The Mechanism of Centriole Inactivation in Starfish Oocytes

Joana Borrego Pinto

Dissertation presented to obtain the Ph.D degree in Cell Biology

Instituto de Tecnologia Química e Biológica | Universidade Nova de Lisboa

Oeiras, May, 2015

INSTITUTO
DE TECNOLOGIA
QUÍMICA E BIOLÓGICA
/UNL

Knowledge Creation

EMBL

PhD defense

Joana Borrego Pinto

Starting date: 1st September 2011

Defense date: 18th May 2015

Supervisors:

Dr. Mónica Bettencourt-Dias, Instituto Gulbenkian de Ciência, Portugal

Dr. Péter Lénárt, European Molecular Biology Laboratory, Germany

Examiners:

Dr. Edgar Gomes, Instituto de Medicina Molecular, Portugal

Dr. Francesca Peri, European Molecular Biology Laboratory, Germany

Dr. Isabelle Vernos, Centre de Regulació Genòmica, Spain

Dr. Jan Ellenberg, European Molecular Biology Laboratory, Germany

Dr. Marie-Hélene Verlhac, Collège de France, France

ACKNOWLEDGMENTS

"Remember to look up at the stars and not down at your feet. Try to make sense of what you see and wonder about what makes the universe exist. Be curious. And however difficult life may seem, there is always something you can do and succeed at. It matters that you don't just give up."

– Stephen Hawking

First of all I would like to thank Péter Lénárt for accepting me as his first PhD student, and also for letting me work on centrioles. I had a great fun! I also have to thank him for all his support and for not complaining (too much) about all my singing and "loudness". I would also like to thank Mónica Bettencourt-Dias for the centriole "bichinho" she transmits to everybody (it is very contagious!), and for all the help provided in this project as co-supervisor and TAC member. I would also like to thank my other TAC members, Jan Ellenberg and Francesca Peri, for all the helpful input in the project and for all their availability.

I would also like to thank to all the people that contributed for this work, one way or another, it was great to work with you all: Julia König and Thomas Müller-Reichert for the EM work, specially for all the hundred serial sections you had to do, Matthia Winter-Karreman and Yannick Schwab for the more serial sections and for all the happiness that you find in your work, Pedro Machado por ser o centriole "buddy" mais próximo, all lab members from Mónica Bettencourt-Dias for letting me participate in their journal club and for all the feedback, especialmente à Inês Bento por partilhar o mundo de eliminação de centrioles comigo, e pelas experiências tão "fixes" que fizemos em Woods Hole. Kreso! For taking such good care of the starfish!

I would also like to thank all the former and current Lénárt lab members for all the great scientific conversations and non-scientific moments that we shared! You've created a great environment to work! Especially for all the "this-pear"s and funny ("S-W-A-T team, "'cause I am happy", "that's magenta", "I had my first

experience...", "I wanna steal your car/heart", "...you know, in the streets of Paris", "are we happy?") moments! Special thanks to Philippe for being a "Rose" weirdo, Natalia for being the crazy mama, Johanna for all the marvelous cakes, Manuela for all the crazy Portuguese talk, Masha for being Masha, Ermin for breaking the centrifuges, Szilárd for being a Hungarian man trapped in an Irish body, Laura for showing her boyfriend around, Sara for being crrrazy, Imre for the craziness of being a physicist! A special thanks for Masashi Mori, my lab brother 2, and Kalman Somogyi, my lab papa, who both helped me so much! It was a pleasure to come to work everyday!

I would like to thank the EMBL community, especially our 4th floor... that rocked! Specially Aastha, Kasia, Thibaut, Deepikaa Deepikaa, Iannaaaa, Ori, Marvin, Alessandra (not-Ginger Ale), Paolita, Gustavo, Oana, Aleksandrita, Ana Rita maluca, Serge, George Cryptic, Vaso, Karin, Simone, Nils Cooling System, Maria mama, Mendi, Dorito and Nicole (oh my, I hope I didn't forget anyone!) for all the great moments: for all the cows, and "sereia à vista no portoooo", for all the barbecues, for all the game nights, for all the flamingos, for all the movie nights, for all the smoothies and warm bretzels and humus and cheese and cakes, for all the chocolates, for all the Moscatel, for all the mentos, for all the grumpy cats, for all the ducks, for all the Muse concerts, for all the crazyyyy stuff, for all the dinners, for all the smiles! It was great to meet you all and spend so many cool moments with you! And always remember: "Um urso rosna quando um galho caiu sobre sua cabeça, mas ele estava sob o peso de uma árvore". I also would like to thank all the Predocs, specially the year of 2011, for all the great fun, for the great community spirit and the great place to do science!

Un petit salut a tous mes amis de Paris, notamment les kiiikiiiissss qui sont toujours lá – c'est toujours beau la campagne et les singes et les petits pijamas – (vous me manquez téllement!), au Gomes lab qui m'a tellement bien accepté comme la petite étudiante de masteur! J'ai appris beaucoup avec vous! Au petit Bruno pour sa tranquilité, ao meu irmão de laboratório número 1 Daniel Osório e ao Edgar Gomes por me ter lançado na minha primeira investigação "à séria" e por continuar sempre disponível para me aturar. Et aussi a tous les autres (les cousins et les Liwerants) qui ne m'oublient pas et a tous mes amis Erasmus! Benno, Lana, Sammy, Ana Banana, Yvonne, JP thanks for still being around!

Um obrigada muito especial a todos os amigos que ficam, mesmo que a distância se alargue! Andreia Panada, Ana Sofia, Carina Men, Sara, Mariana, Melissa, Margarida, Bruno Afonso, Daniel, Neuza, Ana Zhu, Diana por continuarem aí, aconteça ou que acontecer! Porque vocês são lindos e continuam bem pertinho!

Um muito obrigada a toda a minha família que não esquece de mim, embora a "pima" apanhe o avião tantas vezes e só volte esporadicamente. Obrigada especialmente ao Ruizinho que se preocupa mesmo quando finge bem, e à mãezinha que tanto lhe custa que a filhinha esteja tão longe: um muito obrigada por todo o teu apoio e carinho incondicional. Vou, mas trago-vos comigo. Finally, Konradino: what can I say? Thanks for all the help (work and life related). Thank you for being there, sometimes more than 500 miles away, and to be the "man who walks 500 more".

Thank you. Merci. Obrigada. You for sure make my life more colorful.

SUMMARY

"We are drowning in information, while starving for wisdom. The world henceforth will be run by synthesizers, people able to put together the right information at the right time (...)."

– Edward O. Wilson

The centrosome is the major organizing center in a cell, composed by two centrioles, one mother and one daughter, and surrounded by a pericentriolar material, which nucleates microtubules. Centriole duplication and segregation is tightly coupled to cell cycle, which guarantees that centriole number is maintained over generations. During the somatic cell cycle, a pair of centrioles duplicates, after which each daughter cell receives a pair, forming a closed cycle. However, during fertilization, if both cells were to contribute with their pair of centrioles, gamete fusion would result in the double of the normal centriole number. Therefore, centriole number needs to be reduced during meiosis to prevent a surplus in centriole number that would lead to formation of a multipolar spindle in the zygote. Indeed, without exception, centrioles are actively eliminated in oocytes of all animal species, and only the sperm contributes with active centrioles to the zygote. The universality of centriole elimination in female meiosis demonstrates the essential nature of the process in animals. Nonetheless, its mechanisms remain poorly understood.

The timing of centriole elimination varies between species; it may occur early in prophase I of meiosis or just before fertilization. In starfish oocytes (*Patiria miniata*), centrioles are present in fully grown oocytes, and are eliminated during the two consecutive meiotic divisions. I developed GFP markers to specifically label and follow centrioles during starfish meiosis by live imaging in order to visualize when the elimination occurs. I observed that at meiosis onset, two pairs of centrioles are present. One pair out of these is extruded into the first polar body at the end of meiosis I (MI), whereas one pair remains in the oocyte. No

centriole duplication occurs between MI and the second meiosis (MII), and individualized, single centrioles form the poles of the MII spindle.

Strikingly, using the mother centriole marker Odf2-mEGFP I could directly visualize that the mother centriole consistently localizes to the MII spindle's outer pole facing the cell membrane. Consequently, the mother centriole is extruded into the second polar body, whereas a single daughter centriole remains in the mature egg.

By high-resolution 3D tracking of centrioles over time, I identified two steps that are required for this specific orientation of the mother centriole to the outer MII spindle pole: i) a specific transport step, which occurs shortly after PBI extrusion. My data suggests that this transport is independent of dynamic actin, and is occurs independently of polar body extrusion. The proximity to the nuclear region is important, and mother centriole is likely to move to the plasma membrane as a response to a cytoplasmic gradient established upon meiosis resumption. ii) After transport, the mother centriole stably anchors to the cell membrane. This anchoring does not depend on actin or microtubules, for its establishment or maintenance. By confocal light and electron microscopy, the mother centriole can be seen in a close proximity to cell membrane. This suggests that mother centriole is forming a direct contact with the cell membrane, via its mother appendages. This process would be similar to cilia formation, in which mother appendages connect the centriole directly to the plasma membrane, allowing cilia growth.

Additionally, I showed that mother centriole extrusion is physiologically essential: if a mother centriole is artificially retained in the egg, it will remain active, and cannot be eliminated. As a consequence, after fertilization, the mother centrioles organize a multipolar spindle combined with the sperm derived centrioles, which will be detrimental for further embryonic development. In contrast, the daughter centrioles lose microtubule-nucleating activity and are rapidly eliminated from the mature egg's cytoplasm.

In conclusion, in starfish oocytes, the mother centrioles are physically eliminated by extrusion into the polar bodies. In this process, conserved features of the mother centriole are employed to mediate transport and anchoring to the cell membrane. In contrast, the remaining daughter centriole lacks this capacity to be transported and to anchor, and therefore remains in the mature egg. The

mechanism responsible for its elimination is an exciting open question for future studies.

SUMÁRIO

"Tenho em mim todos os sonhos do mundo."

(I have in me all the dreams of the world)

– Fernando Pessoa

O centrossoma é o centro organizador mais importante da célula, composto por dois centríolos, o centríolo mãe e o centríolo filha, e rodeado por material pericentriolar, que é responsável pela nucleação de microtúbulos. A duplicação e segregação dos centríolos está associada ao ciclo celular, o que garante que o número de centríolos é mantido durante as gerações. Durante a divisão celular em células somáticas, o par de centríolos duplica e cada célula filha recebe um par. Porém, durante a fertilização, se ambos os gâmetas contribuíssem com um par de centríolos, isto resultaria no dobro do número normal de centríolos no zigoto. Sendo assim, os centríolos têm que ser reduzidos durante a meiose, de modo a evitar um número excedente de centríolos que levaria à formação de um fuso multipolar no zigoto. De facto, os centríolos são eliminados nos oócitos de todas as espécies animais e apenas o esperma contribui com centríolos para o zigoto. A eliminação de centríolos na meiose feminina ocorre universalmente, o que demonstra como o processo é essencial em animais. No entanto, este mecanismo ainda permanece pouco compreendido.

O estadio em que centríolos são eliminados é variável entre espécies: pode ocorrer durante a profase I ou imediatamente antes da fertilização. É o caso de oócitos de estrela-do-mar (*Patiria miniata*), em que os centríolos são eliminados durante as duas divisões meióticas consecutivas. Foram desenvolvidos marcadores GFP para especificamente marcar e seguir, via *live imaging,* os centríolos durante a meiose da estrela-do-mar, de modo a determinar precisamente quando estes são eliminados. Consequentemente, foi observado que no início da meiose, dois pares de centríolos estão presentes. Um destes pares é extrudido no primeiro corpo polar (CPI) no fim da meiose I (MI), enquanto que o outro par permanece no oócito. Durante a fase MI e a segunda meiose (MII), não há duplicação centriolar, e centríolos individualizados formam

os polos do fuso meiótico II (da segunda meiose). Curiosamente, usando o Odf2-mEGFP, marcador específico do centríolo mãe, observou-se que este se localiza consistentemente no polo exterior do fuso meiótico II, isto é, o polo virado para a membrana celular. Consequentemente, o centríolo mãe é extrudido para o segundo corpo polar (CPII) e o centríolo filha permanece no ovo.

Os centríolos foram observados por 3D *live-imaging* de alta-resolução e verificou-se que o centríolo mãe se posiciona no polo exterior do fuso em duas etapas: i) o centríolo mãe, imediatamente após extrusão do CPI, é transportado para a membrana celular. Este transporte parece ser independente de actina dinâmica e também da extrusão do CPI. A proximidade à região nuclear é importante, o que sugere que o centríolo mãe se desloca para a membrana plasmática em resposta a um gradiente citoplasmático, possivelmente estabelecido aquando da ruptura do invólucro nuclear. ii) Após transporte, o centríolo mãe permanece ancorado à membrana celular. Por microscopia confocal e electrónica de transmissão, o centríolo mãe é visualizado extremamente próximo à membrana celular. Esta ancoragem é independente de actina e microtúbulos, tanto para o seu estabelecimento como para a sua manutenção. Estes dados sugerem que o centríolo mãe está diretamente em contacto com a membrana celular, através dos apêndices do centríolo mãe. Este processo seria similar ao processo que leva à formação de cílios: neste caso, o centríolo mãe está directamente em contacto com a membrana celular através dos seus apêndices.

Adicionalmente, observou-se que a extrusão do centríolo mãe é fisiologicamente essencial: se este ficar artificialmente retido no ovo, permanece ativo, sem ser eliminado. Consequentemente, após fertilização, este centríolo mãe organiza um fuso mitótico multipolar juntamente com os centríolos derivados do esperma. A formação deste fuso mitótico multipolar é prejudicial para o desenvolvimento embriónico. Em contraste, os centríolos filha perdem a capacidade de nuclear microtúbulos no final da meiose e são rapidamente eliminados do citoplasma do ovo.

Em conclusão, em óocitos de estrela-do-mar, os centríolos mãe são fisicamente eliminados por extrusão para os corpos polares. Neste processo, as características do centríolo mãe são empregues para mediar o transporte e a ancoragem na membrana celular. Consequentemente, esta extrusão é essencial

para garantir que os centríolos são devidamente eliminados. Em contraste, o centríolo filha não tem capacidade para ser transportado ou para ancorar, permanecendo no ovo. O mecanismo que leva à sua eliminação é uma questão interessante para ser explorada em estudos futuros.

TABLE OF CONTENTS

"Às vezes ouço passar o vento; e só de ouvir o vento passar, vale a pena ter nascido"

(Sometimes I hear the wind blowing; and just by listening to it, it is worth to be born)

– Fernando Pessoa

ABBREVIATIONS

"Never memorize something that you can look up."

– Albert Einstein

1-MA: 1-methyladenine

CytoD: cytochalasin D

EM: electron microscopy

LatB: Latrunculin B

MI: meiosis I

MII: meiosis II

mGSC: male germ stem cell

MTOC: microtubule organizing center

NEBD: nuclear envelope breakdown

PB/PBs: polar body/polar bodies

PBI: first polar body

PBII: second polar body

PCM: pericentriolar material

γ-TuRC: γ-tubulin ring complex

1. INTRODUCTION

"I learned very early the difference between knowing the name of something and knowing something."

– Richard Feynman

1.1. Centrosome

1.1.1. Historical outlook: the discovery of the centrosome

"Das Centrosoma repäsentiert das dynamische Centrum der Zelle, durch seine Theilung werden die Centren der zu bildenden Tochterzellen geschaffen, um die sich nun alle übrigen Zellbestandtheile symmetrisch gruppiren. (...) Das Centrosoma ist das eigentliche Theilungsorgan der Zelle, es vermittelt die Kern- und Zelltheilung"

("The centrosome represents the dynamic center of the cell; its division creates the centers of the forming daughter cells, around which all other cellular components arrange themselves symmetrically. (...) The centrosome is the true division organ of the cell, it mediates the nuclear and cellular division")

– Theodor Boveri

(Adapted from Boveri, 1887 Ueber den Antheil des Spermatozoon an der Teilung des Eies. Sitzungsber. Ges. Morph. Physiol. München 3, 151-164(Scheer, 2014)).

For the first time in 1887, Theodor Boveri and Edouard van Beneden described centrosomes as the organizing centers of the cell division. Moreover, they recognized centrosomes as cell-autonomous organelles, which are able to duplicate and be transmitted to the daughter cell. Both scholars arrived at these conclusions independently and almost simultaneously. However, Boveri explored

the centrosome's role further and recognized denser granules in the centrosome core, the "centrioles", surrounded by a "centroplasm", a pericentriolar substance from where the aster "arrays", the microtubules, are organized (Moritz and Sauer, 1996; Scheer, 2014) (*fig. 1.1*).

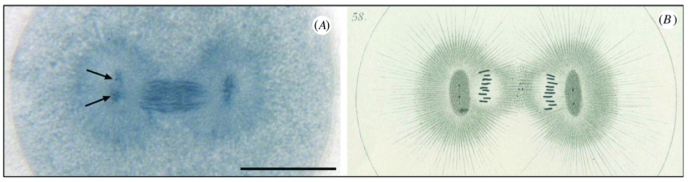

Figure 1.1: First division of a sea urchin zygote. (A) shows an original slide from Boveri (picture taken by Scheer). The two centrioles are identified by the arrows. (B) shows an original of Boveri drawing. Scale 20 μm. Picture adapted from (Scheer, 2014).

Even after more than one century, Boveri's definition of a centrosome is still valid and accurate. A number of studies conducted since then confirmed the existence of a pair of orthogonally arranged centrioles, at the center of the centrosome. These are surrounded by an electron-dense mass, the Boveri's "centroplasm", now referred to as pericentriolar material (PCM). Nowadays, the role of the centrosome, originally proposed by Boveri, as major microtubule organizing center (MTOC) of the cell is well accepted.

In the following chapters I will discuss centrioles from the perspective of their evolutionary origin, detail the molecular mechanisms known to underlie centriole duplication, and specify the centriole behavior during gametogenesis, especially in starfish oocytes, the model system studied here.

1.2. Centrosome function

1.2.1. The ancient function of the centrosome/basal body might have been to anchor flagella and cilia

Evolutionary comparisons show that the most ancient function of the centrosome might have been to act as a *basal body*, the platform for cilia

nucleation (*fig. 1.3*). Indeed, studies suggest that the centrosome as a basal body might have been present in the common ancestor of all ciliated species (*fig. 1.2*) (Azimzadeh, 2014; Azimzadeh and Marshall, 2010). Consistently with this possibility, phylogenetically distant groups, such as plants and protists, all feature the gliding type of locomotion thought to have been present in the common ancestor of all ciliated (Carvalho-Santos et al., 2011). Importantly, the presence of cilia may be the main source of selective constraint for the centriole, its nucleation platform, which may explain its remarkably conserved structure (Bornens, 2012; Carvalho-Santos et al., 2011).

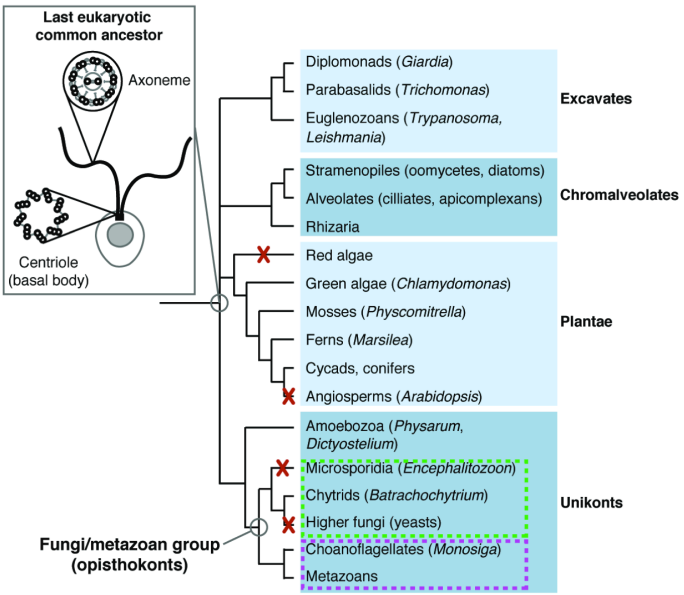

Figure 1.2: Conservation of the centriole and cilia across eukaryotes. These structures were probably present in the last eukaryotic common ancestor. Inset shows a schematic representation of the last eukaryotic common ancestor, as a single-cell organism bearing two motile flagella. Schematic representations of cross-sections through the centriole and the flagellum (inner structure: axoneme) are shown. Red cross: taxa in which all species have lost centrioles and flagella. The green dashed rectangle indicates the fungi group and the violet rectangle indicates the holozoa group. Picture modified from (Azimzadeh and Marshall, 2010).

Centrosomes are likely retained when a species is dependent on cilia at any given developmental stage (*fig. 1.2*). For example, lower plants (such as moss and ferns cells) still have the potential to form centrosomes, likely because their sperm cells are ciliated. However, all of their autosomal cells lack centrosomes

(Marshall, 2009; Roy C Brown, 2011). Species with no requirement for cilia normally lack centrioles, and have other centrosome-like structures at the spindle poles, which acts as MTOCs, such as the spindle pole bodies in yeasts (Bornens, 2012).

In animals, not only sperm cells have cilia. Clearly, cilia acquired important roles in photoreception, olfaction and mechanoreception during evolution. As a consequence, defects in cilia function or structure are a well-known cause of several ciliopathies in humans, such as the Bardet-Biedl syndrome (associated with retinal degeneration and loss of odor sense) and polycystic kidney disease (cyst formation due to loss of mechanosensation of kidney's ciliated cells) (Singla and Reiter, 2006). Consistently, the centriole-less *D. melanogaster* larva die shortly after hatching due to lack of cilia in their neurons, which cause coordination defects (Basto et al., 2006).

1.2.2. Other centrosome functions in metazoan

i. Centrosome function in spindle assembly

Centrosomes are the most important microtubule organizing centers (MTOC) in most animal cells, playing a major role in nucleating microtubules. Centrosomes are most easily recognized as the poles of the mitotic spindle during cell division (*see fig. 1.3*). However, more recently, evidence emerged that centrosomes are dispensable for spindle organization. Interestingly, Boveri already left this option open: "*Ich möchte sagen: die Teilung mit Centrosomen ist die eleganteste Lösung einer Aufgabe, die auch auf andere und wohl mehrfache andere Weise gelöst werden kann." ("I want to say: division involving centrosomes is the most elegant solution to a problem that can also be solved in other and probably multiple other ways")* (Scheer, 2014). Spindles can be organized without centrioles (such as the female meiotic spindles), and even after ablation of centrioles, from cells normally assembling a centriolar spindle, mitosis can still be carried out (Debec et al., 2010; Khodjakov et al., 2000). Furthermore, *D. melanogaster* embryos depleted of centrioles can still develop up to larva stage, although division rate and asymmetric division are affected (Basto et al., 2006). However, one has to note that a maternal pool of centriolar proteins

allowed centriole formation during the early stages of embryogenesis of these flies. If the maternal contribution is completely depleted, *D. melanogaster* embryogenesis is seriously compromised (Arquint et al., 2014; Rodrigues-Martins et al., 2008; Stevens et al., 2007). Similar observations were made during the development of *C. elegans* and mouse: both embryos require the presence of centrioles for the early divisions. Therefore, the importance of the centrosome in spindle organization is likely to be dependent on the cell type, developmental stage and organism (Badano and Katsanis, 2006; Basto et al., 2006).

On the other hand, when present, centrosomes always contribute to spindle assembly. Even though, they might just play a supporting role to facilitate and increase the fidelity of chromosome segregation into the two daughter cells (Marshall, 2001). As the centrosome replication cycle is coupled with the DNA replication cycle, from a centrosome-centered point of view, the participation in a bipolar organization also guarantees the correct segregation of the centrosome into the daughter cells. One hypothesis proposed by J. Pickett-Heaps is that basal bodies became centrosomes just to guarantee their correct inheritance and propagation over the cell generations (Hodges et al., 2010).

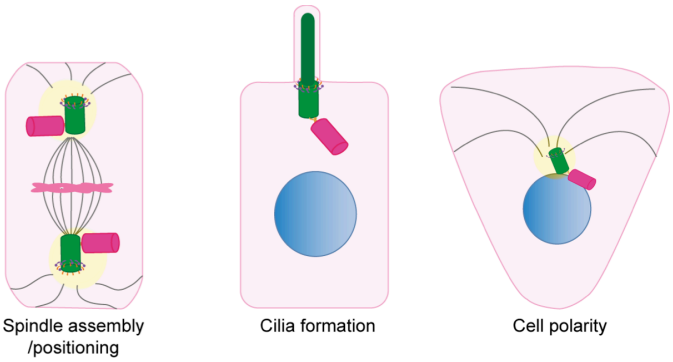

Figure 1.3: Centrosomes have multiple functions in a cell. They participate in spindle assembly and spindle positioning. They organize the cilia/flagella. They organize cell polarity during interphase.

ii. Other centrosomal functions

The centrosome role in spindle assembly is still a controversial topic and, as suggested, might depend on the cell type and organism. However, additional roles of the centrosome in cell cycle progression, cytokinesis and checkpoint

activation have been described for multiple systems (Debec et al., 2010; Doxsey, 2001; Piel et al., 2001). Moreover, centrosomes have a conserved role (from mammals to yeast) in spindle positioning: they nucleate astral microtubules, which are essential to correctly position the mitotic spindle (*see fig. 1.3*) (Doxsey, 2001).

Importantly, during interphase, the centrosome is the major MTOC (*see fig. 1.3*). It is actively positioned at the center of the cell, and creates a microtubule cytoskeleton that defines the "cell's coordinate system" for cell polarity and vesicle trafficking. Moreover, this active positioning defines the localization of other organelles, as the nucleus and the Golgi, to which the centrosome is attached (Bornens, 2012).

1.3. Centrosome structure

As mentioned previously, a centrosome is composed of two orthogonally arranged centrioles, surrounded by a microtubule-nucleating matrix, the PCM (*fig. 1.4*).

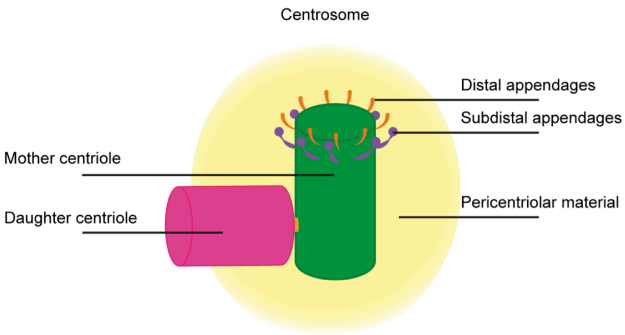

Figure 1.4: A centrosome is formed by two centrioles (one mother and one daughter centriole), surrounded by PCM. Only the mother centriole has two characteristic sets of appendages (distal and subdistal).

Next, I will provide a detailed description of each of these components. In this section, I will focus on the centriole structure and briefly discuss the formation of the PCM. A description of duplication and centriole assembly will be provided in later sections. I will also mention how centriole structure and molecular

composition are so well conserved among organisms, and how this can provide insights into the evolution of this organelle.

1.3.1. Centriole – a well conserved structure across eukaryotes

In the early 1950s, with the advent of electron microscopy (EM), the first centriole ultrastructures exposed the hidden complexity of the centriole. In one of these pioneering studies, Harven and Berhnard showed beautiful transversal and longitudinal sections of centrioles in different cells, revealing the well-conserved 9-fold symmetry of the centrioles and the parallel "tubules" that compose this hollow cylinder (Harven and Bernhard, 1956). Today it is well established that a centrosome has two centrioles, orthogonally arranged. The canonical centriole has 9-triplets of microtubules, which determine its symmetry, a diameter of 250 nm and a length that spans from 150 to 500 nm, depending on the cell type (*fig. 1.5*) ((Winey and O'Toole, 2014). Unrelated species such as mammals, paramecia, tetrahymena and clamydomona have microtubule triplets (Carvalho-Santos et al., 2010). However, there are exceptions to this rule: *D. melanogaster* and *C. elegans* feature microtubule doublets and singlets, respectively (*fig. 1.5*). Curiously, *D. melanogaster* sperm cells have triplets (Azimzadeh and Marshall, 2010; Winey and O'Toole, 2014).

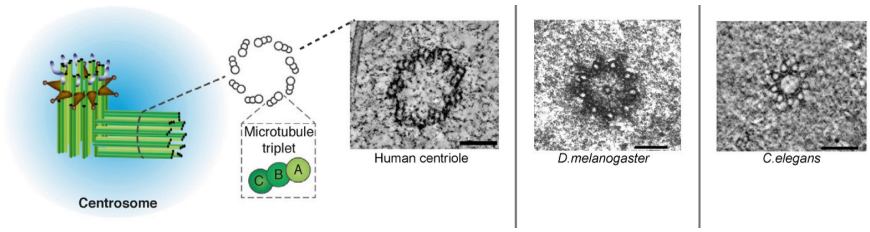

Figure 1.5: Each centriole that composes a centrosome is formed by 9-triplets of microtubules arranged in a cylindrical shape. Mother and daughter centrioles are represented – mother centriole has two sets of appendages. Each microtubule triplet is formed by A-, B-, C-tubules. The canonical centriole has 9 triplets of microtubules (as in the human centriole), but exceptions exist: *D. melanogaster* has 9 doublets, and *C. elegans* 9 single microtubules. Scale bar: 100 nm. Pictures adapted from (Brito, et al. 2012) – schematic, and (Winey and O'Toole, 2014) – EM pictures.

One centrosome has two different centrioles: one mother and one daughter (*fig. 1.4 and 1.5*). The mother centriole has two characteristic sets of appendages, distal and subdistal, which decorate one of its ends (*fig. 1.4 and 1.5*). The distal appendages are involved in ciliogenesis (*see* ***section 1.5***) and are therefore conserved across eukaryotes. In contrast, the subdistal appendages are a new structure that only appeared in vertebrates. These appendages are involved in microtubule anchoring during interphase and they control basal body orientation during ciliogenesis. Similar structures, the basal feet, seem to take their function in other metazoans (Azimzadeh, 2014).

Studies using different methodologies (immunogold labeling, super-resolution microscopy, immunofluorescence studies) mapped the localization of centriolar proteins within the centriole (Brito et al., 2012). These studies very clearly show that mother and daughter centrioles are different in terms of protein composition (*fig. 1.6*). Moreover, protein localization is conserved among species, with multiple homologs localizing consistently in multiple species. For simplicity, I will use the names of the human proteins for the rest of my thesis, but the equivalent homologs can be found in several different studies as (Brito et al., 2012) (*see* ***Appendix section 6.1***).

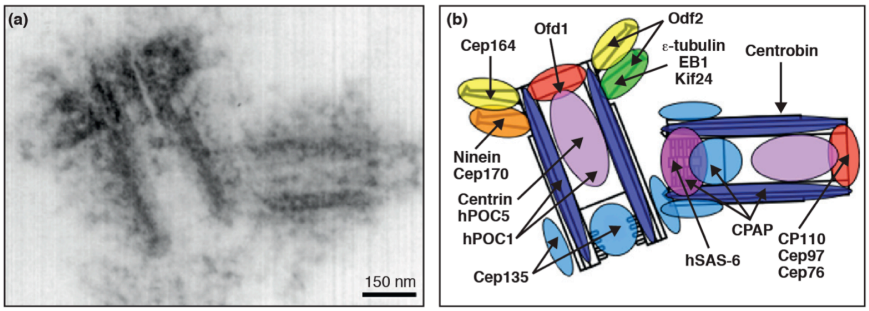

Figure 1.6: Ultrastructural localization of human centriolar markers in a fully mature centrosome. (a) Electron micrograph of a longitudinal section of a centrosome isolated from human lymphoblastoma cells (KE37 cell line). (b) Schematic representation of the picture shown in (a). Several proteins are mother specific and compose the mother appendages (Cep164, Cep170, e-tubulin, EB1, Kif24, Ninein and Odf2). Conversely, Sas6 (in vertebrate cells) and Centrobin only localize to the daughter centriole. Figure and legend adapted from (Brito et al., 2012).

1.3.2. PCM - constitution and formation

As mentioned above, a centrosome has two centrioles, which are surrounded by PCM. Boveri was the first to observe the PCM, and also the first to correctly characterize its main function. Indeed, the PCM works as the “centroplasm”, from where the microtubules are nucleated (reviewed by Scheer, 2014). Gould and Borisy experimentally showed for the first time how isolated PCM can nucleate microtubules *in vitro* (Gould and Borisy, 1977).

Initially, PCM was merely described as an amorphous electron-dense cloud around the centrioles that would expand in size during mitosis. Nowadays, the PCM components start to be better known and described, and advances in super-resolution microscopy revealed the curious PCM organization (Fu and Glover, 2012; Lawo et al., 2012; Mennella et al., 2012; Sonnen et al., 2012). During interphase, the PCM is organized in well-defined concentric layers of proteins (as CEP192, CDK5RAP2, γ-tubulin) around the centrioles, which constitutes the PCM *matrix* (*fig. 1.7*). In this case, γ-tubulin, with a microtubule

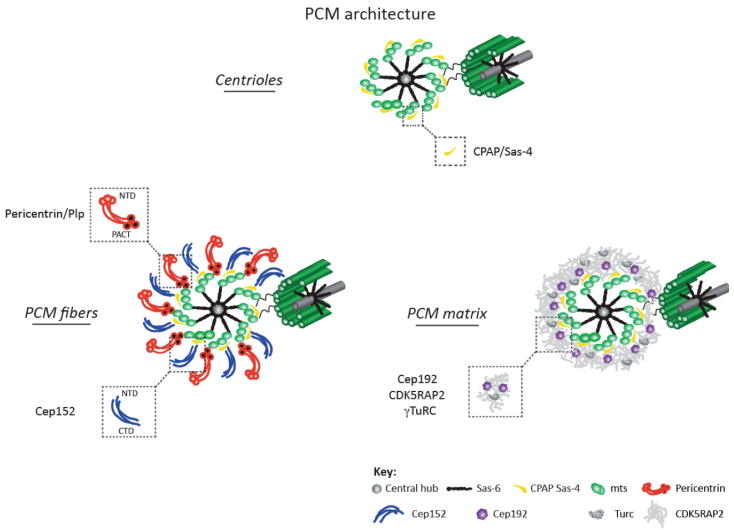

Figure 1.7: PCM organizes around the centrioles. The PCM is organized in two major layers: PCM fibers and PCM matrix (here represented separately to help visualization). PCM fibers comprise the elongated coiled-coil proteins pericentrin/pericentrin-like protein (PLP) and Cep152/Asl. PCM matrix contains: Cep192, CDK5RAP2, γ-tubulin. Picture modified from (Mennella et al., 2014).

nucleating function, localizes in the outer layers. Pericentrin and CEP152 constitute the PCM *fibers* and do not follow this concentric organization, but a more fiber-like organization (*fig. 1.7*) (Lawo et al., 2012; Mennella et al., 2012, 2014). Pericentrin appears to be at the top of the cascade that leads to PCM assembly, recruiting CDK5RAP2 and γ-tubulin (Mennella et al., 2014).

Upon entry into mitosis, more PCM components are recruited, expanding the PCM "cloud". Cell cycle kinases, such as PLK1 and Aurora-A, have a role in PCM expansion. PLK1 phosphorylates PCM components, such as Pericentrin, leading to the accumulation of more PCM components. Aurora-A acts more downstream adding microtubule-associated proteins to the structure. As phosphorylation leads to a PCM extension during mitosis, dephosphorylation of its components, in reverse, causes PCM dissolution at the end of mitosis (Mennella et al., 2014; Woodruff et al., 2014). Hence, the PCM assembly/disassembly is linked to the cell cycle, acting as the major factor to coordinate microtubule assembly.

1.3.3. Protein composition reflects phylogenetic relationships between eukaryotes

As mention before (*see* ***section 1.2.***), it is likely that the centrosome first emerged in evolution as a basal body, the cilia platform, whereas its MTOC function is likely to be a function acquired subsequently. Remarkably, centriole composition supports this idea, with a characteristic set of *ancestral* proteins, appearing in all species that form cilia at any point of their life (*fig. 1.8*). This core of proteins is conserved at least in four major eukaryotic groups: **plantae** (including species as *Clamydomonas reinhardtii* and *Physcomitrella patens*, a type of moss), **excavata** (*Trypanossoma brucei, Naegleria gruberi*), **chromalveolata** (*Paramecium tetraurelia, Tetrahymena termophila*) and **holozoa** (including *Drosophila melanogaster, Caenorhabditis elegans* and vertebrates) (*fig. 1.8*). A single species from the **Fungi** group, *B. denbrobatidis* also contains this set of *ancestral* proteins – *fig. 1.8* (Carvalho-Santos et al., 2011; Hodges et al., 2010).

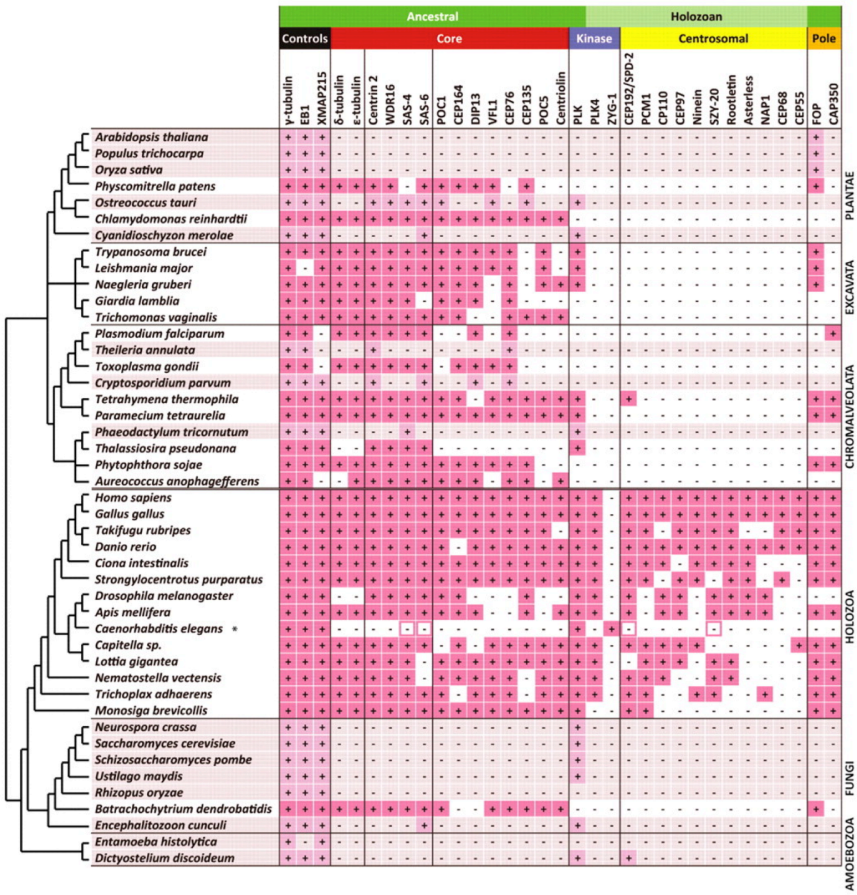

Figure 1.8: Distribution of centriolar and centrosomal proteins among eukaryotes. Protein homologs were identified for 45 eukaryotes (29 ciliated species (white) and 16 non-ciliated species (grey)). (+) Indicates presence of homologs. “Core” proteins are conserved ancestral centriolar proteins. “Centrosomal” proteins are associated with centrosomal functions. “Pole” proteins might have fulfilled a function in the ancestral spindle pole. “Controls” are proteins that are associated with general microtubule dynamics. “Ancestral” proteins are present among extant eukaryotes. “Holozoan” proteins have a restricted presence in holozoa (Metazoa and *M. brevicollis*). The asterisk indicates sequence drift of core and centrosomal proteins in *C. elegans*; divergent homologs known in the literature but not identified by their approach are highlighted with a pink border. Picture and legend adapted from (Hodges et al., 2010).

Among these *ancestral* set, several proteins (such as SAS6, SAS4, CEP135 and CEP164) are involved in the centriolar 9-fold symmetry, microtubule assembly and appendage formation, which suggests that these proteins emerged

early in the eukaryotes and established the centriolar structure (Carvalho-Santos et al., 2011; Hodges et al., 2010).

In holozoa, in which centrioles additionally serve as MTOCs, one can additionally find specific proteins associated with PCM assembly and microtubule nucleation, the *holozoa* set (*fig. 1.8*). This set includes proteins associated with PCM assembly and microtubule nucleation, as CEP192/Spd-2 (Azimzadeh, 2014; Carvalho-Santos et al., 2010; Hodges et al., 2010). Therefore the appearance of this group of proteins likely contributed to the “dual life” of the centrosome. Interestingly, PLK4, the master initiator of centriole duplication, appears also to be restricted to the holozoa group, while other PLK family members, such as PLK1, are identified in many other groups of the tree of life. This suggests that PLK4 possibly had its origin in the duplication of a PLK1-like ancestor, which became specialized in centriole duplication in the holozoa group (Carvalho-Santos et al., 2010).

In summary, centrosomes/basal bodies are highly conserved structures with a conserved protein composition. This protein composition is consistent with the phylogenetic relationships established among organisms, which likely indicates that a centriolar structure was already present in their common ancestor. The study of molecular composition also allows inferring its ancestral and newly acquired functions during the evolutionary pathway.

1.4. Control of centriole number during cell division

1.4.1. Cell division and DNA duplication

Cell division is the basis of cell continuity: cells duplicate and transmit their genetic information to the next generation. In unicellular organisms, cell division is reproduction; in multicellular organisms, cell division produces complexity, in which each cell is specialized for a specific task.

There are two types of cell divisions: to multiply their number, cells follow the mitotic process; to form gametes, and to reduce their chromosome content, cells follow the meiotic process (*see* ***section 1.6.1***).

Both processes are preceded by an interphase that prepares the cell for division, and comprises three distinctive phases: G1, S and G2. During G1, the cell grows in size, synthesizes multiple RNAs and proteins that are necessary for the following cell division. DNA duplication occurs during S-phase. DNA duplication is *semiconservative*, i.e. the parental DNA strands are used as a template for the synthesis of the new DNA strand. DNA has to be *licensed* at the end of the previous division cycle, by pre-replicative complexes, which localize at the regions of *replication origin*, and allows the strand to be duplicated. These complexes are displaced when duplication starts, which turns the DNA to an *unlicensed* state until the next cell cycle (Nishitani and Lygerou, 2002). This assures that DNA is only duplicated once per cell cycle, and guarantees maintenance of genomic content in the long term (Lodish, 2008). At last, the final preparations for cell division are made during G2-phase. After this, a cell enters either mitotic or meiotic division.

1.4.2. Cell division and centriole duplication

i. Centriole duplication is semi-conservative and occurs once per cell cycle

Although Boveri already described the centriole as an organelle able to duplicate, this duplication was first described morphologically using EM (Kochanski and Borisy, 1990; Robbins et al., 1968; Vorobjev and YuS, 1982). Briefly, the pair of centrioles enters a new cell division (G1) in a *disengaged* position, i.e. centrioles are still connected, but no longer in the orthogonal position. During S-phase, each pre-existing centriole duplicates, by "growing" a new centriole, called the "pro-centriole", in an orthogonal position, re-establishing the characteristic orientation. Pro-centrioles then elongate during G2 until prometaphase.

The centriole duplication resembles DNA duplication in four ways: i) it occurs during S-phase, ii) centriole duplication is *semiconservative* – the pre-existing

centrioles are not destroyed, but are instead used as a platform for the emerging centriole (Kochanski and Borisy, 1990). Then, iii) only *licensed* centrioles can duplicate. Centrioles are licensed during mitosis by *PLK1 modification* (Wang et al., 2011) and by *disengagement* through separase and also promoted by PLK1(Tsou and Stearns, 2006; Tsou et al., 2009). Finally, iv) a single *site of origin* ensures that centrioles can duplicate only once per cell cycle (concept adapted from Fırat-Karalar and Stearns, 2014). It is not yet understood how a single site of origin for centriole duplication is assigned. However, it is known that the levels of PLK4, the main regulator of centriole duplication, are tightly regulated during the cell cycle, which is essential to avoid centriole over-duplication (Fırat-Karalar and Stearns, 2014). Other proteins, as SAS-6 and STIL, also stimulate centriole over-duplication and are therefore also tightly regulated (Azimzadeh and Marshall, 2010; Fırat-Karalar and Stearns, 2014).

All this then assures that, similar to DNA, centrioles are duplicated only once per cell cycle, maintaining centriole number over generations. Moreover, at the beginning of a new cell division only the pre-existing centrioles, the *mother centrioles*, are licensed and therefore only these two can duplicate. The new centrioles, pro-centrioles or *daughter centrioles*, are blocked for duplication, because they are not yet licensed.

In the next section, I will provide more details about the mechanism of centriole duplication, including the formation of the *cartwheel* (the base that confers the centriole its 9-fold symmetry), and how microtubules are then positioned around this cartwheel, and centrioles are elongated.

ii. Centriole duplication: the onset and cartwheel formation

At the beginning of a new cell cycle, a pair of disengaged centrioles starts its duplication during late G1/S-phase. Interestingly, a core of only five proteins, identified in *C. elegans*, is essential for centriole duplication: ZYG-1, SPD-2, SAS-4, SAS-5 and SAS-6 (i.e. homologs of the corresponding human proteins: PLK4, CEP192, CPAP/CENJ, STIL, hSAS-6). While this core of five proteins is sufficient for centriole duplication in *C. elegans*, in *D. melanogaster* and human other factors are also essential – for example Asterless in the case of *D. melanogaster*,

and CEP152 and CEP135 in the case of human (Azimzadeh and Marshall, 2010; Hirono, 2014; Nigg and Raff, 2009; Strnad and Gönczy, 2008).

Centriole duplication starts with the recruitment of PLK4 to the origin site, by CEP152 and CEP192, which then recruits SAS-6 (Fırat-Karalar and Stearns, 2014). Lettman MM. and colleagues described, that at least in *C. elegans*, the recruitment of SAS-6 would occur by direct interaction with the *C. elegans* PLK4 (ZYG-1) (*fig. 1.9*) (Lettman et al., 2013).

The first morphological mark of a nascent daughter centriole is the presence of a *cartwheel*, formed by a central *hub* from which nine *spokes* radiate (*fig. 1.9, 1.10 and 1.11*). The cartwheel is evolutionarily conserved among eukaryotes and

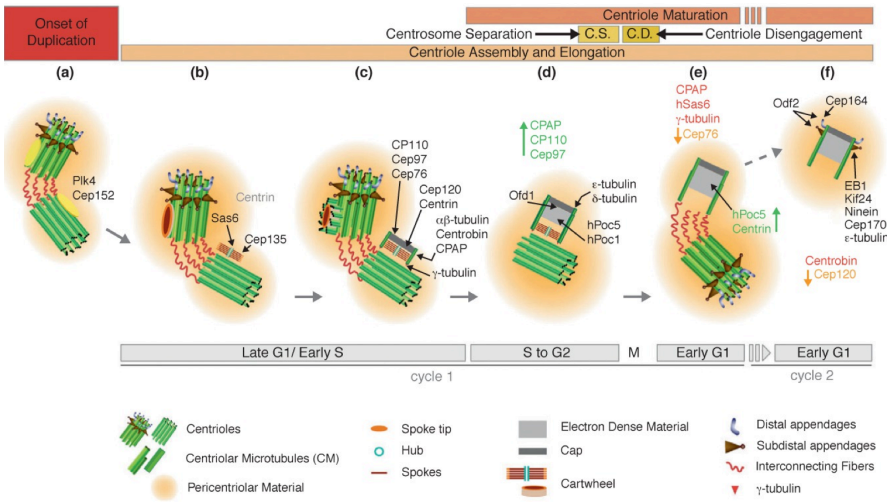

Figure 1.9: Model of the centriole duplication cycle for a human centriole. Briefly, (a) centriole assembly is triggered by Plk4, Cep152 and Cep135. (b) Cartwheel assembly by SAS6. (c) Centriole elongation starts, microtubules assemble around the cartwheel d) Daughter centriole elongation is completed. Centrosome separation, which allows the assembly of a bipolar spindle in mitosis, takes place in late G2-phase. (e) During mitosis, centrioles disengage and lose their orthogonal configuration, a process mediated by Plk1 and separase. (f) The daughter centriole is now a mother, upon full maturation. Centriole duplication and cell cycle stages are indicated at the top and bottom of the image, respectively. Key molecules are shown. Proteins represented in black indicate temporal and spatial localization during centriole assembly; proteins represented in red indicate moment of their displacement from the daughter centriole; proteins represented in green or orange indicate increasing or decreasing levels at the daughter centriole, respectively. Picture and legend adapted from (Brito et al., 2012).

has been reported in protists, algae, fungi and mammals (Hirono, 2014). Moreover, the cartwheel likely creates the characteristic 9-fold symmetry of the centriole. Recently, beautiful *in vitro* studies showed that nine homodimers of SAS-6 oligomerize, forming a ring, through the interaction of their N-terminal domains. This ring forms the *cartwheel hub*, from which the C-terminal domains of the proteins radiate out, forming the *radial spokes* (*fig. 1.10 and 1.11*) (Breugel et al., 2011; Kitagawa et al., 2011). This elegantly shows how a protein can form the scaffold of such a complex structure as the centriole, simply by oligomerization.

The orthologue proteins of STIL in *C. elegans* and *D. melanogaster*, SAS-5 and Ana2, respectively, interact with SAS-6 and appear to facilitate its oligomerization, promoting cartwheel assembly (Hirono, 2014; Leidel et al., 2005; Stevens et al., 2010; Tang et al., 2011).

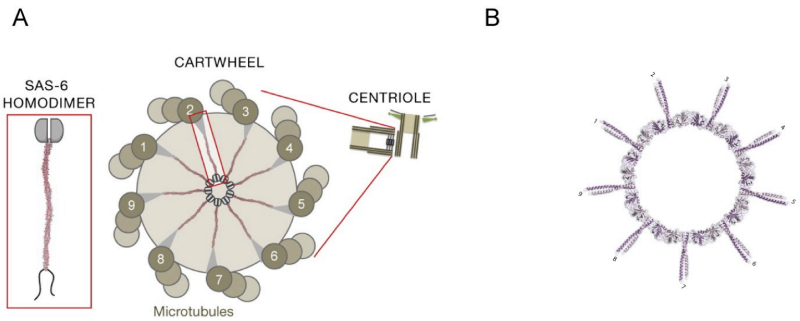

Figure 1.10. Cartwheel is organized by SAS-6 oligomerization. (A) shows a schematic representation of how SAS-6 homodimers organize at the cartwheel. (B) shows the structural model of the SAS-6 related protein, Bld12p (*C. reinhardtii* - cr). Nine crCC-dimers associate such that their N-terminal domains interact, resulting in the 9-fold symmetric ring (diameter of ≈23 nm and a thickness of ≈3.5x5 nm). Figures adapted from (Kitagawa et al., 2011)

iii. Centriole duplication: the centriole growth

After the assembly of the cartwheel, the centriole growth starts with the assembly of microtubules at the tips of the spokes. CEP135 makes the *pinhead*, connecting the cartwheel and the microtubules (*fig. 1.11, yellow*) (Guichard et al., 2013; Hiraki et al., 2007; Matsuura et al., 2004).

Then, each microtubule is individually and sequentially added to the structure, until the formation of a microtubule triplet (*fig. 1.11*) (Azimzadeh and Marshall, 2010; Guichard et al., 2010). These microtubules are named A-, B-, and C-tubule, considering the order in which they are added to the tip of the cartwheel spoke (*fig. 1.11*). The A-tubule is the first to be assembled, consequently requiring the γ-tubulin ring complex (γ-TuRC) for its assembly. This γ-TuRC localizes at the microtubule minus-end and functions here to direct microtubule growth in one direction (Brito et al., 2012). The B- and C- tubules are incomplete microtubules; instead of assembling the 13 new protofilaments, which typically constitute a microtubule, they share some of the protofilaments of the previous tubule, A- and B-tubules, respectively (Guichard et al., 2010; Winey and O'Toole, 2014).

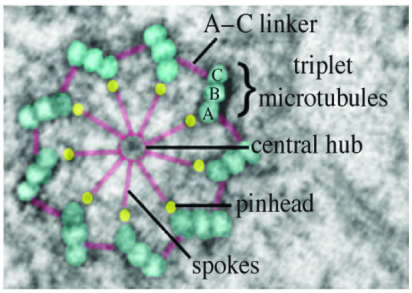

Figure 1.11: Cartwheel ultrastructure and associated microtubule triplets, overlaid by a schematic representation. Cartwheel is shown in the center (pink) formed by the radial spokes and the central hub. In yellow, the pinhead, which connects the cartwheel with the microtubule triplets (A-C). A-tubule is the inner microtubule and interacts with the pinhead. B and C-tubules associate progressively to A. Figure adapted from (Winey and O'Toole, 2014).

The protein CPAP mediates microtubule assembly around the cartwheel (*see fig. 1.9*) (Pelletier et al., 2006), and consequently, mediates centriole elongation, likely by incorporation of tubulin dimers to the microtubule plus-ends of the nascent centriole. CP110 counteracts CPAP action, by limiting centriole growth (Hsu et al., 2008; Kohlmaier et al., 2009; Schmidt et al., 2009). Centriole length appears to be controlled and conserved for each organism.

iv. Centriole and DNA segregation during mitosis

In summary, DNA and centrosomes are duplicated during S-phase as described above (*see previous sections **1.4.2 ii.** and **iii.***). At the G2/M transition, the daughter centrioles are modified by PLK1 (*fig. 1.12*). The cell then enters mitosis with 4N chromosomal content and two pairs of centrosomes, each with a pair of engaged centrioles (Brito et al., 2012; Robbins et al., 1968; Vorobjev and YuS, 1982). Briefly, DNA starts to condense in the beginning of **prophase** and by the time the nuclear envelope breaks down (NEBD), chromosomes are highly condensed entities. The two pairs of centrosomes start to migrate away from each other as NEBD occurs. Progressively, centrosomes capture chromosomes by microtubules, and a bipolar spindle forms. By the end of **metaphase** all chromosomes are properly oriented and aligned at the metaphase plate. Sister chromatid separation occurs in **anaphase** by separase, and each set of chromatids is drawn apart to one pole of the cell, together with one centrosome. Separase is also responsible for the disengagement of the centriole pair. By **telophase,** the nuclear envelope membrane reforms around the decondensed chromatin. At last, **cytokinesis** fully individualizes the two daughter cells (*fig. 1.12*).

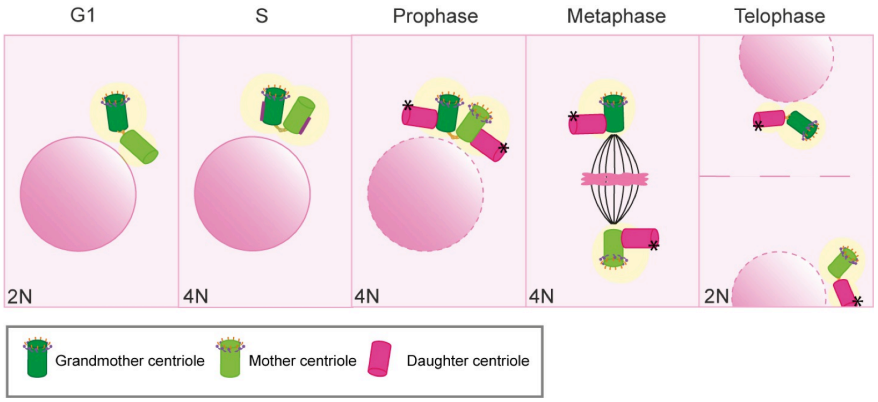

Figure 1.12: Centrosome duplication is coupled with DNA duplication cycle. G1: one disengaged centrosome is present. S-phase: centriole and DNA duplication. Prophase: each mother centriole has a new engaged daughter centriole. NEBD occurs. Metaphase: one pair of centrioles localizes at each spindle pole, chromosomes are aligned at the metaphase plate. At the end of cell division, each daughter cell receives one centrosome and one set of chromatids. (*) indicates modification by PLK1. In the bottom left corner, the DNA content is indicated.

Each daughter cell then contains a diploid set of chromosomes and a single centrosome. Thus, genomic content and centrosome number is preserved over generations (Lodish, 2008). Note that by the end of mitosis, the daughter centrioles are fully licensed (modified by PLK1 and disengaged), and can therefore duplicate in the next cell cycle (*fig. 1.12*).

v. Exceptions to the rule: centriole number is not always conserved

As mentioned, canonical centriole duplication occurs from a pre-existent template: a new daughter centriole grows perpendicularly to the mother centriole during S-phase. The number of new daughters is limited to one per mother centriole (Loncarek and Khodjakov, 2009). This tight control guarantees that each mother centriole duplicates only once per cycle, and each daughter cell inherits one centriole pair, preserving centriole number over the generations. However, exceptions exist and the centriolar cycle does not always follow this canonical pathway.

For example, in some specialized cells, such as those in the multiciliated respiratory epithelia, the canonical cycle could not possibly produce the 200-300 basal bodies formed after cell differentiation. In this case, the rule of one centriole per one pre-existing centriole is broken, and multiple centrioles, in a flower-like organization, assemble around a pre-existing centriole or around a *deuterosome* (*fig. 1.13 B, 1 and 2, respectively)*. A deuterosome is an electron-dense structure that accumulates proteins involved in centriole duplication such as CEP152, PLK4 and SAS6 (Al Jord et al., 2014; Klos Dehring et al., 2013). It is not yet clear how the canonical duplication cycle is broken and which molecular pathways are involved. However, the genes involved in centriole duplication are highly upregulated, which likely accounts largely for the deviation (Fırat-Karalar and Stearns, 2014).

Interestingly, cancer cells often show an amplified number of centrioles, which are likely caused by deregulation of the centriole duplication cycle (by over-expressing the centriolar proteins) or cytokinesis failure, among others (*fig. 1.13 A)*. Despite the abnormal number, cancer cells can still undergo bipolar divisions

by clustering the multiple centrioles at each of the two poles, but they do show an increased rate of aneuploidy (Godinho and Pellman, 2014).

Centrioles can also appear *de novo*, i.e. in the absence of pre-existing centriolar structures, but this only occurs when the centrioles are missing (Marshall, 2009). This phenomenon has been observed for example in insects, in which embryos develop parthenogenetically, without fertilization (*fig. 1.13 C)* (Cunha-Ferreira et al., 2009).

Finally, an extreme case of non-conservation of centriole number occurs during meiosis: centrioles are eliminated in the oocyte, and only the sperm cell contributes the first centrioles to the embryo. As this mechanism is the main focus of my thesis work, I will discuss this process later in more detail.

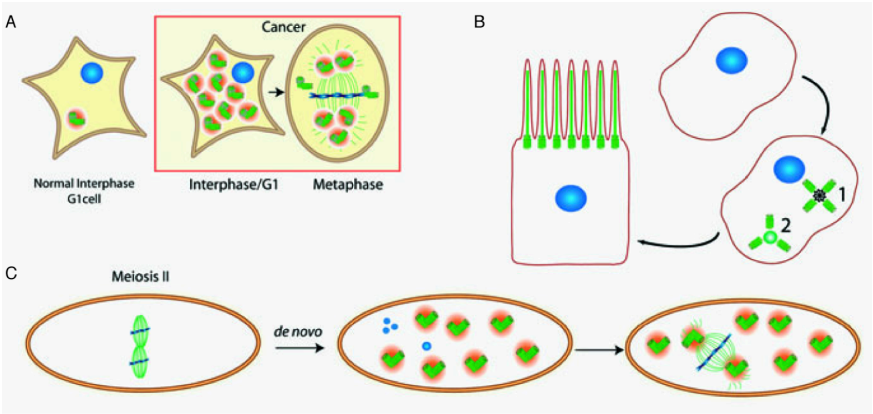

Figure 1.13: Centriole number is not always conserved. (A) Cancer cells often have supernumerary centrosomes. Cancer cells can still conduct mitosis, by clustering the multiple centrosomes at the two poles of the mitotic spindle. (B) Multiciliated cells have to form multiple centrioles at once; they do so either around a pre-existing centriole (1) or a deutostome (2). (C) Centrioles can form *de novo*: in the absence of fertilization, *de novo* centrioles can form the first mitotic spindle, and trigger parthenogenesis. Figure and legend adapted from (Cunha-Ferreira et al., 2009).

1.5. Centriole age: the difference between mother and daughter centriole

1.5.1. Mother and daughter centriole

At the end of mitosis, each daughter cell receives one centrosome, with two centrioles in a disengaged position. These two centrioles were "born" in different generations: the mother centriole is the older centriole, a "progeny" from a previous mitotic cycle, whereas the daughter centriole only just duplicated. Therefore, they differ in age, and moreover they are structurally different. The mother centriole possesses appendages that can easily be seen by EM as small extensions at the distal end of the mother centriole (*fig. 1.14 inset 1 and 2*)

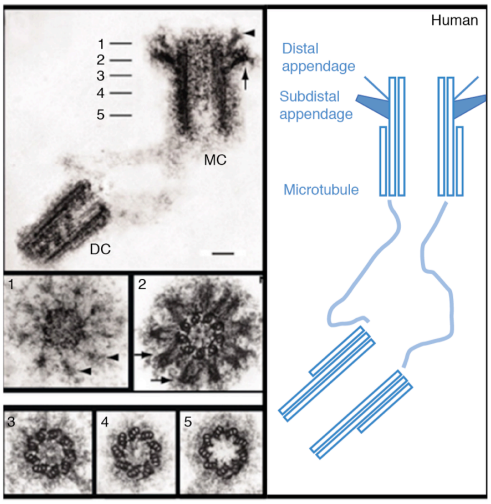

Figure 1.14: Ultrastructure of a centrosome (left) with the respective schematic representation (right). MC indicates the mother centriole, DC indicates the daughter centriole. Mother and daughter centriole differ structurally by the presence of appendages, which localize at the distal end of the mother centriole. (1) Shows a transversal section at the level of the distal appendages (arrowheads). (2) Shows a transversal section at the level of the subdistal appendages (arrows). Note how both sets of appendages follow the 9-fold symmetry of the centriole. (3-5) Transversal sections at different levels of the mother centriole show the nice 9-fold structure organized by microtubule triplets. Scale: 100 nm. Picture adapted from (Fu et al., 2015).

(Paintrand et al., 1992; Vorobjev and YuS, 1982).

Two sets of mother appendages, distal and sub-distal (*fig. 1.14 inset 1 and 2, respectively*), can be observed at the distal side of a mother centriole, following the conserved centriole 9-fold symmetry. However, distal and subdistal appendages carry out different functions. The distal appendages are essential during ciliogenesis and they mediate the centriole anchoring to the plasma membrane. The sub-distal appendages anchor microtubules during interphase and are important for cell polarity. The different functionality reflects the type of proteins that accumulate in each set of appendages. Sub-distal appendages accumulate microtubule-associated proteins as Ninein, CEP170 and ε-tubulin, while distal appendages accumulate proteins such as CEP164 and Odf2 (*see protein localization in fig. 1.6,* ***section 1.3.1***) (Fu et al., 2015; Jana et al., 2014; Tateishi et al., 2013; Winey and O'Toole, 2014). Odf2 is one of the few proteins known to localize to both set of appendages and to be necessary for anchoring to the plasma membrane during ciliogenesis (Ishikawa et al., 2005).

1.5.2. Centriole maturation – the process

At the start of a new cell cycle (G1), the daughter centriole is now licensed to duplicate, and eventually become a mother centriole. One could say that the centriole pair is now formed by a "grandmother", which was already a mother in a previous cycle, and a "new" mother, which is now licensed to duplicate for the first time (*fig. 1.15*). Thus, the now licensed centriole goes through *maturation,* which involves the acquisition of PCM and mother appendages (Brito et al., 2012; Kong et al., 2014; Winey and O'Toole, 2014).

By the end of the following mitosis, the two mothers (grandmother and new mother) have appendages, and each one of them also has a daughter that formed in S-phase. In other words, three generations of centrioles are present in the same cell, in a regular somatic cell division cycle (*fig. 1.15*). Note how the formation and elongation of a new centriole require only one cell cycle, whereas its maturation into a new mother only occurs during the following cell cycle.

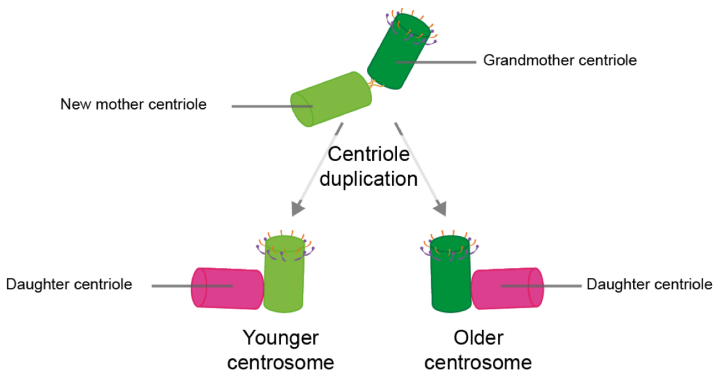

Figure 1.15: There are three generations of centrioles in a dividing cell. At G1, a disengaged centriole pair has a recently licensed “new” mother centriole and a “grandmother” centriole. During S-phase, this pair duplicates, and a new daughter centriole forms in an orthogonal position. The centrosome formed by the “new” mother and a daughter centriole is called the “younger” centrosome, whereas the “older” centrosome, contains the grandmother and a daughter centrioles.

The exact time of appendage assembly is likely to be dependent on the cell type (Kong et al., 2014). Still, PLK1 activity appears to be required throughout S and G2 of the centriole’s second cell cycle, and is essential for appendage formation in the new mother (Kong et al., 2014).

First, appendage proteins start to accumulate at the distal part of the centrioles, and then eventually become appendage structures (Kong et al., 2014; Lange and Gull, 1995). Several studies show that protein accumulation at the mother appendages occurs in a hierarchical way (Ibi et al., 2011; Tanos et al., 2013; Tateishi et al., 2013). Odf2 accumulation in the new mother starts at G2/M transition (Kong et al., 2014; Lange and Gull, 1995) and in fact, Odf2 appears to be one of the most upstream components in the appendage assembly cascade. Consistently, its depletion completely eliminates the formation of either distal or subdistal mother appendages (Ishikawa et al., 2005). How Odf2 is recruited to the new mother centriole is unknown, but the protein 4.1R is likely involved, as upon depletion, Odf2 localization to the centriole is perturbed (Krauss et al., 2008). Odf2 is then required for the proper recruitment of several other appendage proteins as Ninein and CEP164 (Ibi et al., 2011; Tateishi et al., 2013).

As a consequence of the molecular changes outlined above, the centrioles need at least 1.5 cycles to become a functional mother. A daughter centriole, which just duplicated, cannot become a mother (Hoyer-Fender, 2010; Kong et al., 2014; Vorobjev and YuS, 1982), possibly because it needs to disengage first (Kong et al., 2014; Wang et al., 2011).

1.5.3. The role of mother appendages in the anchoring to the plasma membrane

The distal mother appendages mediate the direct anchoring to the plasma membrane during ciliogenesis. However, recently another example of a direct anchoring to the plasma membrane mediated by appendages was described during T-cell activation. I will describe the two processes in the following sections.

i. Ciliogenesis

The mother centriole is required for cilia/flagella formation: it binds to the plasma membrane directly through the mother distal appendages, and once anchored, the mother centriole becomes a *basal body,* i.e. the platform from which cilia or flagella are formed. Cilia and flagella follow the same 9-symmetry as the mother centriole base, but instead have microtubule doublets. Motile cilia/flagella have normally a microtubule doublet in the center, which is not normally present when cilia are non-motile (Reiter et al., 2012).

In order to become a cilia/flagella base, the mother centriole first has to migrate to the plasma membrane, where it then anchors. Details of this process are not entirely clear, but vesicular trafficking appears to be involved. Indeed, one of the current models for ciliogenesis assumes that vesicles dock to the distal appendages of mother centriole, while this is still located in the cytoplasm (*fig. 1.16*) (Sorokin, 1962, 1968; Sung and Leroux, 2013). The mother distal appendage proteins Odf2 and CEP164 are responsible for the interaction with Rab11 and Rab8 vesicles, respectively (Hehnly et al., 2012; Schmidt et al., 2012). More recently, Chibby was found to be involved in mediating the interaction between CEP164 and the Rab8 vesicles (Burke et al., 2014). Subsequently, the vesicles start to fuse with each other, forming a large vesicle,

called the *ciliary vesicle,* at the distal end of the mother centriole. Then, the mother centriole is transported to the plasma membrane along the vesicle transport pathway, where it anchors upon ciliary vesicle fusion with the plasma membrane (*fig. 1.16*) (Reiter et al., 2012; Sung and Leroux, 2013).

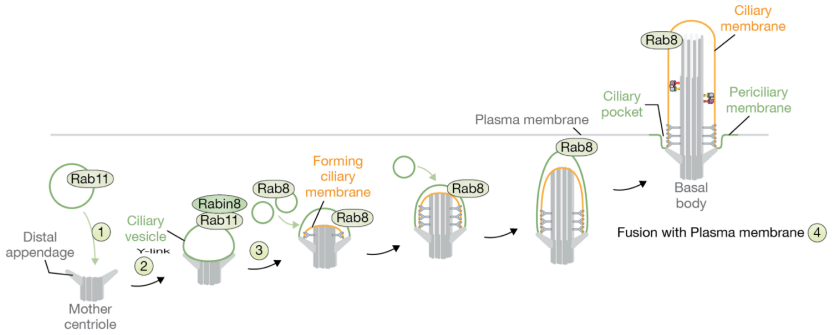

Figure 1.16: Model for ciliogenesis. (1) Mother centriole associates with Rab11 vesicles, which bind to the distal appendages. (2) and (3) Rab8 vesicles associated with the previous vesicles, forming the ciliarly vesicle. The mother centriole is transported to the plasma membrane, hitchhiking the secretory pathway. A pro-axoneme might start to extend while still inside the cell. (4) Vesicles fuse with the plasma membrane, and mother centriole remains anchored directly via its mother appendages. Cilium fully extends. Figure and legend modified from (Sung and Leroux, 2013)

How the mother centriole is transported to the plasma membrane is an unsolved question, but elements of the cytoskeleton are likely involved. The process is best described in multiciliated cells. For example, in multiciliated oviducts, defects in the centriole anchoring are observed upon depolymerization of actin, while microtubule depolymerization has no effect (Boisvieux-Ulrich et al., 1989, 1990; Dawe et al., 2007). It has been shown that the apical surface of multiciliated *Xenopus* embryonic cells are enriched with a dense meshwork of actin, which contributes to basal body spacing and docking, and coordination of cilia beating (Antoniades et al., 2014; Werner et al., 2011). Cytoplasmic microtubules also contribute to this process, by forming a network that polarizes locally the basal bodies (Werner et al., 2011).

ii. Mother centriole movement during T-cell activation

Cytolytic immune cells such as cytotoxic T-lymphocytes kill infected cells by releasing lytic enzymes, which then induce apoptosis. Upon contact with the

target cell, an *immunological synapse* forms, and the T-cell undergoes polarization and re-organization of its microtubule cytoskeleton (*fig. 1.17*). This re-organization is accomplished by centrosome migration to the center of the immunological synapse. Cytolytic granules then move in a microtubule-minus-end directed motion towards the contact site, and are delivered to the target cell (*fig.1.17*) (Stinchcombe et al., 2006, 2011). Microtubules and actin likely play a role in centrosome movement to the plasma membrane, mediated by dynein and formin respectively (Stinchcombe and Griffiths, 2014).

Centrosome movement and association with the plasma membrane are very similar to cilia formation. Indeed, recently Stinchcombe and colleagues identified that in this case mother centriole connects to the plasma membrane through the mother appendages (*personal communication*).

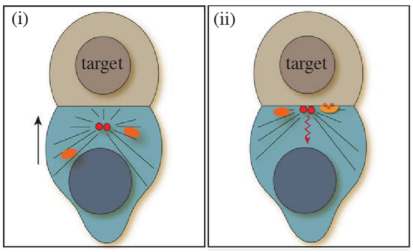

Figure 1.17: Centrosome polarization in T-cells, after interaction with target. Centrosome is shown in red, T-cell in blue, and target cell in light brown. (i) When a T-cell meets its target, the T-cell's centrosome moves towards the contact site. The microtubule network (black lines), including microtubule-associated organelles, such as secretory vesicles (yellow) and cytolytic secretory granules (orange) are reorganized. (ii) Tight centrosome localization at the plasma membrane aligns microtubules, which creates a flow of cytolytic secretory granules towards the contact site. Signalling pathways are activated at the contact site (red arrow). Figure and legend adapted from (Stinchcombe and Griffiths, 2014).

1.5.4. Differential centrosome inheritance and asymmetric division

As mentioned (*see **section 1.5.2***), three generations of centrioles co-exist in a somatic cell. During **metaphase**, at one pole there is the *older* centrosome (which contains the "grandmother" centriole and its daughter), and at the other pole the *younger* centrosome (which contains the "new" mother and its daughter)

(*fig. 1.15*). Therefore, at the **end of cell division**, each daughter cell inherits one of these centrosomes. Due to this asymmetry in centrosome age, a cell division is in fact always asymmetric.

In the standard definition of an asymmetric division two daughter cells are produced that differ regarding their cell fate and/or size. The prime example of this is the stem cell division: stem cells undergo asymmetric divisions and produce a daughter cell that will differentiate, while the other daughter cell maintains its stem cells status and pluripotency.

Is there a link between centrosome age and cell fate? Centrosomes are important for spindle orientation and therefore for establishing the symmetry or asymmetry of cell division. Indeed, multiple studies show that centrosome age determines the division axis of stem cells, which consequently establishes which centrosome each cell inherits. The first report of this was in the **male germ stem cell** (mGSC) line of *D. melanogaster.* Hub cells are important in maintaining the mGSCs pluripotent environment (*fig. 1.18*) (Yamashita et al., 2007). The mGSC divides, maintaining the pluripotent cell close to the hub cells, while the other daughter cell proceeds into spermatogenesis. Interestingly, the older centrosome, due to its higher microtubule nucleating activity, is constrained to the adherens junction between the hub cell and the mGSC during interphase. Consequently, during spindle assembly, the younger centrosome moves distally, defining the future axis of cell division. As a result, the pluripotent stem daughter inherits the older centrosome, while the differentiating daughter inherits the younger centrosome (*fig. 1.18*) (Pelletier and Yamashita, 2012; Yamashita et al., 2007).

However, not always the progenitor cell keeps the older centrosome. In the same organism, in dividing **neuroblasts** the pluripotent cell keeps the younger centrosome, while the differentiating daughter cell, which will give rise to the ganglion mother cell, receives the older centrosome (*fig. 1.18*). This asymmetry is established earlier, during interphase, when the neuroblast has a single pair of centrioles localized apically. The mother centriole rapidly loses its PCM and its apical localization, while the daughter centriole maintains its microtubule nucleating activity and remains connected apically, stabilized by the microtubule aster (*fig. 1.18*) (Conduit and Raff, 2010; Rebollo et al., 2007; Rusan and Peifer, 2007). Interestingly, Centrobin, a daughter centriole marker, is essential for

preserving PCM at the daughter centriole, conserving its MTOC potential during interphase (Conduit and Raff, 2010; Januschke et al., 2013).

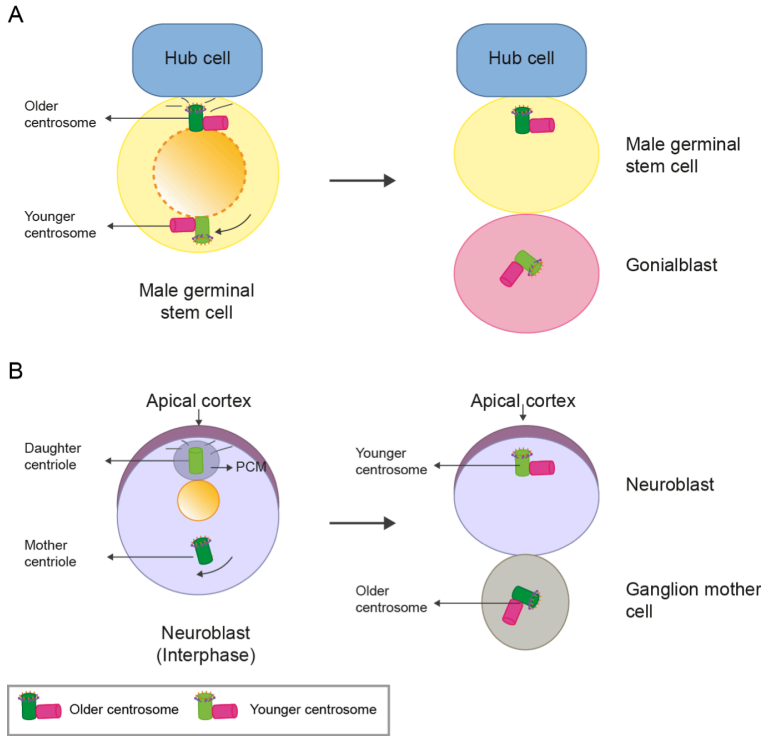

Figure 1.18: Differential inheritance of centrosomes during stem cell division of *D. melanogaster*. (A) Male germinal stem cells (mGSC) (yellow) are associated with hub cells (blue). The older centrosome has a higher microtubule nucleating activity and remains confined to the adherens junction between these two cells. As a consequence, the older centrosome is preferentially inherited by the progenitor stem cell, whereas the goniablast (pink) receives the younger centrosome. (B) During interphase, the daughter centriole retains PCM and microtubule nucleating activity. Therefore it remains at the apical cortex. In contrast, the mother centriole loses PCM and microtubule nucleating activity. When the cell enters division, the progenitor cell (violet) inherits the younger centrosome, whereas the ganglion mother cell inherits the older centrosome (grey).

In the above cases, the connection of either the older or the younger centrosome, respectively in *Drosophila* mGSCs or neuroblasts, to the stem cell niche during interphase, determines the cell division axis, directing the stem cell into an asymmetric division program. However, from these examples, it is not clear whether there is a functional link between the type of centrosome that is

inherited and cell fate. In the **mouse neural cortex**, the apical progenitor cells (also known as radial glia progenitor cells) upon asymmetric division inherit the older centrosome (Wang et al., 2009). The older centrosome retains membrane components, reminiscent of the cilia, which help the progenitor cell to faster reform the cilia than the daughter cell with the younger centrosome. Thereby, Paridean and colleagues showed for the first time the functional importance of inheriting one specific centrosome: the two daughter cells sense and respond differently to the environment, which likely confines their cell fate into a progenitor type cell or into the neuronal differentiation pathway (Anderson and Stearns, 2009; Paridaen et al., 2013).

1.6. Centriole elimination in gametogenesis

As explained in the above sections, centriole duplication and segregation maintains centriole number in somatic cells in a highly controlled manner and with high fidelity. However, deviations exist from the canonical centriole cycle. A prominent example is gametogenesis, where this process is essential for sexual reproduction of all animal species.

During meiosis, oocytes and spermatozoa alter their centrosome activity and composition in a complementary manner. Spermatozoa lose their PCM components, but keep the centriolar structure because of their essential role in cilia formation, and consequently, sperm movement. In contrast, by the end of meiosis, all female gametes lose the centriole structure. Therefore after fertilization, the first embryonic centrioles are a sole paternal contribution. Yet, oocytes accumulate a vast reservoir of proteins necessary for the future embryonic development, and centrosomal proteins are not an exception. Intriguingly, upon fertilization, sperm reduced centrioles use this maternal centrosomal protein pool to fully recover its functionality (Fabritius et al., 2011; Manandhar et al., 2005) .

Again, Boveri already provided us multiple hints about centriole elimination in the beginning of the 19th century. He was the first to describe the lack of centrioles in sea urchins eggs and provide evidence that the embryonic centriole originates from the sperm. Boveri also observed how centrosome number is

important during embryogenesis: an extra number of centrosomes that results from polyspermy (fertilization by more than one sperm) creates multipolar spindles leading to aneuploidy, with consequent defects in embryonic development (Maderspacher, 2008; Moritz and Sauer, 1996; Scheer, 2014).

Following Boveri's pioneering work, multiple studies attempted to characterize the centriole cycle during oocyte and sperm meiosis, referred to as oogenesis and spermatogenesis, respectively. In the next section I will provide a short summary of centriole reduction in spermatozoa, and will focus in more detail on the mechanism of centriole elimination in the oocyte. But first, I will just give a brief introduction to the major steps of meiosis.

1.6.1. Meiosis overview

Meiosis was discovered by Edouard Van Beneden in 1883-84, using the horse roundworm *Ascaris megalocephala* (Hamoir, 1992). Meiosis involves the same steps as mitosis, but in this case the chromosomes still duplicate a single time in S-phase (4N), but undergo two successive divisions – **Meiosis I** (MI) and **Meiosis II** (MII). Hence, four daughter cells originate, each one of them with a haploid set of chromosomes (N). Both female and male gametocytes undergo meiosis, and male meiosis generates daughter cells of equivalent size (sperm cells or spermatozoa) - *fig. 1.19*; female meiosis is extremely asymmetric, originating the oocyte and polar bodies (PBs) – *fig. 1.20* (Lodish, 2008).

Briefly, the steps of meiosis are: **MI** starts with **Prophase I,** normally the longest phase of meiosis, which comprises different steps (only named for future reference): chromosomes get condensed at *leptotene* (from the greek *leptonema,* "thin treads"); then, at *zygotene* (greek *zygonema*, "paired threads"), each chromosome finds its "pair", the other homologous chromosome. At the *pachytene* stage (*pachynema*, "thick threads"), crossing over occurs between the pair of homologous chromosomes. As a consequence, non-sister chromatids exchange genetic material, creating small new rearrangements in the DNA composition; at *diplotene (diplonema*, "two threads"), all crossing overs are established. Most oocytes are arrested at this stage, until fertilization or hormonal stimulation resume the process. Finally, prophase I is completed with *diakinesis*

("moving through"), where chromosomes acquire their maximum condensation, and NEBD occurs (Lesch and Page, 2012).

In **metaphase I**, the paired homologous chromosomes are aligned at the equatorial plate. In **anaphase I**, the pairs of homologous chromosomes separate, and each set of chromosomes migrates to its respective pole of the daughter cell. At **telophase I**, the two daughter cells are individualized, each one of them still diploid, since each chromosome still has two chromatids. A second division starts (**MII**), but no S-phase occurs and thus no duplication of DNA takes place. MII is similar to a mitotic division in terms of chromosome configuration and follows the same steps as MI. Thus, by **telophase II**, each cell receives a single set of chromatids and consequently four haploid cells are formed (*fig. 1.19 and 1.20*).

1.6.2. Centrosome reduction during spermatogenesis

At the last stages of spermatogenesis, the primary spermatocyte (4N) undergoes meiosis, giving rise to four equivalent haploid spermatids (N) (*fig. 1.19*). These cells undergo a major differentiation, reducing all cell components to only those strictly indispensable for fertilization. DNA becomes highly condensed reducing nucleus size, the Golgi apparatus becomes the acrosomal cap and contains enzymes important for fertilization, centrioles organize the flagellar complex, and mitochondria accumulate at the neck of the spermatozoa and provide energy for the flagella movement (*fig. 1.19*) (Lodish, 2008).

As mentioned, centrioles, which are essential for spermatozoa movement, are not eliminated in sperm cells, yet some degree of degeneration is observed. This process, termed *centrosome reduction*, involves loss of PCM proteins and microtubule nucleating activity, with some degree of centriole structure degradation. In some extreme cases, there is the complete elimination of the centriole and respective microtubule triplets. The extent of centriole degradation is variable between species; rodents are the only known species that completely eliminate their sperm centrioles (Manandhar et al., 2005). Moreover, differences also exist in the number of centrioles present in the sperm cells of different species. Next, I will provide an overview of the number and degeneration state of

the centrioles in different organisms, focusing on the most common model organisms.

i. Sperm cells contain one pair of centrioles with different degrees of degeneration

In most species, sperm cells have a pair of centrioles. During spermatids formation in these species, centriole and DNA cycles are uncoupled, and centrioles duplicate between MI and MII, despite the lack of S-phase and thus DNA replication (*fig. 1.19*) (Cunha-Ferreira et al., 2009). It is unknown how the centriole duplication is triggered outside a normal S-phase. In most **mammalian** species (such as bull, sheep, rhesus monkey and human) one of the centrioles, the mother centriole at the base of the flagella, is partially degenerated, and part of the microtubules triplets are disassembled, while the daughter centriole remains intact (Manandhar et al., 2000, 2005). γ-tubulin loss is also observed in the rhesus monkey's spermatozoa.

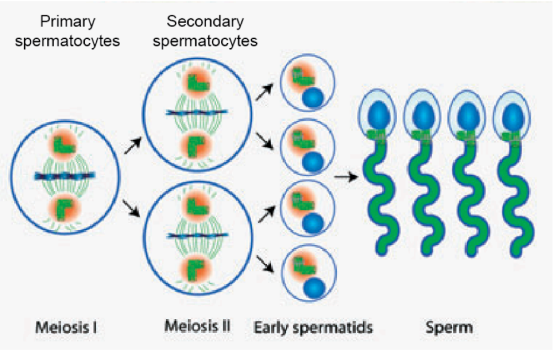

Figure 1.19: Centriole and DNA replication cycles are uncoupled. Centrioles are duplicated in the transition MI to MII, in primary spermatocytes. No DNA replication occurs. Each secondary spermatocyte gives rise to two spermatids, each containing one centrosome. During sperm differentiation, the mother centriole nucleates the flagellum. Figure and legend adapted from (Cunha-Ferreira et al., 2009).

Other non-mammalian species such as **starfish**, **sea urchin** and the ***C.elegans***, also have a pair of centrioles, but it is not known if the mother centriole undergoes any degeneration (Albertson, 1984; Kirkham et al., 2003; Kuriyama and Kanatani, 1981; Manandhar et al., 2005).

ii. Sperm cells contain one single centriole with no degeneration and a proximal centriole-like

In the *D. melanogaster* spermatid, one centriole is present, which nucleates the flagellum (Carvalho-Santos et al., 2012), and does not degenerate its structure. In addition, it has a proximal centriole-like, which lacks the distinctive structure of a centriole. For its formation, the proximal centriole-like requires the same molecular pathways common to the other centriole (such as PLK4 and SAS-6), but it never acquires the centriolar microtubules (mediated normally by SAS-4) (Blachon et al., 2009, 2014).

During differentiation to sperm cells, both centriole and centriole-like undergoes centrosome reduction by losing PCM components as γ-tubulin and centrosomin (equivalent to the human CDK5RAP2), and centriolar proteins such SAS-6 and SAS-4 (Blachon et al., 2014; Manandhar et al., 2005).

iii. Sperm cells do not contain centrioles: complete degeneration

Rodents represent an extreme case of centriole degeneration: spermatids start differentiation with two centrioles, which become completely degenerated by the time spermatozoa reach full maturation. Centriole degeneration comprises the progressive loss of the microtubule triplets and thus the loss of the centriole's inner structure (Woolley and Fawcett, 1973). Degeneration starts with protein loss: γ-tubulin and centrin disappear from the spermatid during maturation to spermatozoa. γ -tubulin is lost first, while the centrin signal progressively fades from the centrioles. Shortly after centrin is lost, the centrioles degenerate. Manhandar et al. proposes that centrin loss in rodent sperm centrioles may be related with the elimination of the structure, since other mammalian sperm cells do not lose this protein (Manandhar et al., 1998, 1999). However, this mechanism was not further characterized.

The only other known species to have centriole-less spermatozoa is the **snail *Lymnae stagnalis***. Protein loss was not described in this species, but ultrastructure studies show loss of the daughter centriole shortly after the end of meiosis. During differentiation, mother centriole microtubules disappear and are replaced by thick electron dense columns (Krioutchkova et al., 1994a).

Interestingly, mouse axonemes show similar columns after centriole deterioration, and similar degeneration processes might be involved in these two species.

1.6.3. Centriole elimination during oogenesis

At the last stages of oogenesis, the primary oocyte (4N) undergoes two consecutive rounds of division with the formation of two PBs (2N and N respectively) and the final mature egg (N), ready to be fertilized. Note that the first PB (PBI) does not normally divide. Female meiosis is highly asymmetric; the mature egg preserves almost all of the primary oocyte's cytoplasm, while the PBs contain just the chromosomes and are destined for decay (*fig. 1.20*).

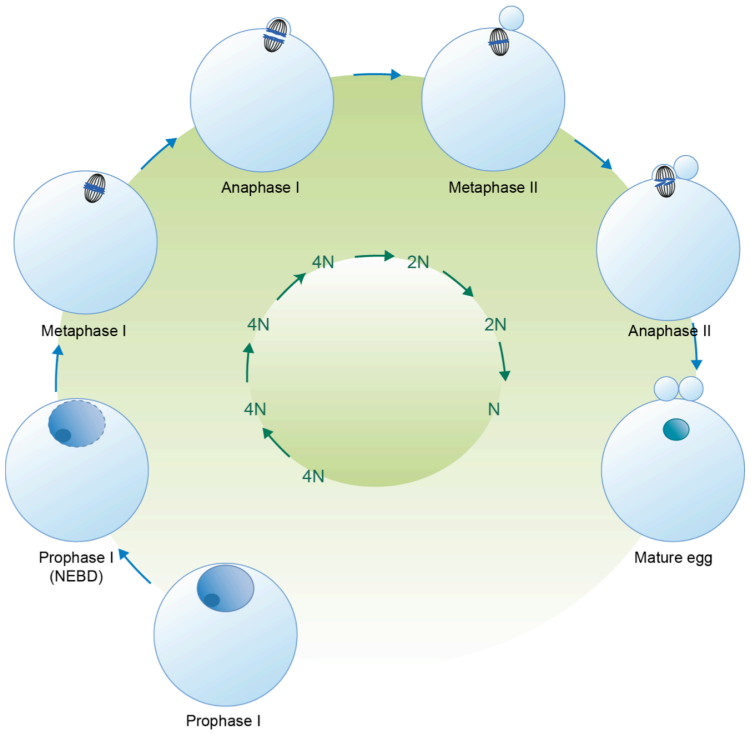

Figure 1.20: General example of meiosis in female oocytes. The oocyte undergoes two consecutive and highly asymmetric divisions, forming two PBs. In MI, each set of homologous chromosomes is segregated to one of the two daughter cells. In MII, each set of sister chromatids is segregated to one of the two daughter cells originating haploid cells. In some oocytes, centrioles are eliminated during Prophase I before NEBD, and spindle is acentriolar (shown), whereas other organize an centriolar spindle. DNA content is shown in the inner circle.

During female meiosis, another important event takes place: female centrioles, as a structure, are eliminated, even though centrosomal proteins are stored in large amounts in the cytoplasm. Upon fertilization, the degenerated centrioles carried by the sperm use the centrosomal proteins stored in the egg, to recover their full functionality (Manandhar et al., 2005).

Centriole elimination is a common process of all oocytes, and by the end of meiosis, no visible centrioles can be found in the egg cytoplasm in any species investigated so far. Depending on the species, centriole elimination occurs at earlier or later stages of meiosis, also determining the mechanism of meiotic spindle assembly. Although multiple studies defined precisely when centrioles are eliminated, the mechanisms underlying the inactivation and elimination of the female centrioles are still largely unknown. Next, I will describe the process of centriole elimination in more detail, grouping different species according to when centrioles are eliminated (*see fig. 1.21 for summary*) and providing, when already described, more information about the mechanism.

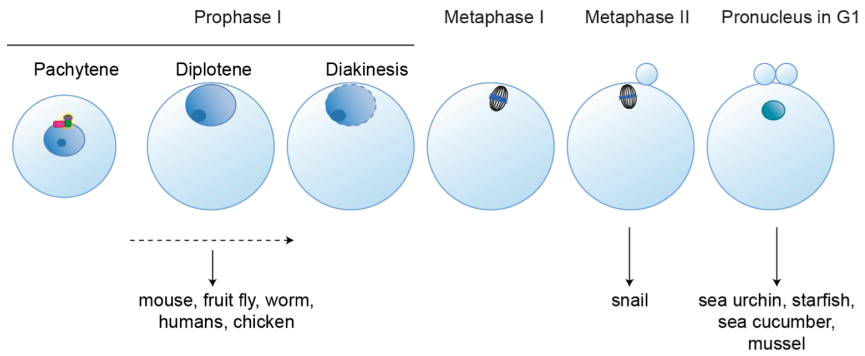

Figure 1.21: Diversity in the centriole elimination timing. Centrioles are present in the pachytene stage of all species that have been described. Centrioles are eliminated by the diplotene stage of prophase I in organisms such as mouse, fruit fly (*D. melanogaster*), roundworm (*C. elegans*), human and chicken (group (i) – see text). In this case the spindle is acentriolar. The snail *Lymnea stagnalis* has one pair of centrioles at meiosis onset. By metaphase II, a single centriole remains (*see details in the main text*), and sperm basal body organizes the other spindle pole. Maternal centriole is then eliminated upon PBII extrusion (group (ii)). In species such as starfish, sea urchin, sea cucumber and mussel (species of the group (iii)), two pairs of centrioles organize the meiotic spindle, which are successfully extruded into the PBs during the meiotic divisions (*see details in the main text*). A single centriole remains in the mature egg and is then eliminated. Dashed line at diakinesis stage indicates NEBD.

i. Centrioles are eliminated before prophase I: spindle assembly is acentriolar

Centrioles are eliminated during prophase I in fruit flies, frogs, worms and mammals. The meiotic spindle is then organized in an acentriolar way.

In mammals such as **humans,** centrioles are observed in the early prophase, but are not present at the poles of MI and MII spindles (Sathananthan et al., 2000, 2006). More data is available in **mouse** oocytes; EM studies show the presence of centrosomes in the pachytene stage of the oocyte, but not in the later stages (Szollosi et al., 1972). Upon NEBD, multiple electron-dense MTOCs, containing pericentrin and γ-tubulin (Calarco, 2000; Carabatsos et al., 2000), are observed around the nuclear envelope. These MTOCs form *de novo* and are functionally equivalent to the centrosomes, clustering to organize the meiotic spindle (Schuh and Ellenberg, 2007). Such electron-dense structures are not observed in the poles of the human meiotic spindle, nor have equivalent structures been described so far (Sathananthan et al., 2006). Besides, these acentriolar MTOCs also have an important role in the first divisions of the mouse embryo: as mentioned above, rodent sperm lacks centrioles, and in addition to meiosis, the first embryonic divisions are also organized by acentriolar MTOCs (Calarco, 2000; Courtois et al., 2012).

Although centriole elimination is less well described in the **frog *X. laevis***, centrioles are also eliminated during diplotene stage (Gard et al., 1995). γ-tubulin appears later around the nuclear region and studies suggest that acentriolar MTOCs might be involved in spindle assembly in these species as well (Gard, 1994).

During ***D. melanogaster*** oogenesis, each egg chamber accommodates a group of 16 interconnected cells, 15 nurse cells and a single oocyte, which will undergo meiosis. The nurse cells only function is to “nurse” the oocyte through the different stages of oogenesis, providing supplies of maternal mRNA and proteins (*fig. 1.22*). Early in oogenesis, nurse cells lose their centrioles, which congress to the oocyte, creating a large MTOC of multiple centrioles, generating an efficient microtubule network that is used to transport all mRNA and proteins towards the oocyte (Becalska and Gavis, 2009; Gonzalez et al., 1998). Up to prophase I, centrioles can be detected by D-PLP and γ-tubulin. As meiosis

proceeds, more precisely during the diplotene stage, the centriolar aggregate is eliminated and no indication of a centriole structure can be detected in the oocyte's cytoplasm (Dåvring and Sunner, 1973; Januschke et al., 2006; Mahowald et al., 1979). Spindle assembly then starts with acentriolar MTOCs.

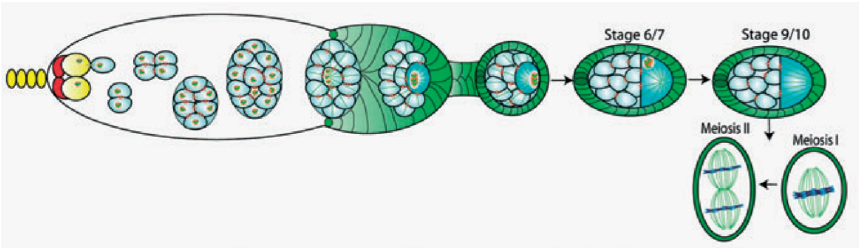

Figure 1.22: Centrioles disappear during *Drosophila* oogenesis. *Drosophila* oogenesis starts with a stem cell that divides asymmetrically. The germline cyst cell divides four times and originates a cyst of 16 connected cells. One of these cells will become the oocyte and undergo meiosis. The other 15 cells become the nurse cells. All the centrioles in the nurse cells migrate to the oocyte. Centrioles disappear at diplotene stage, during stage 9/10 (see figure); as a consequence, female meiosis is acentriolar. Figure and legend adapted from (Cunha-Ferreira et al., 2009).

In the **roundworm *C. elegans***, cells in different stages of differentiation occupy different regions in the gonad: proximally, germ cells undergo proliferation (*fig. 1.23, region 1*), and move distally as they proceed through meiosis (*fig. 1.23, region 2 and 3*), until being fertilized, shortly after NEBD (*fig. 1.23, region –1 to –3*) (Kim et al., 2013). As in fruit flies, by the time the meiotic spindle is formed, centrioles are no longer visible and spindle assembly is acentriolar (Albertson and Thomson, 1993). As different stages of meiosis occupy defined positions inside the gonad, it is possible to precisely time the elimination of the centrioles. Indeed, Mikeladze-Dvali and colleagues observed that, shortly after germ cell entry into meiosis, centrioles lose microtubule-nucleating activity, despite PCM and centriole proteins still being detected at this stage. When the germ cell enters the diplotene stage of Prophase I (*fig. 1.23, region 4*), centriolar and PCM proteins have dispersed and centrioles are no longer observed. Centriole elimination is likely to occur rapidly, as no intermediate or "collapsing" structure has ever been identified (Mikeladze-Dvali et al., 2012).

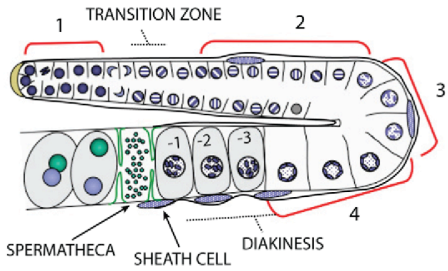

Figure 1.23: Schematic representation of a *C. elegans* gonad. The gonad can be subdivided into four regions: (1) proliferating germ cells; (2) germ cells in pachytene stage; (3) germ cells after pachytene; (4) germ cells in diplotene stage: centrioles are no longer visible at this stage. Note diakinesis oocytes are marked –1, –2, –3 prior to the spermatheca. Sheath cell nuclei are depicted in blue. Figure and legend adapted from (Mikeladze-Dvali et al., 2012).

Centriole elimination in this organism is delayed upon depletion of the germline helicase CGH-1, which associates with certain maternal mRNAs. As a consequence, centriole elimination is defective and oocytes still containing centrioles are fertilized, creating multipolar spindles in the embryos (Mikeladze-Dvali et al., 2012). Although a potential effector or mechanism was not identified, CGH-1 is the first protein known to be involved in centriole elimination.

Taken together, although the species described above are not closely related, their centrioles are eliminated by the diplotene stage, during prophase I (*fig. 1.21*). Whether the underlying mechanisms are conserved is not known.

ii. One single pair of centrioles is present at the beginning of meiosis: the sperm centriole intervenes

The pulmonary snail ***Lymnea stagnalis*** has an alternative centriole cycle during meiosis – a single pair of centrioles is present at the beginning of MI. Consequently, the MI spindle organizes with a single centriole in each pole, with one of the centrioles being extruded into the PBI. The remaining centriole forms the MII spindle pole facing the outside of the cell, whereas the sperm basal body is positioned at the other spindle pole (Krioutchkova et al., 1994b). Although the formation of the MII spindle requires the sperm basal body's intervention, the oocyte centriole pair is successfully extruded into the PBs and therefore eliminated from the egg cytoplasm.

iii. Centrioles are eliminated at the end of meiosis: spindle assembly is centriolar

Not all oocytes organize an acentriolar spindle during meiosis. In fact, ultrastructure studies show that two pairs of centrioles are present at the beginning of meiosis in oocytes of echinoderms (such as **sea urchin** *H. pulcherrimus*, **starfish** *P. pectinifera* and *arnurensis* and **sea-cucumber** *H. moebi*) and bivalves (such as **mussel** *M. edulis*). Although only EM studies were performed in those species, it is described that during MI spindle formation, a pair of centrioles localizes at each pole of the MI spindle. The PBI is extruded with one pair of centrioles. Interestingly, during MII, single centrioles are observed at the MII spindle poles. A second PB (PBII) is extruded with one of the centrioles, and a single centriole remains in the mature egg (Kato et al., 1990; Longo and Anderson, 1969; Miyazaki et al., 2005; Nakashima and Kato, 2001). The remaining centriole is then eliminated, and the sperm provides the embryo with the first pair of centrioles (Saiki and Hamaguchi, 1998). How the remaining single centriole of the oocyte is eliminated remains an unsolved problem. In a next section, more information about the different centriolar behaviors observed in starfish oocytes will be detailed.

The differences in timing of centriole elimination have direct consequences to the type of spindle assembly that is adopted: when centrioles are eliminated before NEBD, the spindle is acentriolar; when centrioles are maintained until the end of meiosis, centrioles organize the spindle. Although the type of spindle assembly, centriolar or acentriolar, has been identified for these species, we are far from understanding what dictates the timing of centriole elimination.

1.6.4. Scaling problems in oogenesis

i. Spindle positioning at the cell cortex

Oocytes are among the biggest animal cells, which undergo highly asymmetric divisions in order to reduce their DNA content to a haploid set of chromosomes. Oocyte asymmetric division is functionally important because it preserves

nutrients and proteins, essential for early embryonic development. Moreover, only the mature egg is fertilizable: the PB cannot bind sperm due to its lack of microvilli, required for sperm entry (Brunet and Verlhac, 2011).

Oocytes' meiotic spindles are small and localize asymmetrically in close proximity to the oocyte plasma membrane, which ensures the extreme asymmetry of the division, so that just a small fraction of cytoplasm is lost during cell division (Chaigne et al., 2012; McNally, 2013). Although asymmetric spindle positioning occurs in all female oocytes, it can happen at different stages of meiosis. In many species, the entire nucleus moves to the animal pole before NEBD (e.g. **starfish**, **sea cucumber**, ***C. elegans***, ***D. melanogaster***), whereas in **mouse** oocytes, the nucleus remains in the center, and migration occurs only after spindle assembly (Fabritius et al., 2011; Miyazaki et al., 2005).

Centrioles, which are retained until the end of meiosis in **starfish** and **sea cucumber** oocytes, localize close to the plasma membrane at the animal pole in the immature oocyte. The nucleus is then positioned to the animal pole in a microtubule-dependent mechanism. In **starfish** oocytes, this nuclear localization to the animal pole happens long before the resumption of meiosis (Miyazaki et al., 2000). In contrast, in **sea cucumber**, the long microtubules nucleated by the centrosome move the nucleus towards the animal pole, shortly after meiosis resumption (Miyazaki et al., 2005). Some studies suggest that centrioles, before elimination, are likely to position the oocyte nucleus in ***D. melanogaster***. Indeed, it has been shown that the (multiple) centrioles grow microtubules, which push the nucleus from a central position until it reaches a lateral one (Zhao et al., 2012).

In ***C. elegans***, the nucleus is also localized to the cortex before NEBD, in a microtubule and Kinesin-1 dependent manner (Fabritius et al., 2011).

In **mouse** oocytes, the mechanism of spindle localization to the plasma membrane is well characterized. Prior to meiotic resumption, the nucleus localizes to the center of the oocyte and only after NEBD and spindle formation, the MI spindle is transported towards the plasma membrane (Verlhac et al., 2000). In mouse oocytes, actin drives spindle transport (*fig. 1.24 B*). Indeed, the oocyte is filled up with an actin network with vesicles at the network's branching points, which act as the organizing centers for this network. On the vesicle surface, actin nucleators (Spire-1 and -2 and Formin-2) and the motor protein

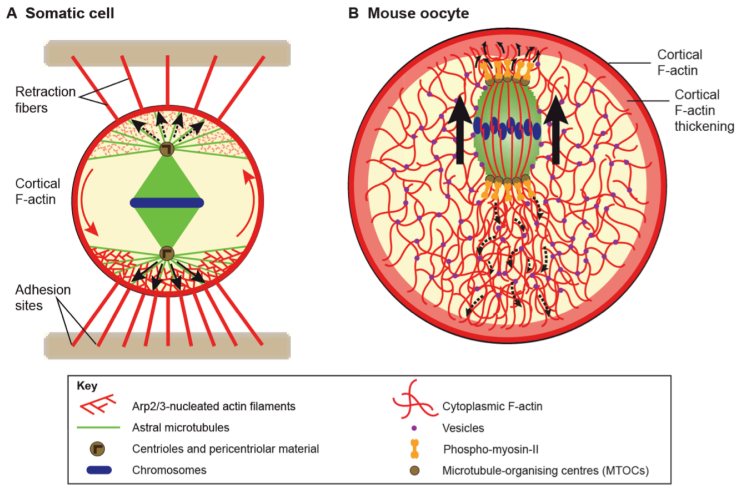

Figure 1.24: Schematic representation of spindle positioning in a mouse oocyte (B) and respective comparison with somatic cell (A). (A) Somatic cell in metaphase of mitosis. Spindle is positioned by astral microtubules. Cortical F-actin anchors astral microtubules to the cortex and increases cell rigidity. (B) Mouse oocyte in metaphase I. A cytoplasmic and highly dynamic actin meshwork drives spindle positioning to the cell cortex. Cytoplasmic meshwork is nucleated from vesicles localizing at its branching points. By localizing at the spindle poles, myosin II likely drives this movement, by pulling on cytoplasmic F-actin (curved black arrows). Figure and legend adapted from (Almonacid et al., 2014).

Myosin-Vb accumulate. Actin is polymerized from these vesicles, and Myosin-Vb generates pulling forces moving these vesicles towards each other. This altogether creates a highly dynamic actin network that serves as a substrate for spindle transport (Almonacid et al., 2014; Azoury et al., 2008; Holubcová et al., 2013; Schuh, 2011). Upon spindle formation, an actin cage forms surrounding the MI spindle, and Myosin-II localizes at spindle poles (*fig. 1.24 B*). The spindle is then transported to the closest cortex on the dynamic cytoplasmic actin network, driven by Myosin-II (Schuh and Ellenberg, 2008). Formin-2 regulation is likely associated with the symmetry-breaking event: before the resumption of meiosis, high levels of Formin-2 keep the nucleus at the center of the oocyte; upon resumption of meiosis, a sudden drop in the levels of Formin-2 changes the actin network organization, and consequently allows off-centering of the spindle (Azoury et al., 2008; Verlhac et al., 2000).

As mentioned earlier, all oocytes position their spindle in close proximity to the plasma membrane before cell division. Moreover, the MI and MII spindle are

orientated perpendicularly to the plasma membrane, a feature that is conserved in all oocytes. For example, in the **worm** *C. elegans,* the MI spindle lies first parallel to the cortex, and then rotates by dynein action, becoming perpendicular to the cortex. Although this rotation is less described in other species, spindles always have a perpendicular orientation before PB extrusion. This perpendicular orientation and the close proximity to the plasma membrane appear to be essential for correct PB extrusion (Fabritius et al., 2011).

ii. Spindle assembly

In a mitotic cell, centrosomes organize the poles of the spindle, nucleating microtubule arrays that capture the chromosomes (*fig. 1.24 A*). In the presence of centrosomes, this centriolar spindle assembly pathway dominates. Nonetheless, chromosomes can also nucleate microtubules, contributing for spindle formation (Walczak and Heald, 2008). In the absence of centrosomes, chromosomes can promote the self-assembly of an acentriolar spindle. This was shown for the first time in *Xenopus* egg extracts: without centrioles, bipolar mitotic spindles are still assembled on sperm chromatin or even around DNA coated beads (Heald et al., 1996). In a simplified way, chromosomal microtubule nucleation depends on a Ran-GTP gradient, which is established around the chromosomes. Ran-GTP then activates several microtubule associated proteins, including TPX2, which recruits the Augmin complex that consequently recruits γTuRC, allowing microtubule nucleation from the chromosomes (Goshima et al., 2008; Gruss et al., 2001; Petry et al., 2013). Other proteins are also involved in the formation of the bipolar spindle: the kinesin Eg5 aligns the nascent microtubules, the motor XKlp1 pushes the microtubule away from the chromosomes, whereas dynein focuses the microtubule ends and contributes for spindle pole formation (Karsenti and Vernos, 2001; Walczak and Heald, 2008).

Acentriolar spindle assembly mechanisms in live oocytes are not as well characterized as in the egg extract. However, in oocytes, acentriolar spindle assembly also occurs from non-centriolar MTOCs, and not only from the chromatin (Dumont and Desai, 2012). Some clarification of these processes arose from the identification of these non-centriolar MTOCs, particularly in ***D. melanogaster,*** **frogs** and **mouse** oocytes.

In **frog** oocytes, a disk-shaped MTOC (referred to as a transient microtubule array) assembles at the base of the nucleus, shortly after NEBD, and then migrates towards the animal pole. This MTOC is likely to collect the chromosomes and function as a precursor of the MI spindle, being subsequently remodeled into a bipolar spindle (Gard, 1992).

In ***D. melanogaster,*** non-centriolar MTOCs appear *de novo* shortly before NEBD, organizing scattered microtubules asters, which then organize into a bipolar spindle. The kinesin Ncd localizes to the initial microtubules asters, and has a central role during MI spindle assembly, by re-shaping these microtubule asters into a bipolar spindle (Megraw and Kaufman, 2000; Sköld et al., 2005).

Again, more data is available in **mouse** oocytes: several studies show the presence of multiple pericentrin and γ-tubulin-containing MTOCs, which form *de novo* shortly before NEBD (*fig. 1.25*) (Calarco, 2000; Carabatsos et al., 2000; Schuh and Ellenberg, 2007). These MTOCs are initially scattered throughout the oocyte, and converge towards each other and to the nuclear region after NEBD, forming a "sphere" of microtubules around the chromosomes (*fig. 1.25 – I to III*). This sphere of microtubules is progressively shaped into a MI bipolar spindle by Kinesin-5 and other molecular motors (*fig. 1.25 – IV to VI*) (Schuh and Ellenberg, 2007).

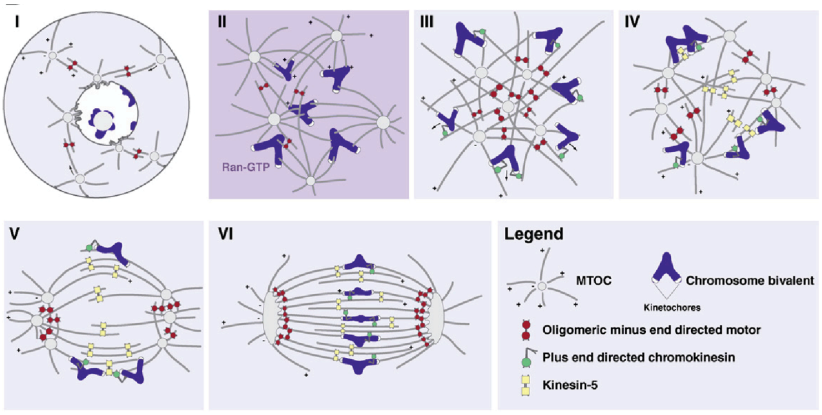

Figure 1.25: Model of acentriolar spindle assembly in mouse oocytes. I-III Acentriolar MTOCs localize first dispersed in the oocyte's cytoplasm. Upon NEBD, a "sphere" of microtubules organize around the chromosomes. IV-V: Acentriolar MTOCs start to cluster and a bipolar spindle is organized (VI), mediated by Kinesin-5. VI: Spindle further elongates. Other molecular motors are likely to be involved. Figure and legend adapted from (Schuh and Ellenberg, 2007).

As mentioned before, microtubule nucleation in frog extracts depends completely on the chromatin generated Ran-GTP gradients. However, in the formation of the MI spindle in **mouse** oocytes, Ran-GTP-dependent nucleation is not essential, yet contributes by accelerating the spindle assembly process (Dumont et al., 2007; Schuh and Ellenberg, 2007). Interestingly, the Ran-pathway is essential for MII spindle assembly, possibly by contributing speeding up the process, which occurs much faster than the MI spindle assembly (Dumont et al., 2007).

In summary, one can consider that acentriolar assembly mechanisms are similar between egg extracts and meiotic oocytes: motor proteins are important for bipolarity, while chromosomes and associated Ran-GTP are a source of microtubule nucleation, yet not the only factor in meiotic oocytes. Even in cells forming acentriolar spindles, MTOCs are present. This suggests that either non-centriolar MTOCs or centrosomes typically accelerate the chromatin-mediated spindle assembly pathway during female meiosis.

1.7. Centriole elimination in starfish oocytes

1.7.1. Overview of starfish meiosis

Starfish oocytes are large cells, with a diameter of 170 μm and when fully grown and arrested in Prophase I, contain a nucleus with 80 μm diameter (*fig. 1.26 A*). The large nucleus localizes closer to the animal pole, defining a clear axial asymmetry in the oocyte. Two pairs of centrosomes localize between the nucleus and the oocyte plasma membrane and actually hold the nucleus at the animal pole by long interphase microtubules (*fig. 1.26 A*) (Miyazaki et al., 2000). Shortly after meiosis resumption, NEBD occurs. Actin has a major role in the early events of meiosis: an actin *shell*, an Arp2/3-dependent structure composed of highly compacted branched actin, transiently accumulates at nuclear envelope and promotes fast fragmentation of the nuclear envelope (*fig. 1.26 B*) (Mori et al., 2014). Shortly after, an actin *meshwork* forms in the nuclear region, which collects the scattered chromosomes across the nucleus (*fig. 1.26 C*). This actin

meshwork is highly dynamic and contracts directionally towards the animal pole. Once the actin network delivers the chromosomes close to the animal pole, they are collected by the centrosomal microtubule asters, which then organize the MI spindle (Lénárt et al., 2005; Mori et al., 2011). The centrosomes organize the spindle (*see* ***section 1.6.3 iii***) and the oocyte undergoes two consecutive meiotic divisions with the extrusion of two PBs.

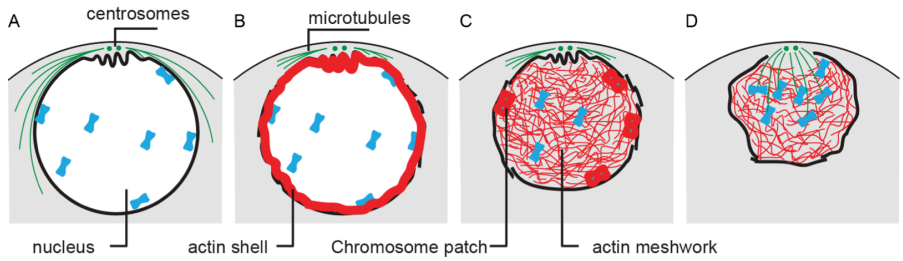

Figure 1.26: NEBD and chromosome congression during starfish meiosis. (A) Oocyte is arrested in Prophase I. (B) After hormone addition, the actin shell transiently accumulates at the nuclear envelope and promotes fast NEBD. (C) Actin meshwork forms inside the nuclear region, actin-rich regions organize around the chromosomes previously localized close to the nuclear envelope. (C) Actin meshwork contracts unidirectionally and chromosomes are transported towards the plasma membrane.

1.7.2. Starfish oocyte as a model to study centriole elimination using molecular markers and live cell imaging

i. Centriole elimination in other model organisms

Centriole elimination is a process characterized by a fast switch from a state including centrioles in the cytoplasm, to another without centrioles. Indeed, no "collapsing" structure has ever been observed. Moreover, it is likely a very fast process (Mikeladze-Dvali et al., 2012), which complicates its observation during the long prophase I, characteristic of all canonical model organisms (frogs, *D. melanogaster*, *C. elegans*, mouse).

Consistently, so far no molecular mechanism has been defined for centriole elimination during female meiosis. For most model systems only the timing of centriole elimination is known, detected by the loss of centriolar proteins and subsequent disappearance of the centriolar structure. With the exception of the helicase CGH-1 in **worms,** no other protein was described to be involved in centriole elimination, and still its role remains unclear.

ii. Centriole elimination in starfish oocytes - what is known so far

Starfish became a model system for meiosis research after the isolation and identification of 1-methyladenine (1-MA) (Kanatani et al., 1969), the hormone responsible for inducing resumption of meiosis, allowing experimentally controlled study of meiotic maturation. Starfish oocytes are a robust system that allows multiple and variable manipulations without affecting the viability of the oocytes. Centriole elimination was first investigated in this system more than two decades ago, because the transparency of the oocyte allowed the visualization of the process by phase-contrast microscopy.

Centriole elimination was initially addressed from the point of parthenogenesis. Unfertilized oocytes rarely undergo parthenogenic development. However, Washitani-Nemoto and colleagues showed that parthenogenesis can be easily triggered in starfish oocytes if PB extrusion is suppressed (Washitani-Nemoto et al., 1994). At the time, a major hypothesis was that the presence of an active centrosome (here merely defined by a large aster visible by transmitted light microscopy) is key for parthenogenesis. A few years later, Saiki and Hamaguchi observed that only the centrioles extruded into the PBs retained a “replicative”, i.e. an aster forming capacity. They proposed for first time that starfish centrioles have an “intrinsic characteristic”, which makes them heterogeneous in their replication capability: the centriole, which remains in the mature egg is “non-replicative”, and as a consequence decays and is eliminated. In contrast, sperm derived centrioles, as well as centrioles derived from re-introduced PBs, are “replicative”, because they maintain their microtubule nucleating activity (Saiki and Hamaguchi, 1998).

Additionally, EM data indicated that at the beginning of meiosis, each centrosome contains a pair of centrioles (Kato et al., 1990). Therefore, out of these four centrioles three would be extruded into the two PBs, and the single centriole remaining in the mature egg would need to be a non-replicative centriole (*fig. 1.27*) (Tamura and Nemoto, 2001). Later, Uetake and colleagues further showed that upon PB suppression, two replicative centrioles remain in the egg, which cannot be eliminated. In fact, they can still duplicate either in parthenogenetic activated eggs or in fertilized eggs (Uetake et al., 2002; Zhang et al., 2004). By further transplantation experiments, it has been shown that these replicative centrioles are already "resistant" to elimination before meiosis resumption (Shirato et al., 2006).

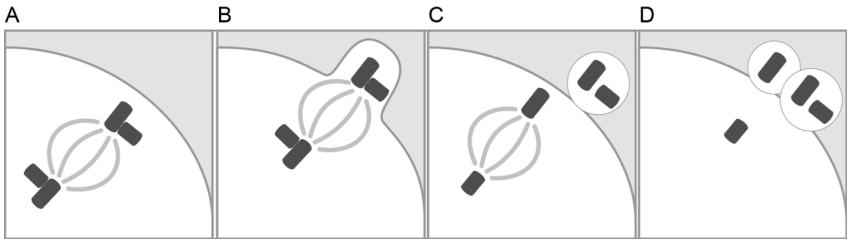

Figure 1.27: Schematic representation of the centriole cycle in a starfish oocyte. (A) Two pairs of centrioles organize the first MI spindle. (B) One pair is extruded into the PBI. (C) A pair remains and single centriole localize at the MII spindle. (D) One centriole is extruded into the PBII. Two replicative centrioles are extruded into the two PBs. The remaining centriole is non-replicative. Note that this cycle was never confirmed with molecular markers for centrioles.

In conclusion, upon starfish oocyte meiosis, earlier studies established that two types of centrioles exist in the oocyte: replicative and non-replicative. The replicative centrioles are extruded into the PBs, whereas a non-replicative centriole remains in the mature egg, where it can be efficiently eliminated in contrast to the replicative centrioles forced to remain in the egg.

iii. Centriole elimination in starfish oocytes – the starting hypothesis

In the above cited literature, a large variety of manipulations were performed, ranging from PB transplantation and PB suppression using either artificially

activated eggs or fertilized oocytes, and even cell fusion between mature and immature oocytes. However, all these experiments were performed using phase-contrast microscopy (Shirato et al., 2006; Tamura and Nemoto, 2001; Uetake et al., 2002; Zhang et al., 2004). Molecular tools available at the time were scarce, and limited to immunostainings for microtubules or γ-tubulin. Additionally, the EM data was relatively limited due to the poor sampling of the large oocyte volume. Thus, altogether the process of centriole elimination was understudied.

The first studies on centriole duplication and the concept of mother and daughter centriole were established around the same time (Lange and Gull, 1995). It was suggested that the “replicative” and “non-replicative” nature of starfish centrioles could be related to the mother vs. daughter difference. However, this hypothesis was never tested.

Therefore, my initial hypothesis was that i) the replicative centrioles correspond to the mother centrioles, and that ii) this difference has a functional role in the process of centriole elimination in starfish oocytes. Namely, the replicative mother centrioles are eliminated so that no centrioles with replicative activity remain in the mature egg.

2. AIMS

"It's the questions we can't answer that teach us the most. They teach us how to think. If you give a man an answer, all he gains is a little fact. But give him a question and he'll look for his own answers."

– Patrick Rothfuss

Common to all metazoa, centrioles need to be eliminated from oocytes before fertilization. However, the mechanism of centriole elimination is still an open and unsolved question. As detailed in the ***Introduction***, it is known for several species when centriole elimination occurs, but how centrioles are eliminated is completely unclear. Part of the problem is technical: centrioles are very small structures in the large oocytes and elimination appears to be a quick process with no obvious intermediate structures of the presumed collapsing centriole ever being identified. Therefore, in samples fixed at specific time points, especially by electron microscopy, it is very difficult to definitively evidence the absence of centrioles.

Quite exceptionally, in starfish oocytes, centriole elimination occurs in the course of meiotic divisions. Furthermore, the laboratory of Peter Lénárt at European Molecular Biology Laboratory (EMBL) has established conditions for high resolution live imaging of oocyte meiosis in this system. This together provided a unique opportunity, and thus I set out to study the mechanism of centriole elimination in starfish oocytes as my PhD project.

The basic characterization of this process in starfish oocytes has already been carried out by Nemoto's laboratory. They have established that centriole number is successively reduced by extrusion into the PBs. They also proposed that "replicative" centrioles are extruded into polar bodies, whereas a single "non-replicative" centriole remains in the mature egg. However, all these studies were based on cellular morphology by transmitted light microscopy of microtubule

asters and EM of cellular ultrastructure. No molecular markers were ever investigated.

Therefore, i) my first aim was to describe the uncharacterized molecular composition of starfish centrioles, and then generate molecular tools to follow the process. Next, ii) I followed how starfish oocytes eliminate centrioles by live imaging, which is a major advantage over most other species in which these stages are only accessible in fixed samples. Specifically, iii) I created markers that allow the distinction between mother and daughter centriole, in order to test whether the mother centrioles are the “replicative” centrioles, and the daughter centrioles are the “non-replicative”. Indeed, I have successfully shown that mother centrioles are the “replicative centrioles. Next, iv) I tested the importance of extruding these mother centrioles and finally v) the mechanisms that led to their extrusions.

Finally, my overall goal is to reveal the mechanism of centriole elimination in starfish oocytes, but use this as an example to gain new insights, and reveal common mechanisms of centriole elimination in other species and of centriole regulation in general.

3. MATERIAL AND METHODS

"I do not know what I may appear to the world; but to myself I seem to have been only like a boy playing on the seashore (...)"

– Sir Isaac Newton

3.1. Identification of homologs of centriolar components in starfish

The Lénárt laboratory in collaboration with the laboratory of Takeo Kishimoto (Tokyo Institute of Technology, Tokyo, Japan) initiated a starfish transcriptome sequencing project. Datasets were generated from mixed tissues using the starfish common in Japan, *Patiria pectinifera* as well as mature eggs of the related species common along the West Coast of the United States, *Patiria miniata*. Overall analysis of these data revealed a high level of similarity between these two species, with intraspecies variation hardly distinguishable from interspecies variability at the amino acid level.

I used this recently available transcriptome to identify homologs of centriolar proteins in starfish. The list of centriole homologs to be identified was selected from two major publications that have established a phylogeny of the most relevant centriolar proteins (Carvalho-Santos et al., 2011; Hodges et al., 2010).

From this list, using BLASTP, I used the human centriole proteins (obtained from http://www.ncbi.nlm.nih.gov/protein), to find sea urchin homologs, the closest related species to starfish with a sequenced genome (http://sugp.caltech.edu/SpBase/wwwblast/blast.php). Subsequently, I used BLASTP again to search for homologs in our *P. miniata* protein database generated from the transcriptome data.

Hits were considered significant homologs when (i) the e-value threshold was below 10^{-20}, and (ii) the reciprocal best hit from reverse blast was the human

protein. Protein domains were further characterized by domain prediction, using SMART (http://smart.embl-heidelberg.de/), or PFAM (http://pfam.xfam.org).

All protein sequences obtained were aligned using the sequence editing program Clone Manager or the online tool Clustal Omega (http://www.ebi.ac.uk/Tools/msa/clustalo/). The phylogenetic tree for Odf2 was generated by Clustal Omega. The alignments for Odf2, Centrin-2, Poc1 and Chibby shown in ***Appendix*** were generated by ESPript (Robert and Gouet, 2014) (http://espript.ibcp.fr/ESPript/ESPript/index.php), using "%Equivalent" for the similarity coloring scheme, which considers amino acids chemical properties.

3.2. Fluorescent markers for live imaging

In order to obtain fluorescent markers for live imaging, I cloned several of the identified homologs. More details will be provided for Odf2, Centrin-2, Poc1, and the recently cloned Chibby, the markers effectively used in this work.

First based on the sequences obtained by transcriptome, forward and reverse primers were designed for the amplification of the full length open reading frame. Then, these primers were used to amplify the full-length cDNA of the sequences of interest by PCR method. For this, a cDNA library, prepared from the total mRNA of mature eggs and embryos, was used. Briefly, this cDNA collection was generated starting with a phenol/chloroform extraction and purification of all cellular RNAs. All polyA-tailed mRNAs were then isolated using a Dynabeads Oligo (dT) kit (Invitrogen). After another step of purification, mRNA was converted to cDNA by reverse transcription, using the GeneRacer kit (Invitrogen).

Odf2, Centrin-2 and Poc1 were obtained by PCR from this cDNA library, whereas Chibby was synthesized by the company Gene Tools. The PCR products were ligated into an intermediary vector, pGEM®-T easy (Promega). A single mEGFP and/or mCherry tag was introduced at the N- and/or C-terminal of the sequences, and ligated in a single step into pGEM-HE plasmid, optimized for *in vitro* transcription.

Briefly, in order to perform *in vitro* transcription, plasmid DNA was first linearized and purified by phenol/chloroform extraction. Purified DNA was then transcribed and *in vitro* 5'end-capped, using the AmpliCap-Max™ T7 High Yield

Message Maker kit (Cellscript). Capped mRNA was then extended with a 3'end-poly(A) tail, using the A-Plus™ Poly(A) Polymerase Tailing Kit (Cellscript). The mRNA was again purified and finally solubilized in 11 µl RNase-free water, with a final concentration of 2-6 µg/µl. The mRNA was then tested by oocyte injection (*see below*), and further diluted if necessary.

All other fluorescent mRNA markers used in this work (including human EB3-mEGFP3 and -mCherry3, starfish CyclinB-mEGFP and PH-mEGFP) were generated in the same way from already existing plasmids in the laboratory. All clonings and mRNA *in vitro* transcription were performed according to (Lénárt et al., 2003).

I also used fluorescently tagged proteins, including H1 from calf thymus (Merck) labeled with Alexa568 or Alexa647 (for DNA labeling), and Cy3- or Cy5-Tubulin (for microtubule labeling). Fluorescently labeled-Tubulin from pig brain was resuspended in BRB80 buffer (400nM PIPES/KOH (pH=6.8), 5mM $MgCl_2$, 1mM EGTA, 40% (v/v) glycerol, 1mM GTP) with 0.05% NP40.

Fluorescently labeled proteins were injected shortly before maturation and live cell imaging, whereas mRNA encoding fluorescent markers were injected the day before to allow protein to express overnight.

3.3. Biological material

3.3.1. Sperm and oocyte collection

Starfish (*P. miniata*) originate from California and were obtained from Southern California Sea Urchin Co. (Corona del Mar, CA), Marinus Scientific LLC (Newport Beach, CA) or Monterey Abalone Company (Monterey, CA). Upon arrival, starfish were maintained at the starfish facility at EMBL in seawater tanks at 16°C.

Oocytes were isolated from the ovaries as described in (Terasaki, 1994). Briefly, pieces of ovaries were obtained from the dorsal side of a female starfish arm through a small hole punctured by a disposable biopsy punch (Miltex). Ovaries were then transferred to calcium-free seawater in order to isolate the oocyte from its surrounding follicle cells. Calcium-free seawater was supplemented with 50 mM phenyl-alanin to prevent spontaneous oocyte

maturation. Ovaries were then transferred to a Petri dish containing fresh filtered seawater, supplemented with acetylcholine (100 μM), to allow ovary contraction and oocyte release. Oocytes were then transferred with a Pasteur pipette to a Petri dish containing fresh filtered seawater, and kept at 14°C for up to two days.

Sperm was obtained by puncturing a small hole on the dorsal side of the arm of a male starfish. Testis were then collected with forceps into an Eppendorf tube and kept “dry” at 4°C.

3.3.2. Fertilization

Starfish fertilization is external, i.e. it occurs naturally in the sea, outside of the parent’s body; thus, embryos are easily obtained by mixing sperm with mature eggs. Nonetheless, to avoid polyspermy, sperm had first to be diluted in fresh filtered seawater (approximately 1:8000), which activates the sperm cells at the same time. Fertilization and embryo development can be followed in the same chambers used for microinjection up to one day, by which time embryos reach the early gastrula stage. Thereafter, the embryos become ciliated and swim away from the injection chambers.

3.4. Oocyte injection

Immature oocytes were mounted into microinjection chambers as described in detail at http://mterasaki.us/panda/injection/. Briefly, the oocytes were mounted between two glass coverslips (one 22 x 22 mm square and a small cut coverslip) held together by double stick tape, referred to as coverslip chamber (*fig. 3.1 A*).

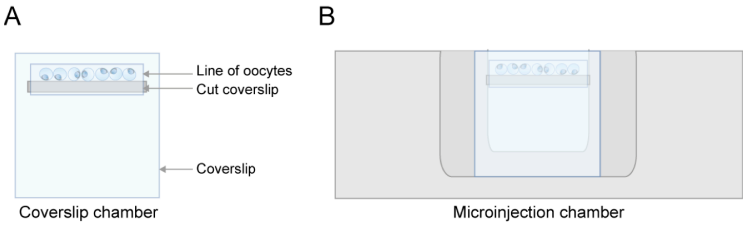

Figure 3.1: (A) Coverslip chamber – where the oocytes are mounted. (B) Coverslip chamber is then mounted in the microinjection chamber – where the oocytes are injected and imaged. See side-view of coverslip chamber in fig. 3.2.

These coverslip chambers were then mounted in a U-shaped chamber and filled up with seawater, forming a microinjection chamber (*fig. 3.1 B*). This chamber keeps the oocytes in place during injection, overnight incubation and subsequent imaging. Moreover, to trigger oocyte maturation, the seawater just has to be exchanged by a 10 µM 1-methyladenine (1-MA) seawater solution.

Microinjection was performed with a CellTram Oil manual injector using mercury-containing needles, as previously described at http://mterasaki.us/panda/injection/. All needles were pulled from Drummond glass capillaries using a Narishige PN-3 Glass Microelectrode Horizontal Needle Pipette Puller.

Prior to injection, mRNAs and proteins were loaded into loading capillaries (Drummond) together with non-reactive silicon oil dimethylpolysiloxane (viscosity: 20 cts, Sigma), as described in http://mterasaki.us/panda/injection/. For each oocyte to be injected, the needle was front-loaded from the loading capillary, with oil, mRNA or protein, and oil. This non-reactive oil prevents mRNA mixing with the seawater and allows the identification of injected oocytes. The mercury localizes at the back (*fig. 3.2*), balances the pressure on the needle and helps controlling the movement of the injected liquid. Only the oocytes with the nucleus facing the top of the chamber (*fig. 3.2*) were injected. During imaging, this side of the chamber faces the objective and therefore imaging conditions are better, as the light has to travel less to the focus, minimizing scattering (*fig. 3.2*).

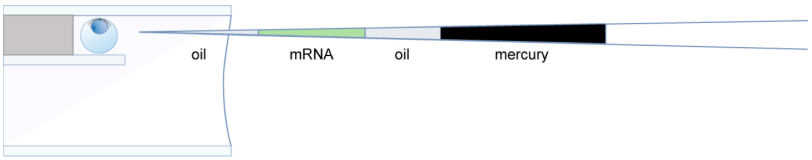

Figure 3.2: Microinjection: needle contains oil – mRNA/protein – oil – mercury. Only the oil and mRNA/protein is injected in the oocyte. Oocyte has a nucleus facing up and it is mounted in the microiniection chamber (side-view).

Fluorescently labeled proteins were injected shortly before maturation and live cell imaging, whereas mRNAs encoding fluorescent markers were injected the day before to allow proteins to be expressed overnight.

3.5. Drug treatment

All the stock solutions were dissolved in DMSO. Before addition, the stock solutions were diluted in seawater and then applied to the oocytes. In order to be able to add drugs at specific time points during meiosis, while continuously imaging, I used a modification of the above described microinjection chamber (*fig. 3.1*). For this, the coverslip chamber was transferred to a small μ-Dish (Ibidi) with a window cut into the plastic bottom of the dish. These dishes are open at the top, which allows direct application of drug solutions, and are single-use, thus avoiding cross-contamination.

I used the following drugs: cytochalasin D (cytoD) (Sigma, stock: 10mM, dilution: 10μM), latrunculin B (latB) (EMD Biosciences, stock: 1mM, dilution: 250nM), taxol (stock: 11μM, dilution: 11nM), Nocodazole (EMD Biosciences, stock: 10 mM, 3.3 μM dilution) and MG-132 (Calbiochem, stock: 50 mM, dilution: 250μM). LatB and cytoD are both actin-depolymerizing drugs, yet they act in a different way: latB sequesters actin monomers, whereas cytoD caps F-actin microfilaments. Both nocodazole and taxol act on microtubules, but have opposite effects: nocodazole depolymerizes microtubules and taxol stabilizes them. MG-132 is a proteasome inhibitor. Each drug has a different time of action: the effect of latB, nocodazole and taxol is visible in less than 2-5 min after drug addition. CytoD and MG-132 take 30 and 45 min, respectively, to act, requiring a longer preincubation of oocytes.

3.6. Confocal microscopy and general image processing

All light microscopy was performed on a SP5II confocal microscope (Leica) equipped with a fast Z-focusing device (SuperZ Galvo stage) and using 40x HCX PL APO 1.10 NA (Leica) water immersion lens.

Starfish oocytes were imaged in 3D and over time at room temperature (20°C). Scan speed was set for 700 or 1000 Hz, using a bidirectional scan and a line average of 3 or 4. Whereas the XY scaling and time resolution are variable

and provided for each figure, I used a Z-step of 1.5 μm for all the experiments, and exceptionally a step of 2 μm for imaging of entire embryos and oocytes. Each stack was taken with 20-25 Z-steps, depending on the orientation of the oocyte. Time resolution depended on the number of stacks and the type of experiment; but an average stack took 30-40 seconds to be acquired. Around 2-5 oocytes were imaged per chamber.

During the fast 3D live imaging acquisition, to track the mother centriole transport, the imaging speed was improved in order to get a good description of such a fast process. In this case, one single oocyte was imaged per chamber, and the number of Z-steps reduced to 10-15. In this case, the imaging was performed with an approximate time resolution of 20 seconds.

3.7. Image analysis and processing

For all data visualization, I used Fiji (http://fiji.sc/Fiji) and Imaris (http://www.bitplane.com/imaris). Fiji is an open source image analysis package, which was used for basic image processing and visualization, while Imaris was used for 3D visualization and 3D tracking.

To reduce shot noise, a Gaussian blur filter (sigma value = 0.8) or Gaussian Blur 3D (X, Y and Z sigma value = 0.8) was applied to all images. Other image processing steps specific for each experiment are described in the appropriate section below.

All processed figures were assembled in Adobe Illustrator. Some panels correspond either to single Z-slices or to maximum intensity projections, or are datasets rendered in 3D by Imaris, which is always noted in the legend. In Imaris, I created a 3D surface model of the oocyte outline using the cytoplasmic background intensities. Note that these models do not represent the real plasma membrane and are just an approximate representation of the cell contour.

Time-lapse panels were generated in Fiji by projecting over time a rectangular ROI, using the “Make montage” function in Fiji.

3.7.1. Validation of mother and general centriole markers

I developed an automatic method to validate our markers and confirm centrosome composition in starfish. In these experiments, oocytes were double injected with Poc1-mCherry as a general centriole marker and Odf2-mEGFP, as a mother centriole specific marker. Oocytes were matured and fertilized, as described above. After 24h, a Z-stack was acquired from a single layer of cells of an early gastrula epithelium (*see schematic representation* ***Results section 4.1.2*** *fig. 4.4 B*).

i. Centriole detection

Centriole detection was performed using the Imaris function "spot detection", in which spots are automatically detected based on their diameter (here 0.3 μm), and intensity threshold. This function also saves the XYZ position of each spot.

Other detection programs were tested as the "Mosaic" plugin (Sbalzarini and Koumoutsakos, 2005) for Fiji. Spots were also detected based on their diameter and intensity (selected radius: 2 pixels, percentile (i.e. which percentage of bright pixels are considered): 0.2%. Different measurements such as spot area and intensity (for each channel), and respective XYZ coordinates were recovered. Imaris was the method chosen for centriole detection (*see below for the comparison between the two methods – fig. 3.4*).

ii. Quantification of overlap between mother and general centriole markers

We implemented a script in R (R Development Core Team, 2009) to automatically quantify the number of Odf2-mEGFP-labeled centrioles ("mother") per pair of Poc1-mCherry-labeled centrioles ("general").

First, spot positions were independently loaded for each channel. To control against any shifts in the images, and to have an initial estimate of the spot colocalization, we plotted all spots in 3D using the "scatterplot3d" package (Ligges and Maechler) for R.

Matches between general-general spots and general-mother spots, i.e. colocalizing spots, were calculated using the Euclidean pairwise distance between all pairs of general and mother spots, and then solving the linear sum assignment problem (Papadimitriou and Steiglitz, 1982) using the “clue” package (Hornik, 2005) – *fig. 3.3*. Mother spots were only assigned to the closest general spots if their distance was less than a fixed threshold based on the cell diameter.

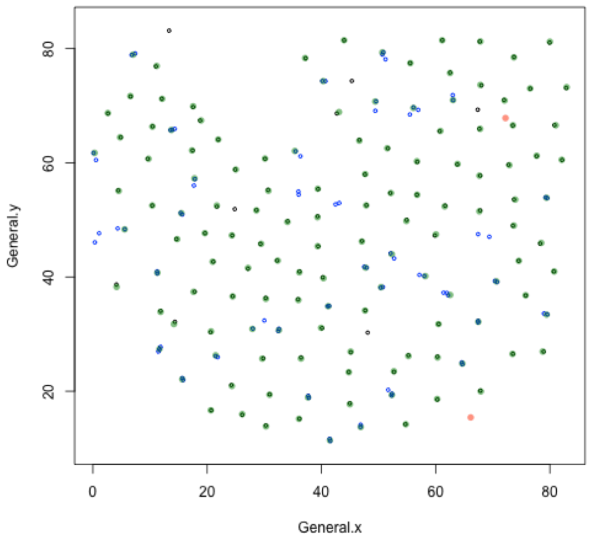

Figure 3.3: Chart for an example case of one embryo, showing colocalizing mother markers (m) and general (g) markers – in green; non-paired mother markers are represented in red; non-paired general markers are shown in blue.

It is important to define a pair of general spots as a single unit (i.e. two centrioles forming a centrosome), to be matched with a single mother spot. If not, one general spot of the pair would be matched with the mother spot, but the other would be categorized as an “unmatched” spot. Hence, we first described the respective pairs of general spots by finding the minimum distances between the pairwise distances. With this information, we calculated the minimum distance between the mother spots and the general spots (paired or not). Thus, the minimum distance directly relates with colocalization of the spots.

All matches were organized in corresponding categories of matched or unmatched pairs, by counting the number of mother (m) spots (one, two or none) colocalizing with the number of general (g) spots (one, two – our biological pairs –, or none): g0m1, g1m0, g1m1, g2m0, g2m1 and g2m2. We tested which

method for centriole detection was more sensitive (*fig. 3.4*). As Imaris was more sensitive in the identification of "g2m1" categories, "centrosome-like" configuration, it was the method selected for further centriole detection.

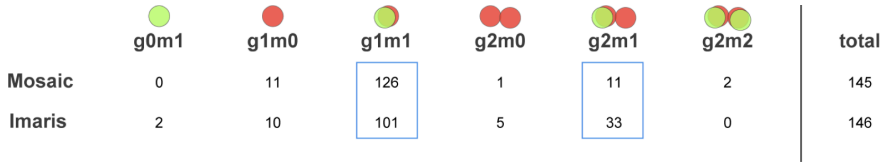

	g0m1	g1m0	g1m1	g2m0	g2m1	g2m2	total
Mosaic	0	11	126	1	11	2	145
Imaris	2	10	101	5	33	0	146

Figure 3.4: Comparison between Mosaic and Imaris for an example case for one embryo. Note that both detect similar total number of pairs. However, Imaris is more sensitive detecting the category g2m1 vs. g1m1 (see blue squares). Therefore, it was the selected method for centriole detection. Categories are indicated (g) represents general, (m) indicates mother, with the respective number of spots found. A schematic representation of the categories is shown: green corresponds to mother, red corresponds to general.

The biological relevance of these categories is discussed in ***Results***. All embryos and their respective centrosomes were categorized, and the total frequency of each category was calculated.

Finally, we considered only the g2 category as biologically relevant and all others results were not considered for the final quantification (*see in* ***Results***).

3.7.2. Quantification of centrioles extruded into polar bodies

To determine the specific mother centriole extrusion during meiosis in starfish oocytes, I double injected oocytes with Odf2-mEGFP (or Chibby-mEGFP), and the spindle markers Poc1-mCherry or Cy3-Tubulin.

i. Vesicle autofluorescence subtraction from the Odf2-mEGFP channel

Data were acquired as a Z-stack and in four different channels: C1-C4. C1 contains the signal corresponding to Odf2-mEGFP matched to mEGFP emission profile, whereas C2 contains a red-shifted detection window to record the auto-fluorescence of cytoplasmic vesicles, taking advantage of the fact that autofluorescence has a much broader emission spectrum than mEGFP (*fig. 3.5*).

In a second scan (using the sequential scan function of the Leica confocal software) C3 contains the signal corresponding to the spindle marker (Poc1-mCherry or Cy3-Tubulin), and C4 records the transmitted light image.

Recording the autofluorescence in a separate channel allowed me to subtract it from the mEGFP channel that contains both the specific signal of Odf2-mEGFP and autofluorescence of the cytoplasmic vesicles (*fig. 3.5*). This improved the images significantly, because it isolates the Odf2-mEGFP signal. Note that the cytoplasmic vesicles are much larger than centrioles and less bright; thus even without background subtraction, centrioles could still be unambiguously identified.

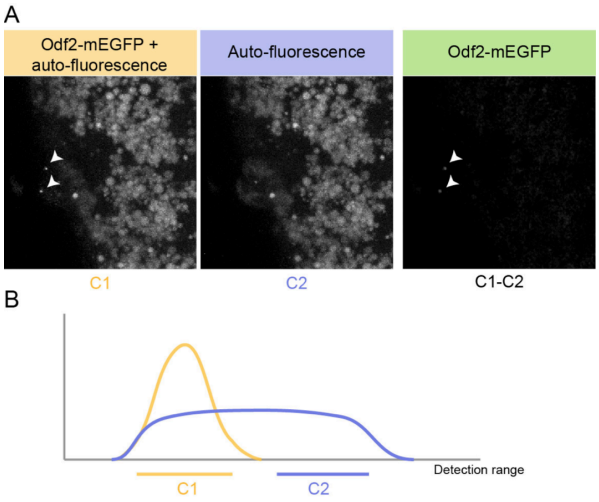

Figure 3.5: Vesicle autofluorescence subtraction from the Odf2-mEGFP channel – schematic representation. (A) Shows the different channels: C1 contains Odf2-mEGFP auto-fluorescence, C2 contains only the auto-fluorescence, C1-C2 shows only the Odf2-mEGFP signal. Arrowheads indicate Odf2-mEGFP signal. (B) Shows a representation of the detection range of the two channels.

I developed a macro in Fiji to automate this autofluorescence subtraction. First, all four channels were separated to individual channels, and C1 and C2 filtered by a “Gaussian blur” (sigma = 0.8). Then, a vesicle was selected using a matching circular ROI. The ROI at the same position was automatically selected in C2. The mean intensity values were obtained for this ROI for each channel, and the ratio between the two calculated. C2 window was then multiplied by this ratio to normalize the fluorescence levels between C1 and C2, followed by

subtraction of C2 intensity levels from C1. This subtraction was applied to all Z-steps of the multidimensional stack.

All panels shown in figures are after subtraction of vesicle auto-fluorescence.

ii. Mother centriole extrusion – quantification

Odf2-mEGFP labeling was sufficient to unambiguously identify single mother centrioles, and it was additionally confirmed by co-localizing with the Poc1-mCherry marker or the spindle pole labeled by Cy3-tubulin.

For quantifying mother centriole localization at the metaphase II spindle, I counted the number of times an Odf2-mEGFP labeled centriole was observed at the MII spindle's outer pole vs. inner pole. For quantifying mother centriole localization at the second polar body (PBII) stage, I counted the number of times Odf2-mEGFP centriole was extruded into PBII vs. the number of times that it remained inside the cytoplasm.

Note that PBI always contains an Odf2-mEGFP- and a non-labeled centriole.

The same quantification was applied to oocytes injected with Chibby-mEGFP.

3.7.3. 3D tracking of centrioles

To follow centriole transport, I developed a method to i) automatically segment out the cell outline based on the cytoplasmic background fluorescence, ii) detect centriole positions over time and in 3D, iii) calculate the minimum distance of centrioles to the plasma membrane over time and in 3D, and finally iv) plot minimum distances over time. Our 3D quantification intends to limit errors associated with different 3D oocyte and spindle orientations, which could affect measurements performed in 2D.

This method was originally developed for Poc1-mEGFP signal, but works equally for EB3-mEGFP with a few changes that will be discussed in the appropriate section.

i. Cell outline segmentation

I developed a Fiji macro to automatically segment the cell outline and turn it into a set of 3D surface coordinates. An initial filtering step was performed using

the in-built plugin “Anisotropic Diffusion 2D” filter (number of iterations: 40, edge threshold height: 2), which efficiently filters out single pixel noise while preserving sharp edges. Next, additional Z slices were added by interpolation resulting in isotropic XYZ resolution. This interpolation “simulates” a plasma membrane closer to a real plasma membrane. This was followed by another filtering step (“3D Gaussian blur”, XYZ sigma=0.8), followed by an automatic thresholding (using Fiji’s “Mean” algorithm) that creates a mask, i.e. a binary 3D image of the cell outline (white: outside of cell, black: inside of the cell). The mask was filtered by the “Analyze particles” function, based on size (size (pixel^2)=5000 to infinity). Finally, cell outlines coordinates were saved using the Fiji function (“Save XY coordinates...”), looping through Z and time to obtain all coordinates in a 4D stack.

ii. Centriole tracking over time and in 3D

The filtered Z stack obtained in Fiji (after “3D Gaussian blur”) was loaded into Imaris to perform centriole tracking, using the automatic “spot detection” function plus the integrated tracking. Again, centrioles were detected based on intensity and size. Spots are then tracked using the “Autoregressive Motion” algorithm. Several parameters can be set, such as the maximum distance (μm) expected and the maximum gap size allowed between time points during the tracking. Tracks were further selected based on their duration.

Spot detection was manually controlled and spots manually edited when automatic spot detection failed. The spots XYZ coordinates were exported to an Excel file.

iii. Minimum distance between centriole and plasma membrane

Using the 3D plasma membrane coordinates and the 3D centriole coordinates (both over time), the final step is to measure the distance between each centriole and the closest point in the plasma membrane (i.e. the minimum distance). For this, a script was written in Matlab (http://www.mathworks.com/products/matlab/). All cell outline XYZ coordinates were loaded into a single table, as well as all centriole coordinates. The minimum distance (in μm) between the two was calculated by searching for the minimum Euclidian distance among any possible

pairs of centriole and cell outline coordinate pairs. This measurement was repeated for each time point.

iv. Plotting minimum distances centriole-cell outline over time

Finally, all minimum distances between centriole and cell outline (plasma membrane) were plotted over time in Excel. In the Y-axis are the values for the minimum distance. “0” represents “plasma membrane”. Thus, distance values near 0, represent closer distances of the centriole to the plasma membrane (*fig. 3.6*). Values larger than 0 represent further distances from the plasma membrane thus deeper into the cytoplasm. The X-axis crosses the Y-axis at its highest values and shows time progression in minutes (min) (*fig. 3.6*).

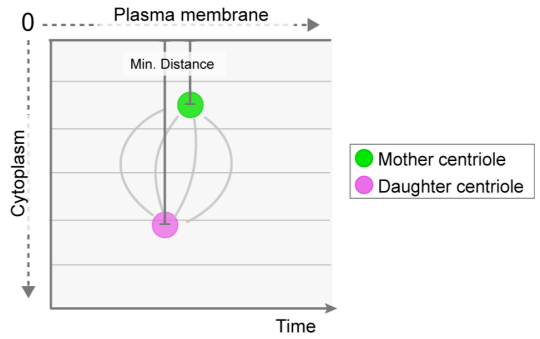

Figure 3.6: Chart shows schematic representation of distance measurements (in 3D) of the centriole to the plasma membrane for a single time point. 0 corresponds to the plasma membrane. The deeper the centriole localizes, the larger the distance to the plasma membrane. The distance measurement over time creates a tracking line.

Note that the filtering methods introduce a small error during membrane segmentation, which is continuously visualized in all analyzed samples and increases the distance measurement to the plasma membrane of ≈1-2 μm.

Calculation of centriole transport velocity

The velocity of mother centriole transport was calculated by fitting a line to the 3D tracks. First, the transport phase was manually defined and plotted in 3D using Matlab. Then, the data was fitted to the data using principal components

analysis, which defined Eigen vectors in the three dimensions. A line was then fitted to the longest vector.

3.7.4. Centrifugation experiments

For centrifugation experiments, the coverslip chamber was placed into a plastic holder in a 50 ml Falcon tube filled with seawater (*fig. 3.7*). The oocytes were centrifuged at 2400 rpm for 1h, at 4°C.

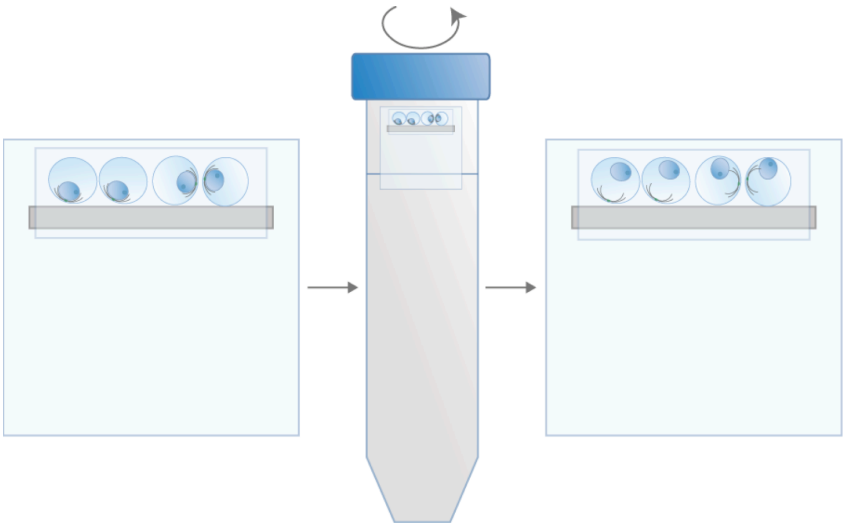

Figure 3.7: Centriole centrifugation: the coverslip chamber is transferred to an adapted falcon tube and then centrifuged. Nucleus is less dense than the cytoplasm and is dislodged from the animal pole. Oocytes have different orientations before centrifugation. Note how this causes variations in the distance nucleus-centrosome, after centrifugation. Centrifugation force, which is constant and applied in the same direction, will create a pool of oocytes in which the nucleus localizes closer or further from the animal pole, depending on the initial orientation of the oocyte.

i. Centriole movement quantification

Similar quantification for centriole movement was performed in centrifuged starfish oocytes. For this, the macro developed for membrane segmentation (*see **section 3.7.3i***) was adjusted to the new imaging parameters. Membrane segmentation was performed for EB3-mCherry and all changes are listed below:

i) “3D Gaussian blur”, XYZ sigma =1, ii) auto-threshold: Triangle, and iii) “Analyze particles”, size (pixel^2)=50000 to infinity, as we are segmenting the entire oocyte.

Membrane segmentation based on EB3-mEGFP signal does not work as well as Poc1-mEGFP, due to a more speckled and less uniform cytoplasmic background. This appears to increase the distance measurement to the plasma membrane of ≈3-5 μm.

ii. Angle quantification

The angle quantification was performed using the “Angle tool” in-built in Fiji. Briefly, prior to NEBD, an angle was created between the nucleus center and the centrosome center, and then measured (*fig. 3.8*). This method assumes that the oocytes are rotationally symmetric (360°, divided in two identical halves of 180° by the axis passing through the nucleus). This method does not discriminate between left and right half, and all angles are measured up to 180°.

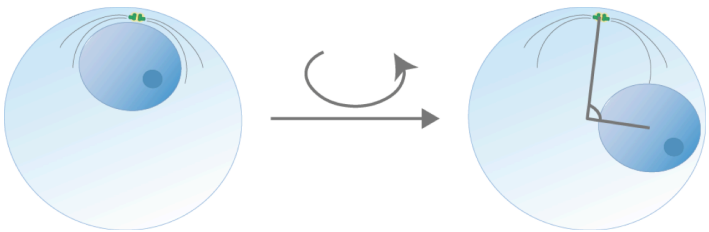

Figure 3.8: Angle quantification after centrifugation. Angle is measured between the center of the nucleus and the centrosome. Note that different angles arise from different oocyte orientation inside the coverslip chamber (see *fig. 3.7*)

3.7.5. MG-132 arrest and quantification

i. MG-132 arrest in metaphase I

In order to optimize the concentration and length of MG-132 treatment, I quantified the kinetics of Cyclin B-mEGFP degradation that was expressed from injected mRNA. MG-132 was added to oocytes together with the maturation hormone 1-MA, or 30 min before. Control oocytes were treated with the same volume of DMSO, added together with the maturation hormone. Control oocytes without DMSO addition were also followed. Imaging of oocytes started around 10

min after addition of 1-MA, and continued for at least 90 min. All control oocytes (both DMSO- and non-DMSO-treated) extruded the two PBs during this time.

Cyclin B-mEGFP intensity quantification

All movies were acquired with the same Z-step of 2.5 μm, for a total thickness of 12.5 μm, containing the middle region of the oocyte. Time resolution varied between 40 s and 1 min depending on the number of oocytes imaged.

Movies were opened in Fiji, and the Z-plane with the largest nucleus diameter was selected. The intensity of Cyclin B-mEGFP was measured over time in a circular ROI at the vegetal pole. No filtering was performed before the intensity measurement. Results were combined in Excel and normalized to the first time point, for each oocyte. Mean curves were calculated in R.

ii. MG-132 arrest in metaphase II

In order to obtain metaphase II-arrested starfish oocytes, oocytes were treated with MG-132, 45-60 min after 1-MA addition. In this case, as MG-132 takes 45 min to act, PBI still extrudes normally (i.e. the metaphase I to anaphase I transition is not blocked). I confirmed that these MG-132 treated oocytes were still arrested in metaphase II 1h45min after 1-MA addition at which time non-treated oocyte would have already extruded PBII. Oocytes were imaged for an additional 30 min before drug treatment, and thereafter for another 30 min (for latB, nocodazole, taxol) or 45 min (cytoD) (*fig. 3.9*).

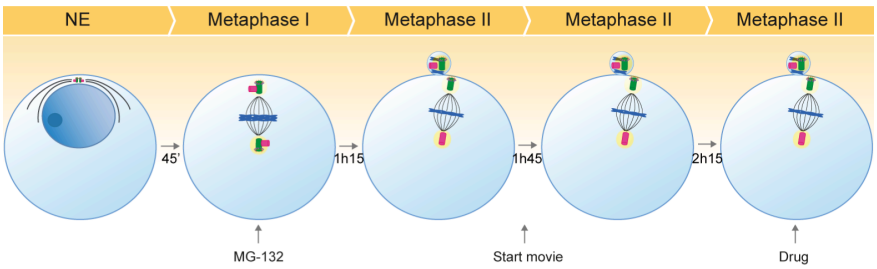

Figure 3.9: MII-arrested oocytes by MG-132. MG-132 is added 45 min after 1-MA maturation and does not affect PBI extrusion. Oocytes are maintained for at least 45 min in an MG-132 induced metaphase II arrest, before drug addition. Oocytes are recorded for 30 min without inhibitory drug, and then 30-45 min under drug treatment.

MG-132 is not a very potent inhibitor, and in a few number of cases, the oocytes exit metaphase. Therefore, all MG-132 treated oocytes, which were not stable in metaphase II before drug addition, were discarded. As no following drug treatment affects metaphase II exit, the same applies: only oocytes still in metaphase II in the end of drug treatment were considered.

3.7.6. Electron microscopy

Two different techniques were employed, differing mainly in i) the immobilization method that was used (high-pressure freezing vs. chemical fixation), and ii) the amount of oocyte that was sectioned (entire oocyte vs. area around the PBI).

i. High-pressure freezing and serial sectioning of the entire oocyte

Sample fixation

Oocytes were injected with Cy3-Tubulin, matured and transferred to cellulose capillaries (Ø 0.2 μm), to facilitate the handling process. Oocytes were then imaged by light microscopy up to the desired meiotic stage (MI and MII). The oocytes were then immobilized by high-pressure freezing (Leica EM PACT 2 with rapid transfer system (Leica Microsystems, Vienna, Austria). Samples were frozen in 20% BSA (in seawater) in the appropriate freezing carriers.

Sample preparation

To prevent ice crystal formation, the water in the cells was exchanged by an organic solvent (1% OsO5, 1%Ua, in aceton), a method referred to as *freeze substitution*, and described previously in (Müller-Reichert et al., 2007). The process was performed in a Leica AFS (Leica Microsystems, Vienna, Austria). Next, samples were gradually infiltrated with Epon/Araldate, followed by resin embedding and polymerization at 60°C for 48h. Once polymerized, samples were sectioned using a Leica EM UC6 microtome and a diamond knife (Diatome) (section thickness: 300 nm). The entire oocyte was serial sectioned, and the

sections were collected on copper slot grids, coated with a FORMVAR film. After sectioning, the samples were post-stained to increase contrast, using 2% uranyl acetate in methanol and 0.4% lead citrate. Finally, fiducial markers were attached to the surface of the sections – in this case gold particles –, which help to reconstruct the tomograms after acquisition.

Sample visualization: scanning for centrioles and tomography

All serial sections were scanned until finding the centrioles, using the electron microscope Zeiss 906.

Some of these sections were used for tomography. Tomograms were acquired with the electron microscope F30 (300 kV TEM, FEI company). Serial tilt images were acquired from -66° to 66° at increment of 1°. The tomograms were then assembled and aligned in IMOD software package (University of Colorado, Boulder), using the fiducial markers.

3D models were performed in the IMOD subprogram 3DMOD.

ii. Chemical fixation and sectioning around the PBI area

Sample fixation

To increase the yield of fixed samples in MII, we matured oocytes and followed them by transmitted light up to PBI. Multiple oocytes were then fixed for 2h at room temperature with 1% glutaraldehyde (Electron Microscopy Sciences) and 2% formaldehyde (Electron Microscopy Sciences) in 0.1 M PHEM buffer (composed of 60 mM PIPES, 25 mM HEPES, 10 mM EGTA and 2 mM $MgCl_2$, pH adjusted to 6.9). The samples were kept at 4°C, overnight, and transferred to cellulose tubes the following day.

Sample preparation

The samples were processed for EM inside the cellulose capillaries, in a PELCO Biowave Pro microwave (Ted Pella, Inc.), which accelerates the processing. The samples were first washed in cacodylate buffer (pH 7.4) and primary post-fixed with 1% OsO_4 (Electron Microscopy Sciences) and 1.5%

$K_4Fe(CN)_6$ (Merck) in 0.1 M cacodylate buffer. Secondary post-fixation was then performed with 1% OsO4 in 0.1M cacodylate buffer. The samples were stained with aqueous UA and gradually dehydrated in increasing concentration of ethanol in water (from 25% up to 100%). The sample was infiltrated with increasing concentration of Epon in ethanol (from 25% to 100%). Oocytes were then mounted in resin molds and left to polymerize for three to four days at 60°C. The resin blocks were finally trimmed using a trimming diamond knife (Diatome) to create a reference surface for future measurements.

X-ray

Before EM image acquisition, we performed Microscopic X-ray computed tomography (microCT) scanning in a Phoenix Nanotom m (GE Sensing & Inspection Technologies GmbH, Germany) operating under Phoenix datosIx 2 and xs control software (GE Sensing & Inspection Technologies GmbH, Germany). Resin-embedded samples were trimmed to a smaller volume (<1 mm^3) and mounted as close as possible to the X-ray source, to obtain a higher resolution upon imaging. The microCT volume was reconstructed using Phoenix datosIx reconstruction software (GE Sensing & Inspection Technologies GmbH, Germany), and the volume was then processed using the VGStudio MAX software (Volume Graphics).

The microCT datasets were then loaded in Amira (FEI company, http://www.fei.com/software/amira-3d-for-life-sciences/), and semi-automatically segmented using the "Labels" module. Then, 3D surface models were generated, which exposed the resin block, the oocyte and more importantly the protruding PBI (*fig. 3.10*). The distance between the PBI and the resin block was then measured in Amira, in order to determine how much material can be trimmed from the resin block until reaching the PBI. Therefore, this X-ray visualization allowed us to create a "distance map" of the PBI and section only the region around the PBI, instead of sectioning throughout the entire oocyte as performed before. Sections of 200nm were cut and collected onto grids for further EM analysis.

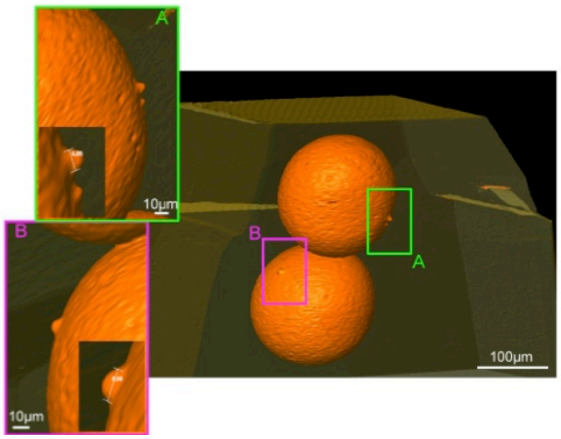

Figure 3.10: MicroCT datasets when loaded in Amira. Oocytes are shown in *orange*, embedded in the resin block (*yellow*). Left panels (A) and (B) show higher magnifications of protruding PBI. Higher magnifications insets of the PBI are equally shown. Matthia Winter-Karreman generated these 3D models.

Sample visualization and tomography

Higher magnification images of the oocytes were acquired using the Biotwin electron microscope (120kV Transmission Electron Microscope, FEI company). Tomograms of the selected 200nm sections were then obtained with F30 (300 kV TEM, FEI company). The tomograms were then assembled and aligned in 3DMOD.

3.7.7. Morpholinos against mother centriole mRNA

Morpholinos are small oligomers that bind target mRNA and block translation, consequently reducing protein levels (Wada et al., 2012). Morpholinos were designed as an antisense sequence for the 5' end of Odf2, Chibby, and CEP164. As control, sense morpholinos were injected (*table 1*).

Each morpholino sequence has a length of 20-30bp and includes the start codon of the target sequence. Each morpholino (synthetized by Gene Tools) was dissolved in water to a final concentration of 1mM.

Table 1: List of morpholinos tested. Antisense sequences are provided, except for the control (sense sequence provided).

Morpholino (antisense)	Sequence 5' – 3'
Odf2	TGGTCATCCTCTACGAGATTTTCCA
CEP164	AGCTGATCTCCCATCATCTTGATAT
Chibby	TGTTACTCGGGAGAAGTGGCATCTT
Control sense	GTTGGTCAATTCAAGATGCCACTTC

i. Experimental details and image acquisition

We performed morpholino depletion in oocytes and embryos. Morpholinos for our target genes were injected into oocytes, which were incubated for a total of three days at 14°C. The day before imaging, oocytes were injected with EB3-mCherry mRNA and re-incubated at the same temperature. These experimental conditions were effective for CEP164 and Odf2, and for Chibby morpholino injection in embryos and oocytes, respectively. Other morpholino concentrations and incubation periods were tested for CEP164 and Odf2 in oocytes.

The oocytes were live imaged during the process of meiosis. Spindle morphology and behavior were recorded using EB3-mEGFP marker.

Embryos were observed at early gastrula stage, 24h after fertilization, using the microscope Zeiss Cellobserver.

ii. Quantification

Oocytes were analyzed and accessed according to the following phenotypes (or lack of): i) spindle anchoring defects and ii) PB extrusion defects. Embryos were accessed according to i) cell division defects, and ii) perturbation in cilia formation.

Acknowledgments:

Kresimir (Kreso) Crnokic (Animal House, EMBL) for taking care of the starfish (and all the other animals from the marine facility).

Kalman Somogyi (Lénárt lab) prepared the starfish cDNA collection (*see* ***section 3.1***). Kalman also cloned Chibby-mEGFP (*see* ***section 3.2***) and tested its localization. Moreover, he performed all morpholino experiments (*see* ***section 3.7.7.***).

Kasia Tarnawksa (Nédelec's group, EMBL) provided the labeled tubulin used in this work (*see* ***section 3.2***).

Konrad Rudolph (Marioni's group, at EMBL/EBI) wrote all the R scripts: i) in the validation of mother and general centriolar markers (*see* ***section 3.7.1 ii***), and for ii) generating the mean curves for the MG-132 cyclinB-expressing oocytes (*see* ***section 3.7.5 i***). Péter Lénárt helped with the Fiji macro to isolate the Odf2-mEGFP signal and the velocity measurements (*see* ***section 3.7.2 I*** *and* ***3.7.3 iv***). Philippe Bun (Lénárt's group) helped with the Fiji macro for cell membrane segmentation (*see section* ***3.7.3 i***). Serge Dimitrieff (Nédelec's group) generated the script in Matlab to calculate the distances between the centriole and the plasma membrane (*see* ***section 3.7.3 iii***).

Together with Julia König (Müller-Reichert's group, at Dresden University of Technology) we immobilized starfish oocytes by high-pressure freezing, which she then processed and thoroughly serial sectioned (*see* ***section 3.7.6 i***). Devrim Acehan (former member of the Electron Microscopy Core Facility, EMBL) helped me acquiring the tomograms for these samples (*see* ***section 3.7.6 i***). Pedro Machado (Electron Microscopy Core Facility, EMBL) helped me with the 3D models generated from the tomograms (*see* ***section 3.7.6 i***). Together with Matthia Winter-Karreman (Schwab's group at EMBL) we fixed the oocytes by chemical fixation. Matthia performed all further processing, X-ray screening, sectioning and tomography of these samples (*see* ***section 3.7.6.ii***).

I would like to thank all for all the great help you provided.

At last, I would like to thank all the actual Lénárt laboratory members, for all the shared equipment and reagents, and a special thanks to Masashi Mori, a former laboratory member, who taught me a lot about starfish oocytes.

4. RESULTS

"The most exciting phrase to hear in science, the one that heralds the most discoveries, is not 'Eureka!' (I found it!) but 'That's funny...'"

— Isaac Asimov

4.1. Establishment of centriole composition and live cell centriolar markers in starfish

4.1.1. Identification of homologs of centriolar proteins

Previous studies have analyzed the ultrastructure of centrioles in starfish, but the molecular composition was not known. The starfish centriole ultrastructure follows the conserved structure of metazoan centrioles with nine triplets of microtubules constituting the centriole's cylinder (Kato et al., 1990). This conserved structure suggests that the centriole's protein composition might also be conserved. To this end, an extensive phylogenetic comparison of centriole structure and molecular composition is already available for a large panel of species (Carvalho-Santos et al., 2010; Hodges et al., 2010). However, these studies did not include information on the molecular composition of starfish centrioles because no genomic or transcriptomic data was available.

Recently, the Lénárt laboratory in collaboration with the laboratory of Prof. Takeo Kishimoto (Tokyo Institute of Technology, Tokyo, Japan) initiated a starfish transcriptome sequencing project for the two starfish species *P. pectinifera* and *P. miniata*. Using these datasets, I identified starfish homologs of centriolar proteins. The identification of the starfish homologs is obviously essential for further molecular analyses of centrosomal processes.

In my search I included centriolar proteins that have been analyzed in the two most comprehensive comparative studies (Carvalho-Santos et al., 2010, 2011; Hodges et al., 2010), as well as the functionally best described centriolar proteins in the literature. Additionally, since our central hypothesis is based on a specific behavior of mother centrioles, I have specifically focused on proteins that localize to the mother centriole-specific appendages.

Strikingly, I was able to successfully identify homologs for all 25 centriolar proteins tested (*fig. 4.1*). First, I identified the homologue of the key component of the microtubule nucleating γTuRC complex, **γ-tubulin** and the key regulator of microtubule growth, the plus tip-localizing **EB1** protein, both of which are widely conserved among eukaryotes (Raynaud-Messina and Merdes, 2007; Tirnauer and Bierer, 2000). I was able to additionally identify all other tubulin-family members in starfish: the components of the microtubule subunits, heterodimer forming **α-** and **β-tubulin**, and also **δ-** and **ε-tubulin** proposed to be involved in the stabilization of the centriolar microtubule triplet (Winey and O'Toole, 2014).

I also identified all the main proteins required for centriole duplication and centriole elongation: **PLK4**, **CEP192**, **CPAP**, **SAS-6** and **STIL**. The same applies

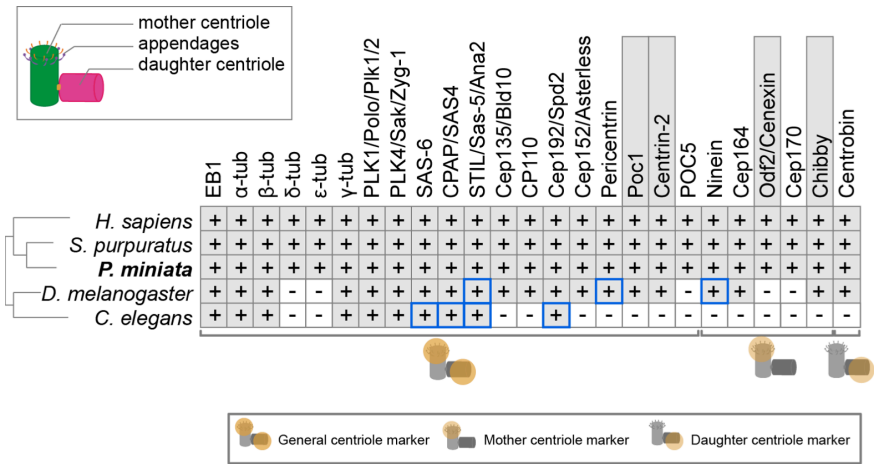

Figure 4.1: Identification of starfish homologs for centriolar markers. The homologs that were successfully identified are indicated by (+). Highly divergent proteins but still considered functional homologs are identified by a blue square. General and mother or daughter specific markers are indicated in the schematic representation at the bottom of the figure. Alternative names for other species are provided.

for the cartwheel stabilizer **CEP135** and the protein **CP110**, which limits centriole growth. The components of the pericentriolar material (PCM) could also be identified (**CEP192, CEP152** and **Pericentrin**), as well as **PLK1**, the mitotic kinase, important for PCM recruitment at mitosis (referred to as centrosome maturation). Additionally, **Poc1** and **Centrin-2** are highly conserved proteins among eukaryotes (Fourrage et al., 2010; Keller et al., 2009; Salisbury, 2007), and I found both to be present in starfish. **Poc1** has important functions in centriole integrity (Venoux et al., 2012) and basal body stability (Pearson et al., 2009). Many studies suggest that **Centrin-2** has a role in centriole duplication, yet its function is not completely understood (Salisbury, 2007). The binding partner of Centrin-2, **hPoc5**, involved in centriole elongation, was also identified.

Furthermore, I also looked for protein homologs specific to the mother and daughter centriole. As mentioned before, the mother centriole has two sets of mother appendages. These include the subdistal appendage proteins **Ninein** and **CEP170**, and the distal appendage components **CEP164. Chibby**, which interacts with CEP164 and localizes to the distal appendages (Burke et al., 2014), was also found in starfish. Additionally, the ubiquitous appendage component **Odf2** was identified. **Centrobin** is a specific daughter centriole marker and also present in starfish oocytes *(see **Introduction** for more information about these proteins).*

Taken together, I was able to unambiguously identify starfish homologs of all tested structural and PCM components in the starfish transcriptome. Comparisons reveal that, consistent with its phylogenetic position, starfish centrioles have a "standard" deuterostome architecture, and therefore similar to **human** (*H. sapiens*) and **sea urchin** (*S. purpuratus*). In contrast, starfish centriole composition is quite distinct from protostome centrioles of the **fruit fly** (*D. melanogaster*) or the **roundworm** (*C. elegans*) (*fig. 4.1*). Notably, although many of the key centriolar proteins and their functions have been first identified in *C. elegans*, it has highly divergent centriolar composition, meaning that its proteins have reduced homology with other centriolar proteins and as a result fail to be detected in comparative studies (*see blue squares in the fig. 4.1*). This highly divergent set of centriole proteins in consistent with the highly divergent centriole ultrastructure also present in this organism (Hodges et al., 2010).

4.1.2. Establishment of centriolar markers

Next I will detail the fluorescent protein centriolar markers that were cloned out of the set of homologs identified above. For each, alignment details and protein domain architecture will be provided. Two types of markers were generated: "general" molecular marker that labels both centrioles of the pair (used as a centriole reference), and also specific mother centriole markers that specifically identify mother centrioles.

Centrin-2 and **Poc1** were tested as general centriolar markers, as both have been broadly used in other species (Fourrage et al., 2010; Keller et al., 2009; Piel et al., 2000; White et al., 2000). Sequence alignments for these proteins show a high similarity between the protein sequences found in starfish and the other organisms analyzed (*see* ***Appendix section 6.3.1 and 6.3.2, respectively***). Moreover, all the characteristic domains, described for these proteins in other species, can be detected. Starfish Centrin-2 contains four Ca^{2+}-binding EF-hands domains (*see fig. 4.2*) and also contains at its C-terminal end the domain KKTSLY, which is characteristic of centriole-associated centrins (*see fig. 4.2, orange domain*) (Salisbury, 2007; Schiebel and Bornens, 1995). Starfish Poc1 contains seven WD40 repeats and the C-terminal coiled-coil which includes the conserved "Poc1" domain (*see fig. 4.2, orange domain*) (Fourrage et al., 2010; Keller et al., 2009) (*see fig. 6.3 and 6.4 in* ***Appendix*** *for protein alignments*).

To generate a mother centriole specific marker I carefully analyzed the literature and selected a short list of potential markers to be initially cloned and tested: **Odf2**, **Chibby**, **EB1** and **ε-Tubulin**. This list was based on i) validation as mother marker in previous studies, ii) sequence length compatible with amplification of the full cDNA sequence. This technical constraint excluded well-described mother centriole markers such as CEP164, CEP170 and Ninein (Chen et al., 2003; Graser et al., 2007; Guarguaglini et al., 2005; Lau et al., 2012; Ou et al., 2002; Wang et al., 2009), which are very large proteins (more than 1500 amino acids) and thus amplification from cDNA is technically more difficult. Odf2 is perhaps the best described mother centriole marker on this list, with multiple papers reporting its role as a mother appendage component (Chang et al., 2013; Ishikawa et al., 2005; Kunimoto et al., 2012; Lange and Gull, 1995; Nakagawa et al., 2001; Schweizer and Hoyer-Fender, 2009; Soung et al., 2006; Tateishi et al.,

2013). Fewer studies report on EB1 and ε-Tubulin as mother centriole markers (Chang et al., 2002; Louie et al., 2004). Chibby was only recently characterized as a mother centriole marker (Burke et al., 2014; Steere et al., 2012) and therefore just recently included in this study. All of these markers were cloned and tested by expression of injected mRNA in starfish oocytes. Out of these, Odf2 and Chibby showed specific fluorescent labeling of the mother centrioles. Since a specific signal could not be detected, EB1 and ε-Tubulin were not further characterized.

Odf2 was first reported in mammalian cells (Brohmann et al., 1997; Lange and Gull, 1995) and although phylogenetic analyses for this protein were never carefully performed, homologs for various species are annotated. However, these described Odf2 homologs are limited to vertebrates (frog, zebrafish, rat, mouse and monkey) and to the hemi-chordate acorn worm (*Saccoglossus*). Odf2 homologs were not previously reported in other phylogenetic groups. Indeed, my analysis identified Odf2 the first time in echinoderms, namely in starfish and the

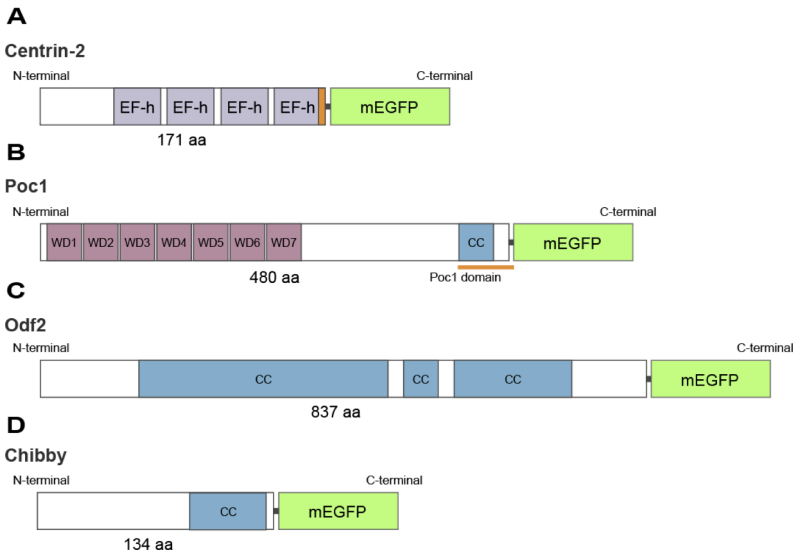

Figure 4.2: Construct design for cloned proteins. All mEGP were placed at the C-terminus of the protein. For each protein, the respective number of amino acids and characteristic domains are indicated. (A) Starfish Centrin-2: EF-h indicates EF-hands domains. In orange, a specific domain identified in centrins associated with centrioles. (B) Starfish Poc1: WD1–7 indicates the seven WD40 domains. The Poc1 domain (orange) can also be identified at the C-terminal end of the protein. CC indicates coiled-coil domains present in Poc1, Odf2 and Chibby.

close-related species sea urchin. The Odf2 protein does not have any characteristic domains, and SMART domain prediction only identifies coiled-coil domains (*see fig. 4.2*). Still, multiple protein alignments show several regions with high degrees of conservation between the multiple species (*see* ***Appendix section 6.3.3*** *for multiple protein alignment and phylogenetic tree*).

Chibby was already characterized phylogenetically and was shown to be very well conserved across species (Enjolras et al., 2012). However, in this previous study Chibby was not identified in starfish or sea urchin. Characteristically, Chibby has a conserved coiled-coil domain at the C-terminus of the protein, which is also present in starfish Chibby (*see* ***Appendix section 6.3.4***).

4.1.3. Live cell centriolar markers are functional

To confirm the utility of these markers in live cells, I expressed mEGFP or mCherry fusions of these proteins in starfish embryos. All four markers were expressed from injected mRNAs, with a wide range of tolerable expression showing no apparent phenotype during oocyte meiosis and early embryonic development.

It is well established that the mother centriole localizes at the base of the cilium, and acts as a platform for cilium growth (Kobayashi and Dynlacht, 2011; Reiter et al., 2012). As starfish embryos develop a ciliated epithelium at the gastrula stage (*fig. 4.4 A and B*), I could show that Centrin-2-mCherry and Poc1-mCherry localize to both centrioles of the pair (*fig. 4.3 for Centrin-2 and 4.4 for Poc1*), while Odf2-mEGFP only localizes to the mother centriole at the base of the cilium, which is labeled with Cy5-Tubulin (*fig. 4.3*).

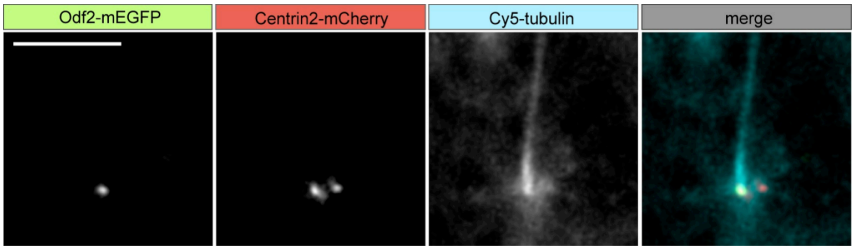

Figure 4.3: Odf2-mEGFP localizes at the base of the cilium of a starfish gastrula. Centrin-2-mCherry labels both centrioles. Cy5-Tubulin labels cilium. Scale: 10μm. Pannels show a Z-projection of the acquired stacks.

Using Odf2-mEGFP and Poc1-mCherry, I wanted to confirm that for each pair of Poc1-labeled centrioles only a single centriole is labeled by Odf2-mEGFP. This is in accordance with the described configuration of a centrosome, composed by a mother and a daughter centrioles. We developed an algorithm for automatically accessing the predominant centriole pair configuration in embryonic cells (*see* ***Material and Methods 3.7.1.*** *for more information*) (*see fig.4.4*).

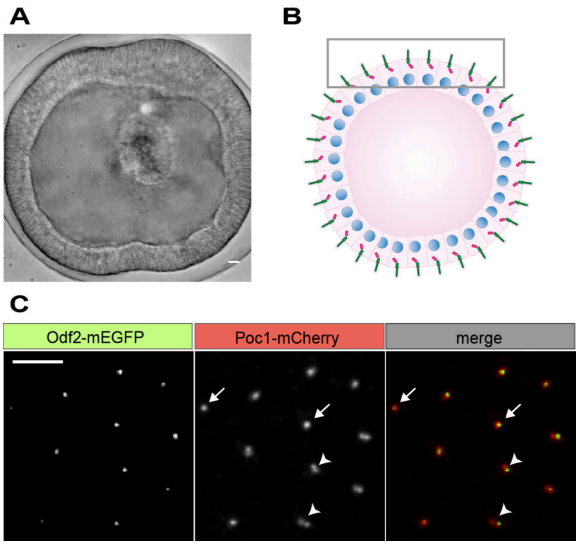

Figure 4.4: (A) Starfish gastrula has a ciliated epithelia (transmitted light). (B) Schematic representation of a ciliated gastrula. The square indicates the section of the epithelium that was imaged. (C) Informative example of one of the regions imaged, and further quantified. Note Odf2-mEGFP labelling is restricted to a single centriole of the pair. Poc1-mCherry labels both centrioles of the pair – "g2" category (arrowheads). Note that not always a pair of Poc1-labelled centrioles can be identified, due to resolution limit constrains (arrows). This corresponds to the "g1" (*see text*). Scale bar: 10 μm. Pannels show a Z-projection of the acquired stacks.

The detection step allows the identification of pairs of centrioles labeled with Poc1-mCherry ("general") and matches them to a respective mother centriole Odf2-mEGFP ("mother"). Different categories are accounted for, considering all possibilities general (g) spots (one, two or none) that may colocalize with mother (m) spots (one, two or none): g0m1, g1m0, g1m1, g2m0, g2m1 and g2m2 (*see fig. 4.5*).

A total of 3866 categorized pairs were obtained from 28 different embryos as shown below (*for the summary table see* ***Appendix section 6.2***):

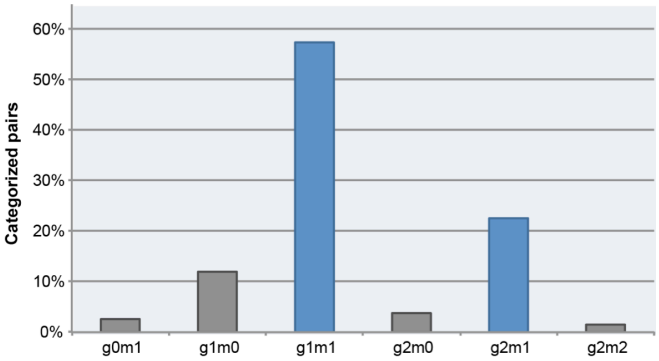

Figure 4.5: Different categorized pairs of general (“g”) and mother (“m”) centrioles. In blue are the categories with the expected labeling pattern (g1m1 and g2m1) – see text for more details. 3866 pairs were categorized, for a total of 28 embryos.

The expected pattern is a centrosome formed by two centrioles (“g2”), one of which is a mother (“m1”) (g2m1) (*see fig. 4.5, blue*), which corresponds to 23% of the pairs analyzed. The largest category (57%) is g1m1 (one “g” spot colabeled with one “m”) - *see fig. 4.5, blue*. The large percentage of g1m1 category can be explained by the small size of the centrioles, close to the defraction limit of the light microscope. These cases correspond to a pair of “g” centrioles that are in such a 3D orientation, they cannot be resolved into two spots, making them appear as a single unit.

Besides these main categories, there are minor deviations from the expected configurations (20%) due to the inability to detect the weak Odf2-mEGFP signal or incorrect assignment of centriole pairs, e.g. at cell boundaries. Thus, in total my automated method confirms for a vast majority of centriole pairs with the expected labeling pattern (g2m1 and g1m1) – 80%.

If one considers only the category in which centriole pairs can be identified (g2) (1080 pairs), 81% of these (874 pairs) correspond to the expected centrosome configuration, with each of the two centrioles of the pair labeled with Poc1-mCherry, and the single mother centriole is labeled with Odf2-mEGFP (*fig. 4.6*).

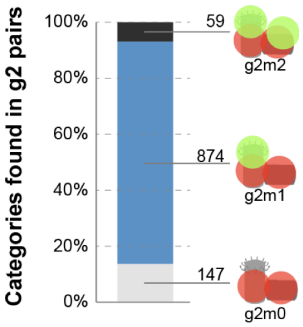

Figure 4.6: The majority of centriole pairs (g2) have a single Odf2-mEGFP labeled centriole (m1), in blue. 874 pairs with the configuration g2m1, out of 1080 g2 pairs were identified.

Taken together, by homology searches in a de-novo assembled transcriptomic dataset, I was able to identify homologs of all major centriole components in starfish, a species previously completely uncharacterized in this regard. Using fluorescent fusions of these proteins, I was further able to establish live cell markers that allow reliable detection of single centrioles, and more importantly to distinguish their maturation state (i.e. mother and daughter centrioles).

4.2. Starfish meiotic spindles are centriolar

4.2.1. Establishing live cell imaging conditions

Several previous studies used electron microscopy (EM), transmitted light microscopy and antibody-immunolabeling (Shirato et al., 2006; Tamura and Nemoto, 2001; Uetake et al., 2002; Zhang et al., 2004) to study centriole elimination in starfish meiosis. However, a major shortcoming of these techniques is the inability to follow the fate of centrioles over time. In particular, disappearance of structures are very difficult to clearly evidence by analyzing cells fixed at specific time points. This is especially problematic for centrioles, which are small structures of only a couple of hundred nanometers in an oocyte with almost 200 micrometer in diameter. Therefore, our major goal was to establish markers and imaging conditions to perform experiments in live cells.

In the previous section, I described the successful identification and establishment of centriole specific markers in starfish. The next step was to establish the appropriate imaging conditions that allow time lapse imaging of the entire process of centriole elimination during oocyte meiosis. In order to do so, I first used two markers that were previously established in the laboratory: EB3-mEGFP3 and fluorescently labeled Histone1 protein (H1), markers for the microtubule plus-end and chromatin, respectively. The combination of these two markers allowed me to optimize imaging conditions, because they label fine structures (e.g. the microtubule tips are very similar in size to centrioles), and at the same time allowed the monitoring of the successful completion of meiosis. Specifically, typical signs of phototoxicity are chromatin bridges visible at anaphase and visible by the H1 marker, and failed cytokinesis that will lead to the formation of multipolar spindles visualized by EB3.

I could find conditions that allow imaging of these two markers in 3D with approximately 30 seconds time resolution throughout meiosis without causing any adverse effects. These imaging conditions did not perturb the timing of the major meiotic events. After 1-MA hormone addition, nuclear envelope breakdown (NEBD) occurs between 20-30 min, the first polar body (PBI) is extruded between 1h15-1h30 after 1-MA addition and the second polar body (PBII) is formed between 1h30-1h45. Finally, meiosis is completed 2h after hormone addition, with the formation of the female pronucleus (*fig.4.7*).

My recordings are fully consistent with previously published observations in fixed samples (Shirato et al., 2006; Uetake et al., 2002): at prophase I, two microtubule asters (from which the EB3 comet tails emerge) are observed, localizing between the plasma membrane and the nucleus. Upon NEBD, the chromosomes are collected to the animal pole, where the first meiotic spindle (MI) assembles (*fig. 4.7 A-B*). During metaphase I, the spindle organizes first parallel to the membrane and then rotates, assuming a perpendicular orientation to the membrane before PB extrusion (*fig. 4.7 C-E*). In fact, this rotation was not previously described in starfish oocytes, but it is consistent with observations made in oocytes of several other species, which also rotate their spindle before PB extrusion (Fabritius et al., 2011).

After PBI extrusion (*fig. 4.7 F-G*), I could visualize for the first time that the second meiotic spindle (MII) assembles with no intermediate parallel orientation.

The MII spindle forms and grows directly perpendicular to the plasma membrane (*fig. 4.7 G-H*). I observed how a massive contraction wave, which moves the entire oocyte, precedes each PB extrusion. Indeed, this contraction wave gives the first indication of PB extrusion, and will be used as a reference for PB extrusion in the following experiments.

Once PBII is extruded (*fig. 4.7 I-J*), a single remaining focal point of EB3 comets remains, which most likely correspond to the remaining centriole. This microtubule focus disappears shortly after pronucleus formation at the end of meiosis (*fig. 4.7 K-L*).

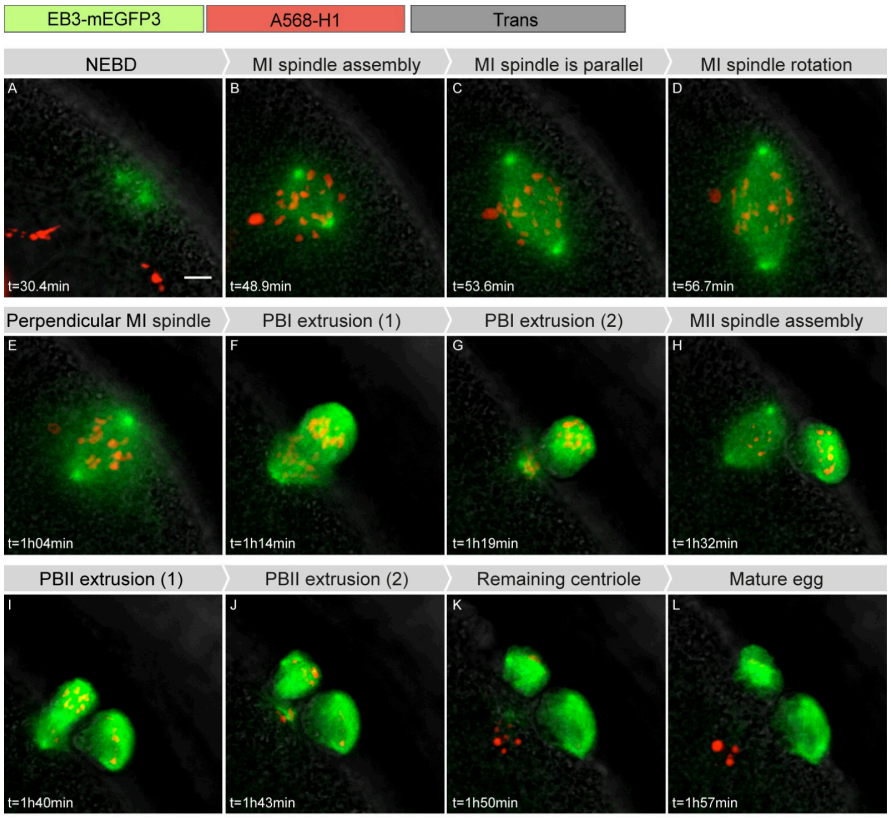

Figure 4.7: Starfish oocyte meiosis observed live. Movie starts 30 min after 1-methyladenine (1-MA) hormone addition. (A-L) show events that are specified in the text. Z-stacks recorded every 30 seconds. Pannels show a Z-projection of the acquired stacks. Scale bar: 10 μm.

In conclusion, I was able to establish conditions to reproducibly image starfish oocytes meiosis in 3D and over time. The selected imaging conditions do not affect the meiotic process, as oocytes undergo meiotic divisions with unaffected

timing, resulting in fully matured eggs that can be fertilized and develop into viable embryos. PB extrusion is preceded by a contraction wave, which causes a substantial movement of the oocyte. My imaging conditions also account for this, which guarantees that at all times the entire spindle is imaged.

Importantly, the live data recapitulate all steps of spindle assembly previously described during starfish meiosis. In addition, it reveals all the delicate details and processes that have remained uncharacterized previously. Accordingly, my live cell data shows for the first time how the MI spindle assembles parallel to the plasma membrane and then rotates to assume a perpendicular position to the cortex before PB extrusion. This clearly differs from the immediate perpendicular orientation of the MII spindle assembly, which I could also show for the first time. Additionally, using EB3-mEGFP3 as a marker, this assay will allow quantification of microtubule dynamics during spindle assembly in future studies.

4.2.2. Live imaging with general centriole markers

Although providing a good overview of microtubule dynamics and spindle assembly and disassembly during meiosis, EB3-3mEGFP3 imaging does not allow to directly investigate the presence of centrioles. EB3 foci are indicative of the presence of centrioles, but could also represent acentriolar microtubule organizing centers (MTOCs) that are seen in mouse oocytes, for example. Therefore, I used the above established imaging conditions and the centriole markers I described in ***4.1*****,** to follow the fate of individual centrioles throughout the meiotic divisions. First, I co-injected both general centriole markers Poc1-mCherry and Centrin2-mEGFP and confirmed that both markers are able to efficiently label the four individual centrioles in starfish oocytes (*fig. 4.8*).

While Centrin2-mEGFP labeling is restricted to the centrioles, Poc1 additionally labels microtubules (*fig.4.8 and 4.9*). This turned out to be an advantage, because this co-labeling of microtubules facilitates the identification of centrioles in the oocyte. Additionally, Centrin-2 often formed additional fluorescent aggregates, also described in other species that were difficult to unambiguously distinguish from the centrioles (*fig.4.8*). Therefore, fluorescently tagged Poc1 was then the preferred centriole marker used in further experiments.

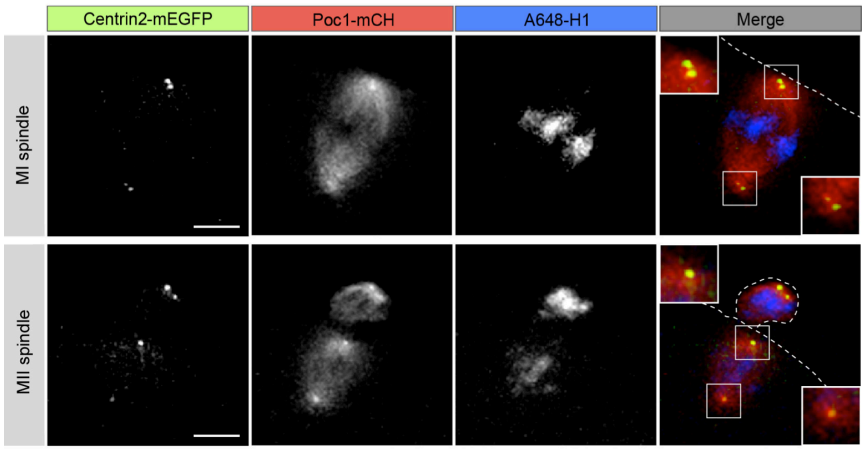

Figure 4.8: Two pairs of centrioles localize at the MI spindle, whereas single centrioles localize at the poles of the MII spindle. Dashed white line shows the outline of the oocyte. Insets show a higher magnification of centrioles. Pannels show a Z-projection of the acquired stacks. Scale bar: 10 μm.

Using these markers, I could determine centriole number at any given meiotic phase, which has not yet been shown in any previous studies of starfish oocytes. Thus, I could observe in a live oocyte that the poles of the MI spindle are organized in a similar manner to somatic cells with one pair of centrioles at each spindle pole (*fig. 4.8 and 4.9, A and B*). Upon PBI extrusion, the pair of centrioles proximal to the cortex is extruded with half of the chromosomes (*fig. 4.8 and 4.9, E*), whereas the other pair remains in the oocyte (*fig. 4.8 and 4.9, C and D*). At the end of MI, as no centriole duplication occurs between MI and MII, this pair splits and the single centrioles form the poles of the MII spindle (*fig. 4.8 and 4.9, F and G*). This configuration is very different from the MI spindle and mitotic spindles. At PBII extrusion, one centriole is extruded into the PBII (*fig. 4.9, K*), and a single centriole remains in the cytoplasm of the mature egg (*fig. 4.9 J*).

Taken together, I could establish live cell imaging conditions to follow centrioles in starfish meiosis over 2 hours in 3D at 30 second time resolution without perturbing the process. Furthermore, using fluorescent centriolar protein markers, I could follow meiosis in live oocytes at a resolution that allowed me to unequivocally identify at all times all single centrioles present at that specific

stage. Consistent with previous electron EM studies, these observations show that in starfish oocytes the MI spindle is organized by a pair of centrioles at each pole, while the MII spindle has an unusual configuration with one single centriole at each pole. Consequently, in meiosis 3 out of 4 centrioles are extruded into the PBs, and only a single centriole remains in the mature egg.

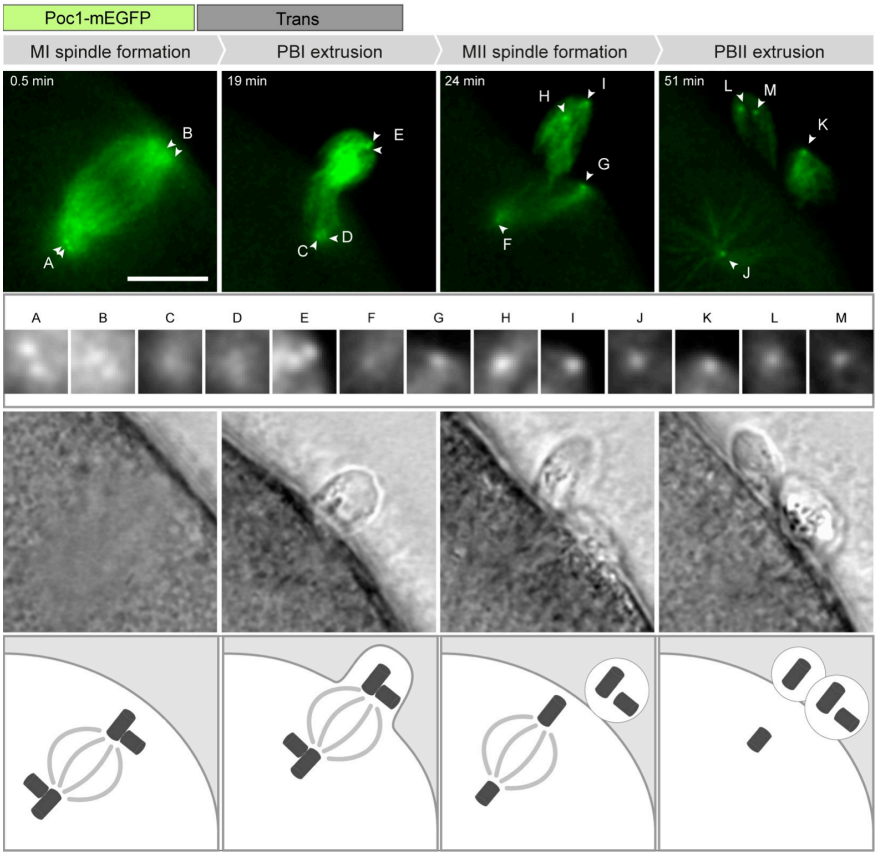

Figure 4.9: Poc1-mEGFP labels centrioles and the microtubules of the spindle. Arrowheads point at centrioles. Insets (A-M) show magnified centrioles for each time point. Movie starts 1h after 1-MA hormone addition. Z-stacks recorded every 30 seconds. Pannels show a Z-projection of the acquired stacks. Scale bar: 10 μm. A schematic representation of the centrioles organizing the meiotic spindles is shown.

4.3. Mother centrioles are extruded into the polar bodies

4.3.1. Each centrosome consists of a mother and a daughter centriole

The above described tools and assays allowed me for the first time to label starfish centrioles with fluorescent markers and follow them live. Indeed, I could visualize single centrioles and show that starfish oocytes have two centrosomes, each of which is composed of a pair of centrioles at meiotic onset. It is well established in the literature that the centrosome is composed of one mother and one daughter centriole. However, until now no definitive data on centriole maturation state was available in starfish oocytes.

To test if the normal configuration of the centrosome is observed in starfish oocytes, I co-expressed one general (Poc1-mCherry or Cy3-Tubulin) and one mother centriole specific (Odf2-mEGFP) marker in oocytes. I could visualize that during metaphase I, a single Odf2-mEGFP-labelled mother centriole localizes at each MI spindle pole, as expected (*Fig. 4.10*). Consequently, one Odf2-mEGFP labeled centriole is extruded into PBI along with one non-Odf2-mEGFP labeled centriole (*Fig. 4.10*). The pair that remains in the oocyte then separates, and the single centrioles organize the MII spindle. This is consistent with the data I obtained using only a general marker (as described in the previous section). However, using the specific Odf2-mEGFP-mother-labelling I observe clearly that the two spindle poles at MII are different in regard of centriole age, one containing mother centriole and the other the daughter (*Fig. 4.10*).

It has to be noted that the mother markers used here cannot distinguish between the “older” mother centriole, i.e. the “grandmother”, and the “new” mother, and I will therefore consider that both poles of the MI spindle are equivalent. It is important to mention that the intensity of Odf2-mEGFP labeling is sometimes variable between the two mother centrioles, with one more intensely labeled than the other. However, this difference is likely to result from optical

effects, i.e. centrioles deeper in the cytoplasm appear dimmer due to light scattering.

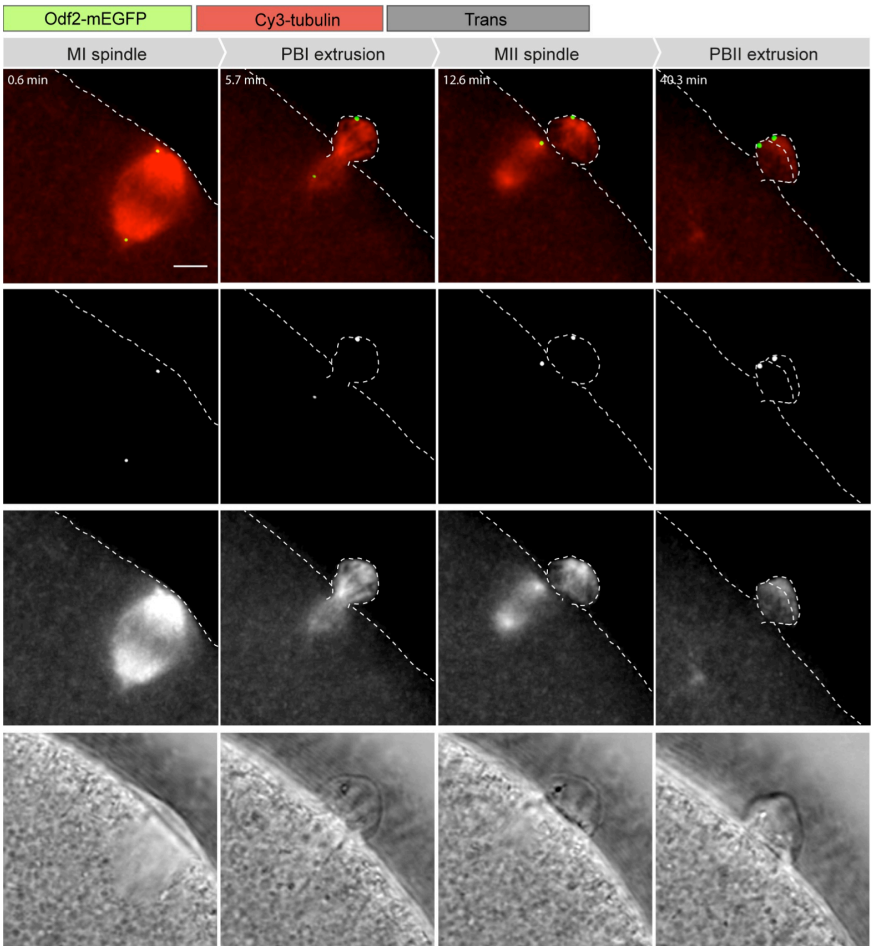

Figure 4.10: Each starfish centrosome has one mother centriole. Movie starts 1h15 after 1-MA hormone addition. Z-stacks recorded every 38 seconds. Pannels show a Z-projection of the acquired stacks. Scale bar: 5 μm. Dashed white line indicates the outline of the oocyte.

4.3.2. The mother centriole is specifically extruded into the second polar body

Intriguingly, I observed in all cases that the single Odf2-mEGFP-labeled mother centriole localizes at the MII spindle pole facing the plasma membrane, the outer pole, whereas the daughter centriole localizes at the pole towards the cell interior, the inner pole (n=17/17) (*fig. 4.11 B*). The 3D data can be difficult to visualize and interpret in 2D, therefore 3D visualization (using the software Imaris) was used to confirm all orientations ((*fig. 4.11 A and B*)

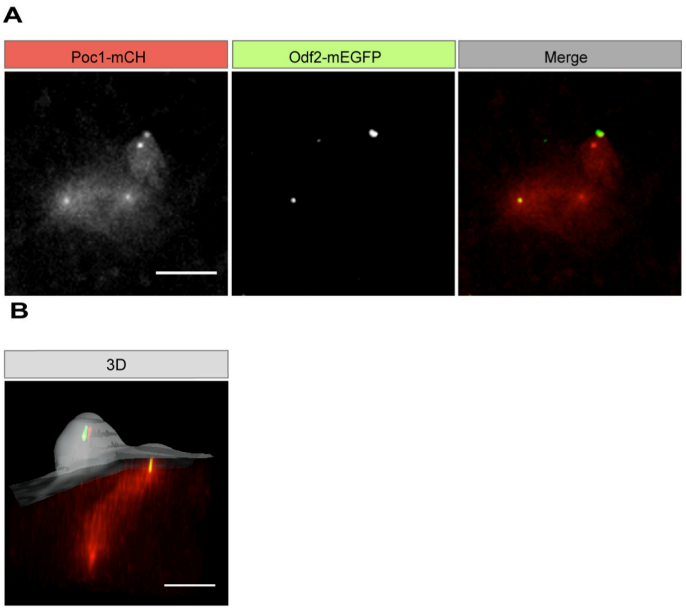

Figure 4.11: The mother centriole always localizes to the outer pole of the MII spindle. (A) Z-projection, generated in Fiji. Scale bar: 10 μm. (B) 3D visualization of the same image, using Imaris. Note how the mother centriole clearly localizes to the outer pole in (B). The oocyte's contour is shown in grey. Scale bar: 5 μm.

As a consequence of its localization to the outer spindle pole, the mother centriole is extruded into the PBII (*fig. 4.10*). To test whether this is a specific mechanism to mother centriole, I expressed the mother marker Odf2-mEGFP together either with a general marker Poc1-mCherry or Cy3-tubulin, and counted how often the mother centriole is extruded into the PBII, in a large number of oocytes (*fig. 4.12*).

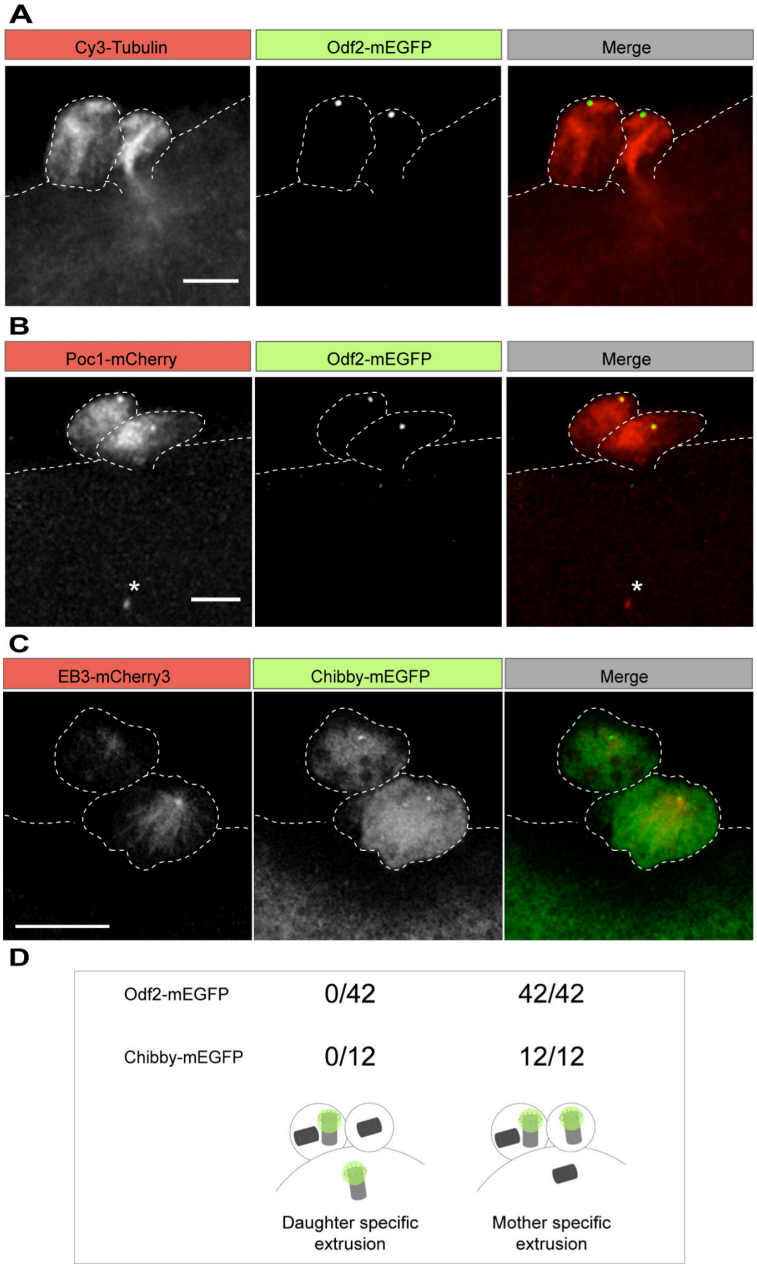

Figure 4.12. Mother centriole is always extruded into the PBs. (A) and (B) show an example of a double injection with the mother centriole marker Odf2-mEGFP and either Poc1-mCherry or Cy3-Tubulin. (*) Indicates the remaining daughter centriole. (C) shows an example of a double injection with the mother centriole marker Chibby-mEGFP and EB3-mCherry3. All pannels show a Z-projection of the acquired stacks. Scale bar: 10 μm. (D) shows the number of cases observed for configuration (depicted below) of extrusion of mother centriole marker.

Strikingly, in all oocytes imaged (n=42), I found the Odf2-mEGFP labeled mother centriole in the PBII, whereas the Odf2-mEGFP negative daughter centriole always remained in the mature egg (*fig. 4.12 A, B and D*). Hence, these observations clearly show that in MII, the mother centriole is specifically extruded into the PBII.

To confirm this pattern with another mother centriole marker, I tested Chibby-mEGFP, recently described as a protein localizing to the distal mother appendages (Burke et al., 2014). Localization of Chibby-mEGFP follows exactly the same pattern as Odf2-mEGFP: one single centriole labeled per centriole pair at MI, an asymmetric localization to the outer MII spindle pole (*see* ***Appendix section 6.4***), and the resulting extrusion of the Chibby-mEGFP-labeled mother centriole into PBII (n=12/12) (*fig. 4.12 C and D*).

Taken together, I validated both Chibby- and Odf2-mEGFP as mother centriole markers, by which I was able to characterize centrosome composition and maturation state of centrioles in starfish oocytes. Most importantly, by following centrioles in live oocytes throughout the meiotic divisions, I could show that at MII, the spindle always orients with the mother centriole facing the cortex, and consequently the mother centriole is extruded into the PBII (*fig. 4.10, 4.11 and 4.12, see schematic representation in fig. 4.13*).

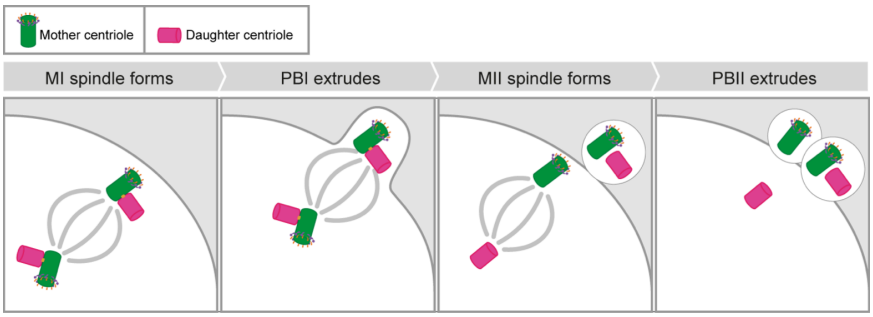

Figure 4.13. Mother centrioles are always extruded into the PBs. One pair of centrioles (each with one mother and one daughter) organizes the MI spindle. During MII, the mother centriole localizes to the outer spindle pole and is consequently extruded into the PBII. A single daughter centriole remains in the mature egg.

Therefore, a clear asymmetry is established between the extruded and retained centrioles: the two mother centrioles are extruded into the PBs, whereas the single daughter centriole remains in the mature egg (*fig. 4.13*). The fact that I have observed this pattern in all oocytes imaged without exception (n>60) indicates that this is a tightly controlled process.

4.4. Extrusion of the mother centrioles is essential for centriole inactivation

4.4.1. The single daughter centriole remaining in the egg does not contribute to the zygotic spindle

It is a pattern general to metazoa that the zygotic spindle is organized by the centrioles provided by the sperm, while the female centrioles are inactivated before the formation of the zygotic spindle. Specifically, starfish oocytes can be fertilized already during meiosis, shortly before the PBI extrusion. In this case, as previously shown (Kitajima and Hamaguchi, 2005), the sperm centrosomes stay "dormant" in the fertilized oocyte up to the completion of female meiosis. After completion of meiosis, the daughter centriole is eliminated shortly after the end of meiosis, and the pronucleus forms. The sperm centrosome aster rapidly grows and captures the female pronucleus, by pulling male and female pronuclei towards each other. The pronuclei then fuse and the first zygotic spindle is organized by the centrioles provided by the sperm (Zhang et al., 2004).

Why do the centrioles not contribute to the zygotic spindle, and at what point are they eliminated? As described above, immature oocytes feature two pairs of duplicated centrioles of which two mother centrioles and one daughter centriole are extruded into the two PBs in the course of meiotic divisions, leaving a single daughter centriole in the mature egg. In EB3-mEGP3 injected oocytes, I could confirm that the same sequence of events occurs in oocytes, which have been

fertilized during meiosis. Indeed, the presence of sperm centrioles does not affect the fate of the oocyte's centrioles – centriole extrusion still occurs (*fig. 4.14*).

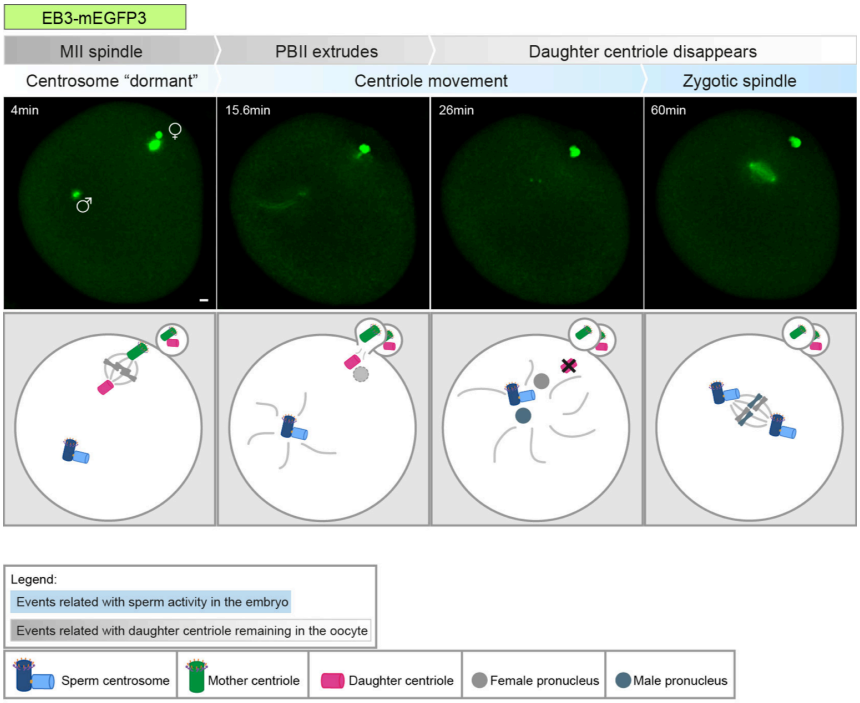

Figure 4.14: The single daughter remaining in the mature egg does not participate in the embryonic spindle. Fertilization occurred after PBI extrusion. Movie starts 1h30 after 1-MA hormone addition. Z-stacks recorded every 79 seconds. Pannels show a Z-projection of the acquired stacks. Scale bar: 10 μm. See schematic representation below.

Importantly, by imaging fertilized oocytes live at the end of meiosis, I could observe how sperm aster extension is synchronous with the disassembly and the disappearance of the remaining daughter centriole aster (*fig. 4.14, t=15.6 min*). Thus, the daughter centriole does not participate in the formation of the zygotic spindle, and no sign of this centriole is detected later, as embryonic development progresses (*fig. 4.14*).

In the literature it is assumed that the daughter centriole is eliminated at the end of oocyte meiosis, and my observations also point towards this direction. Shortly after completion of meiosis the daughter centriole loses its microtubule nucleation activity as detected by EB3-mEGFP3.

How the centriole is eliminated, after the loss of microtubule nucleating activity, is not clear. As from the present data I cannot confirm when and how the centriole structure is eliminated. Thus, I will henceforth refer to this process as daughter centriole *inactivation* rather than *elimination*. The timing of centriole inactivation can be determined very precisely using the EB3-mEGFP3 marker and occurs precisely at the end of meiosis, simultaneously with pronucleus formation.

4.4.2. Mother centrioles artificially retained in the egg, remain active and contribute to the zygotic spindle

To investigate whether the mother centriole would undergo inactivation at the end of MII similar to the daughter centriole, I artificially retained the mother centriole by inhibiting PB extrusion using latrunculinB (latB). This treatment blocks cytokinesis by disrupting the acto-myosin ring required for completion of cell division (Mierzwa and Gerlich, 2014).

Odf2-mEGFP and EB3-mCherry3 expressing oocytes were first fertilized, and then treated with latB after the formation of the MII spindle. At this stage, as expected, the mother centriole already localized at the outer spindle pole facing the plasma membrane (*fig. 4.15 is equivalent to fig. 4.16, t=0min*). However, as also expected, upon latB addition the PB fails to extrude, and therefore the mother centriole that was destined for the PB remains in the egg, as the MII spindle disassembles (*fig. 4.16 A, t=5.5min*).

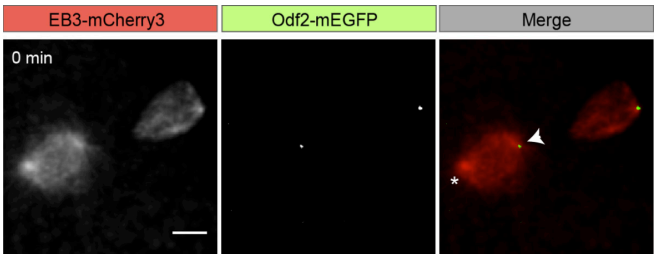

Figure 4.15: Mother centriole localizes at the outer MII spindle pole at the moment of latB addition (arrowhead). (*) Indicates the daughter centriole. Movie starts 1h30 after 1-MA addition and fertilization. Pannels show a Z-projection of the acquired stacks. Scale bar: 10 μm.

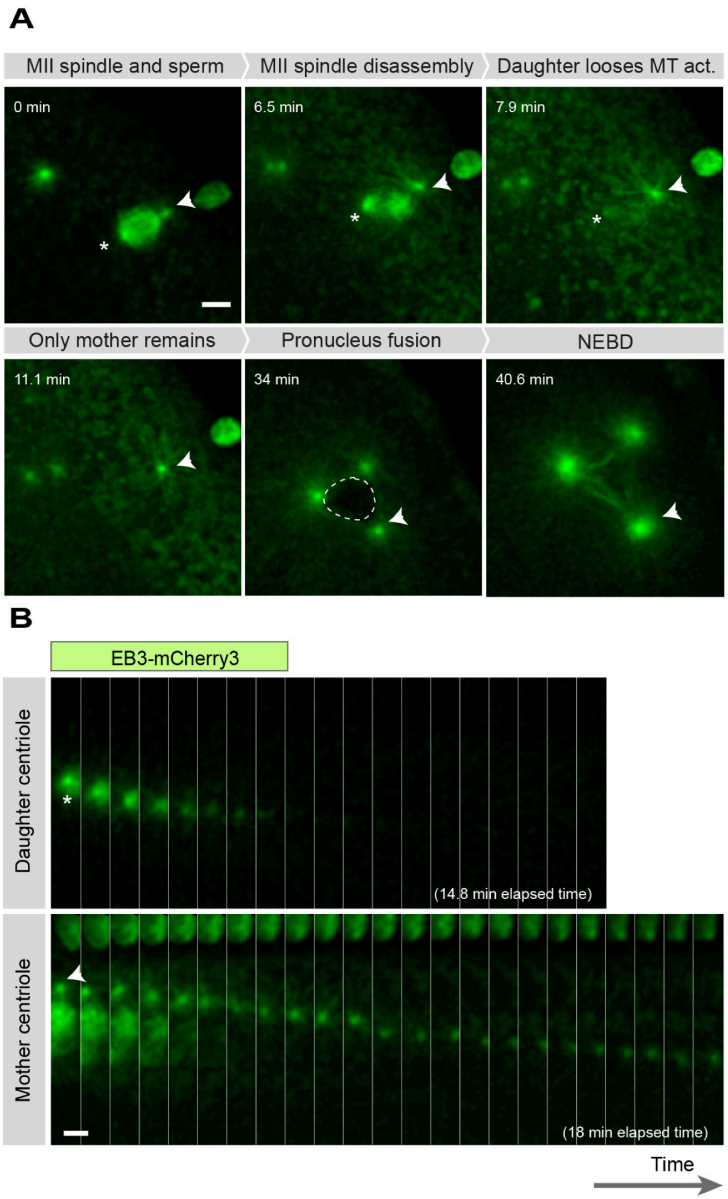

Figure 4.16: (A) Mother centriole remains active and participates in the formation of the zygotic spindle, together with the sperm centrioles. t=0 is a lower magnification of *fig. 4.15*, including the sperm aster. Dashed-line shows the zygotic nucleus. MT corresponds to microtubule, and act. to activity (B) Time-lapse shows the different behavior of maternal mother and daughter centrioles at the end of meiosis. Maternal mother centriole is represented by an arrowhead, and the maternal daughter by a (*). Movie starts 1h30 after 1-MA addition. Z-stacks recorded every 50 seconds. Pannels show a Z-projection of the acquired stacks. Scale bar: 10 μm.

At this point, the mature egg contains in its cytoplasm not only the centrioles inherited from the sperm, but also maternally contributed centrioles: one mother (which failed to extrude to the PBII due to latB treatment) and one daughter. I will refer to these two centrioles as the *maternal* centrioles, to not be confused with the sperm-inherited centrioles, the *paternal* ones. The two maternal centrioles, although present in the same cytoplasm, show a strikingly different behavior: the daughter centriole quickly loses its microtubule nucleating activity as observed in control cells described above (*fig. 4.16 A, t=7.9min, and B*). In contrast, the mother centriole continues to nucleate microtubules (*fig. 4.16 A and B*). Due to this activity, the mother centriole moves deeper into the cytoplasm and joins the sperm centrioles in the assembly of the zygotic spindle resulting in an abnormal tripolar spindle (n=8/8) (*fig. 4.16 A*, arrowhead*, t=40.6min*).

Note that at the end of meiosis, centrioles move deeper into the egg cytoplasm, so the resolution of imaging was compromised in order to follow centriole movement in a larger area. As a consequence, I could not reliably detect the mother specific Odf2-mEGFP signal once centrioles are localized deeper within the cytoplasm. However, by EB3-labeling I could continue to track each of the centrioles and therefore retain the information of which one is the maternal mother centriole (*fig. 4.15 and 4.16 A and B)*.

Next, I tested the consequences of retaining both maternal mother centrioles in the mature egg. For this purpose, I fertilized Odf2-mEGFP and EB3-mCherry3 oocytes and added latB before the PBI extrusion, preventing extrusion of both PBs. In this case, all four centrioles remain in the mature egg: two daughter and two mother centrioles. Strikingly, in this case both daughter centrioles are inactivated, while the two mother centrioles remain active. These, combined with the paternal centrioles, result in the assembly of a tetrapolar spindle (n=5/5) (*fig. 4.17*).

These experiments clearly show the functional difference between mother and daughter centrioles in starfish oocytes. Daughter centrioles lose microtubule-nucleating activity at the end of meiosis, but mother centrioles remain active and contribute to the zygotic spindle, in an equivalent way to the paternal centrioles. Therefore, a mechanism must exist to eliminate the maternal mother centrioles, by extruding them into the PBs, to avoid problems in the zygotic development.

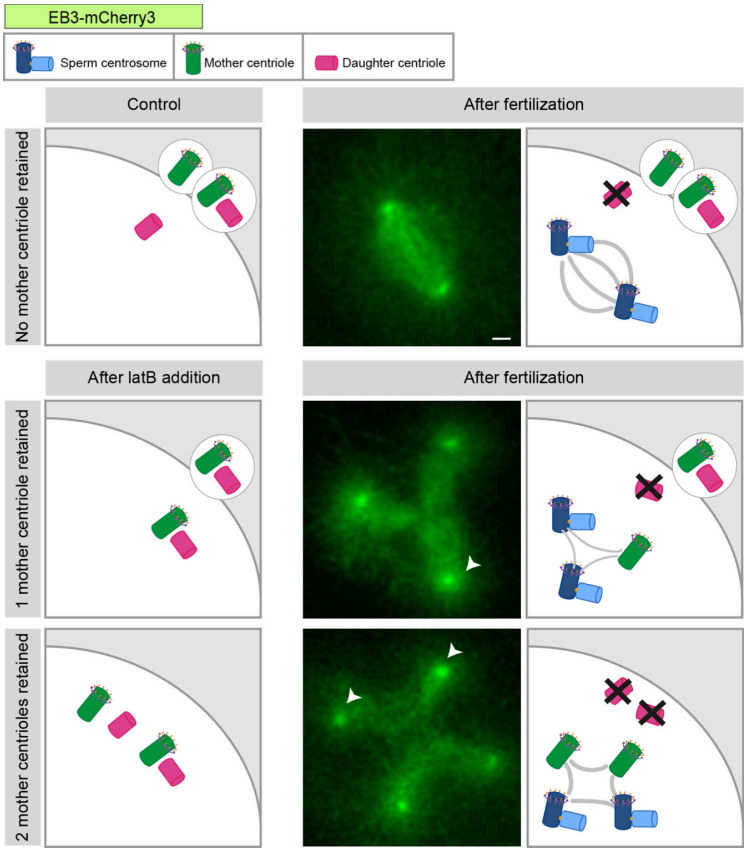

Figure 4.17: If mother centrioles are retained, they will participate with the sperm centrioles in the formation of the zygotic spindle. If one mother is retained (middle pannel) a tripolar spindle is formed. If both mother centrioles are retained, a tetrapolar spindle is formed. See schematic representation. Maternal mother centriole is indicated by an arrowhead. Pannels show a Z-projection of the acquired stacks. Scale bar: 10 μm.

My data thus strongly argues against the presence of a cytoplasmic factor responsible for elimination of all maternal centrioles that was proposed earlier (Sluder et al., 1989). Instead, my experiments clearly show that maternal mother and daughter centrioles can coexist in the same cytoplasm, but only the daughter centrioles are eliminated. This suggests that it is an intrinsic property of the mother centrioles makes them resistant to elimination.

On the other hand, these observations are fully consistent with earlier studies proposing that the “replicative” centrioles are segregated into PBs, but remain able to contribute to the zygotic spindle when artificially retained or injected back

into the egg (*see* ***Introduction section 1.7.2***). I show here for the first time that these “replicative” centrioles are the mother centrioles, while the daughter centrioles are the centrioles that have been previously denoted as “non-replicative” centrioles.

Combining our observations, two mechanisms are employed for centriole elimination in starfish oocytes: (i) physical elimination of mother centrioles by extrusion into PBs, and (ii) a biochemical mechanism that specifically eliminates daughter centrioles in the mature egg (*see fig. 4.13*). Although both mechanisms are important and interesting, I primarily focused on the first one during my PhD work. The second mechanism that is responsible for elimination of the daughter centriole remains a major question to be addressed in future work, which I will detail in the ***Discussion*** section.

4.5. The mother centriole is specifically transported to the plasma membrane

4.5.1. Tracking of the mother centriole reveals a two-step process

The above experiments clearly demonstrated the importance of removing the mother centrioles from the cytoplasm of the mature egg, by extruding them into the PBs. The key question here is how the mother centrioles are extruded into the PBs. In MI, both spindle poles are composed of a pair of mother and daughter centriole, therefore independent of the spindle orientation, one daughter and one mother centriole will be extruded. In stark contrast, in MII a single mother centriole forms the outer spindle pole, while a single daughter centriole forms the inner pole. Therefore, a mechanism must exist ensuring that the mother centriole is at the pole facing the plasma membrane, while the daughter centriole faces inward.

My data presented above also demonstrates that this mechanism functions with high fidelity as I observed the mother centriole facing the plasma membrane

in all oocytes investigated (n>60). Given the critical importance of the process for zygotic development, such a high fidelity process is in fact necessary.

To gain insights into how the spindle is positioned with the mother centriole facing the cell cortex, I performed high spatial and temporal resolution 3D imaging just after anaphase I, using Poc1-mEGFP that conveniently labels both centrioles and spindle microtubules. These time-lapse recordings revealed that shortly after PB extrusion, the mother centriole relocates to the plasma membrane even before the complete disassembly of MI spindle (*fig. 4.18*). Moreover, careful analysis of the live imaging movies using Imaris, a 3D-visualization software, shows that mother centriole movement is directed towards the plasma membrane.

To follow centrioles throughout this process, I developed an algorithm to automatically detect centriole positions in 3D at every time point. In order to quantitatively characterize the transport of the centriole to the cell cortex, I additionally segmented out the cell outline, and calculated the minimum distance of centrioles from the plasma membrane over time and in 3D (*for details and schematic representation, see* ***Material and Methods section 3.7.3***). The resulting tracks, i.e. plots of centriole-cortex distance over time, reveal a two-step mechanism of the mother centriole positioning: i) the mother centriole is transported towards the plasma membrane, and ii) the mother centriole stabilizes at this position, and appears to "anchor" to the cell cortex (*fig. 4.18 A and B*).

Specifically, mother centrioles move to the plasma with an average velocity of 2 μm/min±0.8 (n=13). Interestingly, this velocity is similar to the velocity of centriole movement towards the plasma membrane during T-cell polarization (Kuhn and Poenie, 2002). Moreover, the resulting tracks show how the movement towards the plasma membrane is constant, which is also consistent with the directed movement I observe by live imaging (*fig. 4.18 A and B*).

Poc1-mEGFP was in these experiments simultaneously used for the membrane segmentation and for centriole tracking (*fig. 4.18*). However, Poc1 is a general centriole marker and therefore does not differentiate between mother and daughter centriole. However, based on my data presented above, I can assume that the Poc1-mEGFP-labeled centriole moving to the cell membrane is the

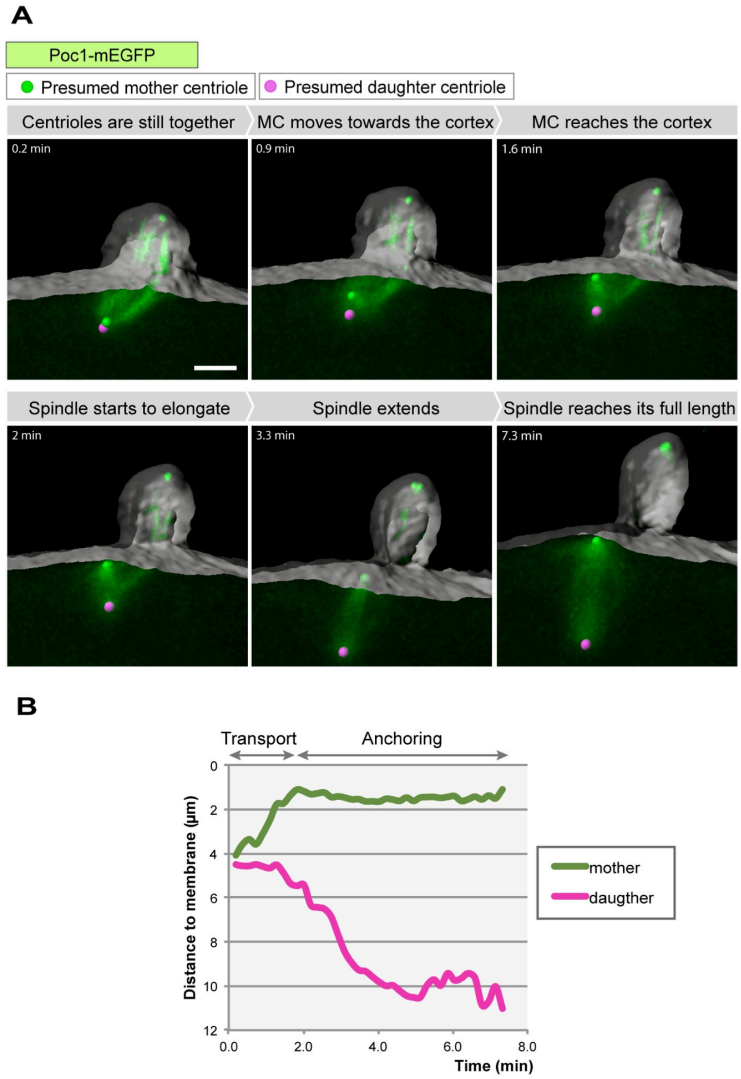

Figure 4.18: (A) Mother centriole transport occurs shortly after PBI extrusion. 3D visualization using Imaris. Oocyte's contour is shown in grey. Z-stacks recorded every 12 seconds. Movie starts after PBI extrusion. Scale bar: 5 μm. MC corresponds to mother centriole (B) Mother centriole is first transported towards the plasma membrane, where it then anchors. Chart shows distance measurements of the centriole to the plasma membrane recorded in 3D and over time.

mother centriole. Additionally, I confirmed this by following the mother centriole transport in double EB3-mCherry3 and Odf2-mEGFP-labeled oocytes (*fig. 4.19*). These data directly confirms that only the mother centriole has the ability to be transported to the cell membrane, and no motion of the daughter centriole towards the cortex was ever observed.

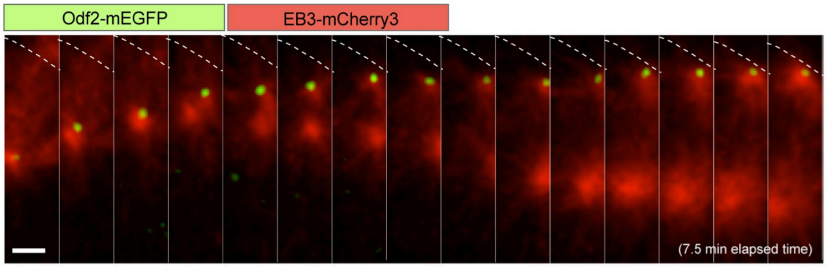

Figure 4.19: Time-lapse shows mother centriole being transported and anchoring to the plasma membrane. Movie starts after PBI extrusion. Z-stacks recorded every 30 seconds. Pannels show a Z-projection of the acquired stacks. Dashed line shows the cell countour. Scale bar: 10 μm.

Together, I conclude that a specific mechanism transports the mother centriole to the plasma membrane shortly after PBI extrusion. Thereafter, the mother centriole remains stably associated with the plasma membrane until the end of MII. At the same time the daughter centriole was never observed to move towards the plasma membrane but rather move into the cell interior through the elongation of the spindle (*fig. 4.18 and 4.19*).

4.5.2. Characterization of the mother centriole specific transport mechanism

The specific and directional transport of the mother centriole towards the cell cortex strongly suggests that this process is mediated by the cytoskeleton. Therefore, to address the mechanisms of the specific transport of the mother centriole to the cell cortex, I used various inhibitors of the actin and microtubule cytoskeleton. However, these treatments turned out to be quite challenging, because centriole transport is a very quick process that occurs shortly after the end of MI, which in turn requires microtubules (telophase) as well as actin (cytokinesis) to be completed. I established protocols to add cytoskeletal inhibitors and thereby affect centriole transport as specifically as possible. Yet, due to the technical difficulties detailed above, these experiments are not yet fully conclusive.

i. Is the mother centriole specific transport driven by microtubules?

To test how microtubules contribute to centriole transport, I treated oocytes with the microtubule-depolymerizing drug, nocodazole, shortly after PBI extrusion in Poc1-mEGFP expressing oocytes (*fig.4.20*).

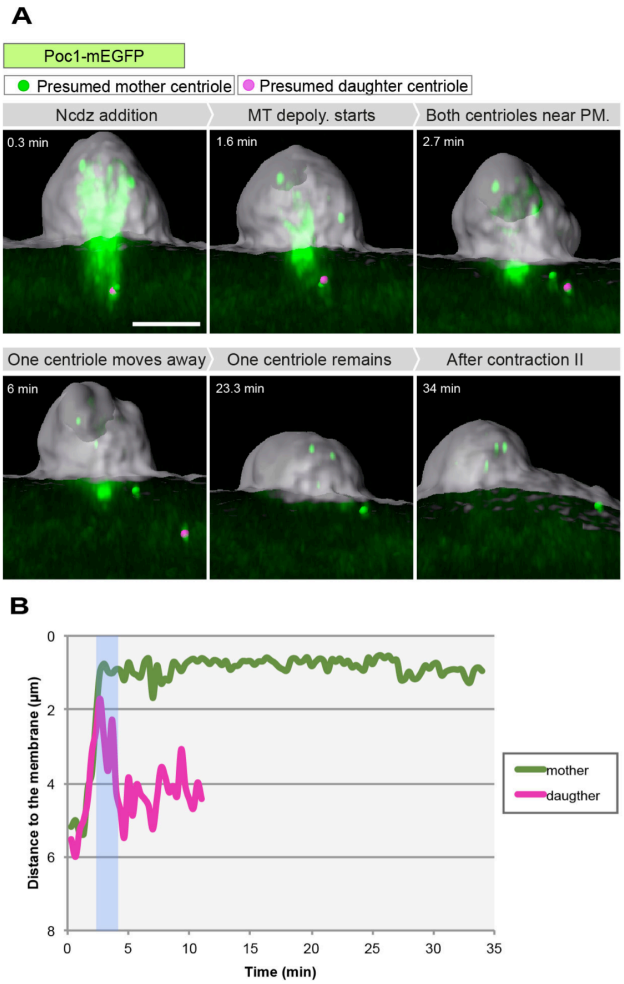

Figure 4.20: (A) Microtubule depolymerization brings both centrioles close to the plasma membrane. 3D visualization using Imaris. Oocyte's contour is shown in grey. Movie starts after PBI extrusion. Z-stacks recorded every 20 seconds. Scale bar: 5 μm. MT corresponds to microtubules, PM to plasma membrane and ncdz to nocodazole. (B) Chart shows distance measurements of the centriole to the plasma membrane recorded in 3D and over time. Note how one of the centrioles the (presumed) mother centriole remains anchored to the plasma membrane, whereas the other ends up being lost from the Z-stack. Blue rectangle shows when the inhibitory drug starts to be active.

Recall that Poc1-mEGFP labels all centrioles and spindle microtubules, but since nocodazole only depolymerizes dynamic microtubules, centriolar microtubules are practically unaffected, as they are highly stable structures. Nocodazole effect is visible 2-4 minutes after addition: microtubules of the MI spindle quickly depolymerize resulting in a rapid inward collapse of the spindle. Unexpectedly, this collapse moves both centrioles near the plasma membrane (*fig. 4.20*).

Thus, I was not able to conclude on the direct involvement of microtubules in the transport of the mother centriole to the plasma membrane: timed addition of nocodazole causes the spindle to collapse towards the cell cortex delivering both centrioles to the cell cortex. This however indicates that indeed the spindle is anchored to the cortex, which justifies why the spindle collapses towards the plasma membrane.

Additionally, these results clearly show that by bringing any centriole close to the plasma membrane is not sufficient for stable anchoring: only the presumed mother centriole is able to anchor, while the presumed daughter centriole diffuses away (*fig. 4.20*).

ii. Is the mother centriole transport driven by actin?

To test the involvement of actin in the mother centriole transport, I treated EB3-mEGFP3-expressing oocytes with latB, shortly after PBI extrusion, i.e. just before the beginning of the mother centriole specific transport to the plasma membrane.

Note that although EB3-mEGFP labels equally mother and daughter centrioles, but they can be distinguished based on the microtubule nucleating at the end of meiosis: as shown above (*see* ***Results section 4.4.2*** *fig. 4.16*) the daughter centriole is inactivated at the end of meiosis, losing its microtubule nucleating activity. In contrast, the mother centriole remains active and is able to nucleate microtubules in the mature egg. Therefore, by following Poc1-mEGFP or EB3-mEGFP3 label up to the end of meiosis, I can track back mother and daughter centrioles.

I observed that upon latB addition, the mother centriole (M2) is transported normally towards the cell membrane (*fig. 4.21*), where it properly anchors (n=6/6). Subsequently, as meiosis progresses, LatB-treated oocytes cannot extrude PBII, because the PBII extrusion is actin dependent. Therefore, the MII

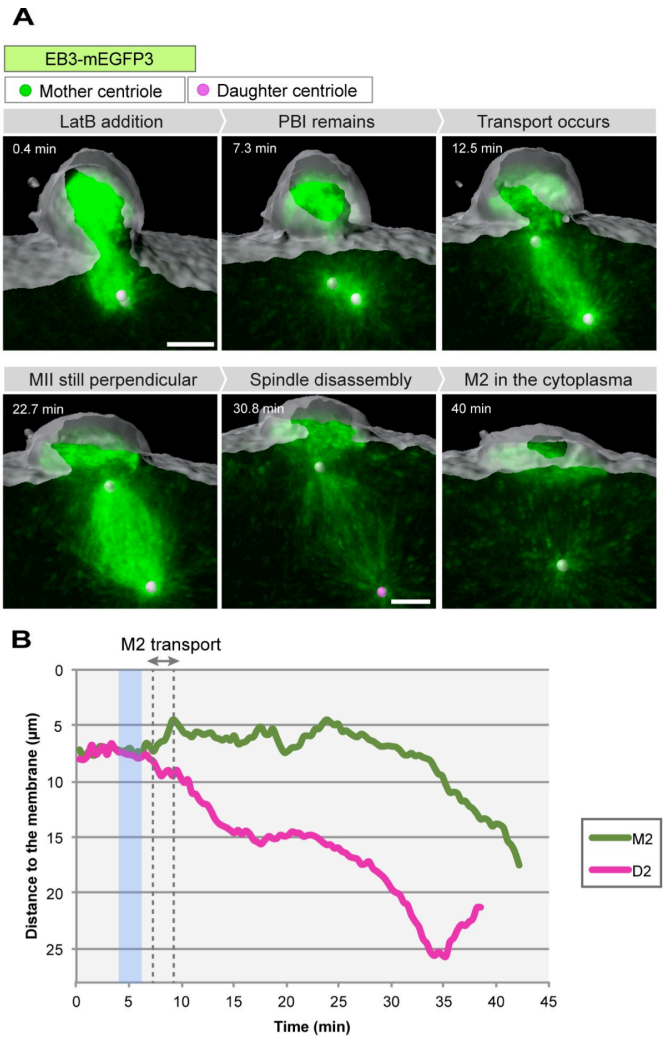

Figure 4.21: (A) Dynamic actin is not involved in the mother centriole transport. 3D visualization using Imaris. Oocyte's contour is shown in grey. Movie starts after PBI extrusion. Z-stacks recorded every 22 seconds. Scale bar: 5 μm. (B) Chart shows distance measurements of the centrioles to the plasma membrane. Transport phase indicated by the dashed lines in the graph. Blue rectangle shows when the inhibitory drug starts to be active. M2 and D2: mother and daughter centriole, respectively, from the MII spindle.

spindle disassembles, and the abnormally retained mother centriole (M2) preserves its microtubule nucleating activity in the mature egg's cytoplasm (note how the daughter (D2) loses microtubule nucleating activity, whereas the mother is still active – *fig. 4.21*).

These data together suggest that dynamic actin is not required for mother centriole transport to the cell membrane. However, similar to nocodazole, LatB sequesters actin monomers, and therefore rapidly affects dynamic or newly forming actin structures, however stable filaments are much more slowly affected. Thus, my protocol of treating oocytes with LatB for only a few minutes before centriole transport can exclude the possibility that the process is driven by dynamic actin structures, but cannot exclude the possibility of involvement of stable filaments.

iii. Is the mother centriole transport dependent on the polar body I cytokinesis?

In the previous section, I only considered oocytes in which PBI formation was completed just before latB addition, and in these oocytes mother centriole transport was normal. However, if latB was added just a little too early, oocytes failed to complete PBI cytokinesis, and the PBI collapses back into the oocyte (*fig. 4.22*).

When I analyzed these oocytes to understand if transport still occurred, I found that, interestingly, the MII spindle does not organize in a perpendicular orientation. Instead, it forms parallel to the cell membrane (note that M2 and D2 are at almost the same distance from the membrane – *fig. 4.22*). Strikingly, the mother centriole is no longer transported to the plasma membrane and the entire MII spindle just sinks into the cytoplasm – *fig. 4.22*. I observed this same phenotype in 8 out of 9 oocytes in which PBI cytokinesis failed: no mother centriole transport occurs and the MII spindle forms parallel to the membrane.

These data suggest that mother centriole transport may happen only if PBI formation is completed. Piel and colleagues showed that mother centriole moves towards the abscission site during cell division in mammalian cells. They hypothesized that this movement occurs because the mother centriole remains connected with the microtubules from the midbody (Piel et al., 2001). Indeed, a

similar mechanism could occur in starfish oocytes: the midbody formation during PBI cytokinesis would cause the mother centriole to move towards the abscission

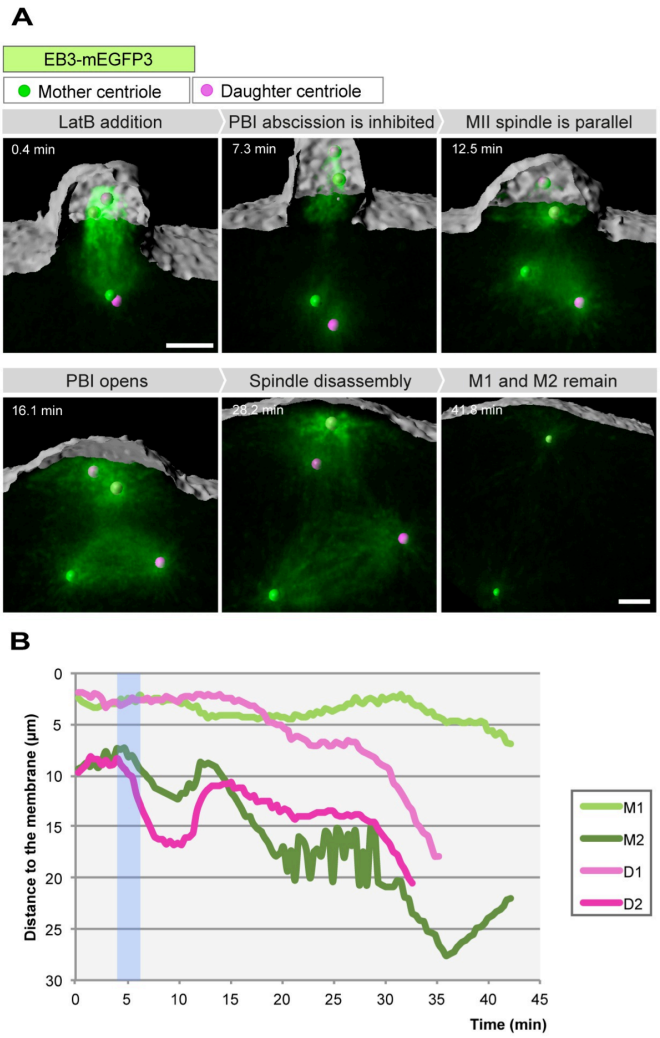

Figure 4.22: (A) PBI formation might be important for mother centriole transport. 3D visualization using Imaris. Oocyte's contour is shown in grey. Movie starts after PBI extrusion. Z-stacks recorded every 22 seconds. Scale bar: 5 μm. (B) Chart shows distance measurements of the centrioles to the plasma membrane. Blue rectangle shows when the inhibitory drug starts to act. M1 and D1 are respectively the mother and daughter centrioles from PBI. M2 and D2 are respectively the mother and daughter centrioles from the MII spindle. Both mother centrioles (M1 and M2) preserve MT nucleating activity at the end of meiosis.

site. Therefore, mother centriole would only occur if PBI extrusion and midbody forms. This movement towards the membrane would then allow the mother centriole to be at a reachable distance to the plasma membrane to allow anchoring.

Mother centriole transport is independent of polar body cytokinesis

R. Matsuura and K. Chiba previously showed that upon gentle centrifugation of oocytes, centrioles maintain a cortical attachment at the animal pole of the oocyte, whereas the nucleus, which is less dense than the cytoplasm, moves away from the cortex (Matsuura and Chiba, 2004) (*see* ***Material and Methods section 3.7.4*** *fig. 3.7*). Centrifuged oocytes still undergo meiosis: NEBD occurs normally, yet PB extrusion does not take place (Barakat et al., 1994; Matsuura and Chiba, 2004). As in these centrifuged oocytes no PB is formed, this constitutes a perfect system to address whether PB cytokinesis or the midbody is required for mother centriole transport to occur, as hypothesized above. Would the mother centriole still move to the plasma membrane in this manipulated system?

Because I needed to cover a larger depth and a larger area during live imaging, I used EB3-mEGFP3 in these experiments. As before, I distinguished mother and daughter centrioles in retrospect by tracking back whether they are active or not at the end of meiosis.

Interestingly, after maturation of these centrifuged oocytes, mother centrioles are still transported to the plasma membrane (n=9/9) (*fig. 4.23 A and B* – note how both mother centrioles (M1 and M2) localize to the plasma membrane). Moreover, mother centrioles localizing twice as deep in the cytoplasm, when compared to centrioles in non-centrifuged oocytes at the beginning of the transport, are still able to move to the cell membrane (compare the distances between *fig. 4.18* and *fig. 4.23*). However, mother centriole transport is slower (0.4 μm/min) than in non-centrifuged oocytes. One idea would be that spindle elongation (in non-centrifuged oocytes) could accelerate the transport towards the plasma membrane. Once mother centrioles reach the plasma membrane, they also remain anchored. In contrast, daughter centrioles (D1 and D2) clearly

lack the potential to move to the plasma membrane, and they just move randomly in the cytoplasm (*fig. 4.23*).

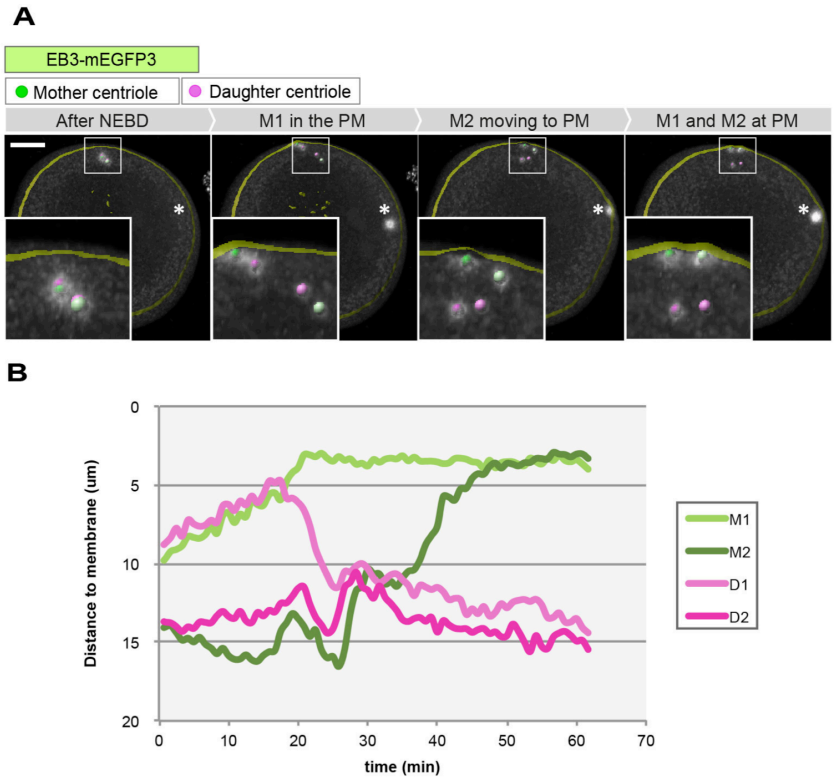

Figure 4.23: (A) Mother centriole transport occurs in a centrifuged oocyte – they do not move as a consequence of midbody formation. “PM” stands for plasma membrane. 3D visualization using Imaris. Oocyte’s contour is shown in yellow. Movie starts after NEBD. Insets show magnifications of the centrioles’ localization. (*) Shows nuclear localization after centrifugation. Z-stacks recorded every 50 seconds. Scale bar: 50 μm. (B) Chart shows distance measurements of the centrioles to the plasma membrane. M1 and M2 are mother centrioles. D1 and D2 are daughter centrioles. In this case, classification as M1 or M2 is arbitrary (in contrast to fig. 4.22). The same applies for D1 and D2.

Taken together, these data indicate that mother centriole transport does not depend on PBI cytokinesis site, as mother centrioles (M1 and M2) clearly move to the membrane in centrifuged oocytes. This movement is also not distance dependent, as mother centrioles localizing deeper in the cytoplasm, can still move to the plasma membrane. On the other hand, this is clearly a specific

property of the mother centrioles, as no daughter centriole (D1 and D2) was ever transported to the plasma membrane.

To reconcile these results with the observations described in the previous section (*fig. 4.22*), it is clear that the cytokinetic site is not a requirement for the specific transport of the mother centriole to the plasma membrane. However, a failed cytokinesis likely introduces an additional microtubule aster from the PBI that might prevent anchoring to occur. The 3D tracks indeed suggest this (*fig. 4.22 B*): when PBI collapses, the daughter centriole D1 (i.e. the daughter centriole from the PBI) has a descending trajectory, which is very similar to the also descending trajectories of the centrioles M2 and D2 (mother and daughter that form the MII spindle). This suggests that the descending microtubule asters of the collapsing PBI likely i) interrupt the formation of the MII spindle in a perpendicular orientation, which therefore becomes parallel to the plasma membrane, and ii) push the MII spindle down, spatially interfering with mother centriole transport to the plasma membrane, and consequent anchoring.

iv. Mother centriole transport requires proximity to the nucleus

I observed that mother centrioles do not always move to the plasma membrane in centrifuged oocytes (*fig. 4.24*) (n=12). In these situations, both mother (M1 and M2) and daughter (D1 and D2) centrioles would remain in the cytoplasm and no directed movement was observed. This was rather intriguing: why would the mother centriole not move in some cases?

Systematic analysis of multiple oocytes revealed that mother centriole movement was related with the centriole distance to the nucleus. Dependent on the initial positions of the oocytes in the coverslip chamber, centrifugation creates a pool of oocytes with variable distances between the new nuclear position and the centrioles (*see* ***Material and Methods section 3.7.4*** *Fig. 3.7 and 3.8*). I characterized this distance between centrioles and nucleus by measuring the angle between the two; an angle of 180° between the two means that nucleus and centrosome are at opposite poles of the oocyte (*see* ***Material and Methods***).

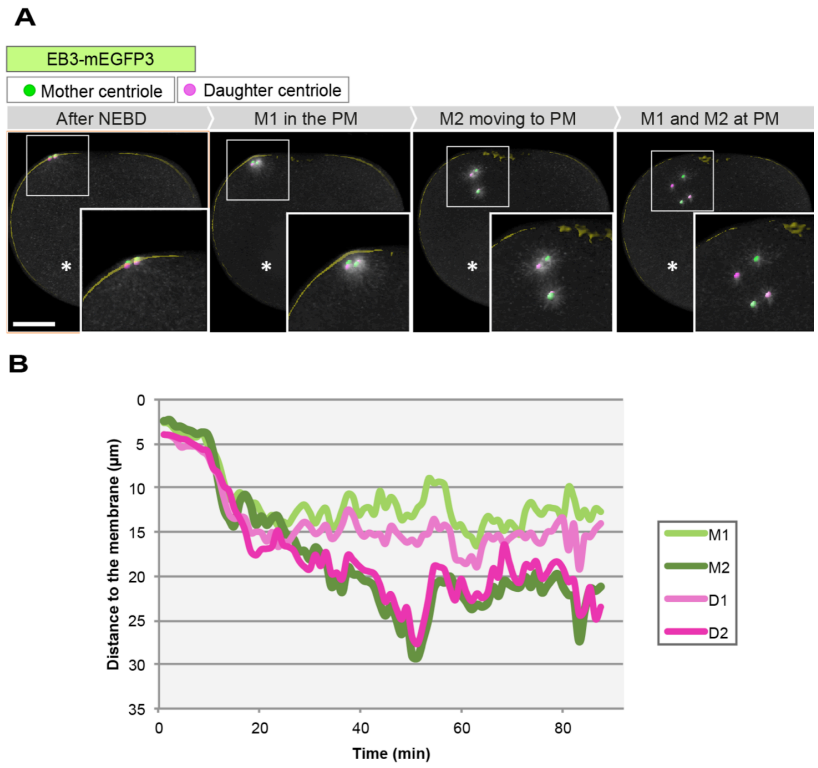

Figure 4.24: (A) No mother centriolar transport is observed. M1 and M2 have a similar behavior as D1 and D2. "PM" stands for plasma membrane. 3D visualization using Imaris. Oocyte's contour is shown in yellow. Movie starts after NEBD. Insets show magnifications of the centrioles' localization. (*) Shows nuclear localization after centrifugation. Z-stacks recorded every minute. Scale bar: 50 *µ*m. (B) Chart shows distance measurements of the centrioles to the plasma membrane. M1 and M2 are mother centrioles. D1 and D2 are daughter centrioles. In this case, as in fig. 4.23, classification as M1 or M2 is arbitrary (in contrast to fig. 4.22). The same applies for D1 and D2.

These angle measurement revealed an interesting relationship (n=27): when the nucleus localize close enough (up to 40°), centrioles can still capture chromosomes and PB extrusion still occurs. When the nucleus localizes between 40-80° away from the centrioles, chromosome capture and PB extrusion does not take place; nevertheless mother centriole transport and subsequent anchoring occur normally. However, as the distance between nucleus and centrioles increases (angle larger than 100°), no transport is observed, and both mother and daughter centrioles show similar, diffusive behavior (*fig. 4.24 and 4.25*).

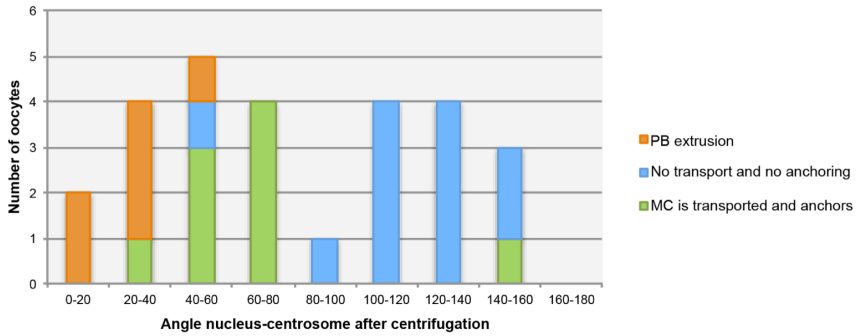

Figure 4.25. Mother centriole (MC) movement requires proximity to the nucleus. In orange, mother centrioles are close enough to the nuclear region and are able to capture (some) chromosomes – PB extrusion still occurs. In green, mother centrioles are transported to the plasma membrane, where they anchor, but PB extrusion does not oocur – as in *fig. 4.23*. In blue, mother centrioles show the random diffuse behavior characteristic of the daughter centrioles, no movement towards the plasma membrane is observed – as in *fig. 4.24*.

Taken together, my results suggest that mother centriole transport is dependent on the distance of the centriole from the nucleus. If the nucleus localizes too far, centrioles can no longer move to the plasma membrane. These results suggest that mother centriole might require a signal originating from the nucleus to be transported to the plasma membrane.

Finally, altogether, I defined a mechanism of transport specific for mother centriole, which occurs shortly after PBI extrusion. This mechanism is likely independent of dynamic actin, and it occurs independently of polar body extrusion. My data suggests that mother centriole transport is dependent on the distance to the nuclear region, which suggests that it might respond to a cytoplasmic gradient established upon meiosis resumption.

4.6. The mother centriole anchors to the plasma membrane

4.6.1. Actin and microtubules are not involved in centriole anchoring

As shown above, after being transported to the plasma membrane, the mother centriole remains stably associated with it. This association is so close that by confocal light microscopy the centriole appears to co-localize with the plasma membrane (*fig. 4.26*).

This strongly contrasts with the normal cell division in which the mitotic spindle is positioned by astral microtubules clearly separating the plasma membrane and the centrosomes – *see* ***Introduction section 1.6.4 i,*** *fig. 1.24* (Almonacid et al., 2014; McNally, 2013).

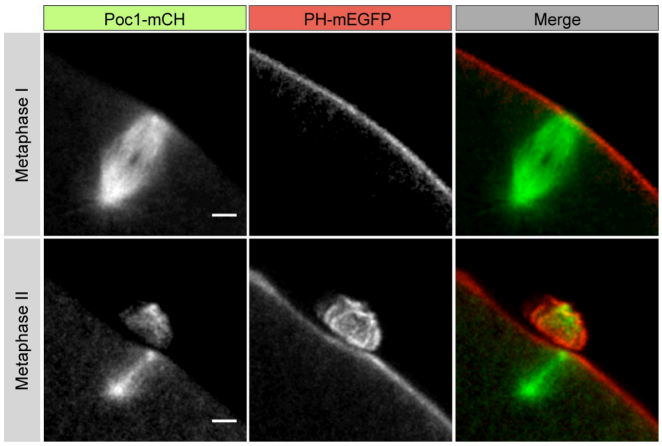

Figure 4.26. Centrioles are in close proximity with the plasma membrane either in metaphase I or II. PH domain (red) labels plasma membrane. Pannels show a Z-projection of the acquired stacks. Scale bar: 10 μm

i. Establishing the conditions to arrest oocytes in MII

To address the mechanism of this tight association of the mother centriole and the plasma membrane, I wanted to rule out that short astral microtubules or

possibly actin filaments mediate the anchoring of the mother centriole to the cell membrane. In order to do so, I developed a method to successfully block oocytes in metaphase II, at which time a single mother centriole faces the cell membrane, and then treat the oocytes with cytoskeleton depolymerizing drugs. In a normal cell division, cyclin B is targeted by ubiquitination for degradation by the proteasome during metaphase (Glotzer et al., 1991) leading to inactivation of cdk1 and consequent mitotic exit. MG-132 is a proteasome inhibitor, which has been previously used in starfish oocytes, to inhibit this cyclin B degradation and maintain the cells in metaphase (Chiba et al., 1997). Thus, this inhibitor was used in order to induce metaphase arrest in starfish oocytes.

First, cyclin B-mEGFP-expressing oocytes were used to establish the MG-132 assay conditions for further use (*fig. 4.27*).

As expected, in control oocytes (with or without DMSO, *pink* and *green*, respectively, *fig. 4.27 B*), cyclin B levels are high before NEBD and decline drastically, at the onset of anaphase I (*fig. 4.27 A and B*). It is important to note that endogenous cyclin B is cell cycle regulated, and its protein levels rise again during MII, followed by degradation in metaphase II to anaphase II transition. However, the injected cyclin B-mEGFP mRNA does not follow the same endogenous regulation and takes longer to be synthesized. As a consequence, cyclin B-mEGFP re-synthesis and degradation cannot be detected during the metaphase II to anaphase II transition.

When oocytes are treated with MG-132 (with or without pre-incubation, *purple* and *orange*, respectively, *fig. 4.27 B*), no cyclin B-mEGFP degradation is observed. Cyclin-B-mEGFP levels remain constant, which indicate an efficient metaphase I arrest (*fig. 4.27 A and B*).

In conclusion, I was able to successfully arrest oocytes in metaphase I upon MG-132 treatment. Equally I established the incubation time required for MG-132 to act (45min) (*see* ***Material and Methods*** *for more experimental details*). This information was then used to arrest oocytes in metaphase II, as proposed, which were then treated with inhibitory drugs.

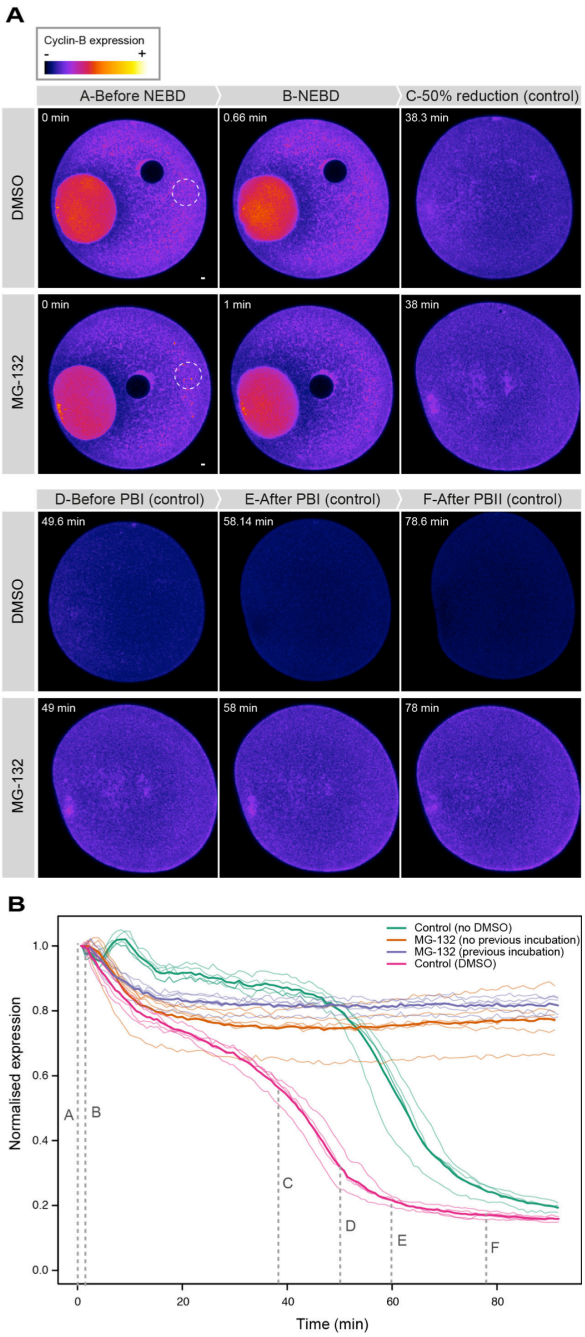

Figure 4.27: (A) Oocytes treated with MG-132 are arrested in Metaphase I – cyclin B-mEGFP is not degraded. Cyclin B levels are visualized by a pseudocolor. The color is indicative of the protein levels: a darker blue/black indicates low protein levels. Z-stacks were acquired every 40seconds and 1minute (DMSO and MG132 respectively). Panels show a single confocal slice, selected accordingly to the largest nucleus diameter. (*To be continued in the following page*)

(*Continuation fig. 4.27*) The intensity of cyclin B-mEGFP was measured over time in a circular ROI indicated in the figure. Scale bar: 5 *μ*m. (B) Plot of the normalized expression of cyclin B-mEGFP levels over time. All datasets are plotted: raw data curves are shown in a pale color, and the mean curve is shown in a bold color. A-F correspond to the panels, which are labeled above. Number of oocytes analyzed: for control (no DMSO), n=6; for control (in DMSO), n=4; MG132 (pre-incubation), n=5; MG132 (no pre-incubation), n=7. For more details *see* ***Material and Methods section 3.7.5***.

All MII-arrested and Poc1-mEGFP expressing oocytes were imaged arrested in MII for 30 min, to control centriole positioning before drug addition. During this period of time, mother centriole remained connected to the plasma membrane (*Fig. 4.28*).

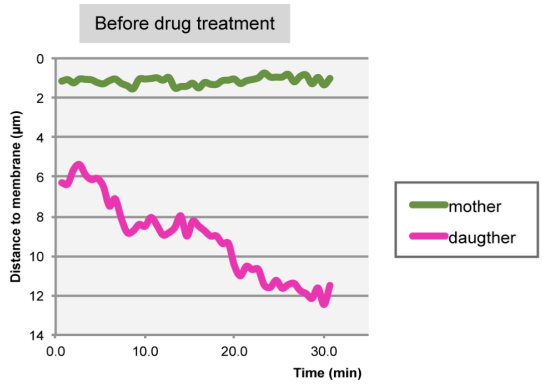

Figure 4.28: All oocytes were imaged for at least 30 min in metaphase II, before drug treatment. Note how mother centriole remains anchored to the plasma membrane during this period of time. Variations in daughter centriole distance to the plasma membrane are due to a slanted orientation of the spindle.

ii. Mother centriole anchoring is independent of microtubules

Next, I tested the effect of microtubule depolymerization, by treating MII-arrested oocytes with nocodazole. Shortly after drug addition, the spindle microtubules quickly depolymerized; yet the tight association of the mother centriole to the plasma membrane was not affected (n=14/14) (*fig. 4.29 A, first panel, and B*). In contrast, the daughter centriole first collapses to the cell membrane, and then moves randomly in the cytoplasm, without preferential

direction. Interestingly, this confirms my above observations (**section *4.5.2.i***): even when the daughter centriole localizes close to the plasma membrane (upon microtubule depolymerization) it cannot anchor.

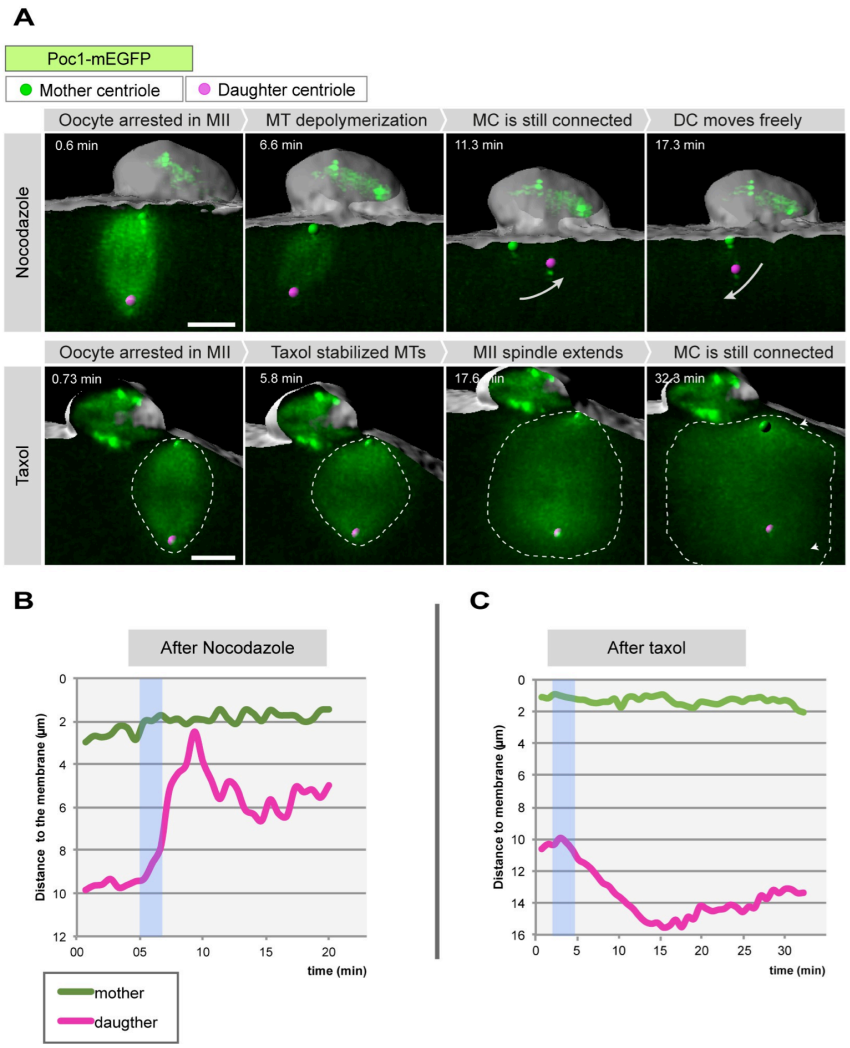

Figure 4.29: A) Mother centriole does not depend on microtubules to anchor to the plasma membrane. Note how astral microtubules grow from the inner pole, whereas in the outer pole, mother positioning is not affected. 3D visualization using Imaris. Oocyte's contour is shown in grey. Movie starts after drug addition. Z-stacks recorded every 40 and 44 seconds, for nocodazole and taxol, respectively. Scale bar: 5 μm. MC and DC correspond to mother centriole and daughter centriole, respectively. MT corresponds to microtubules (B) Chart shows distance measurements of the centrioles to the plasma membrane. Blue rectangle shows when the inhibitory drug starts to be active.

I also tested the effect of taxol treatment and consequent microtubule stabilization: taxol treatment induces spindle growth to the double of its normal length. Still the mother centriole does not detach from the membrane and its position remains stable over time (n=12/13) (*fig. 4.29 A, second panel, and B*). At the same time, the daughter centriole gets "pushed" deeper in the cytoplasm as spindle extends, and astral microtubules expand from the inner spindle pole. However, no growth of microtubules was observed from the outer pole.

iii. Mother centriole anchoring is independent of dynamic actin

To also test whether actin is involved in the anchoring of the mother centriole, I performed similar experiments by treating arrested MII oocytes with actin depolymerizing drugs.

Treatment either with Cytochalasin D (cytoD) or latB had no effect on the mother centriole anchoring (n=8/12, for both cases) (*fig. 4.30*), and for both cases the MII spindle remains attached to the plasma membrane. Interestingly, the MII spindle progressively shows a slanted orientation to the plasma membrane plane (approximately 45°), but still remains anchored (*fig. 4.30 A and B, for latB and cytoD treatment*). Curiously, the mother centriole moves in the plane of the plasma membrane, but never away from it. This suggests that actin, although not involved in the mother centriole *anchoring*, might stabilize the mother centriole *position* at the plasma membrane.

Taken together, I conclude that microtubules and actin are not involved in anchoring the mother centriole to the plasma membrane. Moreover, taxol treatment clearly shows how the two centrioles at the two MII poles are different: astral microtubules grow beyond the inner pole, whereas the same does not occur in the outer pole.

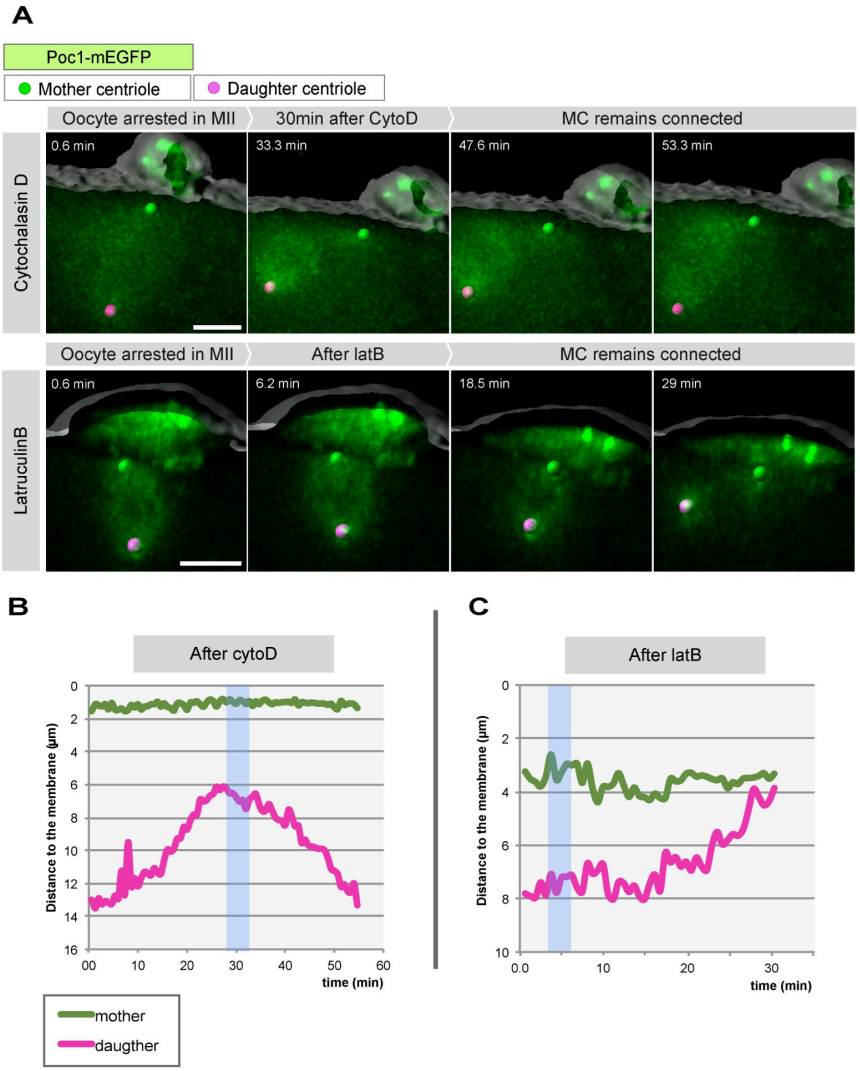

Figure 4.30: A) Mother centriole does not depend on dynamic actin to anchor to the plasma membrane. 3D visualization using Imaris. Oocyte's contour is shown in grey. Movie starts after drug addition. Z-stacks recorded every 40 and 37 seconds, for cytoD and latB, respectively. Scale bar: 5 μm. MC and DC correspond to mother centriole and daughter centriole, respectively. (B) Chart shows distance measurements of the centrioles to the plasma membrane. Blue rectangle shows when the inhibitory drug starts to be active.

4.6.2. Are the appendages connecting the mother centriole to the plasma membrane?

As shown in the previous sections, actin and microtubules do not play a role in anchoring the mother centriole to the plasma membrane during MII. Indeed, such close connection between centriole and the plasma membrane has previously not been documented in cell division. However, cases exist in which the centriole appears in close proximity to the plasma membrane: during cilia and immunological synapse formation (Reiter et al., 2012; Stinchcombe and Griffiths, 2014; Sung and Leroux, 2013, personal comunication). In both cases, the mother centriole anchors to the plasma membrane through its appendages providing the foundation of growing cilia, and the basis to re-organize the microtubule cytoskeleton for the delivery of the cytotoxic granules to the immunological synapse region, respectively.

Because of the similarity of these processes to our studied case, I wanted to test whether the same mechanism of direct anchoring through appendages to the plasma membrane also functions for the mother centriole in starfish oocytes.

i. Visualization of centriole anchoring by electron microscopy

Mother centriole appendages are best visualized by EM. Mother appendages can be observed as small rays radiating from the mother centriole and following its 9-fold symmetry (see ***Introduction section 1.5***). Therefore, we performed EM to assess whether a direct linkage between mother centriole and plasma membrane exists. Starfish oocytes were immobilized by high-pressure freezing or by chemical fixation (*see figure legend and* ***Material and Methods 3.7.6 i and ii***) preferentially at metaphase II, when a single mother centriole localizes to the outer spindle pole. This way we obtained several electron tomography datasets, which show the centriole structure and the relation between centriole and membrane at a much higher resolution than previously reported using thin section EM (Kato et al., 1990).

We could visualize that consistent with our confocal data, centrioles localize in very close proximity to the membrane during MII as well as during MI (*fig. 4.31 B and C, purple*). In the reconstructed tomograms, the conserved 9-fold symmetry

and triplet organization can be nicely recognized (*fig. 4.31 A*), confirming previous reports in starfish oocytes (Kato et al., 1990). The tomograms also allowed measurement of centriole length of ≈320nm (n=4), and a diameter of ≈170nm (n=4), which are also consistent with previous studies (Kato et al., 1990).

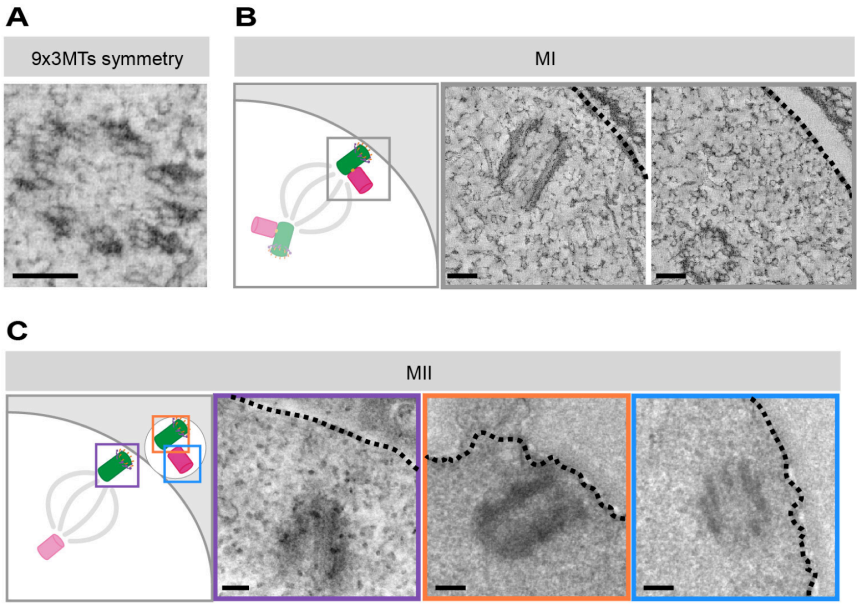

Figure 4.31: Starfish centrioles ultrastructure: starfish centrioles localize in close proximity to the plasma membrane in MI and MII. (A) Starfish centrioles have 9 triplets of microtubules. (B) One pair of centrioles from the MI outer spindle pole localizes in close proximity to the plasma membrane. Note how the two centrioles localize in an orthogonal orientation to each other (see schematic representation). Single sections from two different tomograms, obtained from two consecutive serial sections. (A) and (B) obtained by high-pressure freezing. (C) Starfish in metaphase II. This sample was obtained by chemical fixation. In *purple*, shows the presumed mother centriole close to the plasma membrane. In *orange* and *blue*, two orthogonally oriented centrioles obtained from two consecutive serial sections of the PBI. Note how the perpendicular centriole (*orange*) is closely localized to the plasma membrane. Black dashed lines indicate the oocyte outline. Scale bar: 100 nm.

The best datasets that were obtained correspond to two oocytes both in early MII stage, in which two centrioles can nicely be identified inside the PBI (*fig. 4.31 C and 4.32 A, centrioles in similar orientations are framed with the same colors - orange and blue*). These datasets can be used to extrapolate how the centriole might be anchored while within the oocyte. Meanwhile, we are performing more fixations to obtain centrioles anchored at the MII spindle.

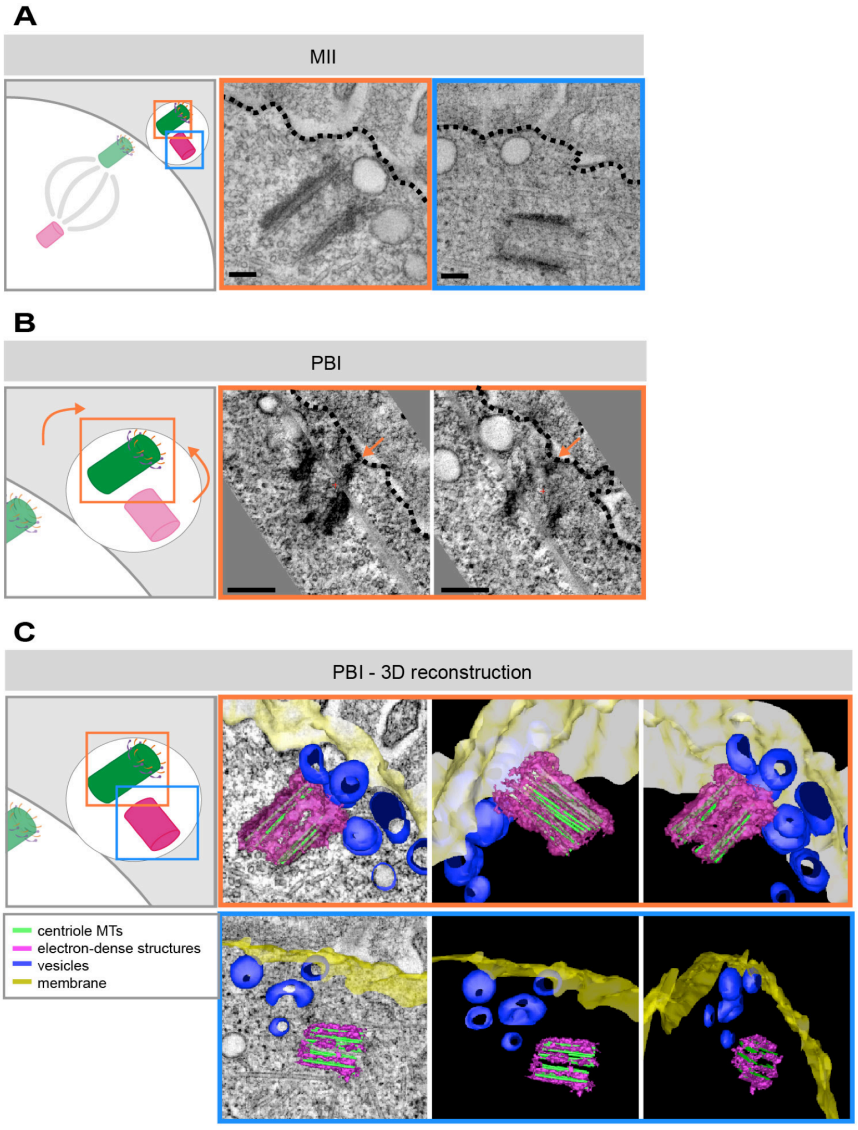

Figure 4.32: Ultrastructure of two centrioles contained in the same PBI. These samples were obtained by high-pressure freezing. (A) The perpendicular centriole inside the PBI is closely localized to the plasma membrane. (B) Same dataset as in (A), *orange*, but tomogram was rotated in a different orientation (see schematic representation, left). Orange arrows indicate points of connection between the centriole and the plasma membrane. Black dashed lines indicate the oocyte outline. Single sections from tomograms are shown. Scale bar: 100 nm. (C) 3D model of (A): each centriole is shown in the same corresponding colors *orange* and *blue*. Left panel shows the 3D model overlaid with the EM. Middle and left panels show two different rotations of the 3D model.

In these data sets, one can identify one centriole perpendicular and other parallel to the membrane (*fig. 4.31 C and 4.32 A, orange and blue, respectively*). This perpendicular orientation is typical of a mother centriole connected to the plasma membrane, acting as a basal body. Therefore this perpendicular centriole might correspond to the mother centriole. Indeed, this centriole clearly localizes in close proximity to the plasma membrane (*fig. 4.31 C and 4.32 A, orange*). Moreover, electron-dense connections are found between this centriole and the plasma membrane, which may correspond to mother appendages (*fig. 4.32 B – arrows – this data set corresponds to a 3D rotation of the tomogram shown in fig. 4.32 A, orange*). Multiple vesicles are found in close proximity to the presumed mother centriole (*fig. 4.32 A and C, orange*).

Interestingly, in both data sets, the centriole in a parallel orientation localizes further away from the plasma membrane, and does not show any type of connection with the plasma membrane (*fig. 4.31 C and 4.32 A*). This is further evidenced by the 3D models (fig. *4.32 C, blue*).

Clearly, more samples will be required to elucidate the ultrastructure of centriole anchoring to the cell membrane during MII. As starfish oocytes are very large cells, sectioning through an entire oocyte proved to be a very challenging and time-consuming process. Therefore, I initiated a collaboration with Matthia Winter-Karreman, who recently introduced an innovative method for single cell of such large proportions: after chemical fixation, an X-ray tomography is performed before serial sectioning (*see* ***Material and Methods section 3.7.6.ii***). This allows the identification of PB positioning and subsequent targeted sectioning of only the region of interest. Using this new technique, within a short time span, we obtained our first dataset (fig. *4.31 C*), and hope to acquire more data in the near future. This data will establish the ultrastructure of mother centriole anchored to the plasma membrane at MII.

In conclusion, the EM data reveals the close proximity of centrioles and the plasma membrane. I could visualize electron-dense connections between one of the centrioles and the cell membrane in the PBI, suggesting that a direct interaction via mother appendages is possible. Our new strategy that involves targeted sectioning using X-ray tomography promises to rapidly increase the

sample number and allow us to firmly establish the ultrastructure linking the centrioles to the plasma membrane in starfish oocytes.

ii. Perturbing mother appendages: an approach to understand centriole anchoring

To complement the EM data, we performed a functional assay by morpholino knockdown to perturb appendage formation. In ciliogenesis, mother centriole anchors to the plasma membrane through its distal mother appendages (composed of Odf2 and CEP164), therefore we targeted the two distal mother appendage proteins which I previously identified in the starfish transcriptome: Odf2 and CEP164.

Odf2 is one of the main upstream factors in the hierarchic process of mother appendage assembly (Ibi et al., 2011; Tateishi et al., 2013), and several proteins (Ninein, CEP164 and Chibby) depend on Odf2 to localize at the mother centriole (Ishikawa et al., 2005). In fact, depletion of Odf2 causes a complete inhibition of mother appendage formation, which directly affects cilia formation (Tateishi et al., 2013). Similarly, depletion of CEP164 in cultured cells impairs the formation of cilia (Graser et al., 2007).

First, in order to test morpholino efficacy, we monitored the effect of morpholinos in embryos. The growing embryo requires active centriolar protein translation as cell division progresses and more centrioles are required. Therefore, if morpholino perturbation is effective, problems in cell division and cilia formation are expected. Indeed we observe a phenotype in embryos treated with morpholinos against Odf2 or CEP164 (*fig. 4.33*) (n=10/10 for each morpholino). These embryos have highly asymmetric cell divisions, problems in development and a reduction in the number of cilia, when compared to control embryos. This indicates that the morpholinos work in embryos and effectively block mRNA translation with consequences at phenotypic level.

We then tested the effect of morpholino injection in oocytes; defects in spindle anchoring were monitored by EB3-mEGFP co-expression. However, both morpholinos (Odf2 and CEP164) did not show a phenotype in oocytes. The spindle still anchors normally to the plasma membrane and PBs form normally (data not shown). Possible explanations for the lack of phenotype could be: i)

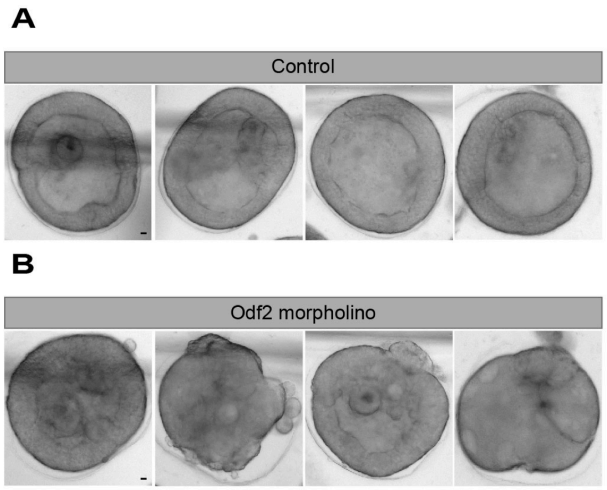

Figure 4.33: Odf2 morpholino affects the normal embryonic development. (A) Shows normal embryos upon injection of a control sense morpholino. See *fig. 4.4 B* for schematic representation. (B) Show mutant embryos after Odf2 morpholino injection. Cep164 morpholino show similar effects. Four examples are shown for each case. Scale bar: 10 μm.

oocytes have a high amount of stored mRNA, which complicates an effective mRNA inhibition, ii) morpholino efficiency strongly correlates with the turnover of the protein, i.e. the balance between protein production and degradation, which is the hardest factor to predict for candidate proteins. Proteins with a high turnover, as cyclin B (Wada et al., 2012), Dysferlin (Oulhen et al., 2014) and Mos (Tachibana et al., 2000), were shown to be effectively depleted upon morpholino injection in starfish oocytes. However, these proteins have a high turnover, which likely explains why morpholino treatment is so effective. Centrioles on the other hand are highly stable organelles, formed by proteins with a low turnover (Nigg, 2006). Therefore, even if the entire mRNA pool is inhibited upon morpholino injection, the mother appendages proteins might still remain, and be stable for several days or even months the time for which oocytes are normally stored in the mother's body. This might explain the lack of a phenotype in the oocyte: mother appendage proteins would still be present and centriole would still anchor. In contrast, during embryonic development, mRNA has to be constantly translated in order to produce more centriolar proteins for the newly forming centrioles. This would explain the strong morpholino phenotype in the embryos.

We have recently started to test morpholino injection against Chibby. Chibby was recently described to interact with CEP164, binding to the distal appendages. Chibby depletion was shown to impair cilia formation and therefore we included it in our study (Burke et al., 2014; Enjolras et al., 2012).

Upon morpholino injection, a phenotype is observed in the oocyte: in several instances the spindle fails to anchor, which directly leads to failure of PB extrusion (*fig. 4.34 A*). Indeed, when comparing to oocytes control (sense), a two-

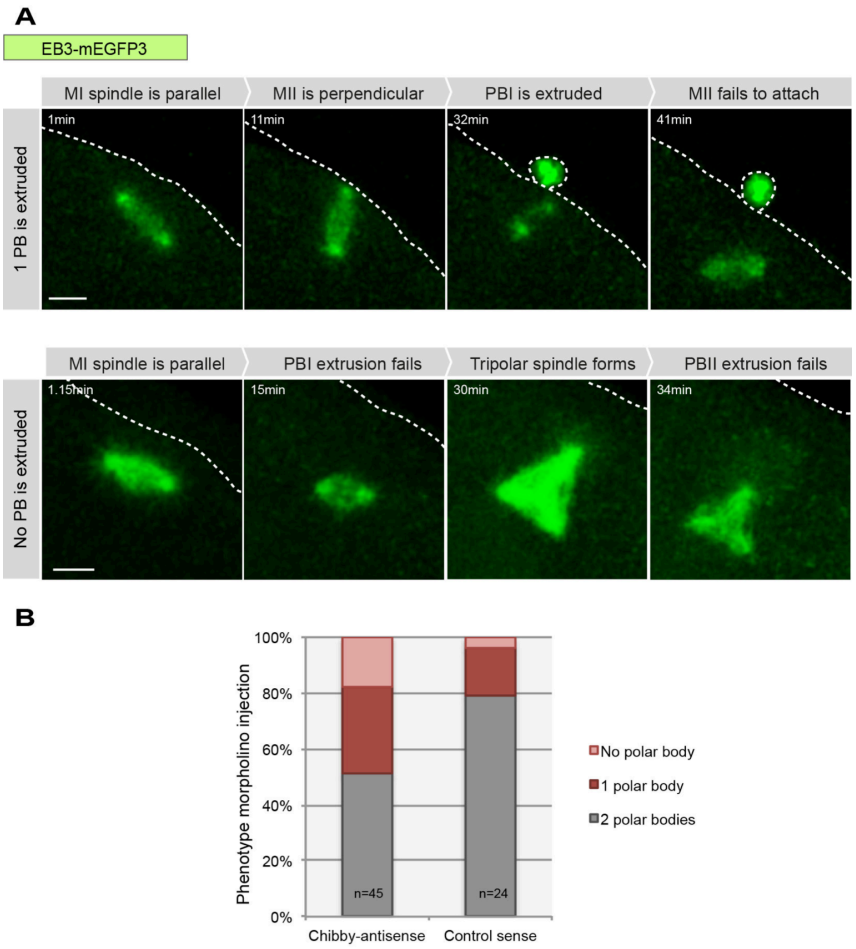

Figure 4.34: Chibby morpholino causes defects in spindle anchoring, and consequently PB extrusion. (A) Movie starts 1h after 1-MA hormone addition. Z-stacks recorded every 1 min (first panel) and 1min9sec (second panel). Pannels show a Z-projection of the acquired stacks. Scale bar: 10 μm. Dashed white line indicates the outline of the oocyte. (B) Quantification of oocytes injected with Chibby-antisense (n=45) morpholino or control (n=24)

fold increase can be observed in the number of oocytes (31% vs. 17% control) that fail to extrude PBI. Moreover, four-times more oocytes (18% vs. 4% control) fail to extrude any PB (*fig. 4.34* B). We are currently performing more experiments to obtain a larger data set (*fig. 4.34*).

Chibby binds to mother appendages, but it is not a stable structural component (Burke et al., 2014). So it might have a higher turnover, which might explain why a phenotype upon Chibby morpholino injection is obtained, in contrast to other appendage protein morpholinos.

Taken together, the preliminary results of Chibby morpholino experiments seem to support the hypothesis that mother centriole appendages are involved in mediating mother centriole anchoring.

Acknowledgements:

All EM data obtained by high-pressure freezing were obtained in collaboration with Julia König (Müller-Reichert's group, Dresden University of Technology), processed, sectioned and scanned all EM data.

Tomograms were acquired at European Molecular Biology Laboratory (EMBL) with the help of Devrim Acehan (Electron Microscopy Core Facility).

All EM data obtained by chemical fixation were obtained in collaboration with Matthia Winter-Karreman (Schwab's group (EMBL), who also performed all X-ray screening, sectioning and tomography of these samples.

Pedro Machado (Electron Microscopy Core Facility, EMBL) explained me how to generate the 3D models with 3DMOD.

Cloning, test and injection of Chibby-mEGFP were performed by Kalman Somogyi (Lénárt's group), who equally performed all morpholino experiments.

I am very grateful for all the help you provided.

5. DISCUSSION

"A thinker sees his own actions as experiments and questions as attempts to find out something. Success and failure are for him answers above all."

– Friedrich Nietzsche

5.1. Centrosomes – an evergreen topic for cell biology

Centrosomes have been a topic of intense investigation for more than a century now, and their structure and mechanisms of function are being uncovered one by one as cell biology progresses. In their role as organizers of the mitotic spindle, centrosomes were first described by Theodor Boveri during his postdoctoral studies around 1887 in the fertilized eggs of nematodes. By using the at the time novel staining by Heidenhain's iron haematoxylin, Boveri and his PhD student Eduard Fürst (Scheer, 2014) saw for the first time the little "dots", the centrioles, at the spindle poles of sea urchin and nematode eggs. After the invention of the electron microscope, the centrosomes became a popular organelle to study in the early 50's, because of their characteristic ultrastructure. More recently genetic screens and biochemical studies identified multiple molecular components that make up the centrioles, revealing the mechanisms of centrosome assembly, duplication and regulation of these. Currently, the newly developing techniques of super-resolution light microscopy are providing insights into the localization and the exact structural details of these molecular components. Biochemical purification and crystallography are also adding important details to correlate between molecular composition and centriole ultrastructure. Hopefully soon, all this can be brought together to result in a complete, molecular level explanation for centriole ultrastructure and function. With the development of all of these new technologies and the new insights

gained, these are great times to study centrioles. Still, with all the current understandings, many new questions remain open or arise anew.

5.2. Centriole elimination as a mechanism to control centriole number

One of the big questions in the centrosome field revolves around how centrosome number is maintained over many cell generations. Indeed, a single centrosome, composed of two centrioles, is present in each cell and duplicates exactly once per cell cycle during S-phase. The pre-existing centrosome is used as a template in a semiconservative duplication mechanism, similar in its principles to DNA replication (Kochanski and Borisy, 1990). After duplication and cell division, each daughter cell inherits one centrosome, composed of two centrioles.

However, during fertilization, the male and female gametes fuse and thus mechanisms are required to avoid a surplus of centrosomes in the zygote. If each gamete were to contribute a pair of centrioles, the embryo would inherit too many. The abnormal number of centrioles would then lead to the formation of multipolar spindles and consequently abnormal divisions and aneuploidy during embryo development. Therefore, prior to fertilization, during female gametogenesis, oocytes lose their centrioles in a process referred to as *centriole elimination*. By the time fertilization occurs, no maternal (i.e. originating from the oocyte) centrioles can be observed. However, microtubule-organizing centers (MTOCs) might be present, which do contain several of the pericentriolar material (PCM) components at their center, but they do not exhibit a centriole structure at their core.

During male gametogenesis, centriole structure is preserved. This is easily explained by the function of the centriole in flagellum formation, which is required for sperm movement. However, even for the sperm centriole structural modifications are observed: in some species sperm centrioles lose PCM proteins and, in some cases, partially loose microtubule triplets, in a process called *centrosome reduction* (*see* ***section 1.6.2***). In this case, the sperm centrosomal

structure has to be again completed after fertilization using maternal centrosomal proteins highly abundant in the egg. Hence, after fertilization, the first embryonic centrosome is in fact a fusion of the paternal (i.e. originating from the sperm) centriole structure supplemented with maternal cytoplasmic centrosomal proteins.

5.3. The mechanism of centriole elimination in starfish oocytes

5.3.1. Starting hypothesis

Although it is roughly known *when* centrioles are eliminated in oocytes of multiple species, it is not at all clear *how* centrioles are eliminated. As detailed in the ***Introduction*** (*see* ***section 1.6.3***), all that has been observed is a sequential loss of centriolar proteins followed by abrupt disappearance of the centriole structure. Apart from this descriptive characterization, no mechanism was identified that would explain centriole elimination. However, I found early descriptions of centriole elimination in starfish oocytes by Nemoto's laboratory (Shirato et al., 2006; Tamura and Nemoto, 2001; Uetake et al., 2002; Zhang et al., 2004). These studies completely lack molecular details, and solely rely on transmitted light microscopy to detect microtubule asters and electron microscopy (EM) to visualize centriole ultrastructure. Still, they were very intriguing for a couple reasons. They proposed the hypothesis that all "replicative" centrioles would be extruded into polar bodies (PBs) and only "non-replicative" centrioles would be retained in the mature egg. These observations motivated my studies and raised the question that became the main line of investigation in this work. As a centrosome is composed of a mother and a daughter centriole, my specific hypothesis were as follows:

i) Is the proposed differential "replicative" and "non-replicative" behavior potentially related to the difference between mother and daughter centriole?

ii) How does this relate to centriole elimination in starfish oocytes?

My intent was to address those questions using specific molecular markers for starfish. Fortunately, Péter Lénárt's laboratory had established conditions for high resolution live cell imaging of the starfish oocytes and a set of tools for molecular biology in this system. Taken together, these formed the basis for my project.

5.3.2. Molecular characterization of centriolar proteins in starfish

Because my main hypothesis was based on a mother/daughter difference, this required the establishment of the respective specific molecular markers. Therefore, for the first time I identified multiple homologs for starfish centriolar proteins, including general centriolar markers that label both mother and daughter centrioles and mother specific markers (*see* ***Results section 4.1***).

Starfish centriole composition is perfectly consistent with its position in the phylogenetic tree of life. Starfish centrosomes contain both *ancestral* and *holozoa* components (*see* ***Introduction section 1.3.3***). *Ancestral* components are present across all extant eukaryotes, and are related with centrosome's ancestral role as a basal body. *Holozoa* proteins are associated with a more recent centrosomal function as MTOC, and are only characteristic of holozoa (Carvalho-Santos et al., 2010; Hodges et al., 2010). Consistently, I could identify both functions in starfish centrosomes: as organizers of the spindle and as basal bodies of cilia in embryos.

I also observed that starfish centriolar protein composition is more closely related to other deuterostomes (*H. sapiens* and *S. purpuratus*), than to the protostomes such as *D. melanogaster* and *C. elegans* (*see* ***Results section 4.1.1***). Again consistent with the position occupied by starfish in the phylogenetic tree of life. Moreover, I was able to identify homologs for all human centriolar proteins, and show that the characteristic protein domains are also present in starfish homologs (*see* ***Results section 4.1.2***).

It is exciting to see that as we know more and more about centriole composition, more comparisons can be established between ultrastructure and molecular composition. Consequently, more comparisons between different species can be made. This will then contribute to a better understanding of

centrosome function and evolution. A few years ago, a project with this aim was initiated in Mónica Bettencourt-Dias' and José Leal's laboratories, available at http://mtoc-explorer.org/, in which I also participated. This project continues now as a community effort to compile and annotate the different centriolar structures that are known from different species. The identification of centriolar proteins and characterization of ultrastructure of starfish centrioles makes a significant contribution to this project.

5.3.3. Live-imaging with centriole molecular markers

After identification of starfish homologs of centriolar proteins, I used this information to generate specific fluorescent-protein-tagged centriolar markers. Centrin-2-mEGFP and Poc1-mEGFP to enable live imaging (*see* ***Results section 4.2.2***). Indeed, these markers allowed me for the first time to follow the entire centriole cycle during starfish meiosis. Moreover, I could at all times identify centrioles at the poles of the meiotic spindles: two pairs of centrioles are present at prophase I, each of which then organizes a spindle pole in metaphase I. The centriole pair closer to the plasma membrane is extruded into the first PB (PBI), and one pair remains in the oocyte. More importantly, I could for the first time clearly show that no centriole duplication occurs between meiosis I (MI) and meiosis II (MII). This results in a specific spindle organization during MII, with single centrioles at the spindle poles. This configuration is very different from the MI spindle and mitotic spindles. Therefore, after formation of the MII spindle, one centriole is extruded into the second PB (PBII), and a single centriole remains in the mature egg.

Taken together, I set up conditions allowing the real-time study of starfish centrioles using specific centriolar markers in live oocytes, for the first time. My observations confirm and also significantly extend previous studies that lacked fluorescent molecular markers and live imaging data. These tools allowed me to perform the first imaging of centrioles throughout the process of centriole elimination described in any animal species. This capacity for live imaging is indeed one of the strongest advantages of our system: in other systems there are

several issues that preclude live observation of centriole elimination. In the majority of these cases, oocytes are too opaque or sensitive for live imaging, or centriole elimination occurs very early in meiotic prophase I, and is therefore hard to access experimentally.

Hence, by establishing the live cell imaging conditions and molecular markers suitable for live imaging, I set the stage to use starfish as a model to study centrioles and to address the mechanism of centriole elimination in oocytes.

5.3.4. A mechanism for centriole elimination in starfish oocytes

Certainly some of the most important tools I developed were the markers specific for mother centriole (Odf2-mEGFP and Chibby-mEGFP) (*see* ***Results section 4.3***). Using these specific mother centriole markers, I could for the first time demonstrate that mother centrioles are specifically extruded into the two PBs. This mechanism works with high fidelity, as I never observed a mother centriole that remained in the mature egg (more than 100 oocytes followed). Moreover, I clearly show that mother centrioles, if retained in the egg, remain active and contribute to the formation of the zygotic spindle together with sperm centrioles. This then results in the formation of a multipolar spindle, which is incompatible with further embryonic development (*see* ***Results section 4.4***).

My observations are consistent with previous studies and show that mother centrioles are the ones with a “replicative” potential. In contrast, the “non-replicative” centrioles are the daughter centrioles, which lose microtubule nucleating activity. Although the mechanism for this is still unclear, my data clearly shows that daughter centrioles can be inactivated and eliminated at the end of the meiosis, which strongly contrasts with the mother centrioles that cannot be eliminated when retained in the mature egg. Indeed, both centrioles can exist in the same cytoplasm, but only the daughter centriole is eliminated (*see* ***Results section 4.4 and 4.5.2***). This rules out the presence of a cytoplasmic factor that would inactivate all maternal centrioles at the end of meiosis, as proposed previously (Sluder et al., 1989). In contrast, it suggests that

an intrinsic difference between mother and daughter centrioles that determines their susceptibility to elimination.

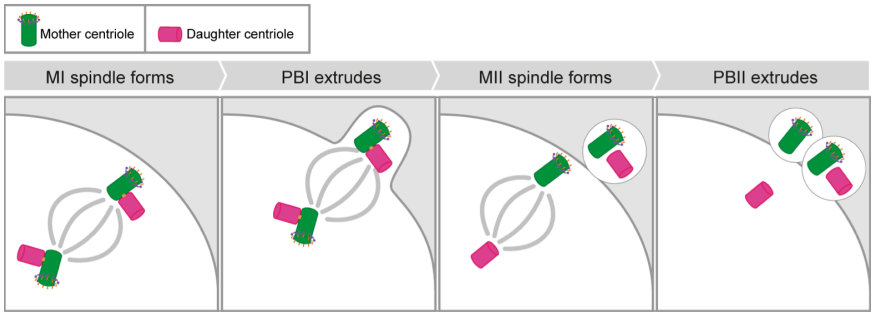

Figure 5.1: Replicative mother centrioles are extruded into the two PBs during starfish meiosis. Note that both spindle poles during metaphase I are equivalent and both contain one mother centriole. During metaphase II, the mother centriole specifically localizes to the outer spindle pole, and is then extruded into PBII. A single non-replicative daughter centriole remains inside the cytoplasm.

In conclusion, I defined a mechanism for centriole elimination, which depends on the differential "replicative potential" of mother and daughter centrioles (*fig. 5.1*). This mechanism of centriole elimination is composed of two main steps: i) replicative mother centrioles are eliminated by extrusion into the PBs, ii) the single non-replicative daughter centriole, which remains in the cytoplasm, is inactivated. For centriole elimination in starfish oocytes, the mother centriole has the active role. Essentially, the mother centriole eliminates itself: it is transported to the plasma membrane between MI and MII, where it anchors, and is thereby extruded into the PBII. Therefore, the mother centriole has to localize at the right place, at the right time, ensuring that it is extruded into the PB.

i. The mother centriole is specifically transported to the cell cortex

To get to the right place at the right time, the mother centriole needs to be transported. This is a specific feature of mother centrioles, and I could not observe a single daughter centriole moving to the plasma membrane. This transport occurs shortly after PBI extrusion, even before the complete disassembly of the MI spindle. The 3D trackings show that mother centriole

movement takes about 5min with an average speed of 2 μm/min ±0.8 to reach the plasma membrane. Strikingly, mother centriole transport is strongly directed towards the plasma membrane, as one can see in the live imaging movies.

My data indicates that dynamic actin is likely not involved in this transport – upon latrunculin B treatment, centriole can still move to the plasma membrane (*see* ***Results section 4.5.2.ii***). However, oocytes are surrounded by a thick and very stable actin cortex (Mori et al., 2011), which is difficult to completely depolymerize. Thus, I cannot exclude that cortical actin has a role in centriolar transport. Although this process is not likely driven by a dynamic actin polymerization, stable actin filaments might still be involved, serving as transport tracks for the mother centrioles. Further experiments are necessary to completely clarify actin involvement in this transport.

When microtubules are depolymerized, mother centriole still localizes to the plasma membrane, which would suggest that microtubules are not involved in the mother centriole transport (*see* ***Results section 4.5.2.i***). However, due to experimental limitations, I cannot rule out the involvement of microtubules in the transport. Nocodazole is added to the oocytes just before the mother centriole transport starts, shortly after PBI extrusion. Rapid depolymerization by nocodazole causes the collapse of the MI spindle, which brings, as a consequence, both centrioles to the plasma membrane. Similar results were observed upon microtubule depolymerization in MG-132-MII-arrested oocytes treated with nocodazole (*see* ***Results section 4.6.1.ii***): daughter centriole moves closer to the plasma membrane, *not* because is *transported*, but as a consequence of the MII spindle *disassembly*. Taken together, due to the multiple essential functions of microtubules at this stage, even if nocodazole is added at a very specific time, one cannot conclude that microtubules are *not* involved in the transport, when microtubule *disassembly* brings the centrioles *closer* to the plasma membrane.

In fact, other observations suggest that microtubules could be involved in mother centriole transport. Microtubule transport is normally associated with long-range directed transport (Atkinson et al., 1992; Langford, 1995; Lodish, 2008). Accordingly, i) mother centriole transport is highly directed towards the plasma membrane (*see* ***Results section 4.5.1***), and ii) mother centrioles can still be transported, even when they localize further to the plasma membrane

(approximately 10 μm away from the cell membrane, as in centrifuged oocytes, *see* ***Results section 4.5.2.iii***). In fact, such long microtubules do exist in starfish oocytes during meiosis, as they can capture chromosomes up to 40 μm away from the animal pole, during Prometaphase I (Mori et al., 2011).

Therefore, further experiments are necessary to clarify the role of microtubules in the mother centriole transport. For example, it would be interesting to test the effect on the transport speed with lower doses of nocodazole, which only partially depolymerize microtubules. One idea would be to use the modified centrifuged oocytes as system to test microtubule (and actin) depolymerization, as mother centrioles move longer distances.

Mother centriole transport is possibly dependent of a cytoplasmic gradient established upon nuclear envelope breakdown

I showed that the further mother centrioles localize from the nucleus, the less likely it is to move to the plasma membrane. This suggests that mother centrioles respond to an activity gradient, possibly established at nuclear envelope break down (NEBD) (*see* ***Results section 4.5.2.iv***). Centrioles are known to be efficient signaling centers, able to respond to multiple external signals (Arquint et al., 2014). Therefore it makes sense that they could interpret a cytoplasmic gradient and move accordingly. Indeed, multiple gradients are known to be established during mitosis (Fuller, 2010), and also in starfish meiosis. For example, Cdk1-cyclinB accumulates in the nucleus upon meiosis resumption, and creates a cytoplasmic gradient upon NEBD (Terasaki et al., 2003).

One interesting observation is that mother centrioles still move to the plasma membrane even when not organizing the meiotic spindle and distant from the chromosomes. This suggests that centriole movement is likely not dependent on a local protein gradient established around the chromosomes, as Ran-GTP.

One could test further this gradient hypothesis, by altering this gradient. One could first remove, by injection, cytoplasm from the animal pole of a non-centrifuged oocyte, and then inject it into a centrifuged oocyte, in which nucleus and centrioles are localized at 180° (recall that no mother centriole movement occurs in these oocytes – *see* ***Results section 4.5.2 iv***). Consequently, this would create a new gradient from the injection site. One could that determine if

the mother centriole movement is restored. Similar experiments of cytoplasm transplantation were performed by a PhD student in my laboratory (Johanna Bischof) and are in principle feasible.

Taken together, my experiments suggest that mother centriole transport does not depend on dynamic actin, and PBI cytokinesis and associated midbody formation. However the role of stable actin and microtubules as drivers of the mother centriole transport needs to be further clarified. Interestingly, mother centriole movement appears to be dependent on the distance to the nucleus, which might suggest that mother centrioles respond to a cytoplasmic gradient established during meiosis resumption.

ii. The mother centriole is anchored to the cell cortex

I could show that after transport, the mother centriole position stabilizes at the plasma membrane, in a process referred to as *anchoring*. By light and electron microscopy, I see that the mother centriole localizes very close to the plasma membrane (*see* ***Results section 4.6***). Indeed, the proximity of the spindle pole to the cortex in oocytes strongly contrasts with that of a regular mitotic spindle, in which long astral microtubules center the spindle in the middle of the cell far from the cell cortex (*see* ***Introduction section 1.6.4****, schematic representation shown in fig. 1.24 A*).

I showed that anchoring still happens if oocytes are treated either with actin- or microtubule-depolymerizing drugs during mother centriole transport. This suggests that neither dynamic actin nor microtubules are necessary for the anchoring to happen (*see* ***section Results 4.5.2i and ii***). Indeed, it is possible that just a close proximity of the mother centriole to the cell membrane might be sufficient for the mother centriole to anchor (*see* ***section Results 4.5.2i***).

Moreover, once anchored, the mother centriole does not detach upon actin and microtubule depolymerization in MII-arrested oocytes. Therefore, once established, neither actin nor microtubules are required to maintain the anchoring (*see* ***section Results 4.6.1***). Interestingly, upon taxol treatment (in MII-arrested oocytes), MII spindle extends and astral microtubules grow from the inner pole of the MII spindle; yet astral microtubule growth does not occur from the outer pole.

Clearly, mother centriole does not detach from the plasma membrane and remains anchored (*see* ***section Results 4.6.1.ii***).

Consistent with these live cell functional data, in our preliminary EM datasets, direct interactions of the presumed mother centriole to the plasma membrane can be seen (*see* ***section Results 4.6.2.i***). These two lines of evidence taken together strongly suggest that mother centriole is connected to the plasma membrane directly by mother centriole specific appendages, in a similar way to cilia formation and T cell activation (Ishikawa et al., 2005; Tanos et al., 2013, and personal communication from Stinchcombe). This suggests that a conserved molecular machinery for anchoring of the mother centriole is used in different situations, and employed to firmly position the mother centriole at a specific cortical location (*see fig. 5.2 for schematic representation*). For example, in ciliated cells, direct anchoring of the mother centriole to the plasma membrane is likely to provide stability as a base to allow ciliary movement. For T-cell activation, a direct mother centriole anchoring would also provide a stable base to allow the entire reorganization of the microtubule cytoskeleton, and create a clear directionality for the cytolytic granules' delivery. In the starfish oocyte, it would allow the entire spindle to stay in close proximity to the plasma membrane and in addition help to ensure the extrusion of the mother centriole. Additionally, through this positioning, it may also contribute to the extreme asymmetry of PB formation

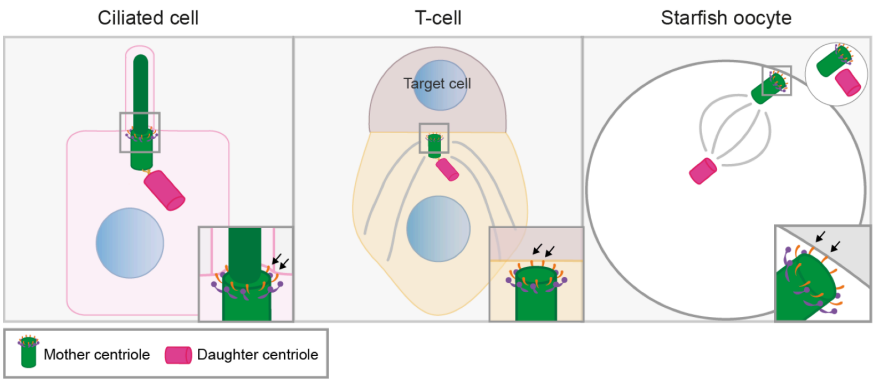

Figure 5.2: Mother centriole anchors directly to the plasma membrane via mother appendages in ciliated cells, T-cell and likely in starfish oocyte. Arrows show connection points to the plasma membrane (higher magnification insets).

(*fig. 5.2*).

Taken together, various lines of evidence indicate that the mother centriole specific appendages are necessary for the anchoring to happen. This explains why only mother centrioles anchor to the plasma membrane and why only these centrioles are extruded. In contrast, the lack of appendages would explain why a daughter centriole was never seen anchored to the plasma membrane, and why it remains in the cytoplasm of the mature egg.

iii. Future directions: the mother centriole is directly anchored to the plasma membrane through mother appendages

I am currently performing experiments to directly test this hypothesis: i) I am preparing samples for EM to obtain a higher number and better quality visualization of the appendages directly linking the mother centriole to the plasma membrane. ii) We are currently performing morpholino-mediated knockdown and following centriole positioning in those oocytes. This would provide a direct and a functional evidence for the involvement of mother centriole specific appendages.

Our morpholino approach against well-known mother distal appendages proteins (Odf2 and CEP164) did not cause defects in spindle anchoring during meiosis (*see in* ***Results section 4.6.2.ii***). Our explanation is that mother centriole appendages are very stable structures, formed by proteins with a low-turnover (Nigg, 2006), and thus remain in the cytoplasm despite the mRNA translational block by morpholinos.

We obtained promising results with another morpholino for the appendage-associated protein, Chibby. Indeed, preliminary tests showed defects in the spindle anchoring upon Chibby morpholino treatment. We are currently performing more experiments in order to further characterize this phenotype. Moreover, we are also currently imaging cells treated with Chibby morpholinos in in higher spatial and temporal resolution, using specific centriolar markers to directly follow centriolar dynamics. Also, we plan to use Chibby-mEGFP-expressing oocytes to control morpholino efficacy: if morpholino effectively blocks mRNA translation, reduced levels of Chibby-mEGFP will be observed by immunoblotting.

In parallel, we have developed mutant forms of Chibby, which might act as dominant negative, following the same strategy as previously described (Burke et al., 2014). We expect that this dominant negative approach may be even more effective than the morpholino approach. Chibby functions as a homodimer and therefore the dominant negative version could form inactive heterodimers, inactivating a large portion of the endogenous protein.

5.3.5. Hypothesis: why only the mother centriole can move and anchor?

Mother and daughter centrioles have a very different behavior during meiosis of starfish oocytes. All my data consistently show that the mother centriole has an intrinsic potential to move and anchor at the plasma membrane, a property that the daughter centriole lacks.

Firstly, regarding centriole structure, mother and daughter are clearly different. Mother centriole contains two sets of appendages that are not present in the daughter centriole (Paintrand et al., 1992; Vorobjev and YuS, 1982). These two set of appendages are involved in different functions: distal appendages bind to plasma membrane during ciliogenesis, whereas subdistal appendages bind to microtubules in interphase. Different proteins form each set of appendages: Odf2 (localizes to both distal and subdistal), CEP164 (distal) and CEP170 and Ninein (subdistal) (Azimzadeh and Marshall, 2010; Brito et al., 2012). These are proteins called *structural* because they "build" the centriole structure. Additional *non-structural* proteins then also bind differentially to the two centrioles: as in the case of Chibby, which binds to CEP164 (Burke et al., 2014).

In the current model for ciliogenesis, the mother centriole first associates with vesicles when still deep in the cytoplasm. Then it migrates to the plasma membrane carried by the vesicular trafficking machinery, where the vesicles fuse with the plasma membrane (*see* ***Introduction section 1.5.3.i***) (Reiter et al., 2012). Chibby binds to the mother appendage via CEP164, and to the vesicles via Rab8 (Burke et al., 2014), and therefore allows the mother centriole to be carried by the moving vesicles to the plasma membrane, where the mother centriole finally anchors (*fig. 5.3*).

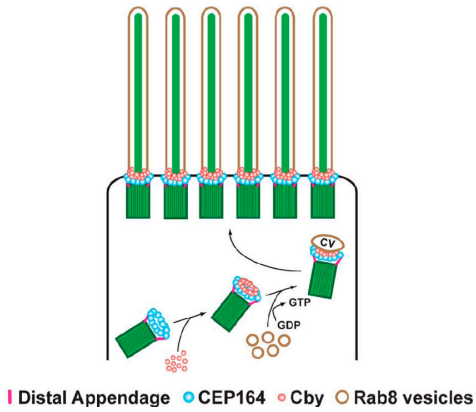

Figure 5.3. Chibby makes the connection between the distal mother appendage component Cep164 and the Rab8 vesicles. This allows mother centriole transport towards the plasma membrane, via the vesicular trafficking pathway. Figure adapted from (Burke et al., 2014).

I propose that in starfish oocytes, the mother centriole could use the same vesicle trafficking machinery to move to the plasma membrane and anchor (*fig. 5.3*). As only the mother centriole can associate with Chibby, and consequently with vesicles, this would explain why only this centriole is transported. Vesicular transport is well conserved among organisms. Two major types have been described: a long-range microtubule-driven, and a short-range actin-driven one (Langford, 1999; Stenmark, 2009). In starfish, both types of transport may occur sequentially and contribute to bring the mother centriole closer to the plasma membrane. Shortly, after the PBI extrusion, the *long-range* transport in microtubules would first occur – which corresponds with the fast movement I observe in the 3D tracks (*see* ***Results section 4.5.1***). At this point, mother centriole would localize close enough to the plasma membrane to anchor. Yet, if necessary, a *local* vesicle transport in actin filaments could mediate the final steps of the anchoring at the plasma membrane. At this point, vesicles would fuse with the plasma membrane and the mother centriole would anchor. My observations are consistent with this: first of all, multiple vesicles are seen in close proximity to the centriole anchored to the plasma membrane by EM (*see* ***Results section 4.6.2.i****, fig. 4.32 A and C, orange*). In contrast, no vesicles appear closely associated with the centriole we assume to be the daughter centriole (*see* ***Results section 4.6.2.i****, fig. 4.32 A and C, blue*).

Furthermore, upon actin depolymerization (*see* ***Results section 4.5.2.ii***), mother centriole is still transported to the plasma membrane. This could be explained because the long-range transport on microtubules is not affected. Upon microtubule depolymerization (*see* ***Results section 4.5.2.i***), both centrioles localize close to the plasma membrane, but then only one anchors. The mother centriole could even use a local vesicle transport mediated by actin to reach the final distance to the plasma membrane. However, actin-mediated transported would provide the last "adjustments", and not be essential, if microtubules are present (*see* ***Results section 4.5.2.ii***).

Other mechanisms might additionally help to direct centrioles towards the plasma membrane during transport. Some of the molecular motors are known to localize specifically to mother centrioles, such as the kinesin Kif24 (Kobayashi et al., 2011) and the dynein regulator NudE/L, which possibly recruits dynein to the centriole in a microtubule-dependent manner (Guo et al., 2006). The NudE/LIS1/Dynein complex could exert a pulling force in the astral microtubules of the mother centriole, as observed in mitosis (McNally, 2013) (*fig. 5.6 – final model*).

i. Future directions: how to evidence the parallels of mother centriole transport between starfish oocytes and ciliated cells?

To assess the similarities of the mother centriole transport in starfish oocytes and ciliated cells, it would also be important to: i) visualize vesicle dynamics and understand if this correlates with the mother centriole transport. ii) Explore the roles of molecular motors. NudE/L and Kif24 are both found in the starfish transcriptome. One could first assess the localization of these proteins, by fluorescent protein fusions. And then test their role in this transport: for example, commercial inhibitors for dynein (cilliobrevin D) are available and could be tested in starfish.

ii. Future directions: how to evidence the parallels of mother centriole anchoring between starfish oocytes, T-cells and ciliated cells?

To evaluate the similarities of the mother centriole anchoring in starfish oocytes, T-cells and ciliated cells, one could examine whether CP110 remains at the tip of the mother centriole marker after anchoring. CP110 is a distal centriole marker that inhibits cilia formation, and is therefore removed from the distal tip to allow ciliogenesis to happen (Schmidt et al., 2009; Spektor et al., 2007; Tsang et al., 2008). Indeed the Griffiths lab (at Cambridge Institute for Medical Research), which described the mother-appendage anchoring of the mother centriole in a T-cell, recently showed that CP110 is removed from the mother centriole's distal tip, when it is attached to the membrane (Stinchcombe, personal communication). As CP110 was also found in our starfish transcriptome, it would be interesting to understand if similarly CP110 is lost from mother centriole distal end during mother centriole anchoring in starfish oocytes. This could be addressed simply by imaging starfish CP110-GFP in live oocytes.

5.3.6. Hypothesis: how is the daughter centriole inactivated at the end of meiosis?

I observed that mother centrioles are replicative and need to be removed from oocyte's cytoplasm not to perturb embryonic development. In contrast, daughter centrioles become inactive in the end of meiosis, losing microtubule nucleating activity. This can be observed in various experiments (*see section* ***Results 4.4 and 4.5.2***). Clearly, an intrinsic difference exists between mother centrioles and daughter centrioles, which protects the mothers against elimination.

Note that the loss of microtubule nucleating activity by the daughter centriole marks when the centriole is *inactivated*, but does not report on its elimination. Centriole elimination is normally referred to as the collapse or disassembly of the centriole structure that is difficult to address with the GFP markers I have available. My assumption is that the daughter centriole is eliminated shortly after becoming inactive – it has been reported in *C.elegans* that centrioles first lose

their microtubule-nucleating activity, and are then eliminated in less than 30 min (Mikeladze-Dvali et al., 2012).

As explained in the ***Introduction***, in order to be fully matured, a centriole needs at least 1.5 cell cycles (Azimzadeh and Marshall, 2010; Hoyer-Fender, 2010; Kong et al., 2014; Vorobjev and YuS, 1982). However, the daughter centriole in starfish oocytes only nearly completed one full cycle, so it is not fully matured. It has been described in the literature, that in order to become a fully matured mother, the daughter centriole has to be *licensed* (*see* ***Introduction section 1.4.2***). For licensing two events have to occur: i) the daughter centriole has to be *modified* by PLK1 during early mitosis, and ii) centriole pairs have to be *disengaged* by separase, i.e. to lose its orthogonal orientation, process that is promoted by PLK1 (*see* ***Introduction section 1.4.2 i***) (Fırat-Karalar and Stearns, 2014; Tsou and Stearns, 2006; Tsou et al., 2009; Wang et al., 2011). Only after this licensing event, a daughter centriole can become a mother and duplicate. Moreover, studies also suggest that engagement is required to initiate appendage assembly in the new mother centriole (Nigg and Stearns, 2011).

In starfish oocytes this full licensing cycle is clearly interrupted: in a mitotic cell, after disengagement the centriole pair remains connected by a loose fibrous connection (Fu et al., 2015). However, in starfish oocytes, single centrioles localize at the MII spindle poles. One could hypothesize that the starfish daughter centriole cannot become a mother, possibly due to the fact that the licensing mechanism is impaired, likely because it is not engaged anymore. Consequently, the daughter centriole becomes non-replicative, cannot duplicate and is eliminated. In contrast, the mother centriole was already licensed in the previous cycle – and so it can further duplicate when retained in the cytoplasm. This overall hypothesis would fit with the idea that centrioles are differentially eliminated because of an intrinsic difference between mother and daughter centriole.

Unfortunately, the mechanisms of centriole disengagement and licensing are not completely understood even in the best characterized model systems. Still, the knowledge and tools that I currently have would allow me to address several key questions:

i. How does the daughter centriole lose its microtubule nucleating activity?

PLK1 localizes at the centrosomes during mitosis and has a role in the expansion of the PCM, which then nucleates microtubules (Kishi et al., 2009; Mennella et al., 2014; Woodruff et al., 2014). However, the detailed localization of PLK1 at centriole level has never been described, which I have the opportunity to access in starfish. I indeed tested for localization of human PLK1-mEGFP in starfish oocytes, and my preliminary data shows that during MII, hPLK1-mEGFP localizes preferentially to the mother centriole (*fig. 5.4*). Could this be an indication that only the mother centriole organizes PCM at this stage?

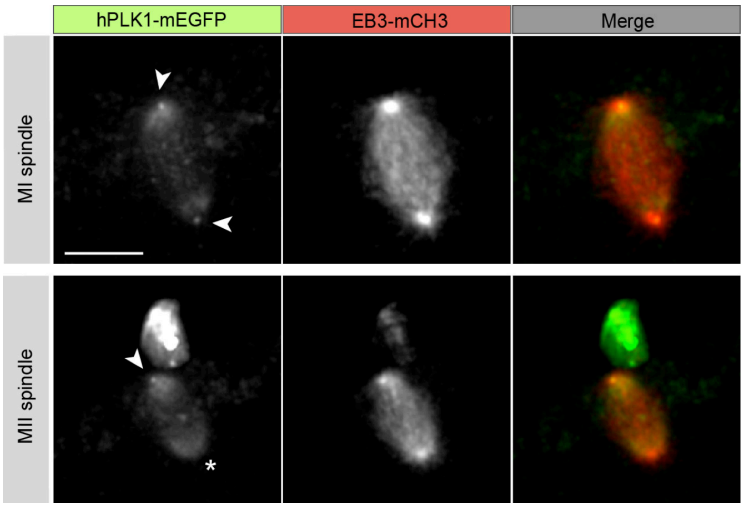

Figure 5.4: hPLK1-mEGFP localization in starfish oocytes. Two meiotic stages are shown: metaphase I and II. Metaphase I: PLK1-mEGFP appears to localize at both poles (arrowheads). Metaphase II: PLK1 shows preferential accumulation at the outer spindle pole (arrowhead), than at the inner pole (*). All pannels show a Z-projection of the acquired stacks. Scale: 10 μm

Previous studies showed that daughter centrioles have to be licensed, i.e. modified by PLK1, in order to recruit PCM (Wang et al., 2011). Therefore, this suggests that if the daughter is not licensed, no PCM is recruited, which will consequently cause the loss of the microtubule-nucleating activity. This would fit with the observed quick loss in the microtubule activity of the daughter centriole. To understand if PCM presence relates with the persistence of microtubule

nucleating activity, one would have to characterize the PCM composition and dynamics during the meiotic process. However, such characterization was never performed in starfish. A single study reports γ-tubulin (a PCM component) localizing to the maternal centriole retained upon PB suppression (Zhang et al., 2004), which I know now corresponds to the mother centriole. Therefore it is possible that only the mother centriole keeps the PCM, and this would explain how it retains its microtubule nucleating activity.

Studies by Wang and colleagues in cultured human cells provide two important conclusions: i) *de novo*-induced daughter centrioles lack PCM-organizing activity, and ii) *de novo*-induced daughter centrioles are segregated randomly during mitosis. Therefore, daughter centriole would likely be a mere passive passenger of the centrosome, segregated correctly during mitosis only because of its association with the mother centriole (Wang et al., 2011). Comparing these results to the starfish system, i) the daughter centriole would be approximatelly the same age as the *de* novo formed centrioles, and ii) the daughter centriole cannot move by itself (*see* ***Results sections 4.5.2***).

In conclusion, one could hypothesize that daughter centriole would drastically lose its microtubule-nucleating activity as a consequence of PCM loss at the end of meiosis. To address this question it would be important to correlate the loss of microtubule activity with a reduction of PCM proteins. This could be addressed by cloning PCM components already found in the starfish transcriptome, and then by monitor their localization by GFP fusions during meiosis.

ii. Are heterologous daughter centrioles equally inactivated at the end of meiosis?

Another very interesting direction would be to investigate the effect of introducing exogenous centrioles into a starfish oocyte. Would they behave similarly to the starfish centrioles? To address this question one could inject purified centrioles (as purification protocols for centrioles exist (Habermann and Lange, 2010; 2011)), and inject them into starfish oocytes. As both mother and daughter centrioles exist in the pool of purified centrioles, one could first distinguish them with my already described fluorescently tagged molecular markers, and then look at their fate during starfish meiosis. This would help to

understand if indeed mother centrioles have something that prevents them to be inactivated.

It could equally be possible to address the fate of *de novo* formed centrioles, by injecting PLK4 mRNA in starfish oocytes. PLK4 overexpression is known to be sufficient to trigger *de novo* formation of centrioles (Rodrigues-Martins et al., 2007). I performed a preliminary experiment injecting fluorescently tagged human PLK4 mRNA in starfish oocytes, and indeed multiple new MTOCs appear in the oocyte's cytoplasm (*fig. 5.5*) (these works were started as a Woods Hole summer project in collaboration with Inês Bento, from Mónica Bettencourt-Dias's group). First one would need to confirm that these new MTOCs are real centrioles by EM, for example, but then it would be very interesting to characterize them in terms of maturation state, using my fluorescent markers. They should be daughter centrioles (as they would need 1.5 cycles to be fully matured). Therefore, they could work as a good comparison to the daughter centriole remaining in the cell, in terms of PCM and microtubule nucleating dynamics during meiosis.

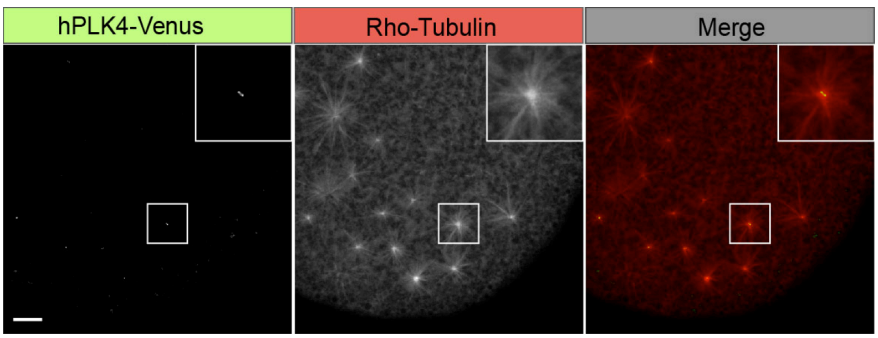

Figure 5.5: hPLK4-Venus induces the *de novo* formation of MTOCs in starfish oocytes. Insets show a higher magnification of the region inside the square. All pannels show a Z-projection of the acquired stacks. Scale: 10 μm

5.3.7. A hypothetical model for the molecular mechanism of centriole elimination in starfish oocytes

Summarizing my results and all the above hypotheses, a comprehensive model for the molecular mechanisms of centriole elimination emerges. I have shown that both mother centrioles and one daughter are extruded into the two PBs during starfish meiosis, with a single centriole remaining inside the mature egg. Mother centriole transport and anchoring would occur similar to that described for mother centriole movement in ciliogenesis; thus, mother centrioles would drive their own extrusion. First, mother centrioles associate with multiple vesicles through their mother appendages. Then, they would move towards the plasma membrane hitchhiking vesicular transport towards the cell periphery.

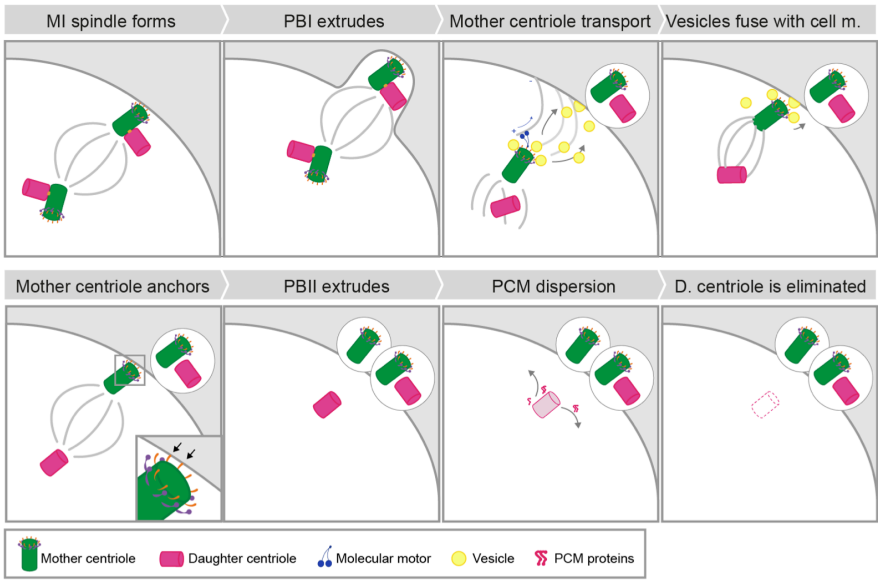

Figure 5.6: Model for centriole elimination in starfish oocytes. Vesicles (yellow) associate with the mother appendages. The mother centriole would be transported to the plasma membrane hitchhiking the secretory pathway. Molecular motors (blue) would direct the transport to the plasma membrane. Once close enough, vesicles would fuse with plasma membrane, and mother centriole would remain connected through mother appendages (black arrows). Daughter centriole would lose PCM at the end of meiosis (grey curved arrows) and would be consequently eliminated. Abbreviations: “m.”, membrane, “D.”, daughter

Molecular motors would direct this transport towards the plasma membrane and guarantee the efficacy of the process. Once close enough, the multiple vesicles at the mother appendages would fuse with the plasma membrane, where the mother centriole would anchor. This tight connection to the plasma membrane would guarantee that the mother centriole is always extruded into the PB.

The extrusion of mother centrioles into the PB would eliminate the replicative centrioles from the mature egg. The non-licensed daughter centriole would not be replicative, losing microtubule nucleating activity by PCM dispersion. As a consequence, its centriolar structure would be destabilized and ultimately collapse. As a result, all centrioles would be eliminated from the mature egg, and embryonic development may take its normal course after fertilization.

5.3.8. A general hypothesis: how to eliminate centrioles during female meiosis in animals

Considering the timing of centriole elimination, and although limited by the modest number of species that are described, I defined two major groups (*see **Introduction section 1.6.3***). One group (i) eliminates the centrioles during the long meiotic prophase (**humans**, **mouse**, **fruit fly**, **roundworm**, **frog**, etc.). The other group (iii) contains the echinoderms **sea urchin**, **starfish** and **sea cucumber**, and the bivalve **mussel**, and preserves their two pairs of centrioles up to the end of meiosis – *fig. 5.7*.

Considering this large diversity in timing of centriole elimination, a ubiquitous conserved mechanism seems rather unlikely. Instead, each group might have independently evolved a mechanism to eliminate centrioles. However, it is likely that only a limited number of possible strategies exist that use conserved molecular mechanisms (e.g. PCM dispersion) as building blocks. Therefore, in this context, the mechanisms discovered in my studies could be generalized to other species.

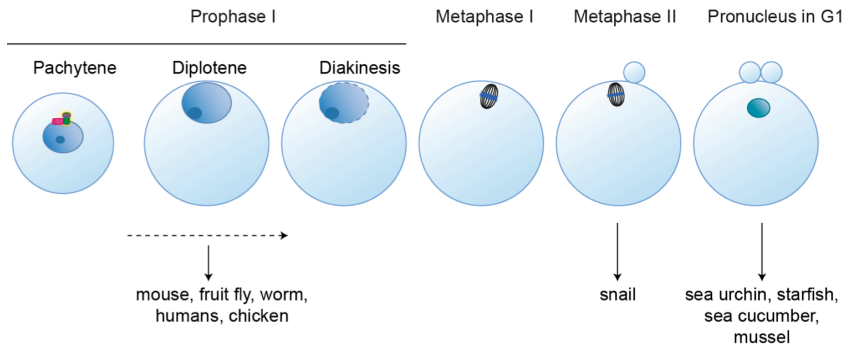

Figure 5.7: Different organisms eliminate centrioles at different meiotic stages. Centrioles are present in the pachytene stage of all species that have been described. Centrioles are eliminated before the diplotene stage of prophase I in organisms of the group (i). In this case the spindle is acentriolar. The snail *Lymnea stagnalis* has one pair of centrioles at meiosis onset. During metaphase II, the sperm basal body organizes the MII spindle with the single remaining centriole. Maternal centriole is then eliminated upon PBII extrusion – group (ii). In species of the group (iii), two pairs of centrioles organize the meiotic spindle, which are successfully extruded into the PBs during the meiotic divisions. A single centriole remains in the mature egg and is then eliminated. Dashed line at diakinesis stage indicates NEBD.

The mechanism described in the previous section (see 5.3.7) takes place in animals that organize a centrosomal meiotic spindle (species group (iii) – *see* ***Introduction section 1.6.3. iii***). Interestingly, for all the species of this group, the ultrastructure studies, which are available, show the close proximity of the centrioles to the plasma membrane, while organizing the meiotic spindle (Longo and Anderson, 1969; Miyazaki et al., 2005; Nakashima and Kato, 2001). This strikingly resembles the close proximity between the mother centriole and the plasma membrane that I reported for starfish, and also consistent with the ultrastructure studies reported in a lower resolution by (Kato et al., 1990). This suggests that in all these species, centriole elimination might occur similarly to starfish: the replicative mother centrioles mediate spindle anchoring and their own extrusion, whereas a single daughter centriole remains in the mature egg. Because this centriole was never licensed, I hypothesized that it would lose PCM and microtubule-nucleating activity, and would be eliminated.

Other species (species group (i) – *see* ***Introduction section 1.6.3. i***), the spindle is acentriolar and centrioles are eliminated during prophase I. In this case, daughter centrioles could be equally eliminated due to PCM and

microtubule-nucleating activity loss. However, this would not be sufficient to eliminate mother centrioles, as we have seen in starfish oocytes (*see* ***Results section 4.4***). Therefore, another specific mechanism or cytoplasmic factor, possibly from maternal origin, would be required to eliminate mother centrioles, which would not be present in the starfish oocytes or the other species of the group (iii).

5.4. Hypothesis: importance of the centrosome during meiosis

5.4.1. Does an acentriolar vs. centriolar spindle correlate with an internal vs. external oocyte maturation?

The centriole elimination timing determines the mechanism by which the meiotic spindle is assembled. If centriole elimination occurs during prophase I, as in group (i), spindle organization is acentriolar – i.e. organized without centrioles. When centriole elimination occurs only in the end of meiosis, as in group (iii), spindle is centriolar – i.e. organized by centrioles.

The centrosome controls the nuclear positioning in multiple systems (Dupin and Etienne-Manneville, 2011). Plus, in female oocytes the nucleus or spindle always localizes close to the cell cortex, which is important to limit PB size during extrusion (Fabritius et al., 2011). Indeed, species that retain centrosomes during meiosis, such as **sea cucumber** and **starfish**, centrosomes position the nucleus close to the cell cortex (Miyazaki et al., 2000, 2005). Also in *D. melanogaster,* nucleus relocalizes before centriole elimination takes place (*see* ***Introduction section 1.6.4 i***) (Zhao et al., 2012). In other species, such as *C. elegans and* mouse, the nucleus and MI spindle, respectively, are positioned to the cell cortex after centriole elimination. In these case alternative mechanisms exist for this correct positioning, which are independent of centrioles (*see* ***Introduction***

section 1.6.4 i) (Almonacid et al., 2014; Fabritius et al., 2011; Holubcová et al., 2013; Schuh and Ellenberg, 2008; Verlhac et al., 2000).

Interestingly, species that eliminate centrioles during prophase I – group (i) – undergo meiosis inside the maternal body. In contrast, most of the animals of group (iii) spawn shortly after NEBD completing oocyte maturation outside the female body (Ettensohn et al., 2004; Shirai et al., 1981). One interesting hypothesis is that nuclear and spindle positioning could occur without centrioles, but only when the oocyte would develop inside the maternal body. Indeed the maternal environment is important to control multiple oocyte maturation steps. For example, hormonal production from the follicle cells causes the release of the prophase I arrest in oocytes (Stetina and Orr-Weaver, 2011). Also in *D. melanogaster*, the nuclear relocalization is likely to be induced by follicle cells, as the nucleus often fails to migrate in *gurken* mutants, in which the follicle signaling into the oocyte is blocked (González-Reyes et al., 1995; Zhao et al., 2012). Therefore, in the absence of maternal environment, such as in the species of the group (iii), the centriole retention could guarantee a correct spindle positioning throughout the meiosis, and equally a source of other valuable polarization cues throughout the meiotic process. In the species of the group (i) developmental cues from the surrounding maternal environment would provide information to guide the different steps of the meiotic process, such as spindle positioning.

It would be interesting to understand whether an external meiotic process correlates with a preferential centriolar retention, and whether an internal meiotic process correlates with an earlier centriole elimination. In this situation, alternative mechanisms for nuclear or spindle positioning, independent of centrioles, might have evolved, which would be regulated by the internal maternal environment in which the oocyte matures.

A phylogenetic approach including more species would be essential to explore this hypothesis, in order to compare the mechanisms of spindle positioning in animals vs. centriole elimination timing vs. centriolar and acentriolar spindle.

5.5. Hypothesis: a preferential inheritance of centrosomes – lessons for stem cells

Starfish meiosis could be considered as a self-renewing asymmetric division that just spans two meiotic divisions: at each cell division the oocyte retains almost all of its initial content, with the exception of a small amount of cytoplasm extruded into the two PBs. More similarities exist between starfish oocytes and stem cells: a differential segregation of centrosomes (or centrioles in case of starfish) is observed between the stem cell and the daughter cells ((*see* ***Introduction section 1.5***).

Interestingly, which centrosome is inherited by the progenitor cell seems to be rather related with the centriole/centrosome that can remain attached during interphase and/or cell cycle. In the case of starfish, the "older" mother centriole is transported and anchored to the plasma membrane, and is consequently extruded into the PBs, whereas the "younger" daughter centriole remains in the mature egg. In *Drosophila* spermatogenesis, the older centrosome has a higher

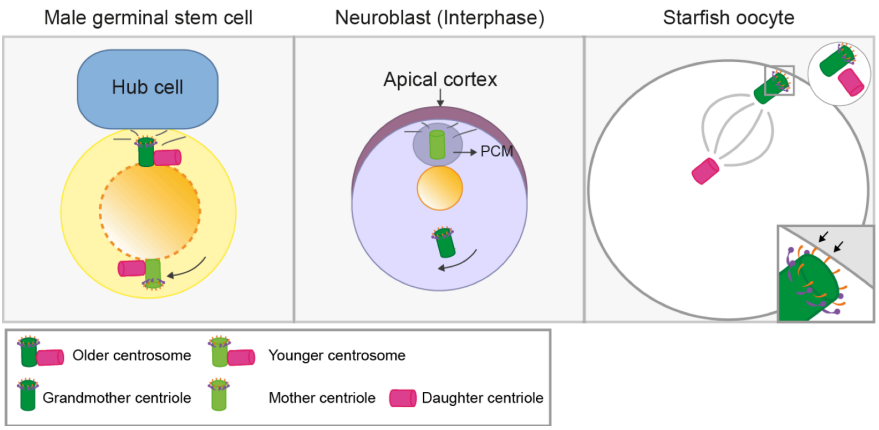

Figure 5.8: The centriole/centrosome inheritance is asymmetric whenever one of centrioles/centrosomes has the potential to remain anchored. In the male germinal stem cell, the older centrosome remains connected to the hub cell due to an higher microtubule nucleating activity. Similarly, in the neuroblast's interphase, the daughter centriole retains PCM and remains connected to the apical cortex. In starfish oocytes, only the mother centriole is able to anchor to the plasma membrane, likely via mother appendages.

microtubule-nucleating activity and is therefore trapped at the adherens junction between the male germ stem cell and the hub cell. In contrast, in *Drosophila* neuroblast, the daughter centriole retains its microtubule nucleating activity during interphase and remains therefore at all times at the apical site (*see* ***Introduction section 1.5.4***). In contrast to the mother centriole, which loses the anchoring to the plasma membrane (*fig. 5.8*).

It is clear that mother and daughter centrioles, and older or younger centrosomes have different microtubule nucleating activity, and therefore anchor differently. This difference appears to be an important factor to determine whether that centriole/centrosome is able to anchor to the plasma membrane and thereby influence spindle position in asymmetric divisions.

Taken together, I consider that the molecular mechanisms described in these studies, are not only relevant for starfish oocytes, but also provide interesting insights into conserved mechanisms of spindle positioning and asymmetric cell division in general.

6. APPENDIX

"So much universe, and so little time."

– Terry Pratchett

6.1. Homologs for centriolar proteins in different organisms

Table 1

Centrosomal proteins, localization and interaction partners

Centrosomal proteins	Homologs	Interaction partners	Centrosomal localization		
			PCM, mother, daughter procentriole	Proximal distal along	Region
Plk4/Sak	Plk4 (Dm), Zyg1 (Ce)	Cep152, CPAP, Sas6, FBXW5, β-TrCP/Slimb	M, D, Pr	P, A	Outer walls, lumen
Cep152	Asl (Dm), Cep152 (Dr)	CPAP, Plk4	M, D, PCM	P	Outer walls
Cep192	Spd2 (Ce, Dm)		M, D, PCM	A	Outer walls
hSas6	Sas6 (Ce, Dm, Dr, Tt, Pm), CrSas6/Bld12p (Cr)	Sas5, Ana2, Zyg1	Pr	P	Cartwheel (spokes, hub)
Cep135	Bld10 (Dm, Pm), Bld10p (Cr)	C-Nap1	M, D, Pr	P	Cartwheel, lumen, outer walls
Centrin	Cdc31 (Sc,Cp), CEN2/3 (Pt), CEN1 (Tt) VFL2 (Cr)	hPoc5, CP110	M, D, Pr	Di	Lumen
Cep120	Cep120 (Mm), Uni2 (Cr)	Ninein, Cep164, Cep290	M, D, Pr	A	Outer walls
CPAP	Sas4 (Ce, Dm)	γ-tubulin, αβ-tubulin, Cep152, Plk2, Plk4	M, D, Pr	P, A, Di	Cartwheel, lumen, walls
γ-tubulin	γ-tubulin (Dm, Pt), Gtu1 (Tt), Tbg1 (Ce), Tubg (Mm), Tug (Cr)	CDK5RAP2, CPAP, Cep170	M, D, Pr, PCM	P	Lumen
Centrobin	CG5690 (Dm), Cntrob (Mm), Nud1p (Sc), Cdc11p (Sp)	αβ-tubulin, Plk1, NEK2	D, Pr	P	Lumen, outer walls
CP110	CP110 (Dm)	Centrin, Cep97, Kif24 Cep76, Cep290,	M, D, Pr	Di	Cap
Cep97	Cep97 (Dm)	CP110, Cep76, Kif24	M, D, Pr	Di	Cap
Cep76	Cep76 (Xl, Dr)	CP110, Cep97, Kif24	M, D, Pr	Di	
ε-tubulin	Bld2 (Cr), Tube1 (Dr, Mm, Xl)	EB1	M, D, Pr	Di, A	Subdistal appendages, outer walls
δ-tubulin	Tubd (Dr, Mm, Xl), Uni3 (Cr), δPT1 (Pt)		M, D, Pr	P	Outer walls
hPoc5	Poc5 (Cr, Pm)	Centrin	M, D	Di, A	Lumen
hPoc1	Poc1 (Dm, Cr, Tt, Pm)	αβ-tubulin	M, D, Pr	Di, A	Lumen, walls
Ofd1	Ofd1 (Mm), BUG11 (Cr)	γ-tubulin	M, D, Pr	Di, A	Lumen
Odf2	Odf2 (Mm)	Ninein, Trichoplein	M	Di	All appendages
Cep164	XP_929307 (Mm), NP_611787 (Dm), XP_697015 (Dr)		M	Di	Distal appendages
Ninein	Nin (Dr, Mm)	γ-tubulin, Odf2, Trichoplein, EB1	M	Di	Subdistal appendages
EB1	Mal3 (Sp), Bim1 (Sc)	CDK5RAP2, FOP, Cep290, Cep170	M	Di	Subdistal appendages
Cep170	Cep170 (Mm)	Plk1, EB1	M	Di	Subdistal appendages
CAP350	Cep350 (Mm)	FOP	M, D	A	
FOP	Fgfr1op (Mm)	CAP350, EB1	M, D	A	Outer walls
Kif24	Kif24 (Mm)	CP110, Cep97	M	Di	Subdistal appendages
CDK5RAP2	Cnn (Dm), CDK5RAP2 (Mm)	Cdc20, PCNT, γ-tubulin, EB1	M, PCM	Di	Outer walls, appendages
C-Nap1	Cep250 (Mm)	Cep135	M, D	P	Linker
Plk1	Cdc5 (Sc), Plk1 (Dr, Mm), Plk1/2 (Ce), Plo1 (Sp), Polo (Dm)	Cep170	PCM		
Plk2	Plk2 (Dm, Mm), Plk2b (Dr)	CPAP	M, D		
β-TrCP	Slimb (Dm), β-TrCP (Mm)	SKP1, Plk4	Centrosome		
Cul1	Cul1 (Ce, Mm, Sp), Cul1a (Dr)	SKP1, SKP2, PPP1CA	M	Di	
Stil	Ana2 (Dm), Sas5 (Ce)	Sas6 (Ce, Dm)	M, D, BB	P, Di	

Figure 6.1: List of human centriolar proteins, which corresponds to the protein nomenclature adopted. A list of known homologs, interaction partners, and centriolar localization details is provided. Centriolar localization was considered accordingly to three classes: (1) mother centriole (M), daughter centriole (D) or procentriole (Pr); (2) proximal region (P), distal region (Di) or along the centriole (A); (*to be continued in the next page*)

(*Figure. 6.1 Continuation*) and (3) detailed ultrastructural description. List of organisms abbreviations: Ce, *Caenorhabditis elegans*; Cr, *Chlamydomonas reinhardtii*; Dm, *Drosophila melanogaster*; Dr, *Danio rerio*; Mm, *Mus musculus*; Pt, *Paramecium tetraurelia*; Sc, *Schizosaccharomyces cerevisiae*; Sp, *Schizosaccharomyces pombe*; Tt, *Tetrahymena thermophila*; Xl, *Xenopus laevis*. Figure and legend adapted from (Brito et al., 2012).

6.2. Summary table for categories

	g0m1	g1m0	g1m1	g2m0	g2m1	g2m2	total
Number	101	464	2221	147	874	59	3866
Percentage (%)	3	12	57	4	23	2	100

Figure 6.2: Centriolar marker validation - detailed description of the categories obtained upon centriole detection and categorization. The blue rectangles indicate the expected categories.

6.3. Protein alignment

6.3.1. Centrin-2

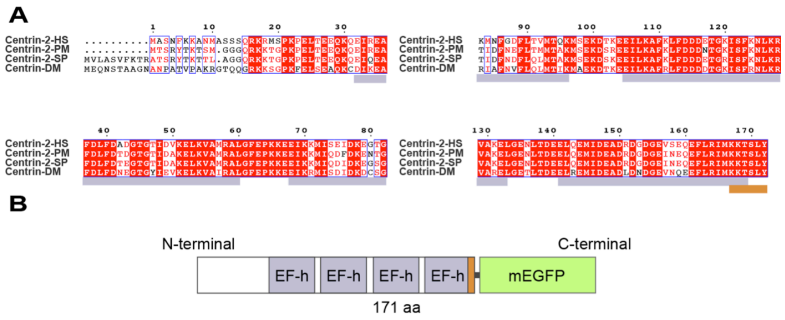

Figure 6.3: Starfish Centrin-2 and protein alignment (*to be continued in the next page*).

(*Figure 6.3 continuation*): (A) Protein alignment for the following organisms: HS, *Homo sapiens*; PM, *Patiria miniata* (starfish); SP: *Strongylocentrotus purpuratus* (sea urchin)*;* DM, *Drosophila melanogaste*r. Red highlight indicates region of homology between all species. Red letter indicates an amino acid substitution from same chemical group. Black letters indicate region of no homology. The colored domains indicate the protein domains in the schematic representation (B). (B) EF-h: EF-hand Calcium binding domain; orange: conserved sequence KKTSLY, characteristic of centriole-associated centrins.

6.3.2. Poc1

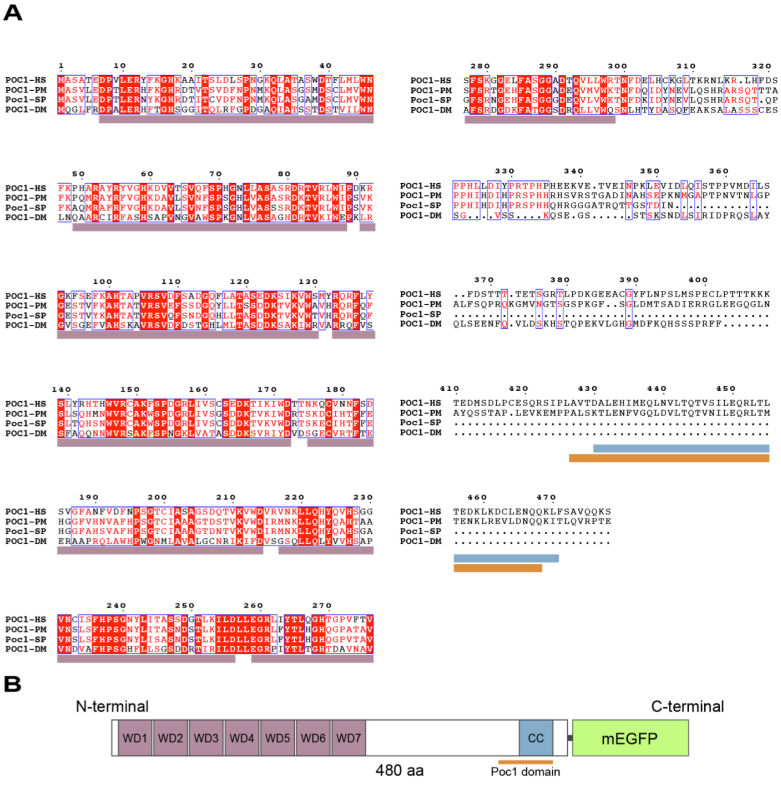

Figure 6.4: Starfish Poc1 and protein alignment. (A) Protein alignment for the following organisms: HS, *Homo sapiens*; PM, *Patiria miniata* (starfish); SP: *Strongylocentrotus purpuratus* (sea urchin)*;* DM, *Drosophila melanogaste*r. Red highlight indicates region of homology between all species. Red letter indicates an amino acid substitution from same chemical group. Black letters indicate region of no homology. The colored domains indicate the protein domains in the schematic representation (B) (*to be continued*).

(*Figure 6.4 continuation*): (B) WD1–7 indicate the seven WD40 domains; orange: Poc1 domain; CC: coiled-coil domain.

6.3.3. Odf2

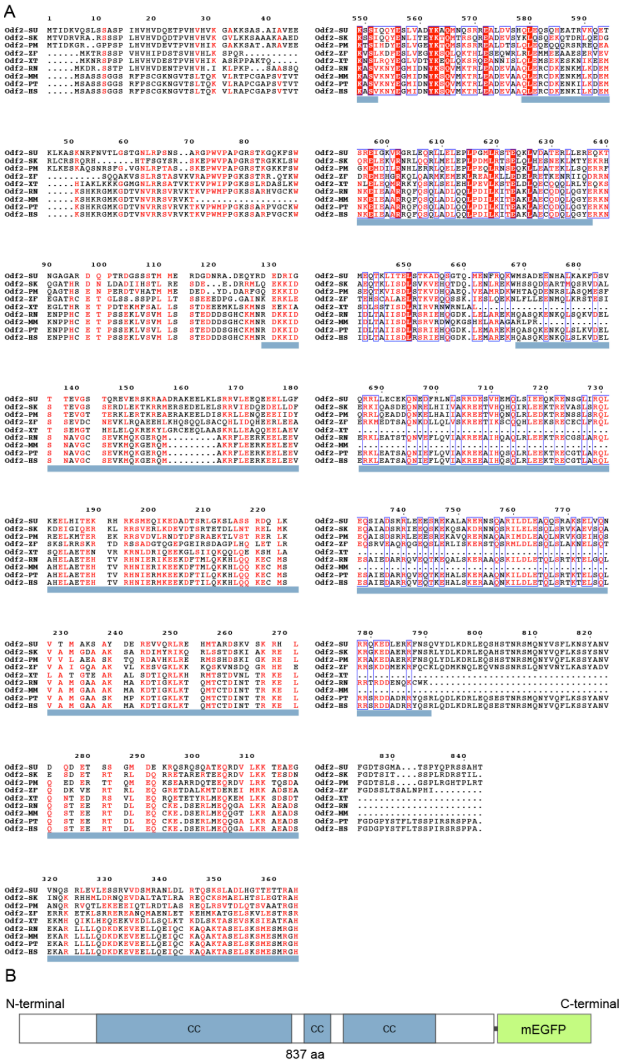

Figure 6.5: Starfish Odf2 and protein alignment. (A) Protein alignment for the following organisms: SU, *Strongylocentrotus purpuratus;* SK, Saccoglossus kowalevskii; PM, *Patiria miniata* (starfish); ZF: *Danio rerio* (zebrafish); XT, *Xenopus tropicalis;* (*to be continued*)

(*Figure 6.5 continuation*): RN, *Rattus norvegicus;* MM: *Mus musculus*; PT: *Pan troglodytes;* HS, *Homo sapiens.* Red highlight indicates region of homology between all species. Red letter indicates an amino acid substitution from same chemical group. Black letters indicate region of no homology. The colored domains indicate the protein domains in the schematic representation (B). (B): CC: coiled-coil domain.

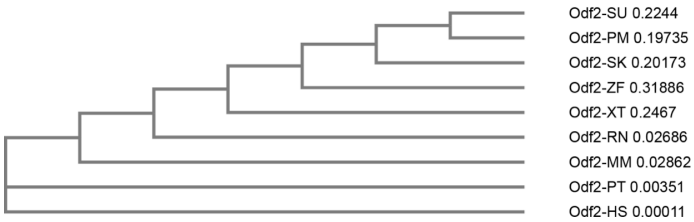

Figure 6.6: Odf2 phylogenetic tree generated by Clustal Omega (*see* ***Material and methods section 3.1***). As expected, starfish Odf2 is more closely related to the sea urchin protein. SU, *Strongylocentrotus purpuratus;* PM, *Patiria miniata* (starfish); SK, Saccoglossus kowalevskii; ZF: *Danio rerio* (zebrafish); XT, *Xenopus tropicalis;* RN, *Rattus norvegicus;* MM: *Mus musculus*; PT: *Pan troglodytes;* HS, *Homo sapiens.*

6.3.4. Chibby

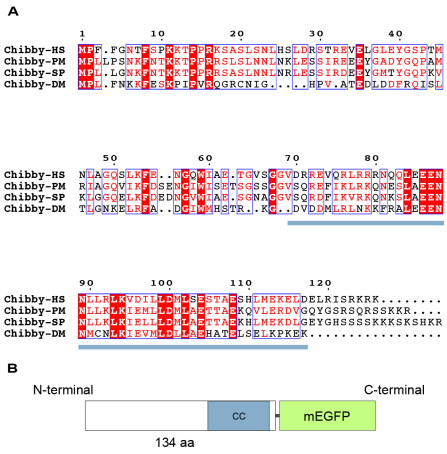

Figure 6.7: Starfish Odf2 and protein alignment. (A) Protein alignment for the following organisms: HS, *Homo sapiens*; PM, *Patiria miniata* (starfish); SP: *Strongylocentrotus purpuratus* (sea urchin)*;* DM, *Drosophila melanogaste*r. Red highlight indicates region of homology between all species. Red letter indicates an amino acid substitution from same chemical group. Black letters indicate region

of no homology. The colored domains indicate the protein domains in the schematic representation (B). (B): CC: coiled-coil domain.

6.4. Chibby localization in MII

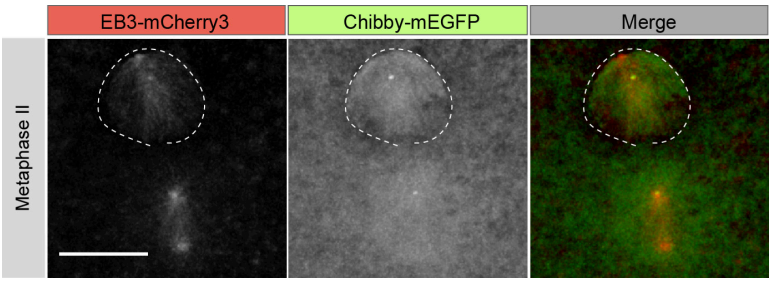

Figure 6.8: Chibby-mEGFP localization to the outer pole of MII spindle. Double injection with the mother centriole marker Chibby-mEGFP and EB3-mCherry3. All pannels show a Z-projection of the acquired stacks. Scale bar: 10μm. Dashed line surrounds the PBI.

REFERENCES

"Le seul véritable voyage, (...) ce ne serait pas d'aller vers de nouveaux paysages, mais d'avoir d'autres yeux, de voir l'univers avec les yeux d'un autre, de cent autres, de voir les cent univers que chacun d'eux voit, que chacun d'eux est."

("The only true voyage of discovery (…) would be not to visit new landscapes, but to possess other eyes, to see the universe through the eyes of another, of a hundred others, to see the hundred universes that each of them sees").

– Marcel Proust

Albertson, D.G. (1984). Formation of the first cleavage spindle in nematode embryos. Dev. Biol. *101*, 61–72.

Albertson, D.G., and Thomson, J.N. (1993). Segregation of holocentric chromosomes at meiosis in the nematode, Caenorhabditis elegans. Chromosome Res. Int. J. Mol. Supramol. Evol. Asp. Chromosome Biol. *1*, 15–26.

Almonacid, M., Terret, M.-É., and Verlhac, M.-H. (2014). Actin-based spindle positioning: new insights from female gametes. J. Cell Sci. *127*, 477–483.

Anderson, C.T., and Stearns, T. (2009). Centriole age underlies asynchronous primary cilium growth in mammalian cells. Curr. Biol. CB *19*, 1498–1502.

Antoniades, I., Stylianou, P., and Skourides, P.A. (2014). Making the Connection: Ciliary Adhesion Complexes Anchor Basal Bodies to the Actin Cytoskeleton. Dev. Cell *28*, 70–80.

Arquint, C., Gabryjonczyk, A.-M., and Nigg, E.A. (2014). Centrosomes as signalling centres. Philos. Trans. R. Soc. B Biol. Sci. *369*, 20130464.

Atkinson, S.J., Doberstein, S.K., and Pollard, T.D. (1992). Moving off the beaten track. Curr. Biol. *2*, 326–328.

Azimzadeh, J. (2014). Exploring the evolutionary history of centrosomes. Philos. Trans. R. Soc. B Biol. Sci. *369*, 20130453.

Azimzadeh, J., and Marshall, W.F. (2010). Building the Centriole. Curr. Biol. CB *20*, R816–R825.

Azoury, J., Lee, K.W., Georget, V., Rassinier, P., Leader, B., and Verlhac, M.-H. (2008). Spindle positioning in mouse oocytes relies on a dynamic meshwork of actin filaments. Curr. Biol. CB *18*, 1514–1519.

Badano, J.L., and Katsanis, N. (2006). Life without Centrioles: Cilia in the Spotlight. Cell *125*, 1228–1230.

Barakat, H., Geneviere-Garrigues, A.-M., Schatt, P., and Picard, A. (1994). Subcellular distribution of aster-nucleated microtubule length: A more or less mitotic status of cytoplasmic areas during meiosis I of starfish oocytes. Biol. Cell *81*, 205–213.

Basto, R., Lau, J., Vinogradova, T., Gardiol, A., Woods, C.G., Khodjakov, A., and Raff, J.W. (2006). Flies without Centrioles. Cell *125*, 1375–1386.

Becalska, A.N., and Gavis, E.R. (2009). Lighting up mRNA localization in Drosophila oogenesis. Development *136*, 2493–2503.

Blachon, S., Cai, X., Roberts, K.A., Yang, K., Polyanovsky, A., Church, A., and Avidor-Reiss, T. (2009). A Proximal Centriole-Like Structure Is Present in Drosophila Spermatids and Can Serve as a Model to Study Centriole Duplication. Genetics *182*, 133–144.

Blachon, S., Khire, A., and Avidor-Reiss, T. (2014). The origin of the second centriole in the zygote of Drosophila melanogaster. Genetics *197*, 199–205.

Boisvieux-Ulrich, E., Lainé, M.C., and Sandoz, D. (1989). In vitro effects of colchicine and nocodazole on ciliogenesis in quail oviduct. Biol. Cell Auspices Eur. Cell Biol. Organ. *67*, 67–79.

Boisvieux-Ulrich, E., Lainé, M.-C., and Sandoz, D. (1990). Cytochalasin D inhibits basal body migration and ciliary elongation in quail oviduct epithelium. Cell Tissue Res. *259*, 443–454.

Bornens, M. (2012). The Centrosome in Cells and Organisms. Science *335*, 422–426.

Breugel, M. van, Hirono, M., Andreeva, A., Yanagisawa, H., Yamaguchi, S., Nakazawa, Y., Morgner, N., Petrovich, M., Ebong, I.-O., Robinson, C.V., et al. (2011). Structures of SAS-6 Suggest Its Organization in Centrioles. Science *331*, 1196–1199.

Brito, D.A., Gouveia, S.M., and Bettencourt-Dias, M. (2012). Deconstructing the centriole: structure and number control. Curr. Opin. Cell Biol. *24*, 4–13.

Brohmann, H., Pinnecke, S., and Hoyer-Fender, S. (1997). Identification and Characterization of New cDNAs Encoding Outer Dense Fiber Proteins of Rat Sperm. J. Biol. Chem. *272*, 10327–10332.

Brunet, S., and Verlhac, M.H. (2011). Positioning to get out of meiosis: the asymmetry of division. Hum. Reprod. Update *17*, 68–75.

Burke, M.C., Li, F.-Q., Cyge, B., Arashiro, T., Brechbuhl, H.M., Chen, X., Siller, S.S., Weiss, M.A., O'Connell, C.B., Love, D., et al. (2014). Chibby promotes ciliary vesicle formation and basal body docking during airway cell differentiation. J. Cell Biol. *207*, 123–137.

Calarco, P.G. (2000). Centrosome precursors in the acentriolar mouse oocyte. Microsc. Res. Tech. *49*, 428–434.

Carabatsos, M.J., Combelles, C.M., Messinger, S.M., and Albertini, D.F. (2000). Sorting and reorganization of centrosomes during oocyte maturation in the mouse. Microsc. Res. Tech. *49*, 435–444.

Carvalho-Santos, Z., Machado, P., Branco, P., Tavares-Cadete, F., Rodrigues-Martins, A., Pereira-Leal, J.B., and Bettencourt-Dias, M. (2010). Stepwise evolution of the centriole-assembly pathway. J. Cell Sci. *123*, 1414–1426.

Carvalho-Santos, Z., Azimzadeh, J., Pereira-Leal, J.B., and Bettencourt-Dias, M. (2011). Tracing the origins of centrioles, cilia, and flagella. J. Cell Biol. *194*, 165–175.

Carvalho-Santos, Z., Machado, P., Alvarez-Martins, I., Gouveia, S.M., Jana, S.C., Duarte, P., Amado, T., Branco, P., Freitas, M.C., Silva, S.T.N., et al. (2012). BLD10/CEP135 Is a Microtubule-Associated Protein that Controls the Formation of the Flagellum Central Microtubule Pair. Dev. Cell *23*, 412–424.

Chaigne, A., Verlhac, M.-H., and Terret, M.-E. (2012). Spindle positioning in mammalian oocytes. Exp. Cell Res. *318*, 1442–1447.

Chang, J., Seo, S.G., Lee, K.H., Nagashima, K., Bang, J.K., Kim, B.Y., Erikson, R.L., Lee, K.-W., Lee, H.J., Park, J.-E., et al. (2013). Essential role of Cenexin1, but not Odf2, in ciliogenesis. Cell Cycle Georget. Tex *12*, 655–662.

Chang, P., Giddings, T.H., Winey, M., and Stearns, T. (2002). ε-Tubulin is required for centriole duplication and microtubule organization. Nat. Cell Biol. *5*, 71–76.

Chen, C.-H., Howng, S.-L., Cheng, T.-S., Chou, M.-H., Huang, C.-Y., and Hong, Y.-R. (2003). Molecular characterization of human ninein protein: two distinct subdomains required for centrosomal targeting and regulating signals in cell cycle. Biochem. Biophys. Res. Commun. *308*, 975–983.

Chiba, K., Sato, E., and Hoshi, M. (1997). Detection of In Vivo Proteasome Activity in a Starfish Oocyte Using Membrane-Impermeant Substrate. J. Biochem. (Tokyo) *122*, 286–293.

Conduit, P.T., and Raff, J.W. (2010). Cnn Dynamics Drive Centrosome Size Asymmetry to Ensure Daughter Centriole Retention in Drosophila Neuroblasts. Curr. Biol. *20*, 2187–2192.

Courtois, A., Schuh, M., Ellenberg, J., and Hiiragi, T. (2012). The transition from meiotic to mitotic spindle assembly is gradual during early mammalian development. J. Cell Biol. *198*, 357–370.

Cunha-Ferreira, I., Bento, I., and Bettencourt-Dias, M. (2009). From zero to many: control of centriole number in development and disease. Traffic Cph. Den. *10*, 482–498.

Dåvring, L., and Sunner, M. (1973). Female meiosis and embryonic mitosis in Drosophila melanogaster. Hereditas *73*, 51–64.

Dawe, H.R., Farr, H., and Gull, K. (2007). Centriole/basal body morphogenesis and migration during ciliogenesis in animal cells. J. Cell Sci. *120*, 7–15.

Debec, A., Sullivan, W., and Bettencourt-Dias, M. (2010). Centrioles: active players or passengers during mitosis? Cell. Mol. Life Sci. CMLS *67*, 2173–2194.

Doxsey, S. (2001). Re-evaluating centrosome function. Nat. Rev. Mol. Cell Biol. *2*, 688–698.

Dumont, J., and Desai, A. (2012). Acentrosomal spindle assembly and chromosome segregation during oocyte meiosis. Trends Cell Biol. *22*, 241–249.

Dumont, J., Petri, S., Pellegrin, F., Terret, M.-E., Bohnsack, M.T., Rassinier, P., Georget, V., Kalab, P., Gruss, O.J., and Verlhac, M.-H. (2007). A centriole- and RanGTP-independent spindle assembly pathway in meiosis I of vertebrate oocytes. J. Cell Biol. *176*, 295–305.

Dupin, I., and Etienne-Manneville, S. (2011). Nuclear positioning: Mechanisms and functions. Int. J. Biochem. Cell Biol. *43*, 1698–1707.

Enjolras, C., Thomas, J., Chhin, B., Cortier, E., Duteyrat, J.-L., Soulavie, F., Kernan, M.J., Laurençon, A., and Durand, B. (2012). Drosophila chibby is required for basal body formation and ciliogenesis but not for Wg signaling. J. Cell Biol. *197*, 313–325.

Ettensohn, C.A., Wray, G.A., and Wessel, G.M. (2004). Development of Sea Urchins, Ascidians, and Other Invertebrate Deuterostomes: Experimental Approaches (Gulf Professional Publishing).

Fabritius, A.S., Ellefson, M.L., and McNally, F.J. (2011). Nuclear and Spindle Positioning during Oocyte Meiosis. Curr. Opin. Cell Biol. *23*, 78–84.

Fırat-Karalar, E.N., and Stearns, T. (2014). The centriole duplication cycle. Philos. Trans. R. Soc. B Biol. Sci. *369*, 20130460.

Fourrage, C., Chevalier, S., and Houliston, E. (2010). A Highly Conserved Poc1 Protein Characterized in Embryos of the Hydrozoan Clytia hemisphaerica: Localization and Functional Studies. PLoS ONE *5*, e13994.

Fu, J., and Glover, D.M. (2012). Structured illumination of the interface between centriole and peri-centriolar material. Open Biol. *2*.

Fu, J., Hagan, I.M., and Glover, D.M. (2015). The Centrosome and Its Duplication Cycle. Cold Spring Harb. Perspect. Biol. *7*.

Fuller, B.G. (2010). Self-organization of intracellular gradients during mitosis. Cell Div. *5*, 5.

Gard, D.L. (1992). Microtubule organization during maturation of Xenopus oocytes: assembly and rotation of the meiotic spindles. Dev. Biol. *151*, 516–530.

Gard, D.L. (1994). γ-Tubulin Is Asymmetrically Distributed in the Cortex of Xenopus Oocytes. Dev. Biol. *161*, 131–140.

Gard, D.L., Affleck, D., and Error, B.M. (1995). Microtubule Organization, Acetylation, and Nucleation in Xenopus laevis Oocytes: II. A Developmental Transition in Microtubule Organization during Early Diplotene. Dev. Biol. *168*, 189–201.

Glotzer, M., Murray, A.W., and Kirschner, M.W. (1991). Cyclin is degraded by the ubiquitin pathway. Nature *349*, 132–138.

Godinho, S.A., and Pellman, D. (2014). Causes and consequences of centrosome abnormalities in cancer. Philos. Trans. R. Soc. B Biol. Sci. *369*, 20130467.

Gonzalez, C., Tavosanis, G., and Mollinari, C. (1998). Centrosomes and microtubule organisation during Drosophila development. J. Cell Sci. *111*, 2697–2706.

González-Reyes, A., Elliott, H., and St Johnston, D. (1995). Polarization of both major body axes in Drosophila by gurken-torpedo signalling. Nature *375*, 654–658.

Goshima, G., Mayer, M., Zhang, N., Stuurman, N., and Vale, R.D. (2008). Augmin: a protein complex required for centrosome-independent microtubule generation within the spindle. J. Cell Biol. *181*, 421–429.

Gould, R., and Borisy, G. (1977). The pericentriolar material in Chinese hamster ovary cells nucleates microtubule formation. J. Cell Biol. *73*, 601–615.

Graser, S., Stierhof, Y.-D., Lavoie, S.B., Gassner, O.S., Lamla, S., Clech, M.L., and Nigg, E.A. (2007). Cep164, a novel centriole appendage protein required for primary cilium formation. J. Cell Biol. *179*, 321–330.

Gruss, O.J., Carazo-Salas, R.E., Schatz, C.A., Guarguaglini, G., Kast, J., Wilm, M., Le Bot, N., Vernos, I., Karsenti, E., and Mattaj, I.W. (2001). Ran Induces Spindle Assembly by Reversing the Inhibitory Effect of Importin α on TPX2 Activity. Cell *104*, 83–93.

Guarguaglini, G., Duncan, P.I., Stierhof, Y.D., Holmström, T., Duensing, S., and Nigg, E.A. (2005). The forkhead-associated domain protein Cep170 interacts with Polo-like kinase 1 and serves as a marker for mature centrioles. Mol. Biol. Cell *16*, 1095–1107.

Guichard, P., Chrétien, D., Marco, S., and Tassin, A.-M. (2010). Procentriole assembly revealed by cryo-electron tomography. EMBO J. *29*, 1565–1572.

Guichard, P., Hachet, V., Majubu, N., Neves, A., Demurtas, D., Olieric, N., Fluckiger, I., Yamada, A., Kihara, K., Nishida, Y., et al. (2013). Native Architecture of the Centriole Proximal Region Reveals Features Underlying Its 9-Fold Radial Symmetry. Curr. Biol. *23*, 1620–1628.

Guo, J., Yang, Z., Song, W., Chen, Q., Wang, F., Zhang, Q., and Zhu, X. (2006). Nudel contributes to microtubule anchoring at the mother centriole and is involved in both dynein-dependent and -independent centrosomal protein assembly. Mol. Biol. Cell *17*, 680–689.

Habermann, K., and Lange, B.M. (2010). Centrosomes: Methods for Preparation. In Encyclopedia of Life Sciences, John Wiley & Sons, Ltd, ed. (Chichester, UK: John Wiley & Sons, Ltd),.

Hamoir, G. (1992). The discovery of meiosis by E. Van Beneden, a breakthrough in the morphological phase of heredity. Int. J. Dev. Biol. *36*, 9–15.

Harven, E. de, and Bernhard, W. (1956). Etude au microscope electronique de l'ultrastructure du centriole chez les vertébrés. Z. Für Zellforsch. Mikrosk. Anat. *45*, 378–398.

Heald, R., Tournebize, R., Blank, T., Sandaltzopoulos, R., Becker, P., Hyman, A., and Karsenti, E. (1996). Self-organization of microtubules into bipolar spindles around artificial chromosomes in Xenopus egg extracts. Nature *382*, 420–425.

Hehnly, H., Chen, C.-T., Powers, C.M., Liu, H.-L., and Doxsey, S. (2012). The centrosome regulates the Rab11- dependent recycling endosome pathway at appendages of the mother centriole. Curr. Biol. CB *22*, 1944–1950.

Hiraki, M., Nakazawa, Y., Kamiya, R., and Hirono, M. (2007). Bld10p constitutes the cartwheel-spoke tip and stabilizes the 9-fold symmetry of the centriole. Curr. Biol. CB *17*, 1778–1783.

Hirono, M. (2014). Cartwheel assembly. Philos. Trans. R. Soc. B Biol. Sci. *369*, 20130458.

Hodges, M.E., Scheumann, N., Wickstead, B., Langdale, J.A., and Gull, K. (2010). Reconstructing the evolutionary history of the centriole from protein components. J Cell Sci *123*, 1407–1413.

Holubcová, Z., Howard, G., and Schuh, M. (2013). Vesicles modulate an actin network for asymmetric spindle positioning. Nat. Cell Biol. *15*, 937–947.

Hornik, K. (2005). A CLUE for CLUster Ensembles. J. Stat. Softw. *14*, 65–72.

Hoyer-Fender, S. (2010). Centriole maturation and transformation to basal body. Semin. Cell Dev. Biol. *21*, 142–147.

Hsu, W.-B., Hung, L.-Y., Tang, C.-J.C., Su, C.-L., Chang, Y., and Tang, T.K. (2008). Functional characterization of the microtubule-binding and -destabilizing domains of CPAP and d-SAS-4. Exp. Cell Res. *314*, 2591–2602.

Ibi, M., Zou, P., Inoko, A., Shiromizu, T., Matsuyama, M., Hayashi, Y., Enomoto, M., Mori, D., Hirotsune, S., Kiyono, T., et al. (2011). Trichoplein controls microtubule anchoring at the centrosome by binding to Odf2 and ninein. J. Cell Sci. *124*, 857–864.

Ishikawa, H., Kubo, A., Tsukita, S., and Tsukita, S. (2005). Odf2-deficient mother centrioles lack distal/subdistal appendages and the ability to generate primary cilia. Nat. Cell Biol. *7*, 517–524.

Jana, S.C., Marteil, G., and Bettencourt-Dias, M. (2014). Mapping molecules to structure: unveiling secrets of centriole and cilia assembly with near-atomic resolution. Curr. Opin. Cell Biol. *26*, 96–106.

Januschke, J., Gervais, L., Gillet, L., Keryer, G., Bornens, M., and Guichet, A. (2006). The centrosome-nucleus complex and microtubule organization in the Drosophila oocyte. Dev. Camb. Engl. *133*, 129–139.

Januschke, J., Reina, J., Llamazares, S., Bertran, T., Rossi, F., Roig, J., and Gonzalez, C. (2013). Centrobin controls mother–daughter centriole asymmetry in Drosophila neuroblasts. Nat. Cell Biol. *15*, 241–248.

Al Jord, A., Lemaître, A.-I., Delgehyr, N., Faucourt, M., Spassky, N., and Meunier, A. (2014). Centriole amplification by mother and daughter centrioles differs in multiciliated cells. Nature *516*, 104–107.

Kanatani, H., Shirai, H., Nakanishi, K., and Kurokawa, T. (1969). Isolation and Identification of Meiosis Inducing Substance in Starfish Asterias amurensis. Nature *221*, 273–274.

Karsenti, E., and Vernos, I. (2001). The Mitotic Spindle: A Self-Made Machine. Science *294*, 543–547.

Kato, K.H., Washitani-Nemoto, S., Hino, A., and Nemoto, S. (1990). Ultrastructural Studies on the Behavior of Centrioles during Meiosis of Starfish Oocytes. Dev. Growth Differ. *32*, 41–49.

Keller, L.C., Geimer, S., Romijn, E., Yates, J., Zamora, I., and Marshall, W.F. (2009). Molecular Architecture of the Centriole Proteome: The Conserved WD40 Domain Protein POC1 Is Required for Centriole Duplication and Length Control. Mol. Biol. Cell *20*, 1150–1166.

Khodjakov, A., Cole, R.W., Oakley, B.R., and Rieder, C.L. (2000). Centrosome-independent mitotic spindle formation in vertebrates. Curr. Biol. *10*, 59–67.

Kim, S., Spike, C., and Greenstein, D. (2013). Control of oocyte growth and meiotic maturation in Caenorhabditis elegans. Adv. Exp. Med. Biol. *757*, 277–320.

Kirkham, M., Muller-Reichert, T., Oegema, K., Grill, S., and Hyman, A.A. (2003). SAS-4 is a C. elegans centriolar protein that controls centrosome size. Cell *112*, 575–587.

Kishi, K., Vugt, M.A.T.M. van, Okamoto, K., Hayashi, Y., and Yaffe, M.B. (2009). Functional Dynamics of Polo-Like Kinase 1 at the Centrosome. Mol. Cell. Biol. *29*, 3134–3150.

Kitagawa, D., Vakonakis, I., Olieric, N., Hilbert, M., Keller, D., Olieric, V., Bortfeld, M., Erat, M.C., Flückiger, I., Gönczy, P., et al. (2011). Structural basis of the 9-fold symmetry of centrioles. Cell *144*, 364–375.

Kitajima, A., and Hamaguchi, Y. (2005). Determination of first cleavage plane: the relationships between the orientation of the mitotic apparatus for first cleavage and the position of meiotic division-related structures in starfish eggs. Dev. Biol. *280*, 48–58.

Klos Dehring, D.A., Vladar, E.K., Werner, M.E., Mitchell, J.W., Hwang, P., and Mitchell, B.J. (2013). Deuterosome-mediated centriole biogenesis. Dev. Cell *27*, 103–112.

Kobayashi, T., and Dynlacht, B.D. (2011). Regulating the transition from centriole to basal body. J. Cell Biol. *193*, 435–444.

Kobayashi, T., Tsang, W.Y., Li, J., Lane, W., and Dynlacht, B.D. (2011). Centriolar kinesin Kif24 interacts with CP110 to remodel microtubules and regulate ciliogenesis. Cell *145*, 914–925.

Kochanski, R.S., and Borisy, G.G. (1990). Mode of centriole duplication and distribution. J. Cell Biol. *110*, 1599–1605.

Kohlmaier, G., Loncarek, J., Meng, X., McEwen, B.F., Mogensen, M.M., Spektor, A., Dynlacht, B.D., Khodjakov, A., and Gönczy, P. (2009). Overly long centrioles and defective cell division upon excess of the SAS-4-related protein CPAP. Curr. Biol. CB *19*, 1012–1018.

Kong, D., Farmer, V., Shukla, A., James, J., Gruskin, R., Kiriyama, S., and Loncarek, J. (2014). Centriole maturation requires regulated Plk1 activity during two consecutive cell cycles. J. Cell Biol. *206*, 855–865.

Krauss, S.W., Spence, J.R., Bahmanyar, S., Barth, A.I.M., Go, M.M., Czerwinski, D., and Meyer, A.J. (2008). Downregulation of protein 4.1R, a mature centriole protein, disrupts centrosomes, alters cell cycle progression, and perturbs mitotic spindles and anaphase. Mol. Cell. Biol. *28*, 2283–2294.

Krioutchkova, M.M., Onishchenko, G.E., and Chentsov, Y.S. (1994a). An Ultrastructural Study of the Centrosome and Centrioles in Gametogenesis and Early Embryogenesis of Lymnaea stagnalis L.: I. Centrosome and Centrioles in Spermatogenesis. J. Struct. Biol. *112*, 49–58.

Krioutchkova, M.M., Onishchenko, G.E., and Chentsov, Y.S. (1994b). An Ultrastructural Study of the Centrosome and Centrioles in Gametogenesis and Early Embryogenesis of Lymnaea stagnalis L.: II. Centrosome and Centrioles in Oogenesis and Early Embryogenesis. J. Struct. Biol. *112*, 59–69.

Kuhn, J.R., and Poenie, M. (2002). Dynamic polarization of the microtubule cytoskeleton during CTL-mediated killing. Immunity *16*, 111–121.

Kunimoto, K., Yamazaki, Y., Nishida, T., Shinohara, K., Ishikawa, H., Hasegawa, T., Okanoue, T., Hamada, H., Noda, T., Tamura, A., et al. (2012). Coordinated Ciliary Beating Requires Odf2-Mediated Polarization of Basal Bodies via Basal Feet. Cell *148*, 189–200.

Kuriyama, R., and Kanatani, H. (1981). The centriolar complex isolated from starfish spermatozoa. J. Cell Sci. *49*, 33–49.

Lange, B.M., and Gull, K. (1995). A molecular marker for centriole maturation in the mammalian cell cycle. J. Cell Biol. *130*, 919–927.

Langford, G.M. (1995). Actin- and microtubule-dependent organelle motors: interrelationships between the two motility systems. Curr. Opin. Cell Biol. *7*, 82–88.

Langford, G.M. (1999). ER transport on actin filaments in squid giant axon: implications for signal transduction at synapse. FASEB J. *13*, s248–S250.

Lau, L., Lee, Y.L., Sahl, S.J., Stearns, T., and Moerner, W.E. (2012). STED Microscopy with Optimized Labeling Density Reveals 9-Fold Arrangement of a Centriole Protein. Biophys. J. *102*, 2926–2935.

Lawo, S., Hasegan, M., Gupta, G.D., and Pelletier, L. (2012). Subdiffraction imaging of centrosomes reveals higher-order organizational features of pericentriolar material. Nat. Cell Biol. *14*, 1148–1158.

Leidel, S., Delattre, M., Cerutti, L., Baumer, K., and Gönczy, P. (2005). SAS-6 defines a protein family required for centrosome duplication in C. elegans and in human cells. Nat. Cell Biol. *7*, 115–125.

Lénárt, P., Rabut, G., Daigle, N., Hand, A.R., Terasaki, M., and Ellenberg, J. (2003). Nuclear envelope breakdown in starfish oocytes proceeds by partial NPC disassembly followed by a rapidly spreading fenestration of nuclear membranes. J. Cell Biol. *160*, 1055–1068.

Lénárt, P., Bacher, C.P., Daigle, N., Hand, A.R., Eils, R., Terasaki, M., and Ellenberg, J. (2005). A contractile nuclear actin network drives chromosome congression in oocytes. Nature *436*, 812–818.

Lesch, B.J., and Page, D.C. (2012). Genetics of germ cell development. Nat. Rev. Genet. *13*, 781–794.

Lettman, M.M., Wong, Y.L., Viscardi, V., Niessen, S., Chen, S.-H., Shiau, A.K., Zhou, H., Desai, A., and Oegema, K. (2013). Direct binding of SAS-6 to ZYG-1

recruits SAS-6 to the mother centriole for cartwheel assembly. Dev. Cell *25*, 284–298.

Ligges, U., and Maechler, M. scatterplot3d - An R Package for Visualizing Multivariate Data. J. Stat. Softw. *08*.

Lodish, H. (2008). Molecular Cell Biology (W. H. Freeman).

Loncarek, J., and Khodjakov, A. (2009). Ab ovo or de novo? Mechanisms of centriole duplication. Mol. Cells *27*, 135–142.

Longo, F.J., and Anderson, E. (1969). Cytological aspects of fertilization in the lamellibranch, Mytilus edulis I. Polar body formation and development of the female pronucleus. J. Exp. Zool. *172*, 69–95.

Louie, R.K., Bahmanyar, S., Siemers, K.A., Votin, V., Chang, P., Stearns, T., Nelson, W.J., and Barth, A.I.M. (2004). Adenomatous polyposis coli and EB1 localize in close proximity of the mother centriole and EB1 is a functional component of centrosomes. J. Cell Sci. *117*, 1117–1128.

Maderspacher, F. (2008). Theodor Boveri and the natural experiment. Curr. Biol. *18*, R279–R286.

Mahowald, A.P., Caulton, J.H., Edwards, M.K., and Floyd, A.D. (1979). Loss of centrioles and polyploidization in follicle cells of Drosophila melanogaster. Exp. Cell Res. *118*, 404–410.

Manandhar, G., Sutovsky, P., Joshi, H.C., Stearns, T., and Schatten, G. (1998). Centrosome reduction during mouse spermiogenesis. Dev. Biol. *203*, 424–434.

Manandhar, G., Simerly, C., Salisbury, J.L., and Schatten, G. (1999). Centriole and centrin degeneration during mouse spermiogenesis. Cell Motil. Cytoskeleton *43*, 137–144.

Manandhar, G., Simerly, C., and Schatten, G. (2000). Highly degenerated distal centrioles in rhesus and human spermatozoa. Hum. Reprod. *15*, 256–263.

Manandhar, G., Schatten, H., and Sutovsky, P. (2005). Centrosome Reduction During Gametogenesis and Its Significance. Biol. Reprod. *72*, 2–13.

Marshall, W.F. (2001). Centrioles take center stage. Curr. Biol. CB *11*, R487–R496.

Marshall, W.F. (2009). Centriole evolution. Curr. Opin. Cell Biol. *21*, 14–19.

Matsuura, R., and Chiba, K. (2004). Unequal cell division regulated by the contents of germinal vesicles. Dev. Biol. *273*, 76–86.

Matsuura, K., Lefebvre, P.A., Kamiya, R., and Hirono, M. (2004). Bld10p, a novel protein essential for basal body assembly in Chlamydomonas. J. Cell Biol. *165*, 663–671.

McNally, F.J. (2013). Mechanisms of spindle positioning. J. Cell Biol. *200*, 131–140.

Megraw, T.L., and Kaufman, T.C. (2000). The centrosome in Drosophila oocyte development. Curr. Top. Dev. Biol. *49*, 385–407.

Mennella, V., Keszthelyi, B., McDonald, K.L., Chhun, B., Kan, F., Rogers, G.C., Huang, B., and Agard, D.A. (2012). Sub-diffraction-resolution fluorescence microscopy reveals a domain of the centrosome critical for pericentriolar material organization. Nat. Cell Biol. *14*, 1159–1168.

Mennella, V., Agard, D.A., Huang, B., and Pelletier, L. (2014). Amorphous no more: subdiffraction view of the pericentriolar material architecture. Trends Cell Biol. *24*, 188–197.

Mierzwa, B., and Gerlich, D.W. (2014). Cytokinetic Abscission: Molecular Mechanisms and Temporal Control. Dev. Cell *31*, 525–538.

Mikeladze-Dvali, T., Tobel, L. von, Strnad, P., Knott, G., Leonhardt, H., Schermelleh, L., and Gönczy, P. (2012). Analysis of centriole elimination during C. elegans oogenesis. Development *139*, 1670–1679.

Miyazaki, A., Kamitsubo, E., and Nemoto, S.-I. (2000). Premeiotic Aster as a Device to Anchor the Germinal Vesicle to the Cell Surface of the Presumptive Animal Pole in Starfish Oocytes. Dev. Biol. *218*, 161–171.

Miyazaki, A., Kato, K.H., and Nemoto, S. (2005). Role of microtubules and centrosomes in the eccentric relocation of the germinal vesicle upon meiosis reinitiation in sea-cucumber oocytes. Dev. Biol. *280*, 237–247.

Mori, M., Monnier, N., Daigle, N., Bathe, M., Ellenberg, J., and Lénárt, P. (2011). Intracellular Transport by an Anchored Homogeneously Contracting F-Actin Meshwork. Curr. Biol. *21*, 606–611.

Mori, M., Somogyi, K., Kondo, H., Monnier, N., Falk, H.J., Machado, P., Bathe, M., Nédélec, F., and Lénárt, P. (2014). An Arp2/3 Nucleated F-Actin Shell Fragments Nuclear Membranes at Nuclear Envelope Breakdown in Starfish Oocytes. Curr. Biol. *24*, 1421–1428.

Moritz, K.B., and Sauer, H.W. (1996). Boveri's contributions to developmental biology--a challenge for today. Int. J. Dev. Biol. *40*, 27–47.

Müller-Reichert, T., Srayko, M., Hyman, A., O'Toole, E.T., and McDonald, K. (2007). Correlative light and electron microscopy of early Caenorhabditis elegans embryos in mitosis. Methods Cell Biol. *79*, 101–119.

Nakagawa, Y., Yamane, Y., Okanoue, T., Tsukita, S., and Tsukita, S. (2001). Outer Dense Fiber 2 Is a Widespread Centrosome Scaffold Component Preferentially Associated with Mother Centrioles: Its Identification from Isolated Centrosomes. Mol. Biol. Cell *12*, 1687–1697.

Nakashima, S., and Kato, K.H. (2001). Centriole behavior during meiosis in oocytes of the sea urchin Hemicentrotus pulcherrimus. Dev. Growth Differ. *43*, 437–445.

Nigg, E.A. (2006). Centrosomes in Development and Disease (John Wiley & Sons).

Nigg, E.A., and Raff, J.W. (2009). Centrioles, Centrosomes, and Cilia in Health and Disease. Cell *139*, 663–678.

Nishitani, H., and Lygerou, Z. (2002). Control of DNA replication licensing in a cell cycle. Genes Cells *7*, 523–534.

Ou, Y.Y., Mack, G.J., Zhang, M., and Rattner, J.B. (2002). CEP110 and Ninein Are Located in a Specific Domain of the Centrosome Associated with Centrosome Maturation. J. Cell Sci. *115*, 1825–1835.

Oulhen, N., Onorato, T.M., Ramos, I., and Wessel, G.M. (2014). Dysferlin is essential for endocytosis in the sea star oocyte. Dev. Biol. *388*, 94–102.

Paintrand, M., Moudjou, M., Delacroix, H., and Bornens, M. (1992). Centrosome organization and centriole architecture: Their sensitivity to divalent cations. J. Struct. Biol. *108*, 107–128.

Papadimitriou, C.H., and Steiglitz, K. (1982). Combinatorial Optimization: Algorithm and Complexity (Prentice Hall).

Paridaen, J.T.M.L., Wilsch-Bräuninger, M., and Huttner, W.B. (2013). Asymmetric Inheritance of Centrosome-Associated Primary Cilium Membrane Directs Ciliogenesis after Cell Division. Cell *155*, 333–344.

Pearson, C.G., Osborn, D.P.S., Giddings, T.H., Jr, Beales, P.L., and Winey, M. (2009). Basal body stability and ciliogenesis requires the conserved component Poc1. J. Cell Biol. *187*, 905–920.

Pelletier, L., and Yamashita, Y.M. (2012). Centrosome asymmetry and inheritance during animal development. Curr. Opin. Cell Biol. *24*, 541–546.

Pelletier, L., O'Toole, E., Schwager, A., Hyman, A., and M^{3}ller-Reichert, T. (2006). Centriole assembly in Caenorhabditis elegans. Nature *444*, 619–623.

Petry, S., Groen, A.C., Ishihara, K., Mitchison, T.J., and Vale, R.D. (2013). Branching microtubule nucleation in Xenopus egg extracts mediated by augmin and TPX2. Cell *152*, 768–777.

Piel, M., Meyer, P., Khodjakov, A., Rieder, C.L., and Bornens, M. (2000). The Respective Contributions of the Mother and Daughter Centrioles to Centrosome Activity and Behavior in Vertebrate Cells. J. Cell Biol. *149*, 317–330.

Piel, M., Nordberg, J., Euteneuer, U., and Bornens, M. (2001). Centrosome-Dependent Exit of Cytokinesis in Animal Cells. Science *291*, 1550–1553.

Raynaud-Messina, B., and Merdes, A. (2007). γ-tubulin complexes and microtubule organization. Curr. Opin. Cell Biol. *19*, 24–30.

R Development Core Team (2009). {R: A language and environment for statistical computing} (Vienna, Austria: R Foundation for Statistical Computing).

Rebollo, E., Sampaio, P., Januschke, J., Llamazares, S., Varmark, H., and González, C. (2007). Functionally unequal centrosomes drive spindle orientation in asymmetrically dividing Drosophila neural stem cells. Dev. Cell *12*, 467–474.

Reiter, J.F., Blacque, O.E., and Leroux, M.R. (2012). The base of the cilium: roles for transition fibres and the transition zone in ciliary formation, maintenance and compartmentalization. EMBO Rep. *13*, 608–618.

Robbins, E., Jentzsch, G., and Micali, A. (1968). THE CENTRIOLE CYCLE IN SYNCHRONIZED HELA CELLS. J. Cell Biol. *36*, 329–339.

Robert, X., and Gouet, P. (2014). Deciphering key features in protein structures with the new ENDscript server. Nucleic Acids Res. *42*, W320–W324.

Rodrigues-Martins, A., Riparbelli, M., Callaini, G., Glover, D.M., and Bettencourt-Dias, M. (2007). Revisiting the Role of the Mother Centriole in Centriole Biogenesis. Science *316*, 1046–1050.

Rodrigues-Martins, A., Riparbelli, M., Callaini, G., Glover, D.M., and Bettencourt-Dias, M. (2008). From centriole biogenesis to cellular function: Centrioles are essential for cell division at critical developmental stages. Cell Cycle *7*, 11–16.

Roy C Brown, B.E.L. (2011). Dividing without centrioles: innovative plant microtubule organizing centres organize mitotic spindles in bryophytes, the earliest extant lineages of land plants. AoB Plants *2011*, plr028.

Rusan, N., and Peifer, M. (2007). A role for a novel centrosome cycle in asymmetric cell division. J. Cell Biol. 200612140.

Saiki, T., and Hamaguchi, Y. (1998). Aster-Forming Abilities of the Egg, Polar Body, and Sperm Centrosomes in Early Starfish Development. Dev. Biol. *203*, 62–74.

Salisbury, J.L. (2007). A mechanistic view on the evolutionary origin for centrin-based control of centriole duplication. J. Cell. Physiol. *213*, 420–428.

Sathananthan, A.H., Selvaraj, K., and Trounson, A. (2000). Fine structure of human oogonia in the foetal ovary. Mol. Cell. Endocrinol. *161*, 3–8.

Sathananthan, A.H., Selvaraj, K., Girijashankar, M.L., Ganesh, V., Selvaraj, P., and Trounson, A.O. (2006). From oogonia to mature oocytes: inactivation of the maternal centrosome in humans. Microsc. Res. Tech. *69*, 396–407.

Sbalzarini, I.F., and Koumoutsakos, P. (2005). Feature point tracking and trajectory analysis for video imaging in cell biology. J. Struct. Biol. *151*, 182–195.

Scheer, U. (2014). Historical roots of centrosome research: discovery of Boveri's microscope slides in Würzburg. Philos. Trans. R. Soc. B Biol. Sci. *369*, 20130469.

Schiebel, E., and Bornens, M. (1995). In search of a function for centrins. Trends Cell Biol. *5*, 197–201.

Schmidt, K.N., Kuhns, S., Neuner, A., Hub, B., Zentgraf, H., and Pereira, G. (2012). Cep164 mediates vesicular docking to the mother centriole during early steps of ciliogenesis. J. Cell Biol. *199*, 1083–1101.

Schmidt, T.I., Kleylein-Sohn, J., Westendorf, J., Le Clech, M., Lavoie, S.B., Stierhof, Y.-D., and Nigg, E.A. (2009). Control of centriole length by CPAP and CP110. Curr. Biol. CB *19*, 1005–1011.

Schuh, M. (2011). An actin-dependent mechanism for long-range vesicle transport. Nat. Cell Biol. *13*, 1431–1436.

Schuh, M., and Ellenberg, J. (2007). Self-Organization of MTOCs Replaces Centrosome Function during Acentrosomal Spindle Assembly in Live Mouse Oocytes. Cell *130*, 484–498.

Schuh, M., and Ellenberg, J. (2008). A new model for asymmetric spindle positioning in mouse oocytes. Curr. Biol. CB *18*, 1986–1992.

Schweizer, S., and Hoyer-Fender, S. (2009). Mouse Odf2 localizes to centrosomes and basal bodies in adult tissues and to the photoreceptor primary cilium. Cell Tissue Res. *338*, 295–301.

Shirai, H., Yoshimoto, Y., and Kanatani, H. (1981). Mechanism of Starfish Spawning. Iv. Tension Generation in the Ovarian Wall by 1-Methyladenine at the Time of Spawning. Biol. Bull. *161*, 172–179.

Shirato, Y., Tamura, M., Yoneda, M., and Nemoto, S.-I. (2006). Centrosome destined to decay in starfish oocytes. Dev. Camb. Engl. *133*, 343–350.

Singla, V., and Reiter, J.F. (2006). The Primary Cilium as the Cell's Antenna: Signaling at a Sensory Organelle. Science *313*, 629–633.

Sköld, H.N., Komma, D.J., and Endow, S.A. (2005). Assembly pathway of the anastral Drosophilaoocyte meiosis I spindle. J. Cell Sci. *118*, 1745–1755.

Sluder, G., Miller, F.J., Lewis, K., Davison, E.D., and Rieder, C.L. (1989). Centrosome inheritance in starfish zygotes: Selective loss of the maternal centrosome after fertilization. Dev. Biol. *131*, 567–579.

Sonnen, K.F., Schermelleh, L., Leonhardt, H., and Nigg, E.A. (2012). 3D-structured illumination microscopy provides novel insight into architecture of human centrosomes. Biol. Open.

Sorokin, S. (1962). Centrioles and the Formation of Rudimentary Cilia by Fibroblasts and Smooth Muscle Cells. J. Cell Biol. *15*, 363–377.

Sorokin, S.P. (1968). Reconstructions of Centriole Formation and Ciliogenesis in Mammalian Lungs. J. Cell Sci. *3*, 207–230.

Soung, N.-K., Kang, Y.H., Kim, K., Kamijo, K., Yoon, H., Seong, Y.-S., Kuo, Y.-L., Miki, T., Kim, S.R., Kuriyama, R., et al. (2006). Requirement of hCenexin for proper mitotic functions of polo-like kinase 1 at the centrosomes. Mol. Cell. Biol. *26*, 8316–8335.

Spektor, A., Tsang, W.Y., Khoo, D., and Dynlacht, B.D. (2007). Cep97 and CP110 suppress a cilia assembly program. Cell *130*, 678–690.

Steere, N., Chae, V., Burke, M., Li, F.-Q., Takemaru, K.-I., and Kuriyama, R. (2012). A Wnt/beta-Catenin Pathway Antagonist Chibby Binds Cenexin at the Distal End of Mother Centrioles and Functions in Primary Cilia Formation. PLoS ONE *7*, e41077.

Stenmark, H. (2009). Rab GTPases as coordinators of vesicle traffic. Nat. Rev. Mol. Cell Biol. *10*, 513–525.

Stetina, J.R.V., and Orr-Weaver, T.L. (2011). Developmental Control of Oocyte Maturation and Egg Activation in Metazoan Models. Cold Spring Harb. Perspect. Biol. *3*, a005553.

Stevens, N.R., Raposo, A.A.S.F., Basto, R., St Johnston, D., and Raff, J.W. (2007). From Stem Cell to Embryo without Centrioles. Curr. Biol. *17*, 1498–1503.

Stevens, N.R., Roque, H., and Raff, J.W. (2010). DSas-6 and Ana2 Coassemble into Tubules to Promote Centriole Duplication and Engagement. Dev. Cell *19*, 913–919.

Stinchcombe, J.C., and Griffiths, G.M. (2014). Communication, the centrosome and the immunological synapse. Philos. Trans. R. Soc. B Biol. Sci. *369*, 20130463.

Stinchcombe, J.C., Majorovits, E., Bossi, G., Fuller, S., and Griffiths, G.M. (2006). Centrosome polarization delivers secretory granules to the immunological synapse. Nature *443*, 462–465.

Stinchcombe, J.C., Salio, M., Cerundolo, V., Pende, D., Arico, M., and Griffiths, G.M. (2011). Centriole polarisation to the immunological synapse directs secretion from cytolytic cells of both the innate and adaptive immune systems. BMC Biol. *9*, 45.

Strnad, P., and Gönczy, P. (2008). Mechanisms of procentriole formation. Trends Cell Biol. *18*, 389–396.

Sung, C.-H., and Leroux, M.R. (2013). The roles of evolutionarily conserved functional modules in cilia-related trafficking. Nat. Cell Biol. *15*, 1387–1397.

Szollosi, D., Calarco, P., and Donahue, R.P. (1972). Absence of Centrioles in the First and Second Meiotic Spindles of Mouse Oocytes. J. Cell Sci. *11*, 521–541.

Tachibana, K., Tanaka, D., Isobe, T., and Kishimoto, T. (2000). c-Mos forces the mitotic cell cycle to undergo meiosis II to produce haploid gametes. Proc. Natl. Acad. Sci. *97*, 14301–14306.

Tamura, M., and Nemoto, S. (2001). Reproductive maternal centrosomes are cast off into polar bodies during maturation division in starfish oocytes. Exp. Cell Res. *269*, 130–139.

Tang, C.-J.C., Lin, S.-Y., Hsu, W.-B., Lin, Y.-N., Wu, C.-T., Lin, Y.-C., Chang, C.-W., Wu, K.-S., and Tang, T.K. (2011). The human microcephaly protein STIL interacts with CPAP and is required for procentriole formation. EMBO J. *30*, 4790–4804.

Tanos, B.E., Yang, H.-J., Soni, R., Wang, W.-J., Macaluso, F.P., Asara, J.M., and Tsou, M.-F.B. (2013). Centriole distal appendages promote membrane docking, leading to cilia initiation. Genes Dev. *27*, 163–168.

Tateishi, K., Yamazaki, Y., Nishida, T., Watanabe, S., Kunimoto, K., Ishikawa, H., and Tsukita, S. (2013). Two appendages homologous between basal bodies and centrioles are formed using distinct Odf2 domains. J. Cell Biol. *203*, 417–425.

Terasaki, M. (1994). Redistribution of cytoplasmic components during germinal vesicle breakdown in starfish oocytes. J. Cell Sci. *107 (Pt 7)*, 1797–1805.

Terasaki, M., Okumura, E.-I., Hinkle, B., and Kishimoto, T. (2003). Localization and dynamics of Cdc2-cyclin B during meiotic reinitiation in starfish oocytes. Mol. Biol. Cell *14*, 4685–4694.

Tirnauer, J.S., and Bierer, B.E. (2000). Eb1 Proteins Regulate Microtubule Dynamics, Cell Polarity, and Chromosome Stability. J. Cell Biol. *149*, 761–766.

Tsang, W.Y., Bossard, C., Khanna, H., Peränen, J., Swaroop, A., Malhotra, V., and Dynlacht, B.D. (2008). CP110 suppresses primary cilia formation through its interaction with CEP290, a protein deficient in human ciliary disease. Dev. Cell *15*, 187–197.

Tsou, M.-F.B., and Stearns, T. (2006). Mechanism limiting centrosome duplication to once per cell cycle. Nature *advanced online publication*, 947–951.

Tsou, M.-F.B., Wang, W.-J., George, K.A., Uryu, K., Stearns, T., and Jallepalli, P.V. (2009). Polo kinase and separase regulate the mitotic licensing of centriole duplication in human cells. Dev. Cell *17*, 344–354.

Uetake, Y., Kato, K.H., Washitani-Nemoto, S., and Nemoto Si, S. (2002). Nonequivalence of maternal centrosomes/centrioles in starfish oocytes: selective casting-off of reproductive centrioles into polar bodies. Dev. Biol. *247*, 149–164.

Venoux, M., Tait, X., Hames, R.S., Straatman, K.R., Woodland, H.R., and Fry, A.M. (2012). Poc1A and Poc1B act together in human cells to ensure centriole integrity. J. Cell Sci.

Verlhac, M.-H., Lefebvre, C., Guillaud, P., Rassinier, P., and Maro, B. (2000). Asymmetric division in mouse oocytes: with or without Mos. Curr. Biol. *10*, 1303–1306.

Vorobjev, I.A., and YuS, C. (1982). Centrioles in the cell cycle. I. Epithelial cells. J. Cell Biol. *93*, 938–949.

Wada, T., Hara, M., Taneda, T., Qingfu, C., Takata, R., Moro, K., Takeda, K., Kishimoto, T., and Handa, H. (2012). Antisense morpholino targeting just upstream from a poly(A) tail junction of maternal mRNA removes the tail and inhibits translation. Nucleic Acids Res. *40*, e173.

Walczak, C.E., and Heald, R. (2008). Chapter Three - Mechanisms of Mitotic Spindle Assembly and Function. In International Review of Cytology, K.W. Jeon, ed. (Academic Press), pp. 111–158.

Wang, W.-J., Soni, R.K., Uryu, K., and Tsou, M.-F.B. (2011). The conversion of centrioles to centrosomes: essential coupling of duplication with segregation. J. Cell Biol. *193*, 727–739.

Wang, X., Tsai, J.-W., Imai, J.H., Lian, W.-N., Vallee, R.B., and Shi, S.-H. (2009). Asymmetric centrosome inheritance maintains neural progenitors in neocortex. Nature *461*, 947–955.

Washitani-Nemoto, S., Saitoh, C., and Nemoto, S. (1994). Artificial parthenogenesis in starfish eggs: behavior of nuclei and chromosomes resulting in tetraploidy of parthenogenotes produced by the suppression of polar body extrusion. Dev. Biol. *163*, 293–301.

Werner, M.E., Hwang, P., Huisman, F., Taborek, P., Yu, C.C., and Mitchell, B.J. (2011). Actin and microtubules drive differential aspects of planar cell polarity in multiciliated cells. J. Cell Biol. *195*, 19–26.

White, R.A., Pan, Z., and Salisbury, J.L. (2000). GFP-centrin as a marker for centriole dynamics in living cells. Microsc. Res. Tech. *49*, 451–457.

Winey, M., and O'Toole, E. (2014). Centriole structure. Philos. Trans. R. Soc. B Biol. Sci. *369*, 20130457.

Woodruff, J.B., Wueseke, O., and Hyman, A.A. (2014). Pericentriolar material structure and dynamics. Philos. Trans. R. Soc. B Biol. Sci. *369*, 20130459.

Woolley, D.M., and Fawcett, D.W. (1973). The degeneration and disappearance of the centrioles during the development of the rat spermatozoon. Anat. Rec. *177*, 289–301.

Yamashita, Y.M., Mahowald, A.P., Perlin, J.R., and Fuller, M.T. (2007). Asymmetric Inheritance of Mother Versus Daughter Centrosome in Stem Cell Division. Science *315*, 518–521.

Zhang, Q.Y., Tamura, M., Uetake, Y., Washitani-Nemoto, S., and Nemoto, S. (2004). Regulation of the paternal inheritance of centrosomes in starfish zygotes. Dev. Biol. *266*, 190–200.

Zhao, T., Graham, O.S., Raposo, A., and Johnston, D.S. (2012). Growing Microtubules Push the Oocyte Nucleus to Polarize the Drosophila Dorsal-Ventral Axis. Science *336*, 999–1003.

(2011). Isolation of Centrosomes from Cultured Cells - Springer. A. Straube, ed. (Humana Press),.